CULTIVATION OF MICROORGANISMS FROM SULFIDIC MINE WASTE AND GENOMIC INSIGHTS INTO *ACIDIBACILLUS FERROOXIDANS* AND *PENICILLIUM* SP.

by

Nathalie Claire Tremblay

A thesis submitted in partial fulfillment
of the requirements for the degree of
Master of Science (MSc) in Biology

The Faculty of Graduate Studies
Laurentian University
Sudbury, Ontario, Canada

THESIS DEFENCE COMMITTEE/COMITÉ DE SOUTENANCE DE THÈSE
Laurentian Université/Université Laurentienne
Faculty of Graduate Studies/Faculté des études supérieures

Title of Thesis Titre de la thèse	CULTIVATION OF MICROORGANISMS FROM SULFIDIC MINE WASTE AND GENOMIC INSIGHTS INTO ACIDIBACILLUS FERROOXIDANS AND PENICILLIUM SP.
Name of Candidate Nom du candidat	Tremblay, Nathalie Claire
Degree Diplôme	Master of Science
Department/Program Département/Programme	Biology
Date of Defence Date de la soutenance	February 25, 2021

APPROVED/APPROUVÉ

Thesis Examiners/Examinateurs de thèse:

Dr. Nadia Mykytczuk
(Supervisor/Directeur(trice) de thèse)

Dr. Gustavo Ybazeta
(Committee member/Membre du comité)

Dr. Nathan Basiliko
(Committee member/Membre du comité)

Dr. Thomas Merritt
(Committee member/Membre du comité)

Dr. Salim Timo Islam Acting Dean, Faculty of Graduate Studies
(External Examiner/Examinateur externe)

Approved for the Faculty of Graduate Studies
Approuvé pour la Faculté des études supérieures
Dr. Lace Marie Brogden
Madame Lace Marie Brogden

Doyenne intérimaire, Faculté des études supérieures

ACCESSIBILITY CLAUSE AND PERMISSION TO USE

I, **Nathalie Claire Tremblay**, hereby grant to Laurentian University and/or its agents the non-exclusive license to archive and make accessible my thesis, dissertation, or project report in whole or in part in all forms of media, now or for the duration of my copyright ownership. I retain all other ownership rights to the copyright of the thesis, dissertation or project report. I also reserve the right to use in future works (such as articles or books) all or part of this thesis, dissertation, or project report. I further agree that permission for copying of this thesis in any manner, in whole or in part, for scholarly purposes may be granted by the professor or professors who supervised my thesis work or, in their absence, by the Head of the Department in which my thesis work was done. It is understood that any copying or publication or use of this thesis or parts thereof for financial gain shall not be allowed without my written permission. It is also understood that this copy is being made available in this form by the authority of the copyright owner solely for the purpose of private study and research and may not be copied or reproduced except as permitted by the copyright laws without written authority from the copyright owner.

ABSTRACT

With increasing pressure to support sustainable mining initiatives, the advancement of biotechnologies is essential for dealing with mine waste in Canada and around the world. These improvements require a thorough understanding of microorganisms that inhabit different waste materials. This study used classic culturing techniques to isolate acidophilic iron-oxidizing bacteria and genomic sequencing to characterize microbial isolates from different source materials. Two organisms were isolated from an enrichment culture that was inoculated with low-sulfur waste rock from a Canadian mine site. They were identified as a strain of *Acidibacillus ferrooxidans* and a fungus of the genus *Penicillium*. Some of the genes that were annotated from the sequenced prokaryotic genome were absent in available genomes of *Ab. ferrooxidans* and others were associated with metabolic abilities that have not been described in this organism, such as respiratory nitrate reduction. A total of 59 stress response genes were identified including for resistance to several heavy metals and multiple antibiotics. Fungal biomass displayed iron oxidation as well as accumulation, and 4 genes encoding for multicopper oxidase enzymes were annotated which have been associated with the adaptation of fungi in metal-rich environments. This study also tailored selective media with the aim of isolating bacteria from the genera *Leptospirillum* and *Sulfobacillus* from sulfidic bioreactor cultures. These groups were not identified but we started to isolate at least 2 different colonies of interest. This project provides insight into microorganisms from these waste materials and their potential in biotechnologies. It also emphasizes the importance of assessing fungi in these environments.

KEY WORDS: Acidophile, iron oxidation, mine waste, bioleaching, iron-oxidizers, isolation, *Acidibacillus ferrooxidans*, fungi, *Penicillium*, bioaccumulation, metabolism, heavy metals.

ACKNOWLEDGEMENTS

I would like to sincerely thank my supervisor, Dr. Nadia Mykytczuk, for giving me the opportunity to be part of her lab group which has been an invaluable experience. I am tremendously grateful for her guidance with this project, and for the general mentorship she has provided over the years which has profoundly impacted my development as a young researcher. A special thank you to my committee members. Dr. Gustavo Ybazeta for advancing my knowledge in bioinformatics and for all of his help with processing the whole-genome sequencing data. Dr. Nathan Basiliko, Dr. Thomas Merritt, and Dr. Salim Timo Islam for the time they invested in guiding this project and reviewing my work.

A huge thanks to Nicole Valiquette for introducing me to the Mykytczuk lab group, for all that she taught me, and for trusting me to work with her cultures. I'd like to thank everyone from the Living with Lakes Centre including Dr. John Gunn and Karen Oman. Special thanks to Emily Smenderovac, Dr. Varun Gupta, James Seward, and Saskia Hart for helping me with various things around the lab and with learning bioinformatics. Thank you to Megan Smith and Madison Cooper for helping with culture work. I feel very fortunate to have worked around so many great people.

Finally, a heartfelt thank you to my family and friends for all of their support through this challenging process and for being a constant source of joy in my life.

TABLE OF CONTENTS

LIST OF FIGURES

LIST OF TABLES

LIST OF ABBREVIATED TERMS

AMD: Acid Mine Drainage

BLAST: Basic Local Alignment Search Tool

CBB cycle: Calvin-Benson-Bassham cycle

EC number: Enzyme Commission number

ED pathway: Entner-Doudoroff pathway

EDTA: Ethylenediaminetetraacetic Acid

EMP pathway: Embden-Meyerhof-Parnas pathway

FeTSB medium: Iron Tryptone Soya Broth medium

FTIR: Fourier-Transform Infrared Spectroscopy

ISP medium: Iron Salts Purified medium

ITS region: Internal Transcribed Spacer Region

LMCO: Laccase-Like Multicopper Oxidase

MCO: Multicopper Oxidase

MG-RAST: Metagenomic Rapid Annotations using Subsystems Technology

NCBI: National Center for Biotechnology Information

PATRIC: Pathosystems Resource Integration Center

PCR: Polymerase Chain Reaction

PP pathway: Pentose Phosphate pathway

QC: Quality Control

RAST: Rapid Annotations using Subsystems Technology

ROS: Reactive Oxygen Species

rTCA cycle: Reverse Tricarboxylic Acid Cycle

RISC: Reduced Inorganic Sulfur Compounds

SEM: Scanning Electron Microscopy

TCA: Tricarboxylic Acid Cycle

TOC: Total Organic Carbon

TK medium: Iron Salts medium

WL pathway: Wood-Ljungdahl pathway

GENERAL INTRODUCTION

Proper disposal of reactive mine-waste material is expensive and failure to contain the toxic compounds that leach over time can have serious environmental impacts. Waste management is therefore a large liability for mining companies and there is significant interest in developing affordable and sustainable biotechnologies for metal removal or stabilization. The development and optimization of such technologies requires a multidisciplinary approach, but one of the key aspects is understanding the microbial populations that influence metal leaching.

Chapter 1 consists of a literature review that introduces microbiology as a multidisciplinary field which includes the use of culturing methods, DNA sequencing technology and computational data processing tools. It discusses the value of molecular analyses but emphasizes the importance of obtaining pure cultures when possible. Literature is also provided for the generation of mine waste and acid mine drainage (AMD). This includes the microbial organisms that have been identified and described in these environments as well as community interactions. The presence and roles of fungi in AMD is introduced in this chapter. The application of both bacteria and fungi in different biotechnologies pertaining to metal-rich mine waste are reviewed.

Chapter 2 presents the first part of this study which focused on isolating, identifying and describing bacteria from enrichment cultures that were inoculated with sulfidic mine waste material. It also focused on isolating the fungus that was observed to grow from the enrichment culture of low-sulfur waste rock from a mine site in Northern Ontario.

Chapter 3 constitutes the second part of this project that used whole-genome sequencing to gain insight on genes and enzymes from *Acidibacillus ferrooxidans* and *Penicillium* sp. that were cultivated from the waste rock culture. Potentially active metabolic

pathways and important genes such as those pertaining to energetic metabolism, stress responses and metal resistance are discussed.

Findings from both experimental chapters are combined in Chapter 4 to provide concluding remarks, to suggest future directions, as well as to discuss how these results relate to the leaching of metals into the environment and to optimizing biotechnologies for metal recovery.

CHAPTER 1:

MICROBIOLOGY OF AMD AND APPLICATIONS IN BIOTECHNOLOGIES

1.1 Importance of environmental microbiology and challenges encountered in the field of study

Due to many factors such as their ubiquitous nature, rapid growth rate and metabolic diversity, microorganisms have been recognized as primary agents of geochemical cycling (Madsen, 1998). Reaction rates of thermodynamically unstable compounds are accelerated by enzymes, such as those produced by microorganisms to survive and grow in their environments (Madsen, 1998). This particular class of enzymes catalyzes oxidation/reduction reactions which are of ecological significance pertaining to geochemical cycling, detoxification of contaminants, and to making conditions conducive for life (Madsen, 1998). Knowledge of environmental microbiology is now considered a critical part of understanding the function of the biosphere because processes carried out by microorganisms have significant global-scale impacts on issues such as environmental quality, agriculture, and climate change (Madsen, 1998). Furthermore, due to advancements in the understanding of these processes, microbial technologies have emerged in the last few decades in which microbial activities are manipulated for a variety of purposes, such as for the degradation of toxic substances from contaminated sites (Hurst, 2007).

Despite this understanding and the dynamic nature of knowledge in this field, answering fundamental questions such as those pertaining to the presence of various microorganisms and their physiological activities, have remained a challenge since the nineteenth century (Madsen, 1998). This has largely been attributed to inadequate methodologies

when compared to the complexity of field sites, as well as the minuscule scale of the organism, and the generation of artifacts by analyses conducted in the laboratory (Madsen, 1998). Complexity is further increased by the understanding that each habitat has different microbial consortia which synergistically induce geochemical changes, the particular activities of which vary in time and space (Madsen, 1998). Unfortunately, a Heisenberg uncertainty-type principal has been associated with environmental microbiology demonstrating that the closer one examines microorganisms from a natural environment, the information becomes increasingly less likely to be representative of the original field site conditions due to habitat disturbance and alterations (Madsen, 1998).

Assigning the role of specific members of microbial communities to different geochemical processes has been a challenge due to the degree of field-site complexity, but pure culture-based analyses (which have simplified this) can overlook small populations of ecologically important species while favoring more abundant yet less relevant species (Madsen, 1998).

These challenges have partially been overcome by using tools for DNA sequencing and downstream analyses, which have revolutionized the field of environmental microbiology (Tyson et al., 2004). As technology advanced rapidly, many valuable tools emerged such as metagenomics, which made the analysis of genetic material from a whole environmental community possible (Bashir et al., 2014). This has led to the discovery of many microorganisms that have yet to be cultured (Bashir et al., 2014; Overmann, 2013). In addition, the potential to carry out different biogeochemical processes could be understood by examining the genomes of individual species (Madsen, 1998). Advancements in sequencing technologies and computational approaches have largely overcome the challenges associated with assembling

individual genomes from complex microbial community datasets that can contain thousands of species and uncultured organisms (Ayling et al., 2020). Metagenomic assembly tools have been created to process short reads from random shotgun whole genome sequencing, and new tools for assembling long reads from metagenomic data will likely be developed in the near future as the use of third generation platforms is increasing to improve the contiguousness of assembled genomes (Ayling et al., 2020).

Culture-independent techniques have provided an abundance of data that was previously considered to be unattainable, but with isolated cultures, predictions based on genetic information can accurately be tested by such means as biochemical tests (Overmann, 2013). Novel cultivation efforts include selective media that better resemble environmental conditions to target organisms of interest, as well as *in situ* cultivation methods to expand cultivatable diversity (Overmann, 2013; Stewart, 2012). Furthermore, phenotypic characterization is of importance because bacteria that are phylogenetically similar based on genetic analyses can exhibit different biogeochemical capabilities (Pace, 1997).

To overcome the classic challenges of environmental microbiology, disciplines of classic culturing and of modern DNA sequencing should be combined. Using molecular tools, organisms of interest can be identified within complex samples, and can then be enriched by using selective culturing techniques. With genomic information, hypotheses can be formulated pertaining to the expression of traits in target organisms and they can be tested with additional laboratory experiments. The combination of culturing and genomic data provides essential insights on the metabolic abilities of target organisms and responses to changes in environmental conditions (Goltsman et al., 2009). These findings must then be considered in the context of the environment in which the samples came from, while keeping in mind the Heisenberg

uncertainty-type principle which applies to these types of studies. One system of interest in the field of environmental microbiology is found in mine waste.

1.2 Formation of AMD and general properties

Although metals are increasingly in finite supply, mining-related activity has seen a global increase with modern mining industries extracting thousands to billions of tons of metal ore per year (Auld, 2014). Pure metals cannot directly be extracted from the soil. They are instead found in heterogenous structures within minerals, such as pyrite that can be processed for valuable gold but that also contains less valuable iron (Auld, 2014; Yadav & Jamal, 2015). When these minerals are mined, lower-grade materials are discarded as waste and become increasingly reactive due to increased surface areas from the crushing and grinding processes (Baker & Banfield, 2003). Failure to properly contain the waste materials can cause the mineral to enter a state of chemical and physical disequilibrium due to exposure to oxygen (O_2) and water (H_2O) (Auld et al., 2013; Das et al., 2009). This causes a complex cycle of reactions that lead to the development of AMD.

The generation of AMD is described as being a positive feedback loop. Once the process begins, reactions are accelerated until the necessary agents, which are usually sulfide materials, have been entirely depleted (Yadav & Jamal, 2015). Reactions can differ due to water geochemistry and due to the minerals being degraded, but a buffering system is generally formed between iron(III) hydroxide ($Fe(OH)_3$) and sulfate (SO_4^{2-})/sulfuric acid (H_2SO_4), which keeps the pH value at ~2.0 (Amaral Zettler et al., 2003; Auld, 2014). The reactive cycle starts with the chemical oxidation of pyrite compounds, lowering the pH to ~4.0 (Auld et al., 2013).

$$2FeS_2\ (s) + 7O_2\ (g) + 2H_2O\ (l) \rightarrow 2Fe^{2+}\ (aq) + 4SO_4^{2-}\ (aq) + 4H^+\ (aq)$$

Dissolved ferrous iron (Fe^{2+}) can be chemically oxidized to ferric iron (Fe^{3+}) that will either form an orange $Fe(OH)_3$ precipitate that will further reduce the pH, or which will not precipitate and will oxidize additional pyrite (Auld, 2014).

$$FeS_2\ (s) + 14Fe^{3+}\ (aq) + 8H_2O\ (l) \rightarrow 15Fe^{2+}\ (aq) + 2SO_4^{2-}\ (aq) + 16H^+\ (aq)$$

This reaction highly increases acidity and iron content as evidence shows that Fe^{3+} oxidizes pyrite 18 to 170 times more rapidly than O_2 (Sanchez-Andrea et al., 2011).

The increase in acidity and dissolved metals in solution provides optimal conditions for microbiological oxidation to occur by chemolithotrophic bacteria (Amaral Zettler et al., 2003). Dissolution rates are highly influenced by the number of viable microbial cells in solution. Studies have found that 75% of AMD was generated specifically by microbial activity (Baker and Banfield, 2003). Furthermore, studies have suggested that the oxidation of Fe^{2+} is the rate-limiting step in the generation of AMD (Auld, 2014). Bacteria are able to accelerate this reaction by up to 1,000,000 times the rate at which it would occur abiotically (Haferburg et al., 2007).

In addition to being acidic as well as sulfate- and iron-rich, AMD contains various heavy metals including cadmium, manganese, nickel, lead, copper, and zinc (Yadav & Jamal, 2015). Yellow-orange $Fe(OH)_3$ precipitates, commonly known as “yellow boy”, give AMD its characteristic color and cause light attenuation (Das et al., 2009). The system is also deficient in dissolved oxygen and total organic carbon (Das et al., 2009). Warm temperatures are typically found in AMD due to microbial activity, such as the highly exothermic oxidation of sulfides (Smith et al., 2015). For example, temperatures at the Richmond Mine at Iron Mountain in Northern California, US, have been recorded to be between 35 °C to 57 °C (Baker et al., 2004).

However, low temperatures (< 5 °C) have been recorded for AMD in northern climates during the winter months (Ben Ali et al., 2019).

1.3 Microbiology of AMD

Microorganisms in AMD can be found living in solution, as well as in subaqueous and solution-air interface biofilms (Baker et al., 2009). Sites have different microbial niches based on their biogeochemical and physical properties, but diversity is generally limited due to extreme conditions (Baker & Banfield, 2003). The main factor causing this selective pressure is high acidity levels, but others include temperature, ionic species, total organic carbon, and dissolved oxygen (Mendez-Garcia et al., 2015). Multiple studies have examined the microbial diversity found in the Rio Tinto river that runs through the Iberian Pyritic Belt in southwestern Spain (Amaral Zettler et al., 2002). Possessing a pH of 1.7 to 2.5, this system has a higher species diversity than many other AMD sources due to diverse nutrient inputs from surrounding watersheds, and due to sunlight being able to penetrate the water column (Amaral Zettler et al., 2003; Baker et al., 2009). In contrast, the subsurface Richmond Mine, located in northern California, USA, is considered to be more of a closed system and is more acidic than the Rio Tinto river (pH 0.5 to 0.9) (Baker et al., 2004). Due to the limited sources of nutrients, species diversity and richness are lower at the Richmond Mine (Baker et al., 2009).

1.3.1 Bacterial communities in AMD

Bacterial communities in AMD have been well documented, and they have been found to contain relatively few phylogenetically-diverse lineages (Baker et al., 2009). It has been

suggested that these bacteria have lived in this type of extreme environment for a very long period of time due to the distinct lineage of strict acidophiles to which they belong (Baker et al., 2009). A diverse range of physiological, metabolic, and genetic traits have been recorded including the ability for many bacterial species to alternate between autotrophic and heterotrophic metabolism based on environmental conditions (Dall'Agnol et al., 2016). Fe^{2+}, elemental sulfur (S^0), and reduced inorganic sulfur compounds (RISCs) are used as electron donors for many chemolithotrophic species (Dall'Agnol et al., 2016). By oxidizing the chemically generated Fe^{2+}, Fe^{3+} is produced and by oxidizing RISCs, H_2SO_4 is formed (Schippers, 2007; Valenzuela et al., 2006). This increase in acidity further promotes the dissolution of metals into solution (Schippers, 2007).

Documented phyla often include Proteobacteria (e.g. *Acidithiobacillus ferrooxidans*), Nitrospirae (*Leptospirillum ferrooxidans* and *Ferromicrobium acidophilus*), Firmicutes (*Acidimicrobium ferrooxidans* and *Sulfobacillus* sp.), and Acidobacteria (*Acidobacterium capsulatum*) (Baker & Banfield, 2003). Community composition in solution from the Rio Tinto river was analyzed by Gonzalez-Toril et al. (2003) using 16S rRNA gene amplification. Most of the bacteria detected were involved with iron cycling such as *L. ferrooxidans*, *At. ferrooxidans*, and *Acidiphilium* spp. (Gonzalez-Toril et al., 2003). Despite diversity being minimal at the Richmond Mine site, a novel group of Deltaproteobacteria and a novel Acidobacteria isolate similar to *A. capsulatum* were recovered (Baker & Banfield, 2003). At this site, *Leptospirillum* spp. were found to be the dominant bacteria at temperatures up to 50 °C and pH values below 0.5, as well as the main components of subaerial slimes (Baker & Banfield, 2003).

In addition, a study comparing the community composition in summer and winter at Vale's Copper Cliff central tailings facility in Sudbury, Ontario, Canada, found that samples mostly contained organisms belonging to the Proteobacteria phylum (Auld et al., 2017). They documented that diversity was lower in the summer with the dominance of organisms from the genera *Acidithiobacillus* and *Acidiphilium* (Auld et al., 2017). In the winter, chemolithotrophs such as *Acidithiobacillus* spp. still generated AMD, but heterotrophic bacteria of the genus *Acidiphilium* were essentially absent during the cold winter months when pH was moderately higher and when available nutrients were increasingly limited (Auld et al., 2017).

The role of bacteria in this biological system has been extensively studied since they are the primary drivers of AMD formation (Baker & Banfield, 2003). The focus is often on organisms involved in iron cycling such as *At. ferrooxidans* and *L. ferrooxidans* (Mendez-Garcia et al., 2015). Another important group of bacteria are those that can oxidize and/or reduce sulfur compounds including *Thiomonas* spp. (Auld et al., 2013). Sulfur-oxidizing bacteria contribute to the generation of H_2SO_4 by oxidizing hydrogen sulfide (H_2S), S^0, and thiosulfates (Ranalli et al., 2009). Microorganisms are the primary producers in AMD (Mendez-Garcia et al., 2015). In areas with lower temperatures (< 30 °C) and higher pH (> 2), organisms including *At. ferrooxidans* are mainly responsible for carbon dioxide (CO_2) fixation, but at higher temperatures and lower pH, other autotrophic organisms such as *Leptospirillum* spp. and *Sulfobacillus* spp. take over this role (Baker & Banfield, 2003). Certain bacteria, such as *At. ferrooxidans* and *L. ferriphilum*, can incorporate nitrogen into the biological system by fixing dinitrogen (N_2) (Baker & Banfield, 2003; Mendez-Garcia et al., 2015). Heterotrophic bacteria, such as *Acidiphilium* spp., consume organic compounds including lysates and exudates which are inhibitory for many of the previously mentioned organisms (Mendez-Garcia et al., 2015). The

biogeochemical cycling of elements by bacteria influence many other forms of life, such as by increasing the bioavailability of toxic heavy metals, by absorbing and releasing gases from/into the atmosphere, as well as by incorporating essential compounds into the biological system that can be utilized by other members (Haferburg et al., 2007).

1.3.2 Presence and roles of fungi in AMD

The successful colonization of different environments by fungi has been associated to their polymorphic nature as well as their mode of reproduction by spore dispersal (Fomina et al., 2006). Increasing evidence is showing that the microbial communities inhabiting AMD are more complex than what was previously acknowledged, and a growing number of studies are investigating the presence as well as the role of fungi in AMD and in AMD-contaminated soils (Auld et al., 2016; Das et al., 2009; Glukhova et al., 2018; Hao et al., 2010; Hujslova et al., 2017; Mardanov et al., 2016; Oggerin et al., 2016; Simonovicova et al., 2010; Simonovicova et al., 2013; Saxena et al., 2006; Wang et al., 2018).

Many species of fungi experience significant stress when exposed to toxic levels of metals and acidity (Das et al., 2009). Metals disrupt essential metabolic processes through protein denaturation as well as by rupturing cell membranes, and an additive effect has been observed when fungal cells are exposed to multiple metals (Das et al., 2009). They are however considered to be resilient organisms, and fungi often dominate metal-contaminated soils due to being more resilient to metals than bacteria found in these environments (Saxena et al., 2005; Santelli et al., 2010). They are found ubiquitously in soil and water, and so have often been exposed to toxic levels of metals found naturally in solution from mineral deposits (Siegel et al., 1990). Resistance factors to protect the cell from metal toxicity are therefore present in fungi,

especially in those which have adapted due to the long-term exposure to extremely high metal concentrations (Bourzama et al., 2019; Haferburg et al., 2007; Mardanov et al., 2016).

They can avoid metal toxicity by adsorbing ions onto their cell surface instead of absorbing them (Kapoor et al., 1999). This occurs passively since fungal cell walls are rich in metal-binding polysaccharides such as chitin and chitosan as well as polyuranides, glycans, proteins, and lipids (Siegel et al., 1990). Chitin has been documented to take up zinc, lead, copper, cadmium, mercury, and iron (Kapoor et al., 1998; Simonovicova et al., 2010). These properties are due to amine, amide and carboxylic functional groups found in these molecules that act as sorption sites (Guibal et al., 1995). Adsorption can occur via complexation, chelation, ion exchange, and reduction reactions (Kanamarlapudi et al., 2018). In addition to providing the cell with metal resistance, adsorption is advantageous for fungi since these binding sites on the cell wall can subsequently accept H^+ ions and release accumulated micronutrients if they become scarce in the surrounding environment (Siegel et al., 1990). Alternatively, active mechanisms of accumulation include uptake into the cell, proton pumps, reduction, and the secretion of metal-complexing metabolites like polysaccharides and inorganic phosphates (Guibal et al., 1995).

Fungi inhabiting AMD environments have been found to be closely related to neutrophilic isolates of the same species, which suggests that the strains found in AMD adapted to these conditions relatively recently (Amaral Zettler et al., 2003). Most fungi in these systems are documented to be acid-tolerant, but some acidophilic species have been identified in environments such as volcanic hot springs and AMD (Baker et al., 2004). Acid-tolerant fungi possess mechanisms to tolerate acidic conditions, such as by pumping protons out of their cells and by establishing low membrane permeability to maintain intracellular neutral conditions (Gross & Robbins, 2000). The presence of ubiquitous fungi in many extreme systems which can

grow in a wide range of pH values supports that they adapted to colonize these environments and compete with other extremophiles (Hujslova et al., 2017). For example, Glukova et al. (2018) examined two strains of *Penicillium* from highly metal rich water at a mine site in Siberia, Russia. Both could grow in pH values from 1.5 to 13, but *Penicillium* ShG4B was deemed acidophilic since it grew best at a pH value of 2.5 whereas optimal growth for the acid-tolerant *Penicillium* ShG4C was found at both pH 2.5 and 7.0 (Glukhova et al., 2018). The acid-tolerant species would keep the pH around 1.5-2.0 and would otherwise bring it up to pH 7-8 if the value raised above 2.5 (Glukhova et al., 2018). The most extreme cases of fungal acid tolerance may be in the mitosporic fungi *Scitadilium acidophilum* and *Acontium velatum* that have been found growing in solution at pH values as low as 0.0 (Baker et al., 2004).

In the Rio Tinto river, which receives external nutrient inputs, diversity appears to be much higher for eukaryotes than prokaryotes and most microbial biomass in samples was found to be eukaryotic (Amaral Zettler et al., 2002). Sequencing analysis of these samples suggests that the dominating fungal phylum at this site is Ascomycota, and that Basidiomycota as well as Zygomycota are present in lower abundance (Oggerin et al., 2016). Within the Ascomycota phylum, sequences were assigned to the classes Eurotiomycetes, Dothideomycetes, Sordariomycetes, and Helotiales (Oggerin et al., 2016) At the Richmond Mine site, which is considered to be more of a closed system, significant amounts of fungal hyphae were found in biofilms especially in those growing in flowing solution (Baker et al., 2004). Using both 18S rRNA and beta-tubulin genes, Baker et al. (2004) identified the presence of fungi belonging to the phylum Ascomycota and classes Dothideomycetes as well as Eurotiomycetes at this site. It was only in surface biofilms that the Basidiomycota phylum was found to be the most abundant

(Baker et al., 2009). *Acidomyces richmondensis* was isolated from this site, and its role in nitrogen cycling was highlighted due to its ability to perform denitrification (Mosier et al., 2016).

Eukaryotic diversity was observed to be lower than prokaryotic diversity in a study of an AMD site in Copper Cliff, Ontario, Canada, but fungi were documented to be present in substantial amounts at this location during both summer and winter months (Auld et al., 2017). Fungal classes included Saccharomycetes, Agaricomycetes, Leotiomycetes, Dothideomycetes, and some were found to be unclassified (Auld et al., 2017). Eukaryotic communities appeared to change significantly less than bacterial communities with the change of seasons, and a higher abundance of eukaryotes was found in the winter than was expected (Auld et al., 2017). Schlief and Mutz (2005) also found higher fungal biomass during the fall and winter seasons, and they associated this to the organic carbon input from fallen leaves.

Prokaryotes have been considered to be the organisms that are mainly responsible for geochemical cycling in AMD, but multiple studies have discussed the important roles of fungi in this environment as well (Amaral Zettler et al., 2003; Baker et al., 2004; Baker et al., 2009; Das et al., 2009; Mosier et al., 2016; Oggerin et al., 2016). For instance, their importance has been highlighted in biofilms, which is considered a habitat for microorganisms and a medium for reactions to take place, as they provide them with rigidity and structure (Amaral Zettler et al., 2003; Baker et al., 2004; Baker et al., 2009). The formation of biofilms on minerals is beneficial since Fe^{2+}-oxidizing bacteria need to be in contact or in close proximity to the metal to accomplish the oxidation reaction (Baker & Banfield, 2003).

Pertaining to carbon cycling, fungi are considered to be the primary degraders of complex organic matter in this extreme system that does not contain invertebrates (Das et al., 2009). As heterotrophic organisms, they keep organic carbon levels low and produce dissolved

carbonate ions that acidophilic bacteria require for growth (Amaral Zettler et al., 2003; Baker et al., 2004). Schlief & Mutz (2005) examined respiration performed by fungi following the input of carbon from leaf fall during autumn in an AMD stream and in a contaminated lake. During peak respiration rates, fungi were responsible for 57% of it in the stream and 47% in the lake (Schlief & Mutz, 2005). As previously discussed, heterotrophic bacteria such as *Acidiphilium* spp. have been found to be almost absent in the winter due to changes in conditions, including colder temperatures and slightly higher pH, but fungi remained present in relatively high abundance (Auld et al., 2017).

In addition, these eukaryotes contribute to the weathering of minerals and to the formation of new ones (Fomina et al., 2005). Their ability to solubilize metals is due to the organic acids, protons, and other metabolites that they synthesize and excrete which induce acidolysis, chelation, and complexation (Deng et al., 2019; Fomina et al., 2005). Several oxidative enzymes produced by fungi can have pH values as low as 2.0 (Das et al., 2009). Metabolites also induce the precipitation of soluble metals and the formation of minerals, such as metal oxalates caused by oxalic acid that many fungi produce (Glukhova et al., 2018).

1.4 Bioremediation of AMD-contaminated sites and biomining of low-grade material

Mine waste is actively generated as a by-product at operational mine sites, but the abandonment of operations without proper remediation has also left behind a legacy of environmental damage that needs to be resolved (Lyon et al., 1993). Contamination by AMD has severely polluted aquatic systems, food crops, and soil environments (Yadav and Jamal, 2015). At low pH, metals are more soluble which makes them more bioavailable and leaching can

contaminate the surrounding soil and water table (Auld, 2014; Haferburg et al., 2007). Mining companies are now liable for managing the waste that they generate, and this responsibility is very expensive (Haferburg et al., 2007; RoyChowdhury et al., 2015).

Additionally, since metals are a non-renewable resource that is being depleted at rising rates, it is becoming increasingly important to recover metals from lower-grade sources, but standard chemical methods are inefficient for these low concentrations. Separating metals by means of chemical treatment is expensive, and the need to use large amounts of reagents for this process have negative environmental impacts (Bourzama et al., 2019). For reasons like these, the development of biotechnology utilizing native microorganisms to increase the rate of metal dissolution and precipitation is of significant interest as it provides a more economical and sustainable method to remove metals from reactive materials (Gross & Robbins, 2000). Common terms used for this application include bio-oxidation, bioleaching, and biomining. These technologies can serve to remediate contaminated soil with methods of extraction or neutralization, and/or to process the extracted metals for financial gain (Baldrian, 2003; Guibal et al., 1995; Wang et al., 2018). They can either be in the form of passive or active treatment (Rambabu et al., 2020).

Passive treatment for AMD involves the design and construction of systems such as aerobic and anaerobic wetlands to systematically remove contaminants like sulfates and heavy metals as well as to raise alkalinity (Skousen et al., 2017). Passive treatment is considered to be more economical over time since it does not require continuous inputs (Rambabu et al., 2020). The typical lifespan of these constructed systems before they require additional inputs is 25 years, but this also means that the process is a long-term one (Trumm, 2010). Other drawbacks include that they require a lot of space which may be unavailable, and changes in abiotic factors

over time (e.g. aeration, pH, temperature) can alter the system in a way that it no longer accomplishes its function (Rambabu et al., 2020). Passive treatments are often ideal to remediate non-operational mine sites as the chemistry and flow rates at these locations are often more stable (Trumm, 2010).

Higher costs are typically associated with active forms of treatment because they utilize equipment such as tanks, mixers, and pumps that are continuously operating and they are regularly maintained with the addition of inputs (Trumm, 2010). They are however of significant interest because they have multiple advantages. Active treatment systems require less space for operation, and they are considered to be highly effective at removing metals and acidity (Trumm, 2010). Systems in tanks can be optimized for treating mine waste based on their specific chemical and biological properties, and conditions can be controlled throughout the process for maximal results (Trumm, 2010). Active forms of treatment for AMD offer faster results than the passive form and are beneficial for active mine sites that experience variations in drainage chemistry and flow rates (Trumm, 2010). The processing of refractory sulfidic gold-bearing concentrates using bioreactor tanks was first commercialized in 1986 and was followed by the initiation of several other industrial bioreactor operations (Natajaran, 2013). One of the major companies involved with the development of biomining has been the BacTech Environmental Corporation, leaching copper sulfides and refractory sulfide gold concentrates (Natajaran, 2013).

Chemolithotrophic bacteria have been the focus when it comes to microorganisms utilized in mine waste biotechnology since they directly solubilize or precipitate metals in order to obtain energy. Most of the species that have been described in industrial applications are also found in the natural mine waste environment, and they are often sulfide-oxidizing acidophiles (Norris et al., 2000). Bioreactors can be operated at temperatures ranging from 40-50 °C and so

they often utilize mixed cultures of thermophiles and occasionally of thermotolerant organisms. (Norris et al., 2000). Studies have found that chemolithotrophic bacteria can solubilize various metals from minerals which include zinc, copper, manganese, nickel, lead, and uranium (Abhilash & Pandey, 2012; Chen & Lin, 2004; Couillard & Mercier, 1990; Mousavi et al., 2005). As in the case of the BacTech bioreactors mentioned previously, bacteria are used to indirectly solubilize gold particles by oxidizing Fe^{2+} from the arsenopyrite-containing minerals in waste material so that the precious metal can subsequently be recovered (Norris et al., 2000). A table listing acidophilic prokaryotes that have been identified in bioleaching operations of various mineral concentrates was created by Rawlings & Johnson (2007).

Fungi have gained attention in the field of biotechnology for their roles in weathering and in bioaccumulation/biosorption (Table 1.1). The potential of fungi in remediation applications as biosorbents to remove contaminants has been discussed in numerous studies (Baldrian, 2002; Deng et al., 2019; Glukhova et al., 2018; Guibal et al., 1995; Hujslova et al., 2016; Kapoor et al., 1998; Mardanov et al., 2016; Saxena et al., 2005; Siegel, 1990; Simonovicova et al., 2013). The placement of hyphal mats in water contaminated by AMD has been suggested as an option for metal removal (Das et al., 2009). *Penicillium chrysogenum* is used for the recovery of metals and has been found to bioleach 60.4% of total heavy metals (Deng et al., 2019). It removed 19.8 mg of cadmium, copper, lead, and zinc from 2.5 g of soil (Deng et al., 2019).

Fungi have some other advantages such as rapid growth rates that make them easily and affordably accessible for biotechnological applications (Mardanov et al., 2016). In addition, dead cells are able to continue to passively adsorb or chelate metals onto their cell walls (Kapoor et al., 1998). Following accumulation, metals can possibly be recovered by eluting the

metals off of the fungal biomass by using reagents such as ethylenediaminetetraacetic acid (EDTA), sodium hydroxide (NaOH), and hydrochloric acid (HCl), and the biomass can subsequently be re-used to extract more metals (Siegel, 1990).

Table 1.1: **Summary of findings pertaining to the solubilization and immobilization of metals by fungi for biotechnological applications**.

Process	Findings	References
Metal dissolution	Solubilization of cuprite, galena, rhodochrosite and calcite by *Aspergillus niger*	Glukhova et al., 2018
	Removal of iron from stainless Fe-Ni-Cr alloys by *Penicillium*	Siegel, 1990
Metal immobilization	Precipitation of copper and cadmium oxalates by certain species of *Penicillium*	Glukhova et al., 2018
	Accumulation of retgersite in the mycelium of certain species of *Penicillium*	Glukhova et al., 2018
	Accumulation of uranium by *Penicillium*	Galun et al., 1982
	Sorption of selenite, lead, cadmium, and copper by *A. niger*	Ardejani et al., 2005; Galun et al., 1982
	Precipitation of cobalt and nickel sulfates via the oxidation of sulfur by some fungi	Glukhova et al., 2018
	Precipitation of manganese by fungi growing with bacteria in bioreactors	Santelli et al., 2010
	Removal of copper, manganese and zinc from contaminated water by wild type strain of *A. niger*	Simonovicova et al., 2013
	Accumulation of iron, magnesium and calcium by *A. niger*	Simonovicova et al., 2010
	Removal of selenite from samples of AMD by lyophilized cell suspension of *A. niger*	Faramarz et al., 2005
	Production of hydronium-jarosite by *Purpureocillium lilacinum* in controlled laboratory experiments	Oggerin et al., 2013

CHAPTER 2:

ISOLATION OF MICROORGANISMS FROM ENRICHMENT CULTURES OF SULFIDIC MINE WASTE

2.1 Abstract

The optimization of bioremediation and bioleaching technologies requires an understanding of the microorganisms that solubilize and precipitate metals. Community diversity varies for different waste materials due to environmental conditions and mineralogical composition; therefore, optimization is site and project specific. This study aimed to isolate and describe Fe^{2+}-oxidizing bacteria from enrichment cultures inoculated with i) low-sulfur waste rock (BWR) and ii) sulfidic tailings from 2 different sites (ECT and BT), specifically targeting the genera *Leptospirillum* and *Sulfobacillus* in the latter. Due to initial observations that fungal growth from BWR seemed to be more rapid and consistent than bacterial growth in/on media, and that quantities of Fe^{3+} appeared to be higher in cultures with fungal biomass, identifying the fungus from this culture became a parallel focus. The 16S rRNA gene sequence of the bacterium isolated from BWR was most similar to sequences from the Fe^{2+}-oxidizing bacteria *Alicyclobacillus* BGR 73 and *Acidibacillus ferrooxidans* SLC66, and the sequence from the ITS region of the fungus was most similar to sequences from species of *Penicillium*. Fungal colonies from BWR consistently accumulated Fe^{3+} and results supported that they were likely oxidizing Fe^{2+} in/on media. In addition, 8 bacterial colonies were isolated from the enrichment cultures of sulfidic tailings. Preliminary results indicated that the 16S rRNA gene sequences of 2 colonies isolated from the ECT culture were most similar to those from bacteria which may be of interest, but additional sub-culturing would have provided more accurate identifications. Further efforts to isolate colonies from the genera *Leptospirillum* and *Sulfobacillus* are likely required.

2.2 Introduction

Bioleaching is a viable solution to address the re-processing and treatment of reactive mine waste materials to prevent long term AMD-contamination from mine waste stockpiles. Maximum metal extraction requires a thorough understanding of microorganisms which drive mineral dissolution so that optimal conditions can be provided and maintained in the biotechnological system (Chen & Lin, 2004). Mineral leachate liquors from stirred-tank and heap pile applications have been found to almost always contain primary iron- and sulfur-oxidizing chemolithotrophs as well as tertiary acidophilic heterotrophs (Johnson et al., 2008). When selecting microorganisms to use, it is important to choose those that will generate a sufficient amount of biomass throughout the process and those which will most efficiently perform the desired mineral dissolution and/or precipitation reactions (Van Der Gast et al., 2004).

The genus *Leptospirillum* classified as belonging to the Nitrospirae phylum and Nitrospirales order was first described in 1972 (Schippers, 2007). These mineral sulfide-oxidizers have been found in numerous AMD systems around the world, like at the Richmond mine, and in bioreactor tanks (Goltsman et al., 2009). These members are Gram-negative obligate aerobes and acidophiles (grow in pH < 4), with cells in the shape of vibrioids or spirilla (potentially cocci or pseudococci) (Schippers, 2007). *Leptospirillum* have been found to be the predominant organisms at temperatures between 35-50 °C and when the pH is below 1.0 (Schippers, 2007). They gain energy by oxidizing Fe^{2+} but cannot do so with sulfur compounds (Schippers, 2007). To this date, species from this genus have been classified into 4 groups including *L. ferrooxidans* (group I), *L. ferriphilum* and *L. rubarum* (group II), *L. ferrodiazotrophum* (group III), and *L.* group IV UBA BS (group IV) that was most recently discovered (Goltsman et al., 2009). Isolate characterization has indicated that groups I and III are

able to fix N_2, and metagenomic sequencing data for the group IV organism suggests it may also be involved in N_2 fixation as well as CO_2 fixation (Goltsman et al., 2009). *Leptospirillum* species with these capabilities have been described as keystone species in newly-forming soil systems (Fujimura et al., 2012). Strain identification and characterization has been described as difficult for this organism since it is challenging to obtain and maintain in pure cultures (Fujimora et al., 2012). Tyson et al. (2005) were able to cultivate and isolate the iron-oxidizing free-living diazotroph, *L. ferrodiazotrophum* sp. nov., by using genetic information that indicated the presence of a *nif* operon to tailor the culturing medium and conditions accordingly for N_2-fixing organisms. Their study is one that highlights the value of using environmental sequencing data to guide culturing methods for organisms that have not been previously cultivated (Tyson et al., 2005).

Another group which is found commonly in acidic environments and consistently in bioleaching reactors is bacteria of the genus *Sulfobacillus* (Justice et al., 2014). These Firmicutes in the order Clostridiales were first described in 1978 and several isolates have been established including *S. acidophilus*, *S. thermosulfidooxidans*, and *S. thermotolerans* (Johnson et al., 2008; Justice et al., 2014). These have been successfully applied in bioleaching sulfide-containing ores and concentrates (Panyushkina et al., 2019). They are Gram-positive acidophiles which are capable of producing spores when conditions are unfavorable (Johnson et al., 2008). The pH range for growth has been found to differ in Fe^{2+}-containing medium (pH 1.2-2.4) and S^0-containing medium (pH 2.0-5.0) (Bogdanova et al., 2006). Most bacteria in this genus are moderate thermophiles, with the exception of *S. thermotolerans* and *S. benefaciens* that are thermotolerant (Panyushkina et al., 2019). They have been reported to grow in temperatures ranging from 20-60 °C, with optimum temperatures such as 40 °C (Bogdanova et al., 2006). The

metabolic capabilities of *Sulfobacillus* are diverse. They are facultative chemolithotrophs that oxidize Fe^{2+} and RISCs including S^0 and tetrathionate, and which can grow heterotrophically when necessary (Bogdanova et al., 2006; Panyuskina et al., 2019). Optimal mixotrophic growth has been documented when levels of organic matter in the medium are 0.02-0.05% w/v total organic carbon (TOC) (Bogdanova et al., 2006). Organic carbon sources used for both energy and assimilation when the bacteria exhibit heterotrophic or mixotrophic metabolism are yeast extract and glucose (Bogdanova et al., 2006). In addition, they can perform anaerobic respiration using Fe^{3+} as the final electron acceptor in the absence of O_2 (Justice et al., 2014). Despite their application in bioleaching approaches for low- and high-grade sulfidic material, their metal tolerance is usually lower than the concentrations of soluble metals found in bioreactors (Watling et al., 2008). Their ability to sporulate has been speculated to assist with their survival in such hostile conditions (Watling et al., 2008). As described by Johnson et al. (2008), species of *Sulfobacillus* have been differentiated from each other by using a combination of phylogenetic and physiological traits.

In AMD environments, these bacteria are part of communities. Considering this and the fact that conditions in bioreactors change throughout the operation process that results in alterations of the community profile, it is reasonable that pure cultures may not have the best results in bioleaching applications (Norris et al., 2000). The successful use of mixed cultures in sulfide-leaching bioreactors has been documented. Yang et al. (2012) compared the percentage of copper extracted from low-grade copper ore between a pure culture of *At. ferrooxidans* and a mixed culture of this organism with the heterotrophic bacterium *Acidiphilium* sp. They found that over 117 days (15 days pre-leaching and 102 days bioleaching), the mixed culture extracted 20.11% whereas the pure culture extracted only 14.87%.

The literature is lacking on how fungi affect chemolithotrophic bacteria in AMD and bioleaching operations such as in reactor tanks. Mariner et al. (2008) reported the presence of both manganese-oxidizing bacteria and fungi in bioreactors to treat manganese-contaminated water. They mention their potential for removing other metals such as iron, aluminum, arsenic, and copper from mine waters, but interactions between the organisms were not discussed in this study. No literature was found to indicate that any experiments have been performed that resemble those which have examined the benefit of using mixed cultures containing *Acidiphilium* spp. in bioleaching reactor tanks. Analyses of bacterial-fungal biofilms have revealed that fungi can influence physiological traits of bacteria such as by providing resistance to antibiotics and other stressors, as well as by altering the expression of virulence genes (Frey-Klett et al., 2011). Studies of consortia formed between these organisms have numerous applications in various fields (Tarkka et al., 2009).

Although the description and isolation of bacteria from AMD is extensive, especially for individuals that are most successful in bioleaching applications, it is important to continue this type of research considering different microbial niches exist based on a site's biogeochemical and physical properties (Baker & Banfield, 2003). In both bioleaching operations and at waste sites, phylogenetic diversity at the strain level is substantial (Goebel & Stackebrandt, 1994). This information supports that there are likely many organisms in these environments that remain to be described. In terms of evolutionary understanding, it is important to identify adaptive traits in organisms that are closely related (Goltsman et al., 2009).

The focus of this chapter is the isolation and identification of bacterial colonies from an enrichment culture that was inoculated with low-sulfur waste rock from a mine site in

Northern Ontario, as well as 2 enrichment cultures that are maintained for the optimization of bioleaching applications in bioreactor tanks. Culturing media used for all of these samples specifically selected for Fe^{2+}-oxidizers. Despite this selectivity, substantial growth of fungal biomass was observed in liquid and on solid media. For this reason, the description of fungi found in these samples and their effects on Fe^{2+}-oxidizing bacteria became a parallel focus of this study, and we attempted to isolate the fungal organism that proliferated in one of the AMD enrichment cultures (BWR). Based on results from targeted 16S rRNA metagenomic sequencing which indicated that the bioreactor enrichment cultures were dominated by bacteria of the genera *Leptospirillum* and *Sulfobacillus*, species-selective media were used to try to isolate these members. Results from this study will provide insight on microorganisms which are part of the native microbial communities from these source materials, and some may be valuable for bioremediation and bioleaching applications. Obtaining these organisms in isolation is essential for accurate biochemical and phenotypic characterization as well as to assess their metabolic responses to different variables in the environment. An increased understanding of fungi in these systems, specifically on how they interact with Fe^{2+}-oxidizing bacteria and with metals from substrates, is necessary to distinguish whether these organisms could be used to optimize industrial bioleaching operations and how they should be managed in biotechnological systems.

2.3 Materials and methods

2.3.1 Starting material: enrichment cultures

The first culture used in this study was previously enriched and described by Valiquette (2018) (Appx. A-1). The inoculum source was low-sulfur waste rock from a nickel-

copper-mixed element mine located in Northern Ontario. Samples of waste rock were enriched in iron tryptone soya broth (FeTSB) medium (Table 2.1). Cultures from this source were labelled as BWR (Bin 1 waste rock).

The 2 other enrichment cultures of sulfidic waste materials were provided by BacTech industrial partners and are maintained in iron salts (TK) medium (Table 2.1) to optimize bioleaching of valuable metals from mine waste in bioreactor tanks (Mykytczuk, 2014). One was labelled BT (BacTech), and the other ECT (Ecuadorian Tailings) (Appx. A-2).

2.3.2 Bacterial colony isolation

Inoculum from the BWR enrichment culture was streaked for isolation onto solid media. This was performed in triplicates on FeTSB and iron salts purified (ISP) medium (Table 2.1). Gellan gum was used as a solidifying agent at a concentration of 0.8 g/L (0.8% w/v). It was used as a substitute for agar because the latter is considered to be unsuitable for culturing extremophiles (Deguchi, 2011; Rygaard et al., 2017).

Inoculum was collected and streaked by means of an inoculation loop. Once colonies were isolated on solid media, they were sub-cultured into the same type of liquid medium so that the cultures would become increasingly pure. We tried to isolate the bacterial and fungal components that were observed in the BWR culture, and we were able to repeat the sub-culturing process described above 4 times, aiming for purity in the last generation. The 5th and final culture was inoculated with a bacterial colony that appeared to be separated from its counterpart in 50 mL of FeTSB. When growth was observed, it was streaked onto plates in attempt to confirm isolation. All liquid and solid cultures were incubated at room temperature (~25-27 °C), and liquid cultures were shaken at 120 rpm. Phenotypic traits that were observable

Table 2.1: **Composition of media utilized for selectively growing and isolating acidophilic microorganisms**.

Medium	Microorganisms being selectively enriched	Media composition			References
		Iron content ($FeSO_4•7H_2O$)	Nutrients	Final pH	
FeTSB	Acidophilic heterotrophic iron-oxidizing bacteria	10.0 g/L	1.26 g/L $(NH_4)_2SO_4$; 0.49 g/L $MgSO_4•7H_2O$; 0.25 g/L tryptone soya broth	2.0-2.5	Johnson, 1987
TK	Acidophilic chemolithoautotrophic iron-oxidizing bacteria	33.4 g/L	4% (w/v) $(NH_4)_2SO_4$; $MgSO_4•7H_2O$; K_2HPO_4	2.0-2.5	Tuovinen & Kelly, 1973
ISP	Acidophilic heterotrophic iron-oxidizing bacteria	10.0 g/L	1.165 g/L $(NH_4)_2SO_4$; 0.275 g/L $MgSO_4•7H_2O$; 0.055 g/L KCl	2.0-2.5	Manning, 1975
Modified TK (liquid)	*Leptospirillum* spp.	33.4 g/L	4% (w/v) $(NH_4)_2SO_4$; $MgSO_4•7H_2O$; K_2HPO_4	~1.8	Rainey & Oren, 2006
Modified ISP (solid)	*Leptospirillum* spp.	10.0 g/L	1.165 g/L $(NH_4)_2SO_4$; 0.275 g/L $MgSO_4•7H_2O$; 0.055 g/L KCl	~1.9	Rainey & Oren, 2006
SM	*Sulfobacillus* spp.	4.2 g/L	3.00 g/L $(NH_4)_2SO_4$; 0.2 g/L yeast extract; 0.50 g/L K_2HPO_4; 0.50 g/L $MgSO_4•7H_2O$; 0.10 g/L KCl; 0.01 g/L $Ca(NO_3)_2$	~1.8	Rainey & Oren, 2006
TSB	Fungus from BWR (inhibiting growth of iron-oxidizing bacteria)	0.0 g/L	1.26 g/L $(NH_4)_2SO_4$; 0.49 g/L $MgSO_4•7H_2O$; 0.25 g/L tryptone soya broth	2.0-2.5	Modified from Johnson, 1987.

were documented and light microscopy was performed on the bacterial colony that was identified with the fungus in BWR. A Gram stain was performed as well as a methyl green stain to assess endospore formation.

Dilutions of the bioreactor enrichment cultures were first spread and streaked onto solid FeTSB and ISP media. These included cell concentrations of 1, 1/10 and 1/100. Each dilution for ECT and BT was streaked in duplicates onto both types of media, and 200 μL of each dilution was spread onto both types of plates. Colonies that grew on FeTSB plates were transferred to this liquid medium, and those that grew on ISP were transferred to TK. Once growth was observed in these cultures, they were streaked onto both FeTSB and ISP plates. The first plate was inoculated using the standard protocol of flaming the inoculation loop between each set of streaks for a sample, and the second plate was inoculated without flaming the loop in between sets of streaks. This was done to increase the number of cells across the surface of the medium since colonies are difficult to obtain and require a long time to grow.

Results from metagenomic sequencing performed in another student project (Bieniek, 2019) indicated that *Leptospirilli* and *Sulfobacilli* were the dominant organisms in these cultures, therefore species-selective media were made based on the protocols described by Rainey & Oren (2006). To isolate *Leptospirillum* spp., TK liquid medium was used with a modified pH of ~1.8 rather than ~2.0, and for solid medium this modification was done with FeTSB at a final pH of 1.89 (Table 2.1). The composition of liquid and solid medium utilized to isolate colonies of *Sulfobacillus*, referred to as SM (*Sulfobacillus* medium), is listed in Table 2.1. The concentration of gellan gum had to be increased from 0.8% to 1.0% since the media did not solidify with the lower concentration, especially for modified ISP plates. Cultures in selective media were created by transferring 0.3 mL of the enrichment cultures BT and ECT to 9.7 mL of

media. Both types of selective media were inoculated with both enrichment cultures in triplicate. These were incubated at 40 °C and shaken at 120 rpm. When growth was observed in these cultures, volumes were taken from each replicate to create a pooled sample. Serial dilutions were performed from 10^{0}-10^{-5} with each of the pooled samples, and they were used to inoculate plates of the corresponding selective medium. The volume of inoculum was increased as cell concentration decreased throughout the dilution series (increments of 25 µL from 50-200 µL). Plates were incubated at 28 °C.

2.3.3 Isolation and analysis of fungal isolates

The initial intention was not to culture fungi, and so they were first obtained by trying to isolate bacterial colonies as described above. They became a focus in this project since substantial fungal growth was observed for most of the cultures and in/on all types of media. Characteristics were documented for fungi from all samples, but to closer analyze the eukaryotic organism, isolation was attempted solely with the BWR enrichment culture. This was done by repeatedly transferring plugs of mycelium on solid media (~1 cm x 1 cm) into liquid FeTSB and ISP media.

Most of the plates with fungal growth displayed Fe^{2+} oxidation that is typically an indicator of chemolithotrophic bacterial growth, therefore a small fungal colony that did not have Fe^{3+} around it was transferred to 50 mL of FeTSB (F). A sample of fungal mycelium with Fe^{3+} was also transferred to 50 mL of FeTSB to analyze if it consisted of both fungal and chemolithotrophic organisms (BF). Samples were taken for light microscopy. Antibiotics and antimycotics were used to try to ensure separation of the fungal and bacterial organisms, but this was unsuccessful. Information on this experiment can be found in Appx. B. In addition, the

fungal culture was streaked onto FeTSB medium that did not contain iron (TSB) with the intention of inhibiting growth of bacteria that require this metal for energy. The effect of growing in absence of heavy metals on mycelial growth was documented. Mycelium from the fungus that grew on these plates was inoculated into liquid FeTSB medium to assess effects on Fe^{2+} oxidation. All liquid and solid cultures were incubated at room temperature (~25-27 °C) and liquid cultures were shaken at 120 rpm.

2.3.4 Identification via Sanger sequencing

DNA was extracted from bacterial colonies that were obtained from BWR, BT and ECT. BWR fungal DNA was extracted from 3 plugs of mycelium on solid medium and using aliquots from two different liquid cultures. The Mobio Ultra Clean Microbial DNA Isolation kit was utilized. Polymerase chain reaction (PCR) was performed amplifying the 16S rRNA bacterial gene using the primer pair 27f (5'-ACAGTTTGATCMTGGCTCAG) (Lane, 1991) and 1492r (5'-GGTTACCTTGTTACGACTT) (Turner et al., 1999). Amplification of the Internal Transcriber Spacer (ITS) region of nuclear DNA was used for identification since it is recognized as being able to taxonomically differentiate between species of fungi (Fajarningsih, 2016). Primers used were ITS1 (5'-TCCGTAGGTGAACCTTGCGG) and ITS4 (5'-TCCTCCGCTTATTGATATGC) (Korabecna, 2007). One of the mycelial plugs that appeared to also contain bacterial DNA due to visible Fe^{2+} oxidation (BF) was sequenced with both ITS and 16S rRNA primers in attempt to confirm the presence of chemolithotrophic bacteria. DNA quantification was done using the BioTek microplate spectrophotometer by measuring absorbance at a wavelength of 260 nm, and purity was assessed using 260/280 values (Barbas III et al., 2007). PCR was performed using HotStart Taq Polymerase and thermocycler conditions

were optimized for each primer pair (Table 2.2). Amplification was confirmed using gel electrophoresis. PCR products that successfully amplified were sent to Genome Quebec for Sanger Sequencing.

Data quality was provided by the sequencing company. The 4Peaks (v. 1.8) (https://nucleobytes.com/4peaks/) software was used to view DNA sequence trace files in order to trim primer sequences and low-quality base calls from the start and end of the sequences, as well as to call mixed bases when possible. Consensus sequences were generated using BioEdit (v. 7.2) (https://bioedit.software.informer.com/7.2/) that performed a pairwise alignment allowing ends to slide, and these were considered to be partial sequences due to being shorter than the entire targeted genes. The Basic Local Alignment Search Tool (BLAST) was used to query the consensus sequences against the National Center for Biotechnology Information (NCBI) nucleotide database.

2.4 Results

2.4.1 Low-sulfur waste rock enrichment culture

Following the initial enrichment culture transfers of BWR, a total of 75 cultures were obtained in liquid or on solid media that had visible Fe^{2+} oxidation and microbial growth. Of these, 66 showed fungal growth (37 from FeTSB medium; 29 from ISP medium) and 9 seemed to only have bacterial proliferation (5 from FeTSB; 4 from ISP). For the latter, bacterial biomass typically appeared after at least a month's time as a lawn on the first isolation streaks, and very few colonies were obtained. Fungal biomass appeared rapidly compared to its bacterial counterpart becoming visible after about one week, and Fe^{2+} oxidation quickly followed. On

Table 2.2: **Optimized concentrations of reagents and thermocycler parameters for PCR reactions**.

A) Composition of 10 µL single PCR reaction:

Reagent	Volume (µL)
Phire Green Hot Start II PCR Master Mix	5
Water	3.6
Forward primer	0.3
Reverse primer	0.3
DNA template	0.8

B) Thermocycler conditions to amplify the prokaryotic 16S rRNA gene using the primer pair 27F-1492R:

Reaction step	Temperature (ºC)	Duration
1. Initial denaturation	98.0	30 seconds
2. Denaturation	98.0	5 seconds
3. Annealing	55.5	5 seconds
4. Extension	72.0	25 seconds
5. Final extension	72.0	1 minute
* Steps 2-4 cycled 30 times		

C) Thermocycler conditions to amplify the nuclear ribosomal internal transcribed spacer (ITS) region in fungi using the primer pair ITS1-ITS4:

Reaction step	Temperature (ºC)	Duration
1. Initial denaturation	98.0	30 seconds
2. Denaturation	98.0	5 seconds
3. Annealing	56.7	5 seconds
4. Extension	72.0	10 seconds
5. Final extension	72.0	1 minute
* Steps 2-4 cycled 30 times		

plates, the fungus grew as flat granular vegetative mats. Small initial colonies appeared white, almost opaque and were mostly circular. Larger mature colonies were less opaque, were more of a salt and pepper color, and were often irregularly-shaped. The black pigments appeared more concentrated in the center of the colony and diffused towards the filamentous edges. Most of those colonies were visibly covered in Fe^{3+} (Figure 2.1). When grown on TSB plates that did not contain Fe^{2+}, filamentous colonies of various sizes from 1-4 cm were circular and black pigments were more pronounced, especially in the aging zone. Transferring fungal mycelium from 5-month-old TSB plates to Fe^{2+}-containing media did not slow down Fe^{2+} oxidation but instead accelerated it. Within one week, both fungal growth and Fe^{2+} oxidation were observed. On FeTSB medium, fungal colonies appeared to be covered in Fe^{3+} precipitates whereas on ISP plates, Fe^{3+} seemed to accumulate less evenly on the biomass (Figure 2.2). Only a few bacterial colonies were obtained from BWR. These were small, smooth and dull, opaque dark orange colonies that were circular, entire and slightly raised.

Two of the final cultures were presumed to be isolated, one with the fungal organism (F) and the other with the bacterium (B). We suspected that the third culture (BF) might contain both organisms since Fe^{2+} oxidation is typically an indicator of chemolithotrophic bacterial growth in iron-rich media (Figure 2.3). Oxidation in each of the cultures started after approximately a week, starting with F and BF. Turbidity was observed in the bacterial culture, but it remained translucent. Precipitation of Fe^{3+} was observed as a dark orange ring on the bottom of the flask. The F culture was less turbid and more translucent than the B culture, and it did not contain as much precipitated Fe^{3+} at the bottom of the flask. Fungal biomass in F was string-like filaments that formed aggregates, and these had a dark orange color. The BF culture was also more translucent than B, but appeared more opaque than F. Similarly, less Fe^{3+}

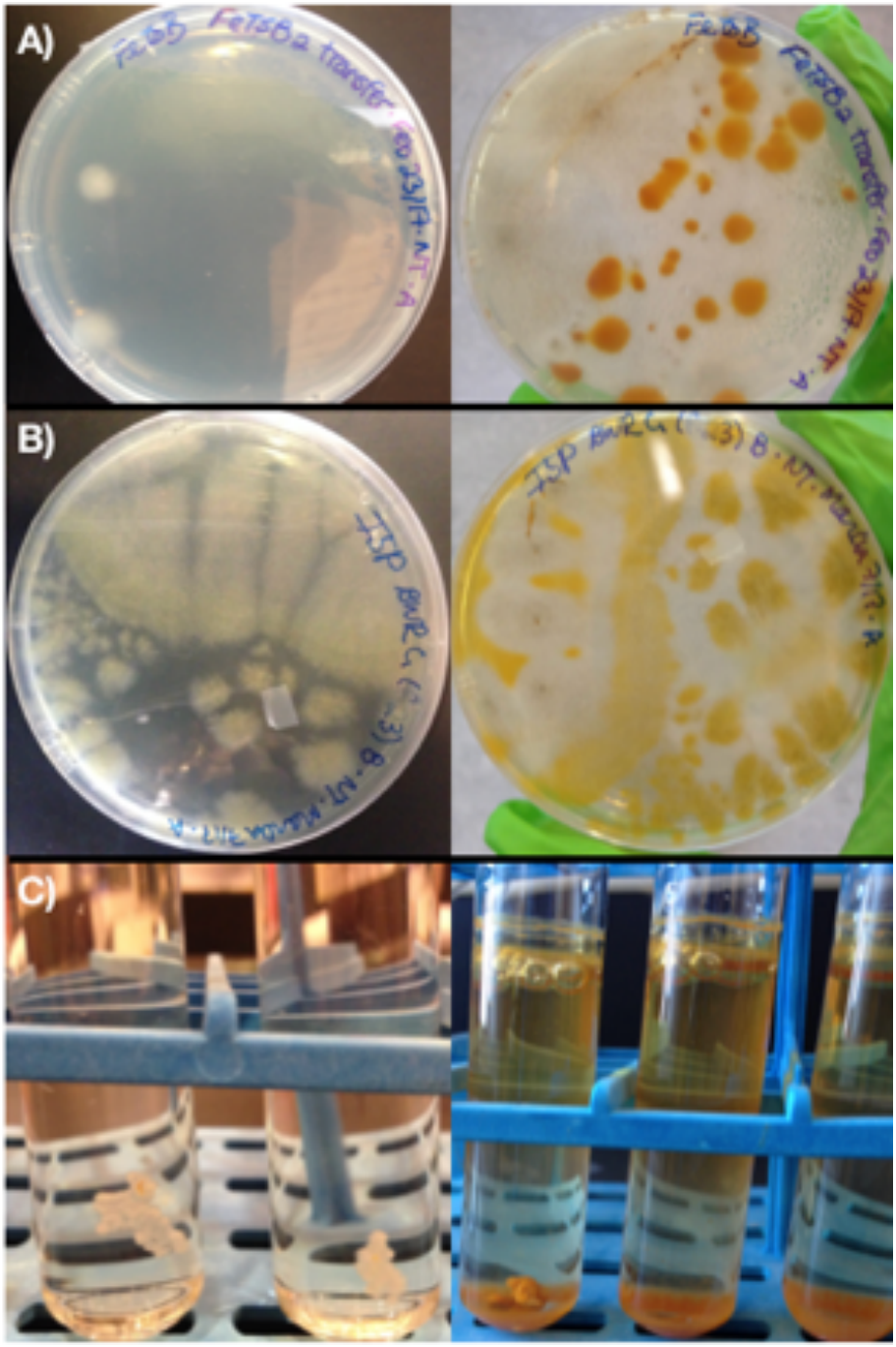

<u>Figure 2.1</u>: Fungal growth from BWR, oxidation of Fe^{2+} in media, and precipitation of Fe^{3+} onto mycelia (orange colored precipitates on biomass). Pictures to the left were taken after a week since inoculation, and pictures to the right after a month's time. Row A) grown on FeTSB medium; Row B) on ISP medium; Row C) in liquid FeTSB medium.

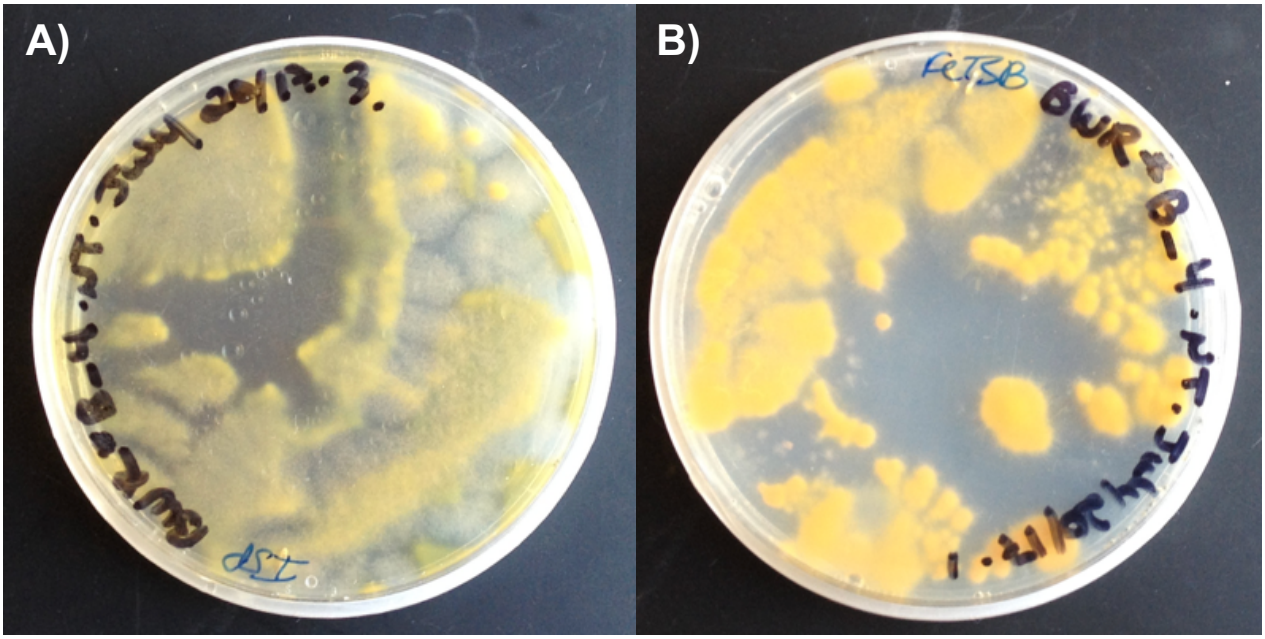

<u>Figure 2.2</u>: **Fungal colony morphology grown in the absence of iron**. Bottom photos are results from inoculating iron-containing media with fungal mycelium from the top photo. A) Growth on ISP medium where fungal colonies accumulated Fe^{3+} in different mycelial zones; B) Growth on FeTSB medium where colonies were fully covered in Fe^{3+}.

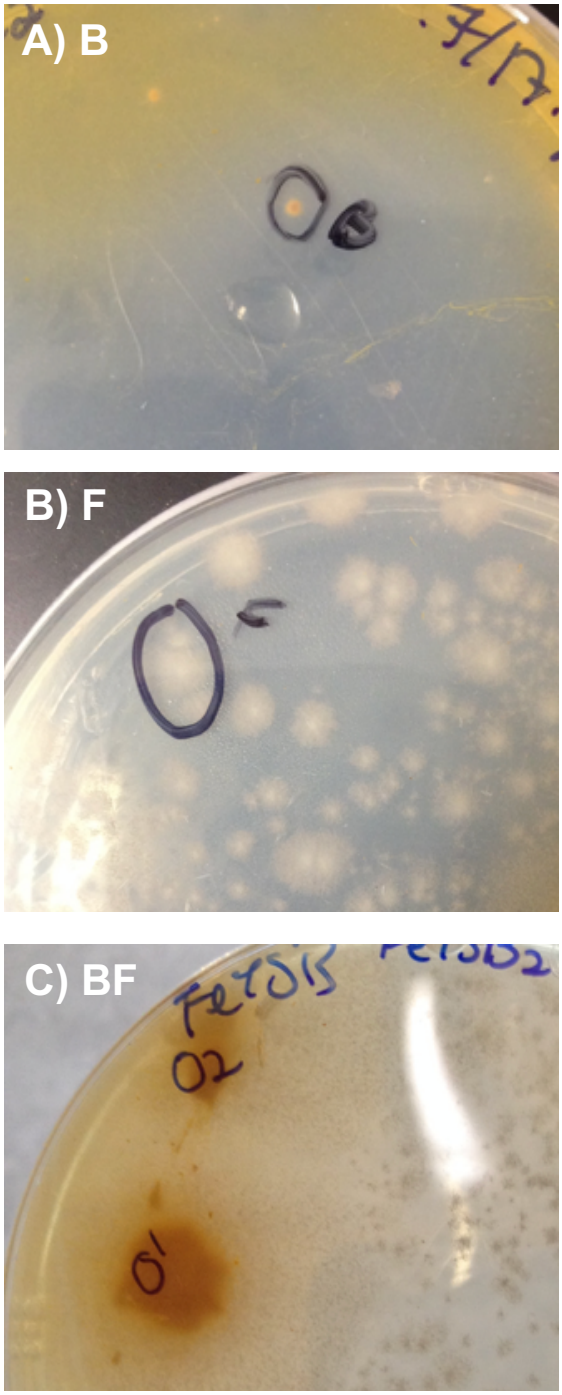

Figure 2.3: **Bacterial** (A) **and fungal** (B) **organisms that appeared to be isolated compared to a plate that was hypothesized to contain both bacterial and fungal cells** (C). **These colonies served as inoculum for the cultures B, F, and BF**.

appeared to have precipitated to the bottom than B but more than F. In this culture, fungal biomass formed round fungal pellets of various sizes that were light orange in color. The inoculation of the B culture on solid medium resulted in Fe^{2+} oxidation along one of the first streaks where bacterial biomass grew, and a translucent halo of oxidation was observed covering the entire plate. The F and BF cultures were largely indistinguishable (Figure 2.4). Fungal biomass covered approximately half of the plates and colonies of various sizes were scattered around. Fe^{2+} oxidation was substantial, but there was no other evidence to support the presence of bacteria. Fe^{3+} appeared to heavily precipitate on the fungal colonies considering fungal mycelia were fully covered in orange precipitates. Slight differences included that halos of oxidation were more pronounced on the BF plates and certain colonies appeared to be thickly concentrating precipitates in the aging zone of the colony rather than being fully covered. This appeared to be the case as colonies approached the halo of Fe^{2+} oxidation, but the halo did not appear to affect colonies in this manner on plates inoculated with F.

Preliminary microscopic analyses of fungal mycelium revealed intertwined branches of hyphae covered in Fe^{3+} precipitates. Septates and several structures resembling conidia were observed. Bacterial cells were very small Gram-positive rods that appeared to produce endospores. Most of them had been released into the culture and a few cells were identified that appeared to contain a terminally located endospore, but images were not obtained.

16S and ITS gene sequences were obtained for the organisms. Fungal sequences were most similar to sequences from species of *Penicillium*, and the sequence from the bacterial colony was most similar to sequences from *Alicyclobacillus* sp. BGR 73 and *Acidibacillus ferrooxidans* SLC66 (Table 2.3) (Appx. C). Sequencing of the ITS region for the BF culture was successful, but sequencing of the 16S gene failed.

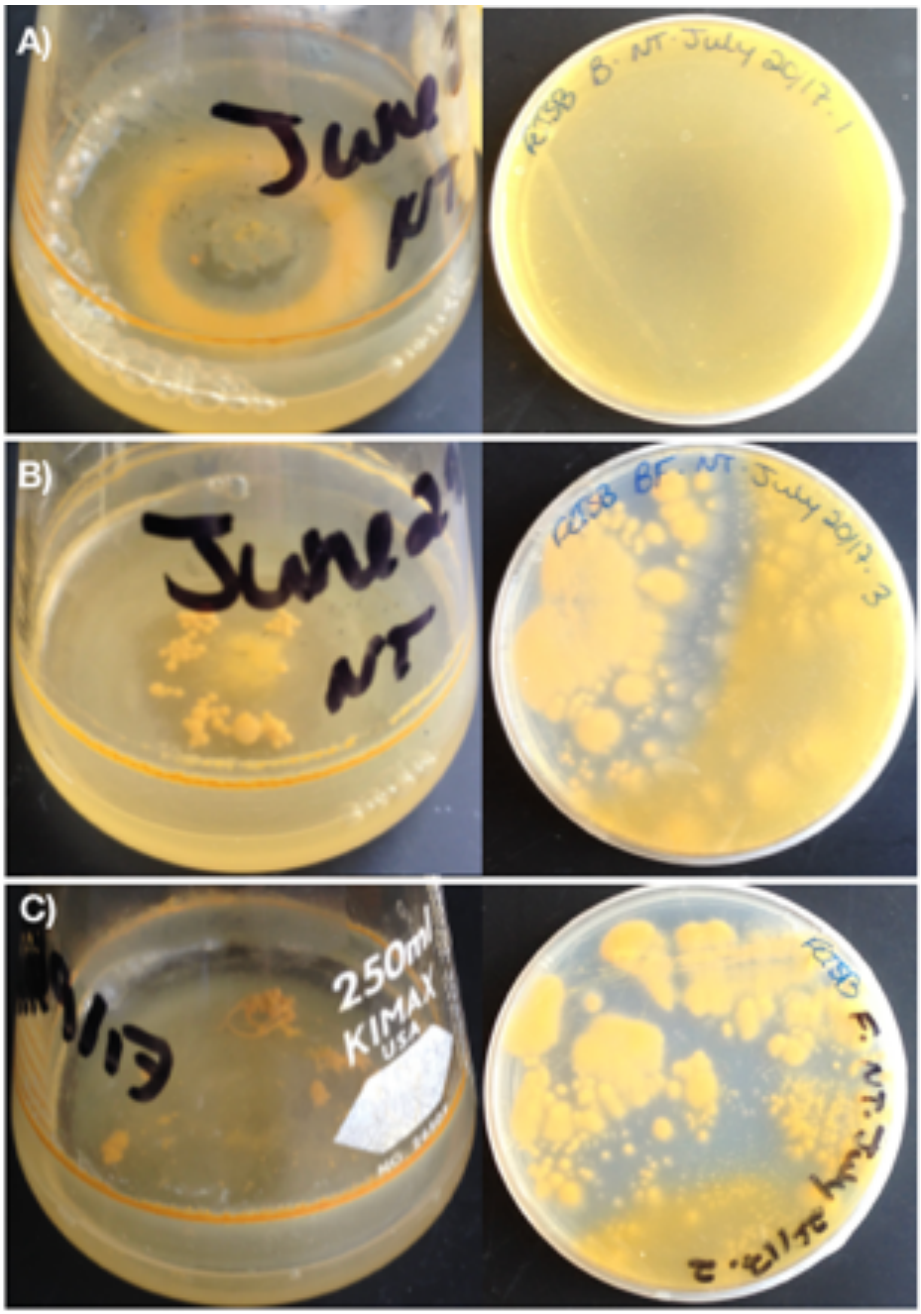

Figure 2.4: **Presumably isolated cultures:** A) **B,** C) **F**. B) **Compared with a culture (BF) that inoculum was suspected to contain cells from both bacterial and fungal organisms**.

Table 2.3: **Identification of the bacterial and fungal organisms from BWR**. PB was obtained from a bacterial colony on solid medium. The first row shows BLAST results with degenerate bases in the sequence, and the second row shows the increase in percent identity when degenerate bases were called if they corresponded with the base at this position in the most similar sequences from the NCBI database. PF represents fungal mycelium from solid medium whereas F1 and F2 were fungal cultures in liquid medium. DNA for BF was extracted from solid medium and was suspected to contain genetic material from both the bacterial and fungal organisms. Sequencing of the 16S rRNA gene failed for this sample. NCBI Accession numbers for most similar sequences are provided.

Sample	Size (bp)	Most Similar Sequences in NCBI Database	Query Cover	Percent Identity	Accession Number
PB	851	*Alicyclobacillus* sp. BGR 73	99%	65.51%	GU167996.1
		Uncultured bacterium clone G26	98%	65.51%	DQ364429.1
		Uncultured bacterium clone SA26	98%	65.11%	FR683050.1
PB	851	*Alicyclobacillus* sp. BGR 73	98%	91.42%	GU167996.1
		Acidibacillus ferrooxidans strain SLC66	98%	90.82%	AY040739.1
		Uncultured bacterium clone G26	98%	90.81%	DQ364429.1
PF	525	*Penicillium albidum* strain CBS 286.53	100%	100%	MH857203.1
		Penicillium daleae strain CBS 211.28	100%	99.81%	MH854984.1
		Penicillium sp. isolate TTC172	100%	99.81%	KX640498.1
F1	525	*Penicillium albidum* strain CBS 286.53	100%	100%	MH857203.1
		Penicillium daleae strain CBS 211.28	100%	99.81%	MH854984.1
		Penicillium sp. isolate TTC172	100%	99.81%	KX640498.1
F2	525	*Penicillium albidum* strain CBS 286.53	100%	100%	MH857203.1
		Penicillium daleae strain CBS 211.28	100%	99.81%	MH854984.1
		Penicillium sp. isolate TTC172	100%	99.81%	KX640498.1
BF	525	*Penicillium albidum* strain CBS 286.53	100%	100%	MH857203.1
		Penicillium daleae strain CBS 211.28	100%	99.81%	MH854984.1
		Penicillium sp. isolate TTC172	100%	99.81%	KX640498.1

2.4.2 Bioreactor enrichment cultures

Growth from the first dilution series was observed on almost all of the plates of each type of medium, but 8 plates from BT had to be thrown out because they had too much fungal growth and some ECT plates had very minimal growth. Fungi still proliferated at 1/100 dilution and growth of ECT was minimal even for undiluted inoculum. A total of 3 ECT colonies and 4 BT colonies were transferred to respective medium that all grew on FeTSB except for one ECT colony on ISP (Appx. A). Five of these colonies were obtained by using undiluted inoculum and 2 of them grew from 1/10 dilutions. Five of the colonies were on spread plates and 2 on isolation streaks. Many bacterial colonies from BT grew on bacterial lawns and with substantial fungal biomass (Figure 2.5). Growth on certain plates and additional colonies were identified over 2 years after inoculating the first set of plates and these were not passaged as part of this project. Subsequent streaking of the colonies showed that the BT colony cultures still had fungal biomass that proliferated on the plates. Only BT1 did not have visible fungal colonies. DNA from a total of 4 ECT colonies on FeTSB medium were extracted and one colony from BT on FeTSB (Table 2.4).

Following the inoculation of selective liquid media, substantial turbidity of the cultures was observed which indicated microbial growth in both types of media. The majority of the BT plates were disposed of due to excessive fungal growth and most of the others displayed little-to-no microbial growth or oxidation at all, even after a year since inoculation. One single colony was obtained on a plate of modified ISP medium that was inoculated by spreading 50 μL of the undiluted enrichment culture, and its DNA was extracted. This smooth and dull opaque yellow colony was tiny, flat, entire, and circular. Relatively short partial gene sequences were obtained from Sanger sequencing and of the 5 colonies, only 2 fairly confident preliminary

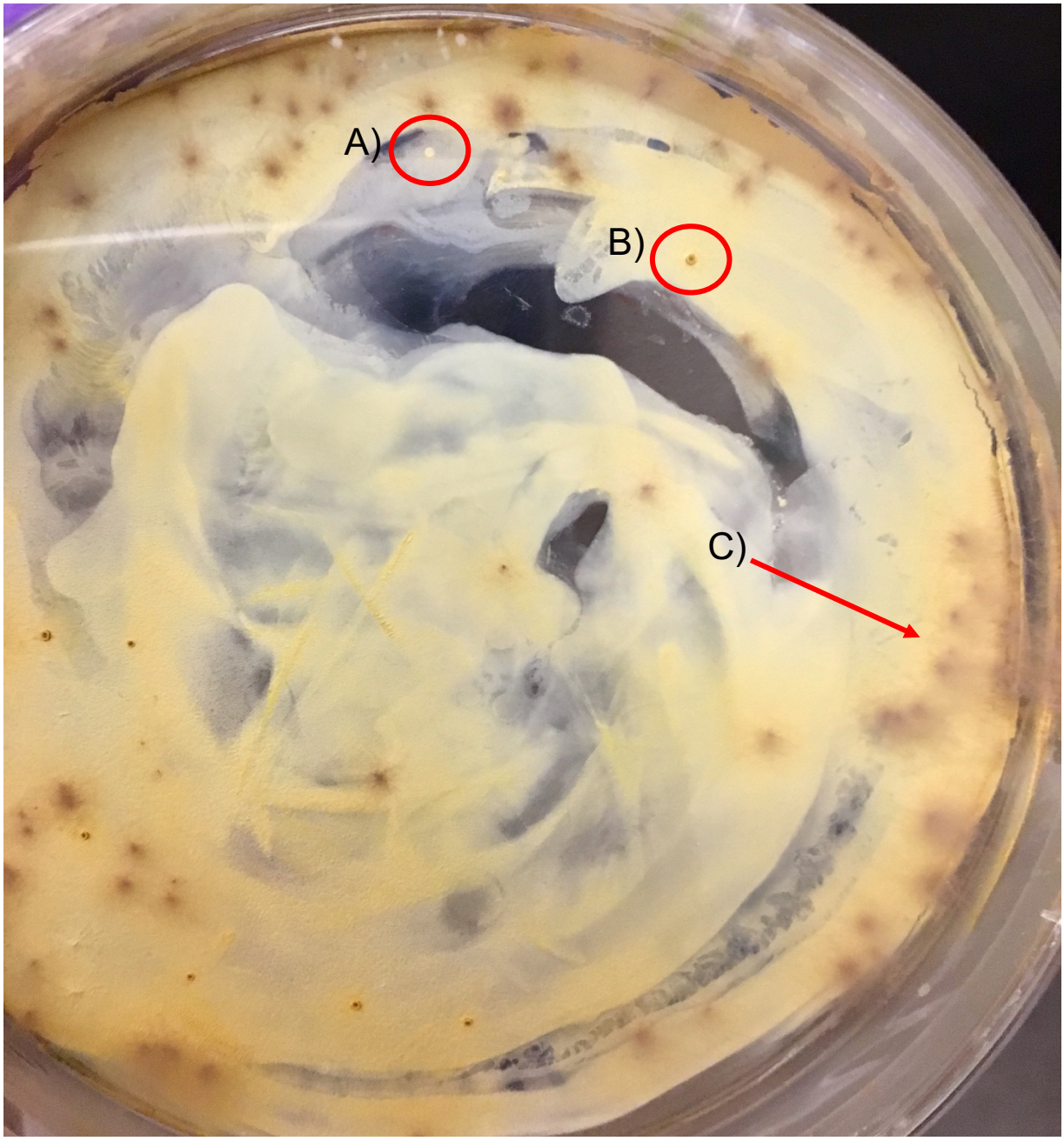

<u>Figure 2.5</u>: **Yellow** (A) **and red** (B) **colonies from BT that grew on FeTSB medium**. These colonies grew on bacterial lawns and were surrounded by small fluffy brown fungal colonies. The formation of aerial hyphae by the latter can be observed in this photo around the edge of the plate (C).

Table 2.4: **Morphology of BT and ECT colonies that were sent for Sanger sequencing**.

Colony	Medium	Size	Shape	Elevation	Margin	Color + Opacity	Surface
ECT1	FeTSB	Very small	Circular	Flat	Entire	Opaque light orange	Smooth and dull
ECT1	FeTSB	Small	Circular	Raised	Entire	Opaque orange	Smooth and dull
ECT3	FeTSB	Small	Circular	Raised	Entire	Opaque red	Smooth and dull
ECT3	FeTSB	Small	Circular	Raised	Entire	Opaque red	Smooth and dull
BT1	FeTSB	Small	Circular	Raised	Entire	Opaque dark orange	Smooth and shiny

identifications were obtained from forward and reverse sequences. Given the length of the sequences and Phred scores below the recommended value of 40, consensus sequences were not assembled (Appx. C). As demonstrated in Table 2.5, these were for an ECT colony on modified ISP medium and ECT3 on FeTSB medium (Appx. C).

Fungal growth was only observed on BT plates. Filamentous colonies on FeTSB plates were relatively small, circular and were brown with a darker circle in the center. Fe^{3+} did not appear to cover these colonies as previously described with the BWR fungus. On ISP medium that demonstrated less apparent bacterial growth, grey colonies were larger and more irregular in shape as well as were covered in Fe^{3+}. Black mold also grew on some of these plates (Figure 2.6). Plates that were discarded had colonies which had cottony/woolly textures with "fluffy" aerial mycelium that rapidly covered the plates. A total of 5 plates with selective media (both SM and ISP mod.) contained only visible fungal colonies that did not display Fe^{2+} oxidation following one year since inoculation. These were irregular in shape, of various sizes, grey in color and had filamentous margins. Some plates had smaller colonies that were scattered whereas others had only a couple large colonies that nearly covered the whole plate (Figure 2.7).

2.5 Discussion

2.5.1 Low-sulfur waste rock enrichment culture

Despite using low-carbon media selecting for acidophilic Fe^{2+}-oxidizers, substantial fungal growth was observed in most of the cultures. The solidifying agent in solid media provides an additional source of carbon, but visible fungal biomass appeared quickly in

Table 2.5: **Preliminary identifications obtained for ECT colonies**. Alignments of forward and reverse reads were not successful therefore the sequences were individually queried against the NCBI database using BLAST. We were unable to obtain identifications for the other colonies listed in Table 2-2 due to the low quality of the sequences. NCBI Accession numbers for the most similar sequences are provided.

Colony	Sequence Direction	Sequence Size (bp)	Most Similar Sequences in NCBI Database	Query Cover	Percent Identity	Accession Number
ECT on ISP mod.	Forward	331	Uncultured bacterium clone E07 627 Jing	96%	72.76%	KJ023499.1
			Uncultured bacterium clone F10 642	96%	72.76%	KJ023498.1
	Reverse	508	Uncultured gamma proteobacterium	70%	74.93%	FR670390.1
			Uncultured bacterium clone EA10-13s22	71%	74.73%	HQ899717.1
ECT3	Forward	591	*Candalkalibacillus thermarum* strain HA6	100%	94.08%	NR_043169.1
			Bacillus sp. TX3	100%	94.08%	AB043863.1
	Reverse	512	*Candalkalibacillus thermarum* strain HA6	100%	89.45%	NR_043169.1
			Bacillus sp. TX3	100%	89.45%	AB043863.1

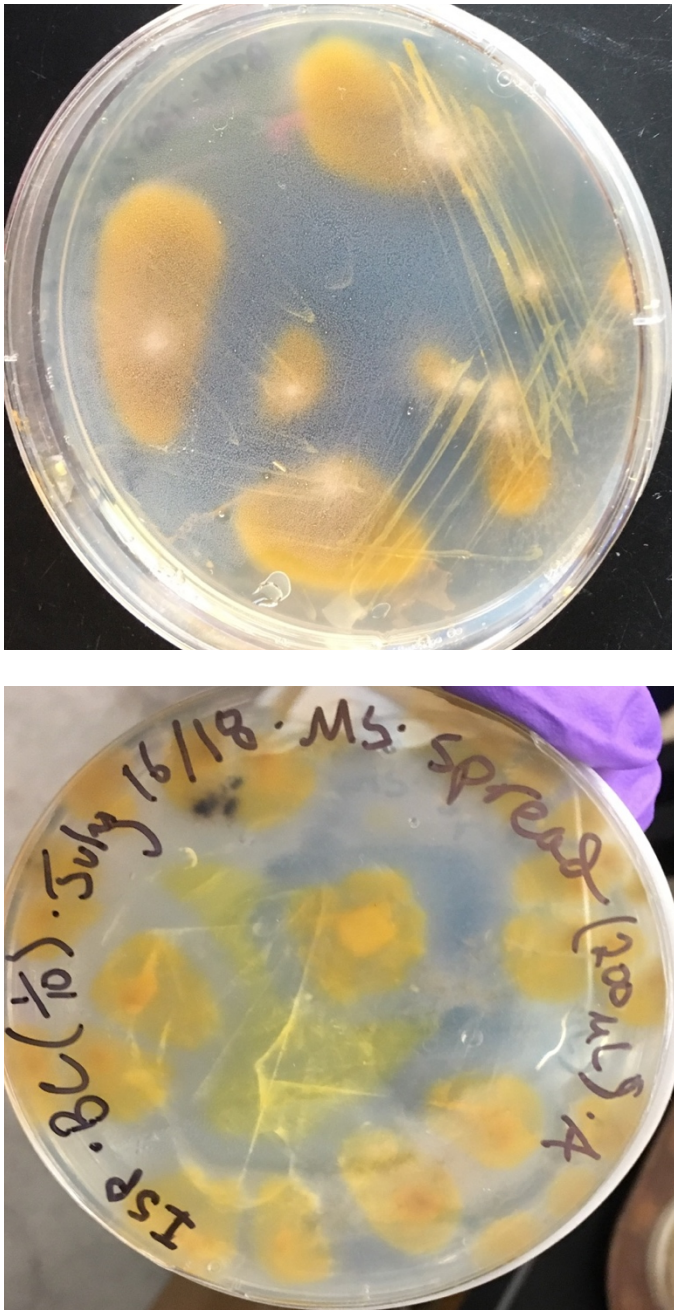

<u>Figure 2.6</u>: **Different fungal colonies observed from the BT culture when growing on FeTSB medium** (top photo) **and ISP medium** (bottom). Small brown colonies were the third type of observed morphology when grown on FeTSB medium as shown in Figure 2-5.

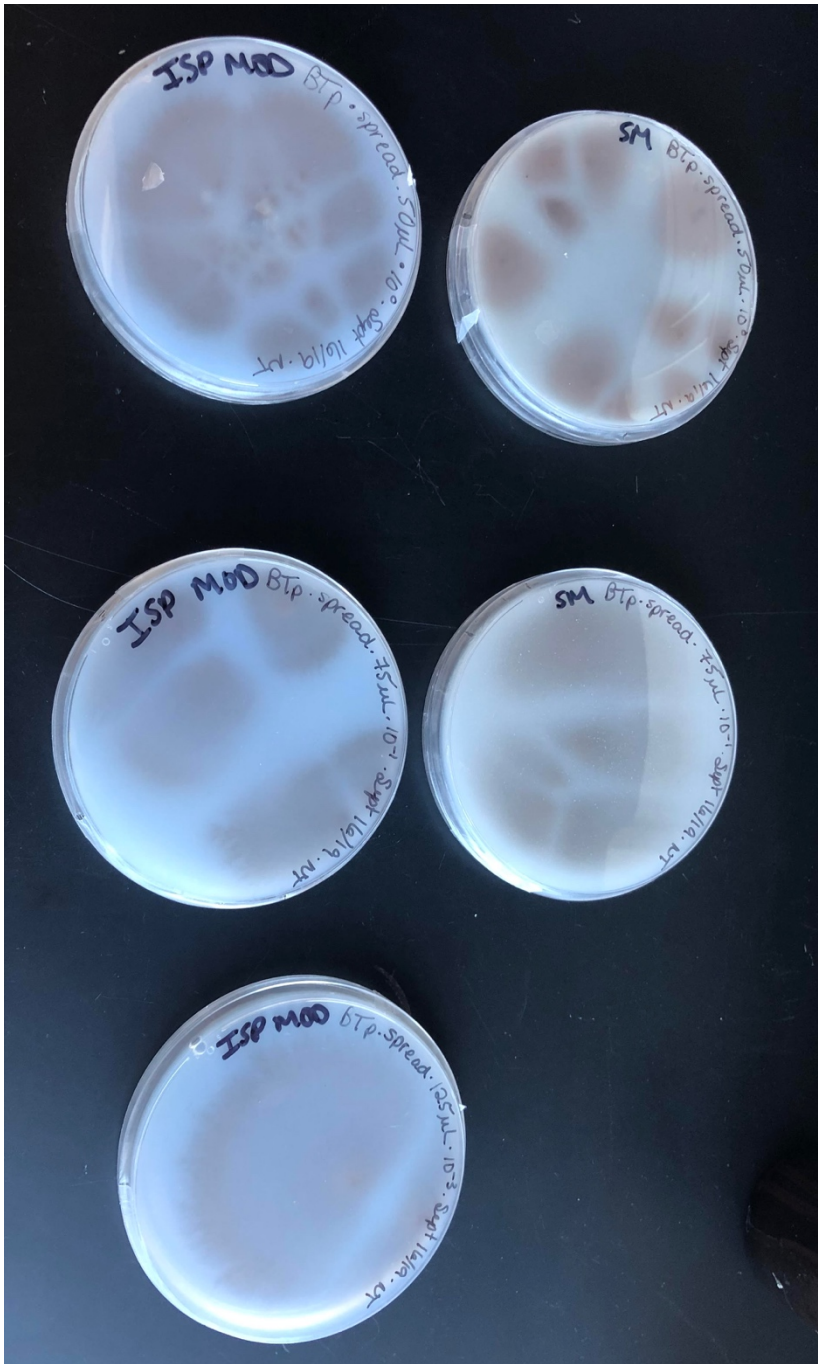

<u>Figure 2.7</u>: Fungal colonies on solid media selecting for *Leptospirillum* spp. and *Sulfobacillus* spp. These were the only fungal colonies with this morphology that did not visibly oxidize Fe^{2+}.

liquid cultures as well. These results are similar to the experiment by Glukhova et al. (2008) that tried to isolate sulfide-reducing bacteria. Fungi, including some species of *Penicillium*, are fast growers and can proliferate over a wide range of pH values (Glukhova et al., 2008; Soo Park et al., 2019). This gives them a competitive advantage over slow-growing chemolithotrophs when provided with limited nutrients such as in laboratory cultures.

Maturation of the fungal colonies on solid media was relatively consistent with the morphology of *Penicillium* colonies. They often start off white in color and mature into flat filamentous colonies that can become blue-green or gray-green (Larone, 1995; St-Germain & Summerbell, 1996). We observed that colonies either remained white or turned grey with darker, almost black, spots that were concentrated in the ageing zone and became more diffuse towards the white fruiting zone. The findings that colonies remained small, some even punctiform, and white may suggest that colony maturation was negatively affected either from high Fe^{2+} concentrations, low organic carbon, or low pH. These observations are consistent with the findings by Deng et al. (2014) that mycelial colonies exposed to bioleaching had smaller lengths and diameters than control samples. Dark pigments are typically associated with the production of melanin, and *P. chrysogenum* has been found to produce pyomelanin when grown in tyrosine-containing minimal salts medium (Lujan et al., 2016; Vasanthakumar et al., 2015). This pigment is typically produced to help fungi survive in adverse conditions but Vasanthakumar et al. (2015) documented that fungi ceased to produce the pigment once grown in medium without tyrosine, whereas we observed that dark pigmentation was more pronounced when the fungus was grown on minimal salts medium without Fe^{2+}. *Penicillium* spp. do typically form dense felts of conidiophores and conidia can appear as shades of grey which could explain these observations (Bullerman, 2003). There have also been reports of heavy metals causing discoloration in fungi

(Baldrian, 2003). Reduced colony size and discoloration similar to the results from this study were observed by Mohammadian Fazli et al. (2015) when exposing *Terichoderma* sp. to 200 mg/L of cadmium. However, it is important to consider that these results are not accurate identifiers since standard media for the growth of *Penicillium* should be used for this purpose, which include Czapek Yeast Autolysate agar (CYA) and Czapek Malt Extract Agar (MEA, Oxoid) (Visagie et al., 2014). Even the brand of agar used for culturing has been documented to influence the appearance of colonies, and no information was found in the literature about the cultivation of fungi using gellan gum (Visagie et al., 2014).

There were noticeable differences in patterns of Fe^{3+} precipitation on and around fungal colonies that grew on FeTSB and ISP plates. There seemed to be less Fe^{2+} oxidation on ISP plates considering that fungal mycelia were still visible as opposed to being densely and fully covered on FeTSB plates. Accumulation of Fe^{3+} on this medium was hard to interpret since some colonies appeared to accumulate the metal in the aging zone, others mainly in the fruiting zone and some accumulating mainly in both of these areas. Additionally, some colonies had halos of oxidation that remained on the medium surrounding them. It is possible that these two types of media selectively enriched different fungal organisms, but colony morphology did not seem to differ, suggesting it was at least the same genus. Both types of media contained 10 g/L of $FeSO_4 \cdot 7H_2O$ and had pH values between 2.0-2.5. The biggest difference was the small amount of glucose provided from the minimal amount of tryptone soya broth in FeTSB which may have been the largest inhibitor of growth and Fe^{3+} accumulation. Glukhova et al. (2018) used Czapek medium that contained 40 g/L of yeast extract to screen tolerance to arsenical compounds and heavy metals by *Penicillium spp.* They reported that the colonies were greenish in color and they did not report that heavy metals were inhibitory for fungal growth (Glukhova et

al., 2018). Deng et al. (2009) found that *P. chrysogenum* most likely extracts heavy metals via acidolysis and chelation due to the increased production of organic acids from the TCA cycle. Tianwei & Cheng (2003) also describe the biosorption of metals by *P. chrysogenum* which includes chelation via chitosan in the mycelium. These findings indicate that *Penicillium* sp. in this study can likely utilize both mechanisms of passive biosorption and active accumulation, and that an increase in organic carbon availability may be contributing to a rise in the production of organic acids. This could explain why it appears as though more Fe^{3+} is precipitated on fungal colonies from FeTSB plates. Halos of oxidation around small white colonies suggested that these colonies may have secreted minimal amounts of metabolites. It is expected that they'd at least excrete protons to maintain intracellular homeostasis in acidic conditions. Another possibility could be that FeTSB supports bacterial growth along with the fungus better than ISP, and that the increased amount of precipitated Fe^{3+} on fungal colonies was caused by Fe^{2+}-oxidizers growing in the mycelia. To assess these theories, Fe^{2+} oxidation by *Penicillium* sp. should be assessed by modifying Czapek medium to be acidic and to contain iron. Gellan gum contains minimal carbon, therefore ISP plates would serve as a great comparison.

We wanted to rule out that chemolithotrophic bacteria were causing Fe^{2+} oxidation therefore we tried to completely inhibit bacterial growth by inoculating FeTSB plates that did not contain Fe^{2+} (TSB). As expected, no bacterial growth was observed. To ensure that bacterial organisms would be eliminated, we waited 5 months before transferring inoculum back into Fe^{2+}-containing medium. However, spore formation was observed by microscopic analysis and the ability to sporulate has been documented for *Alicyclobacillus* spp. as well as one species of *Ab. ferrooxidans* to date, SLC66 (Ciuffreda et al., 2015; Holanda et al., 2016). Doing so would have provided the bacterium with a means to survive while on medium devoid of Fe^{2+}

once glucose concentrations had quickly been depleted by the fungus. We expected that transferring fungal inoculum from the TSB plate into FeTSB and ISP media would at least cause a lag time in Fe^{2+} oxidation, but it occurred faster than with any other culture in this study and Fe^{3+} precipitation remained substantial. It is possible that this was induced by the bacterial organism considering that ribosomes have been found to be rapidly activated once germination is initiated, but this short lag phase has not been observed with any other bacterial organism in this entire study and would be surprising from a slow growing chemolithotrophic organism (Lior et al., 2014). These results could potentially indicate an acute stress response by the fungus induced by re-exposure to the metal, either to tolerate it or potentially to accumulate it, since it would not have had access to this micronutrient on TSB medium that did not contain any assimilable iron at all. Selecting the fungus would have probably been more successful by ensuring it would dominate with the use of modified Czapek medium that contained micronutrient concentrations of iron.

The presumed isolated bacterial culture did not contain any visible fungal growth and absence was supported on solid medium. One distinguishable difference was that this entire plate was entirely covered by a halo of oxidation whereas the other two were not. This could therefore potentially be an indicator of bacterial growth. Fe^{2+} oxidation visibly began in F and BF cultures which indicated that this precipitation could have been induced by the fungal organism. The timing was also consistent with other fungal cultures in this study as opposed to longer lag phases that were observed with bacterial cultures. It was difficult to determine if the BF culture contained bacterial cells. This culture showed no sign of a bacterial lawn under the fungal colonies, and the only main difference that could indicate bacterial growth was the halo of oxidation which covered half of the plate. It was also very difficult to interpret patterns of Fe^{2+}

oxidation and Fe^{3+} accumulation. We could not explain the reason why fungal colonies around the halo of oxidation on BF did not accumulate any Fe^{3+} on their mycelium. Further work should assess why precipitates clustered in different areas of the fungal colony considering iron concentrations should have been homogeneous throughout the plate and metal-chelating groups are present in the walls of each cell. Glukhova et al. (2018) found that *Penicillium* sp. had different tolerance mechanisms depending on the metal. Most of them formed clusters of precipitates on the mycelium and extracellular vacuoles were synthesized on the mycelium to store copper when grown in medium containing this metal (Glukhova et al., 2018). Smaller amounts of precipitates were observed in the F and BF cultures that suggested metal accumulation by fungal biomass. This is supported by the fact that the biomass was initially white and became increasingly orange in color.

The cultures F and BF displayed different fungal morphology. Dimorphism has been reported in species of *Penicillium* such as *P. chrysogenum* that can exhibit several morphological forms when submerged in liquids that range from dispersed hyphae to the formation of pellets (Veiter & Herwig, 2019). Many factors have been reported to influence the formation of fungal pellets including agitation rate, availability of nutrients, pH value, and inoculum size (Liu et al., 2007). Of these factors, the only one which could have varied substantially was the inoculum size. The aggregation of fungal cells is induced by hydrophobin proteins that are located on the surface of cells, which drive the formation of pellets via inter-cellular adhesion forces (Siqueira & Lima, 2012; Veitner et al., 2018). This was consistent with the agglomeration of fungal cells to some degree in all liquid cultures. These hydrophobic interactions in combination with electrostatic interactions allow bacteria to attach to the surface of fungal cells which could be possible in BF, forming bacterial-fungal pellets (Siqueira & Lima,

2012). Fungal pellets have been found to be less productive and complicate biotechnological processes (Veiter & Herwig, 2019). Access to O_2 and nutrients is limited in the densely packed core therefore activity becomes restricted to the external hairy region of intertwined hyphae (Veiter et al., 2018). This was supported by the findings that less densely packed agglomerates of fungal biomass in the F culture were a substantially darker orange color than the light orange pellets in BF, indicating that more precipitated Fe^{3+} had been adsorbed onto the fungal biomass in the F culture.

The ITS gene sequences from samples of the fungal isolate on solid and liquid FeTSB medium were identified as being most similar to sequences from *Penicillium* species, such as *P. albidum* strain CBS and *P. daleae* strain CBS. The other top hit, *Penicillium* sp. isolate TTC172 was isolated using iron-containing medium as part of a study on heavy metal tolerant fungi in surface soils of a temperate pine forest (Torres-Cruz et al., 2018). Identification was also the same for the BF culture. These results support with confidence that the fungal organism is a species of *Penicillium* that may be heavy metal tolerant. The length of the ITS region can be variable in fungi but considering the top BLAST hit was 806 bp, we managed to obtain over half of the sequence which provides strong evidence that the genus identification is correct. Obtaining the complete sequence of the ITS region could potentially alter results of species identification. In addition, results from microscopic morphology were consistent with this genus considering the findings of septate mycelium and the production of conidiophores (Visagie et al., 2014).

It was much more challenging to obtain an identification for the bacterial organism, but we managed to do so for one colony on solid medium. The percent ID was initially quite low due to the assignment of many degenerate bases following assembly of the consensus

sequence. These mixed base calls were compared with the most similar sequences in the NCBI database in order to assign a putative base call when the degenerate base corresponded with the base at that position in the most similar sequences, and otherwise the degenerate base was left as a "N". By doing so, the percent ID increased to just above 90%. Aside from uncultured isolates, identifications remained consistent with top hits belonging to *Alicyclobacillus.* sp. BGR 73 and *Ab. ferrooxidans* SLC66. All of these organisms were acidophilic Fe^{2+}-oxidizers obtained from high-grade metal ore and bioleaching systems (Breuker et al., 2009; Holanda et al., 2016). These results were consistent with the microscopic observations of Gram-positive bacilli. This colony was cultured in FeTSB, but both *Alicyclobacillus* spp. and *Acidibacillus* spp. have been described by multiple studies to prefer yeast extract as a complex carbon source, which was absent in this medium (Holanda et al., 2016; Nancucheo et al., 2016). Increased cell concentrations of the bacterial organism would have likely been obtained if media containing yeast extract would have been utilized for cultivation. However, doing so would have likely also increased fungal growth.

The failed amplification of the 16S rRNA gene for the BF culture indicated that the bacterial organism may not be present, at least not in detectable numbers. These results support the observation that Fe^{2+} oxidation can be induced by the fungal organism.

2.5.2 Bioreactor enrichment cultures

Cultures of the ECT sample only displayed bacterial growth whereas fungal growth from the BT sample often consumed the plate. The brown fungal colonies did not appear to accumulate Fe^{3+} but mycelia from grey colonies were covered as described with BWR. Many grey colonies did not remain flat and instead produced fluffy aerial hyphae. This could have been

caused by an increase in cell concentrations either in the culture or due to a larger inoculum size on the plate. However, the increased production of aerial hyphae has been observed in *S. commune* when it was transferred on solid medium containing cadmium (Baldrian, 2003).

The proliferation of bacteria on solid media seemed to be more successful when the amount of inoculum was increased and was undiluted. This however often caused the fungus to take over the plate making the isolation of bacterial colonies difficult. The increase of bacterial cell concentrations across the surface of the medium was helpful in obtaining colonies from these organisms, and multiple colonies formed on FeTSB and ISP media.

Growth appeared to be successful in liquid genus-level selective media, but the opposite was observed on solid media. Only one modified ISP plate displayed minimal bacterial growth including a colony. Other ECT plates did not have any growth, and BT plates either had excessive fungal growth or no growth at all. Greyish-brown colonies on these plates generally had larger diameters suggesting a lower inhibition of growth. Fe^{2+} oxidation was not observed on these plates, even on modified ISP medium that was identical to ISP, other than having a pH value below ~1.8 and 0.2% more gellan gum. These findings indicated that the fungus is able to grow despite increased acidity, but the fungal colonies did not oxidize Fe^{2+}. Bacterial oxidation was substantially lower than all of the other cultures in this study as well, which suggested that a factor which inhibits microbial growth must have been introduced when producing these selective types of solid media. We know that the solidification of gellan gum was affected at pH 1.8 and that increasing its concentration by 0.2% helped. Such problems have been reported with agar plates at pH 3 and doubling the concentration of both the solidifying agent and of basal salts has been suggested. The increased amount of salts in SM medium may have helped with buffering acidity which would explain why these solidified better than modified ISP plates. No

information was found about making any type of solid medium at pH values lower than 2.0, but pH 1.8 may be close to the stability limit of gellan gum. Carbohydrates can be hydrolyzed into toxic by-products when autoclaved, especially when acidified (de Lange, 1989). It is therefore suggested to autoclave the unacidified solidifying solution separately from the basal salts solution, and to adjust the pH following sterilization. This is what we did, but gellan gum solidifies much quicker than agar therefore the solidifying solution was mixed into the acidified basal salts solution while they were still very hot. The presence of an additional toxic substance could also explain why the fungus on these plates did not oxidize Fe^{2+}.

It is also possible that bacterial growth would have required more time considering additional growth, including colonies, was observed on the initial FeTSB and ISP plates 2 years after inoculation. Long lag times and slow growth are factors that increase the difficulty of isolating chemolithotrophic bacteria, and which indicate that the process to obtain purity (sub-culturing an isolated colony at least 3 times) for these types of organisms can take longer periods of time.

This was further supported by the failure to obtain identifications for most BT and ECT colonies that were extracted and sequenced. The low confidence of assigned bases for these sequences was likely induced by the presence of DNA from multiple organisms. Considering that most of the colonies had only been sub-cultured once prior to extraction and that the ECT colony on modified ISP had not been sub-cultured, it is reasonable that the colonies were not pure and additional work is required to complete this process (Shrestha et al., 2013). Morphology of the sequenced ECT colony on modified ISP was consistent with small flat yellow colonies of *Leptospirillum* spp., but the most similar sequences to the one from the ECT colony on this medium were from uncultured chemolithotrophic bacteria isolated from low-carbon and extreme

environments including lava flows in Iceland and deep subsurface sediments, which was consistent with the types of bacteria that we expected would be present in these samples (Chen et al., 2014; Crépeau et al., 2011; Dong et al., 2014; Kelly et al., 2014). Morphology of ECT3 on FeTSB was relatively consistent with "fried egg" shaped colonies of *Sulfobacillus* that are orange in the center, and the most similar 16S rRNA gene sequences included those from *Candalkalibacillus thermarum* strain HA6 and *Bacillus* sp. TX3. The former is a spore producing Gram-positive rod that is aerobic and organotrophic (Xue et al., 2006). Like *Sulfobacillus* spp., this organism is thermophilic with optimal growth at 60 °C, but it is characterized as alkaliphilic growing optimally at pH 8.5 (Xue et al., 2006). The second top hit, *Bacillus* sp. TX3, was also isolated as part of a project cultivating thermophilic and alkaliphilic species from the Bacilli class (Nogi et al., 2000). Further work is required to isolate and identify these colonies, as well as to isolate colonies from the target genera *Leptospirillum* and *Sulfobacillus*.

2.6 Conclusion

The goal of this study was to isolate and describe microorganisms from enrichment cultures of mixed metal sulfidic waste material. Using media selecting for acidophilic heterotrophic Fe^{2+}-oxidizing bacteria, substantial fungal growth and Fe^{3+} precipitation was observed from the enrichment culture of low-sulfur waste rock. By repeatedly passaging this culture, we were able to isolate a bacterial colony that was identified as an Fe^{2+}-oxidizing bacterium which was most similar to *Alicyclobacillus* sp. BGR 73 and *Ab. ferrooxidans* SLC66 (16S rRNA genes). The fungal organism was identified repeatedly as *Penicillium* sp., and these identifications were consistent with macroscopic colony morphology

as well as microscopic cell characteristics. All of these organisms have been associated with Fe^{3+} precipitation in AMD systems, and their potential in bioremediation as well as bioleaching applications has been of interest. However, our understanding of them remains incomplete, especially for the relatively novel *Ab. ferrooxidans* strains and for acidophilic *Penicillium* spp.

Results suggested that the bacterium grew best when the fungus was present as well as supported with confidence that the fungus was contributing to the oxidation of Fe^{2+} and was bioaccumulating Fe^{3+}. These observations were supported by the knowledge that *Penicillium* species are efficient at extracting metals and immobilizing them.

We started isolating bacterial colonies from the bioreactor enrichment cultures, but further passaging of these BT and ECT cultures is required to obtain pure colonies and reliable identifications. Putative identifications obtained for 2 ECT colonies supported that these organisms could be chemolithotrophic and thermophilic bacteria of the genus *Bacillus*. Solid selective media to isolate the genera *Leptospirillum* and *Sulfobacillus* were found to likely require optimization. Fungal growth from the BT culture was observed on all types of media, and 3 different colony types were suspected to be present due to differences of morphology when grown on solid medium. As seen with BWR, oxidation of Fe^{2+} and precipitation of the metal onto fungal mycelia was observed for some BT colonies.

This study provides additional insight about these organisms. Our findings support that fungi are competitive organisms that are ubiquitously found in acidic and metal-rich environments, and that at least one species which was observed likely contributes to iron oxidation as well as accumulation. Metal leaching could potentially be improved with mixed cultures of bacteria and fungi such as those assessed in this study, and the use of fungal mycelium as a biosorbent could facilitate the metal recovery process.

CHAPTER 3:

GENOMIC DESCRIPTIONS OF *ACIDIBACILLUS FERROOXIDANS* NOWR-5 AND *PENICILLIUM* SP. FROM AN ENRICHMENT CULTURE OF LOW-SULFUR WASTE ROCK

3.1 Abstract

Genomic descriptions can provide substantial insight about organisms that reside in AMD in order to assess their roles in these systems and their potential in biotechnological applications. The acidophilic Fe^{2+}-oxidizing bacterium, *Acidibacillus ferrooxidans*, is a newly described genus and species for which additional analyses are required to complete the annotation of draft genomes as well as to understand this organism's metabolic abilities. In AMD environments, many aspects of fungal physiology, such as metal resistance, are also not well understood. In this chapter, I describe findings from sequencing, assembling, and annotating the genomes of a bacterium and a fungus that were isolated from enrichment cultures of low-sulfur waste rock. These were identified with confidence to be a strain of *Ab. ferrooxidans*, that we designated NOWR-5 for this study, and *Penicillium* sp. Gene annotation supported that the bacterial organism was a metal-tolerant heterotrophic acidophile, and genes from various subsystem categories were identified that have not been annotated or described in existing draft genomes, such as *nar* genes encoding enzymes for respiratory nitrate reduction. However, none of the identified genes could be confidently associated to the respiratory Fe^{2+}-oxidation pathway. The identification of fungal multicopper oxidase-encoding genes supported that the fungus from BWR has adapted to metal rich environments, and these enzymes could potentially be oxidizing divalent cations such as Fe^{2+} and Cu^{2+}. Findings from this study provide insight into the relatively uncharacterized genomes of *Ab. ferrooxidans* and acidophilic *Penicillium* spp.

3.2 Introduction

There is significant interest in the optimization of bioleaching technologies as it provides a more sustainable and cost-effective method to extract and recover metals from low-grade reactive mine waste materials that could contaminate the environment (Gross & Robbins, 2000). Microorganisms which are natural inhabitants of the waste material to be leached have been documented to perform most effectively in some cases (Van der Gast et al., 2004). For this reason, their identification is important so that those which are best suited for the application can be selectively enriched, and an understanding of their requirements for maximum growth and activity will provide insight into the conditions that should be provided throughout the operation process for maximized leaching efficiency (Norris et al., 2000).

High-throughput sequencing allows for the assembly of draft or complete genomes and for the speculation of roles that different organisms have, some of which may be contributing directly or indirectly to the leaching process (Quatrini et al., 2007). Comparing newly sequenced genomes to others found in publicly available databases, such as those from phylogenetically similar organisms, can assist in making assumptions about protein functions and can provide insight into differences in metabolic abilities between closely related species (Quatrini et al., 2007).

Studies often focus on mechanisms of energetic metabolism considering its direct relation to bioleaching but have also analyzed genes with speculated involvement in metal resistance, quorum sensing, and the production of extracellular polysaccharide precursors for the formation of biofilms (Jerez, 2008; Valenzuela et al., 2006). The diversity of bacterial genetics and physiology found in AMD environments as well as the metabolic plasticity that these

organisms exhibit to ensure survival in such extreme conditions have been recognized (Dall'Agnol et al., 2016; Quatrini et al., 2007).

The metabolic mechanism of Fe^{2+} oxidation is best understood in *At. ferrooxidans* (Johnson & Hallberg, 2009). There have been two main types of electron transfer models that have been proposed, but the one which has been supported by many studies is: $Fe^{2+} \rightarrow$ Cyc2 $\rightarrow$ Rus $\rightarrow$ Cyc1 $\rightarrow$ Cox $\rightarrow O_2$ (Zhan et al., 2019). Genes have been documented to be organized in operons such as those in the Rus operon as described by Zhan et al. (2019). Other genes that have been speculated to be involved in Fe^{2+} oxidation in *At. ferrooxidans* are described by Quatrini et al. (2009). Zhan et al. (2019) and Levican et al. (2002) describe complexes and proteins involved in the uphill pathway to synthesize NAD(P)H. Although information on the Fe^{2+} oxidation mechanisms in other acidophiles is limited, it is known that differences exist from those which have been documented in *At. ferrooxidans* (Johnson & Hallberg, 2009). For instance, key proteins that have been associated with Fe^{2+} oxidation in *Leptospirillum* spp. include cytochrome 572 and cytochrome 579 (Chen et al., 2014).

Heterotrophic bacteria are unique since they can use more than one of several pathways for the oxidation of glucose (Jurtshuk Jr., 1996). Alternatives to the Embden-Meyerhof-Parnas (EMP) pathway are presented by Flamholz et al. (2013). A pathway that is ubiquitously found in combination with these two glycolytic pathways is the pentose phosphate (PP) pathway. (Shuttleworth et al., 2005; Soderberg, 2005). The glyoxylate shunt is a variant of the TCA cycle which skips the steps that generate CO_2 to conserve carbon atoms (Ahn et al., 2016).

To date, there are six metabolic pathways that have been described for autotrophy (Bender et al., 2011). Enzymes which catalyze distinctive steps in these pathways are conserved,

and their presence in an organism's genome strongly suggests that the associated metabolic pathway is active (Berg, 2011). Evidence has suggested that certain microorganisms may be able to switch between using the Calvin-Benson-Bassham (CBB) or reverse tricarboxylic acid (rTCA) cycles (Campbell & Cary, 2004).

The ability to maintain a neutral intracellular pH is due to membrane impermeability and cation efflux systems that have been found to be encoded in all sequenced acidophile genomes (Baker-Austin & Dopson, 2007). Microorganisms found in AMD strictly maintain metal homeostasis and they have developed various defenses against high concentrations of toxic elements (Arguello et al., 2013; Lewinson et al., 2009; Moller et al., 2014; Suzuki et al., 1998).

Alicyclobacillus spp. of the Firmicutes phylum, are a commonly documented group of heterotrophic acidophiles (Johnson & Hallberg, 2009). They are Gram-positive organisms which can produce resistant spores (Ciuffreda et al., 2015). A total of 17 *Alicyclobacillus* species have been discovered, and many of them were isolated from hot springs in Yellowstone National Park (Johnson & Hallberg, 2009). Some species, including *Alb. ferrooxidans*, are mesophilic whereas others, like *Alb. sulfuroxidans*, are moderately thermophilic (Nancucheo et al., 2016). Many *Alicyclobacilli* are mixotrophic being able to utilize both organic and inorganic substrates for energy, but they require a complex organic carbon source such as yeast extract, which has been found to be preferred by these organisms (Nancucheo et al., 2016). Fe^{2+} and RISCs are electron donors that they have been documented to use, and growth using Fe^{3+} as an electron acceptor in anaerobic conditions has been observed in a few isolates (Johnson & Hallberg, 2009). Optimal pH for growth varies with different species (Nancucheo et al., 2016). *Alb. acidocaldarius* was isolated from Yellowstone National Park and

is characterized as strictly preferring aerobic conditions (Tianli et al., 2014). It is a thermophilic acidophile which grows optimally in temperatures of 45-70 °C and at pH values between 2-6 (Tianli et al., 2014).

The most recent genus of acidophilic Firmicutes described is *Acidibacillus* which was isolated from mine waste material (Nancucheo et al., 2016). Two species have been distinguished which include the mesophilic and acidophilic *Ab. ferrooxidans* that grows optimally at pH 2.9 and 30 °C, and the moderately thermophilic *Ab. sulfuroxidans* that grows optimally at pH 1.8 and 43 °C (Nancucheo et al., 2016). The former can use Fe^{2+} oxidation for energy whereas the latter can use Fe^{2+}, S^0, as well as tetrathionate, and both can use Fe^{3+} as an electron acceptor from the oxidation of organic carbon when O_2 is not available (Nancucheo et al., 2016). However, just like *Alicyclobacillus* spp., a source of organic carbon is required, and yeast extract is preferable (Holanda et al., 2016). The first strain isolated was *Ab. ferrooxidans* SLC66^T and the draft genome of a second existing strain, *Ab. ferrooxidans* ITV01 was announced a year later which came from an acidic stream that was draining from a pile of low-grade chalcopyrite ore (Dall'Agnol et al., 2016). Holanda et al. (2016) highlighted that *Acidibacillus* species may be widely distributed in acidic environments and that they may have potential for use in bioleaching consortia since they can oxidize Fe^{2+} as well as remove inhibitory Fe^{3+} and organic carbon substrates. Knowledge about these organisms to date includes that they appear to have a gene which is related to the one that transcribes the blue copper rusticyanin protein, and that they do not have the ability to fix N_2 (Holanda et al., 2016). Studies are still required to confirm whether they would in fact be beneficial to use in industrial applications (Holanda et al., 2016).

As emphasized by Kanti Das et al. (2008), the metabolic analysis of fungi in

AMD is required to analyze their potential for remediation. The use of enzymes and metabolites produced by fungi in AMD for bioremediation of contaminated sites has been proposed (Hujslova et al., 2016). Genes of interest include those for the tolerance of heavy metals and extreme acidity, their carbon sources, and active mechanisms of accumulation such as metal uptake, proton pumps, reduction reactions, and the secretion of secondary metabolites with metal-complexing abilities (Guibal et al., 1995; Kanti Das et al., 2008; Siegel & Speitel, 1975). Glukhova et al. (2018) reported working on a transcriptomic analysis of the *Penicillium* isolates which they obtained from metal-rich water at a mine site in order to understand their resistance to high copper and arsenic concentrations.

This chapter focuses on the annotation of genes that were sequenced from a prokaryotic genome and from a fungal genome. These organisms, which evidence suggests is a strain of *Ab. ferrooxidans* or *Alb. acidocaldarius* and a fungus belonging to the genus *Penicillium*, grew together while attempting to isolate bacterial colonies from a sample of low-grade sulfidic ore that was obtained as part of a bin leaching experiment (Valiquette, 2018). The description of genes and pathways were mainly focused on the prokaryotic organism to gain understanding of mechanisms including (i) dissimilatory pathways for inorganic and organic substrates, (ii) metal homeostasis and resistance, (iii) maintenance of intracellular pH and responses to other stressors, (iv) sporulation and dormancy, and (v) biofilm formation. These results were compared to a few draft genomes available in public databases that were from the closest phylogenetic relatives. The metabolic description of the fungal organism served to gain some preliminary insight about how it is affecting metal transformations, such as the oxidation and precipitation of iron, as well as how it may be influencing bioleaching prokaryotes. Bacterial genes for Fe^{2+}-oxidation were expected to be identified in the data based on literature of this

acidophile and on Fe^{3+} generation from qualitative analyses (Chapter 2). It was hypothesized that the fungus would have genes for the production of chitin or chitosan, and that other genes for metal-chelating compounds would be identified to support the qualitative data that this organism was exhibiting Fe^{2+} oxidation and Fe^{3+} accumulation (Chapter 2). We expected to find stress response genes such as for metal resistance and maintenance of intracellular pH in both target organisms. We speculated that the analysis would support that the bacterium could be benefiting from the consumption of carbon or the formation of biofilms by *Penicillium* sp.

3.3 Materials and methods

3.3.1 Extraction and sequencing of DNA

We identified an acidophilic bacterium (*Ab. ferrooxidans/Alicyclobacillus* sp.) and a fungus (Penicillium sp.) from an enrichment culture of sulfidic mine waste (Chapter 2). Extractions were performed on bacterial colonies and on fungal mycelium using the Mobio Ultra Clean Microbial DNA Isolation Kit. DNA quantification as well as sample quality were assessed using the BioTek microplate spectrophotometer by measuring absorbance at a wavelength of 260 nm and 280 nm (Barbas III et al., 2007). PCR was performed to confirm successful amplification and appropriate band size of the amplicon. The bacterial 16S rRNA gene was amplified using the primer pair 27f (5'-ACAGTTTGATCMTGGCTCAG) (Lane, 1991) and 1492r (5'-GGTTACCTTGTTACGACTT) (Turner et al., 1999). The fungal ITS region of nuclear DNA was amplified using the primer pair ITS1 (5'-TCCGTAGGTGAACCTTGCGG) and ITS4 (5'-TCCTCCGCTTATTGATATGC) (Korabecna, 2007). Two samples of unamplified DNA, one containing DNA from a colony of the bacterial target organism (12 µL of 19.403 ng/µL) and one

containing DNA from fungal mycelium (12 µL of 10.586 ng/µL), were sent to Metagenom Bio for whole-genome shotgun sequencing. The former was labelled Metagenome 1 and the latter Metagenome 2.

DNA samples were shipped on dry ice to the National Research Council (Montreal, QC) where they were stored at -80 °C until they were processed. An ethanol precipitation and purification protocol was employed to concentrate nucleic acids and remove potential contaminants in the DNA samples. Following the manufacturer's procedure, the Quant-iT PicoGreen assay (Thermo Fisher, #P7589) was used to quantify purified DNA samples prior to shotgun sequencing. Libraries were created according to the manufacturer's instructions using the Illumina Nextera XT library preparation kit (FC-131-1024) from 2 ng of purified gDNA. A TapeStation instrument and High Sensitivity D5000 ScreenTape (Agilent, #5067-5592) were used to assess the quality of individual libraries, and library normalization was done by pooling equimolar amounts of libraries based on molarity values from the TapeStation analysis. Libraries were then sequenced on a HiSeq4000 system (Illumina) using the paired-end 100 bp configuration for 216 cycles.

3.3.2 Data processing and gene annotation

Quality of the raw reads was assessed using the FastQC (v. 0.11.8) software (https://www.bioinformatics.babraham.ac.uk/projects/fastqc/) (Brown et al., 2017). Paired-end mode trimming was performed on the reads using the Trim Galore wrapper tool (v. 0.6.4) (https://www.bioinformatics.babraham.ac.uk/projects/trim_galore/) around Cutadapt (v. 2.6) (Martin, 2011) (https://github.com/marcelm/cutadapt) with a Phred score cutoff of 30, and to specifically remove Nextera adapters that were present. The minimum required sequence length

for both reads was set to 20 bp. The successful removal of adapters was confirmed with FastQC before continuing with data processing. Contigs and scaffolds were assembled using the SPAdes (v. 3.14.0) (https://github.com/ablab/spades/releases) algorithm (Bankevich et al., 2012). We assigned taxonomic labels in the form of NCBI taxonomy to the scaffolds using the Kraken2 (v. 2.0.8-beta) (https://zenodo.org/record/3520272#.X-1hc2YZPPA) program, and prokaryotic genes were annotated using the Prokka (v. 1.14.0) (https://github.com/tseemann/prokka/milestone/2) software tool (Seemann, 2014; Wood & Salzberg, 2014). Bacterial contigs were additionally submitted to the Rapid Annotations using Subsystems Technology (RAST) and Metagenomic RAST (MG-RAST) to analyze gene annotations and to compare the data from these servers with annotations generated from Prokka (Aziz et al., 2008; Keegan et al., 2016). Preliminary results from binning the scaffolds of the metagenomic samples were obtained using MetaBAT 2 (v. 2.12.1) (https://bioconda.github.io/recipes/metabat2/README.html) and CONCOCT (v. 1.1.0) (https://github.com/BinPro/CONCOCT). Genome quality was assessed with the CheckM (v. 1.1.3) (https://anaconda.org/bioconda/checkm-genome) software (Parks et al., 2014). For fungal reads, taxonomic assignment and gene annotation were mainly performed using MG-RAST.

3.3.3 Phylogenetic analyses and genomic descriptions

I used BLAST (https://blast.ncbi.nlm.nih.gov/Blast.cgi) to identify the 16S rRNA genes that were annotated by Prokka from the contigs of Metagenome 1, and the one belonging to *Ab. ferrooxidans* was used for the phylogenetic analysis. The phylogenetic tree was constructed using the SeaView (v. 4.7) (https://packages.debian.org/buster/seaview) graphical user interface (Gouy et al., 2009). We added closely related sequences from NCBI to build an alignment and reconstruct a phylogenetic tree to understand these sequences' taxonomical

relationships. These sequences were from organisms that were identified as most closely related to the *Ab. ferrooxidans* strain obtained in this project, which included *Ab. ferroxidans* strain SLC66 and *Alb. acidocaldarius* subsp. *acidocaldarius* DSM 446. We used the PHYML (v. 3.1) (https://toolshed.g2.bx.psu.edu/repository/display_tool?repository_id=e3d7e14082eb4a6a&tool_config=%2Fsrv%2Ftoolshed%2Fmain%2Fvar%2Fdata%2Frepos%2F002%2Frepo_2263%2Fphyml.xml&changeset_revision=6dd988b4b760) software to estimate the maximum likelihood of the most likely phylogeny that fit the evolution model, Generalized Time Reversible (GTR) + Gamma distribution (G) + Invariant sites (I) and the aligned sequences. The tree showed confidence values ranging from 0.00-1.00 (equivalent to bootstrap values) (Guindon et al., 2005). The 16S rRNA gene sequence from a strain of *Geobacillus thermoleovorans* was used as an outgroup.

Genes identified in the data that we obtained for Metagenome 1 were compared to those in the draft genomes available on the Pathosystems Resource Integration Center (PATRIC) database, including *Ab. ferrooxidans* strain Huett2 (Genome ID: 1765683.8), *Ab. ferrooxidans* strain SLC66 (Genome ID: 1765683.11), and *Alb. acidocaldarius* subsp. *acidocaldarius* DSM 446 (Genome ID: 521098.5). The literature on what is known about the metabolisms of these bacteria and on the genes that were annotated by Prokka, combined with gene functions assigned by RAST and MG-RAST, were used to predict gene functions and attempt to describe the genome of the bacterium that we obtained. We implemented this protocol for the fungal genes that were annotated using MG-RAST. Specific gene sequences were queried against the NCBI database using BLASTn to acquire more information about which organisms possess similar sequences, and to assess assigned protein products.

3.4 Results

3.4.1 Metagenome 1: bacterial target

A total of 190 bacterial contigs were assembled with an average cover value of 14.03X. The largest contig (#1) was 502,177 bp with a coverage value of 13.72X. All of the contigs up to and including contig #9 were larger than 100,000 bp. Contig size dropped below 1,000 bp at contig #44 with substantially higher coverage values (17X-123X), and all contigs following #63 were very small (< 200 bp).

Kraken was able to assign an NCBI taxonomic label to 32 bacterial scaffolds. *Ab. ferrooxidans* was not labelled, and the only contig that was assigned to one of the most closely related organisms, *Alb. acidocaldarius* subsp. *acidocaldarius* DSM 446, was contig #3 (Table A.C-1). Most of the labels assigned belonged to the family *Bacillaceae*, in which the genus *Acidibacillus* is classified. The label "Homo sapiens" was given to scaffolds #16, 17, 169, 185, 187, and 176-178. These were manually submitted to BLASTn in order to identify the most similar sequences from the NCBI database. BLAST results indicated that the sequence was not of *Homo sapiens* origin and instead appeared to be fungal, specifically being most similar to sequences from *Penicillium* spp. and *Aspergillus* spp. For instance, the sequence on contig #17 matched with 82% query cover and 86.20% identity to a sequence from the complete genome of *P. chrysogenum* Wisconsin 54-1255.

The data generated by Prokka had 4 hits for 16S rRNA gene sequences, of which the size for 2 of them was approximately 1,500 bp and the other 2 were under 1,000 bp. These sequences were used to query the BLASTn database. Results indicated that the 16S rRNA (1,541 bp) gene from contig #27 was highly similar to the 16S rRNA gene sequences of *Alicyclobacillus* sp. BGR 73 and *Ab. ferrooxidans* strain SLC66 from the NCBI database. The

length of this contig was 5,132 bp with a coverage of 47.85. The gene found on contig #17 (1,431 bp) was a very similar to a mitochondrial sequence from the complete genome of *Penicillium* sp. ShG4C. The sequences on contig #22 also appeared to correspond to fungal DNA since the rRNA sequences identified from this contig were most similar to 18S rRNA gene sequences from strains of *P. oxalicum*, *P. janthinellum*, and *P. decumbens*, as well as DNA from the chromosome of *Blumeria graminis*. Details of these BLAST results are shown in Table 3.1. Sequences can be found in Appx. C.

Preliminary results from binning the contigs with MetaBAT 2 suggested that there were 2 groups of contigs. One appeared to correspond to the size of a bacterial genome (average: ~3.87 Mb) (diCenzo & Finan, 2007), and the other group had low coverage and appeared to belong to a larger genome such as in fungi (average in Ascomycota: 36.91 Mb) (Mohanta & Bae, 2015). A few very small contigs were excluded from these groups, and further processing is required to assess whether these are real groups or artifacts that need to be removed.

The 16S rRNA gene sequence from contig #27 was used to construct a phylogenetic tree with species and strains of *Acidibacillus* and *Alicyclobacillus*, as well as with *Geobacillus thermoleovorans* as an outgroup (Figure 3.1). Branches were constructed based on maximum likelihood assumptions from analyzing our dataset and supported with a high level of confidence that the 16S rRNA gene sequence on contig #27 clustered with the rate class containing *Ab. ferrooxidans* strains, and significantly differed from the rate classes of *Ab. sulfuroxidans* as well as *Alb. acidocaldarius.* The most closely related strains of *Ab. ferrooxidans* were identified as BOR5, Huett2, and SLC66. We therefore assigned the strain ID "NOWR-5" to the strain of *Ab. ferrooxidans* in this study. The uploaded and post quality check (QC) sequence

Table 3.1: **Results from using BLASTn to query the 16S rRNA gene sequences identified in the sample against the NCBI database**.

Contig	Length (bp)	Position	Most Similar Sequences in NCBI Database	Query Cover	Percent Identity	Accession Number
27	1541	3436-4976	*Alicyclobacillus* sp. BGR 73 16S ribosomal RNA gene	94%	99.79%	GU167996.1
			Acidibacillus ferrooxidans strain SLC66 16S ribosomal RNA gene	95%	99.25%	AY040739.1
22	932	4481-5412	*Penicillium oxalicum* strain 114-2 18S ribosomal RNA gene	100%	99.89%	KF152942.1
			Penicillium janthinellum genes for 18S rRNA	100%	99.89%	AB293968.1
22	589	5651-6239	*Blumeria graminis* f. sp. Tritici genome	100%	100%	LR026995.1
			Penicillium decumbens strain ZQ001 18S ribosomal RNA gene	100%	100%	KX553859.1
17	1431	2683-4113	*Penicillium* sp. ShG4C mitochondrion	100%	95.96%	KX931017.1
			Blumeria graminis f. sp. Tritici genome	100%	95.82%	LR026995.1

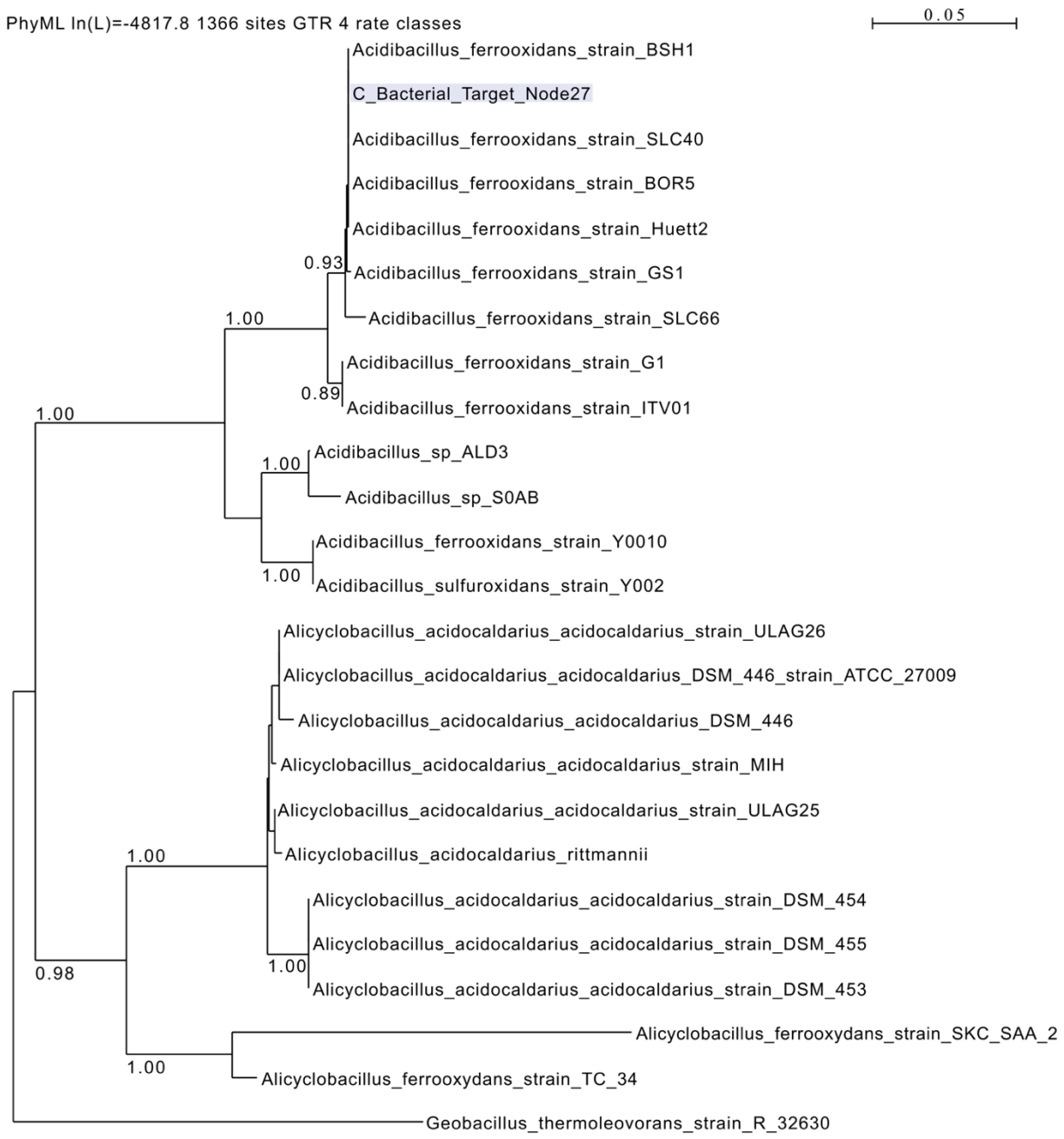

Figure 3.1: **Maximum-likelihood phylogenetic tree based on the 16S rRNA gene sequence from contig #27 showing the relationship of the target bacterium from BWR with strains of *Ab. ferrooxidans* and *Alicyclobacillus* sp**. Outgroup: *Geobacillus thermoleovorans*. Constructed from the sequence alignment of 1,366 sites. Inferred under the GTR+G+I evolution model. Numbers at nodes correspond to confidence values ranging from 0.00-1.00. Branches are scaled to the expected number of substitutions per site. Bar, 0.05 substitutions per nucleotide position.

count from submitting the scaffolds to MG-RAST was 191 (split contig #1 > 50,000 bp maximum) with 2,518,408 bp, and a mean sequence length of 13,185±52,875 bp. MG-RAST predicted 1,440 protein features and 17 rRNA features, as well as identified 1,040 protein features and 7 rRNA features. Figure 3.2 demonstrates identification at the domain level, and bacterial phyla are presented in Figure 3.3. The majority of hits (81.49%) within the Firmicutes phylum were classified as Bacilli and most of the others as Clostridia (17.81%). Of the 1,171 hits assigned to the Bacilli class, 1,143 of them were identified as belonging to the Bacillales order and the remaining hits as Lactobacillales. Hits in the Bacillales order were mainly assigned to 3 families (Figure 3.4). Most (93.10%) of the fungal hits were classified as belonging to the class Eurotiomycetes with 51 hits for the *Trichocomaceae* family. Over half (54.90%) of these hits were assigned to the genus *Penicillium*, 25.49% to *Aspergillus*, and 9.80% each of *Neosartorya* and *Talaromyces*.

Gene subsystem categories which were identified by MG-RAST for the genus *Alicyclobacillus* are shown in Table 3.2. Considering many general genes were annotated and that only 102 hits were classified as belonging to *Alicyclobacillus* sp., the scope of genes which could belong to this organism was widened to include hits from the *Bacillaceae* family. Figure 3.5 shows the number of genes that were annotated for both *Alicyclobacillus* sp. and *Bacillaceae*, and their combined total. These total numbers were used to compare the amounts of genes found in each subsystem category with numbers from the draft genome of *Ab. ferrooxidans* strain Huett2 (Figure 3.6).

Prokka identified 2,453 coding genes from 190 of the contigs. These included 49 tRNA, 32 miscellaneous RNA, 9 rRNA, and 1 tmRNA. One CRISPR sequence was removed, and 1,102 proteins were labeled as hypothetical. RAST identified 2,605 protein coding

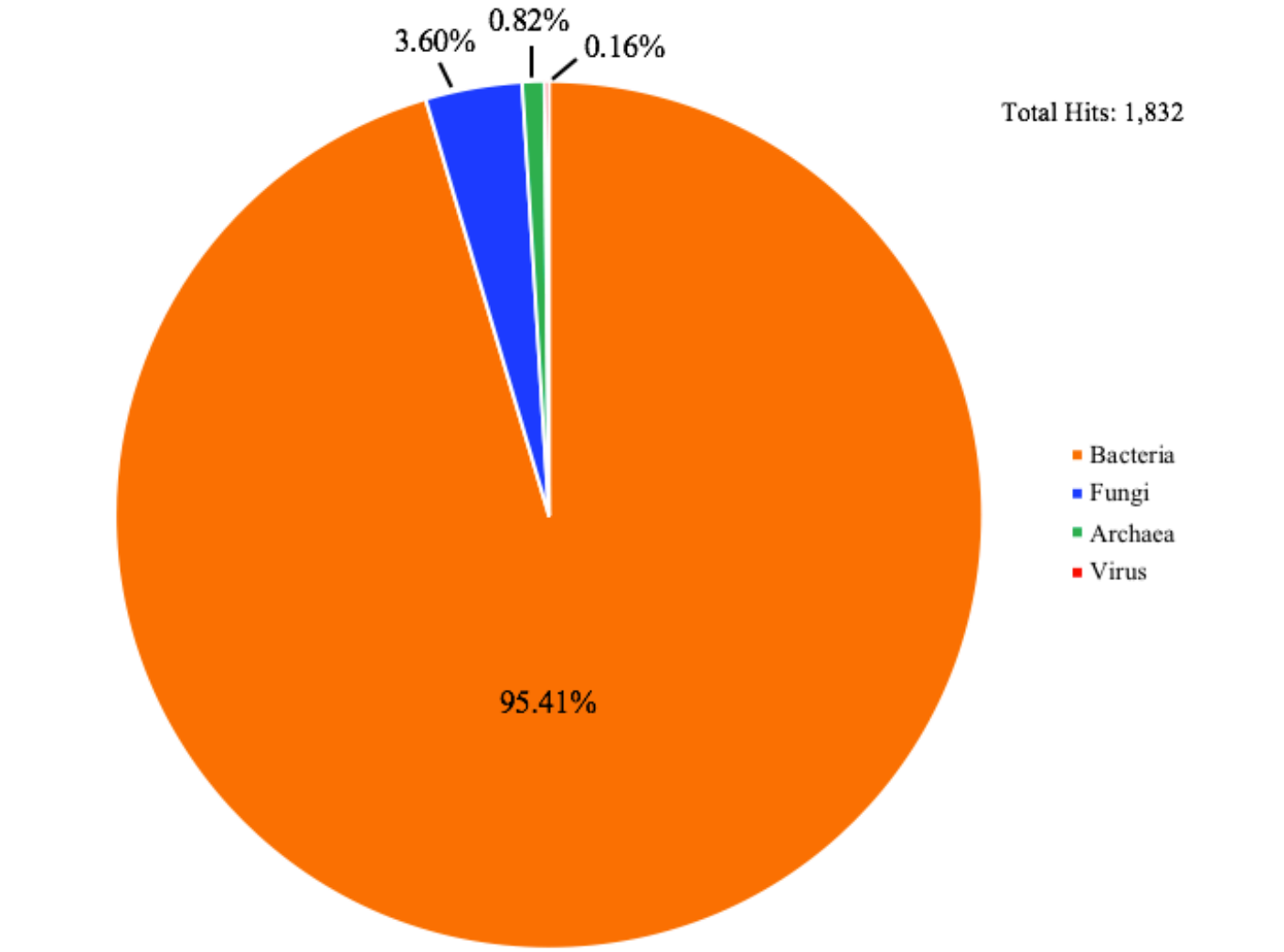

Figure 3.2: **Percentage of sequences from the Metagenome 1 sample assigned to different microbial domains by MG-RAST**.

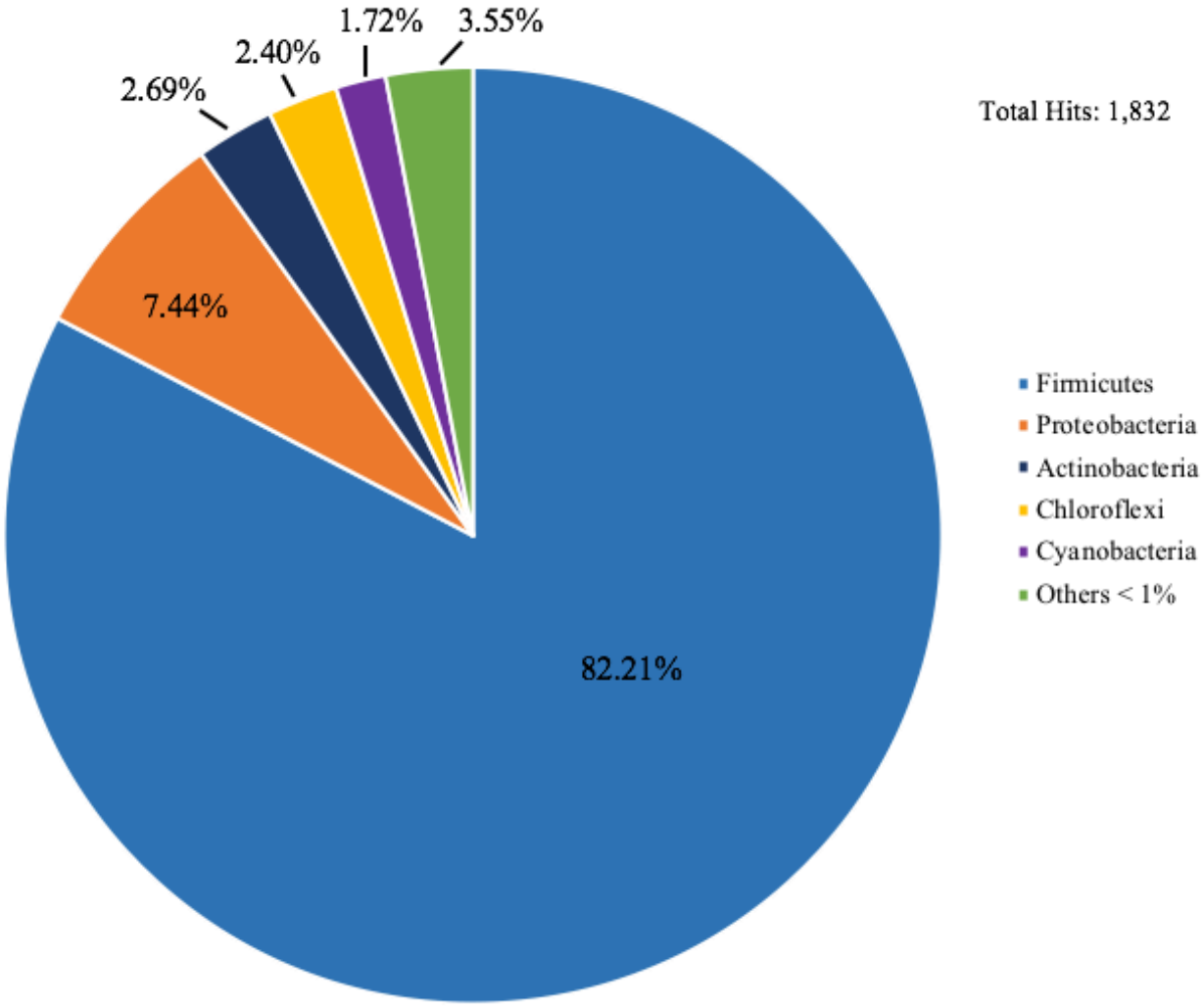

Figure 3.3: **Classification of bacterial sequences from the Metagenome 1 sample into phyla**.

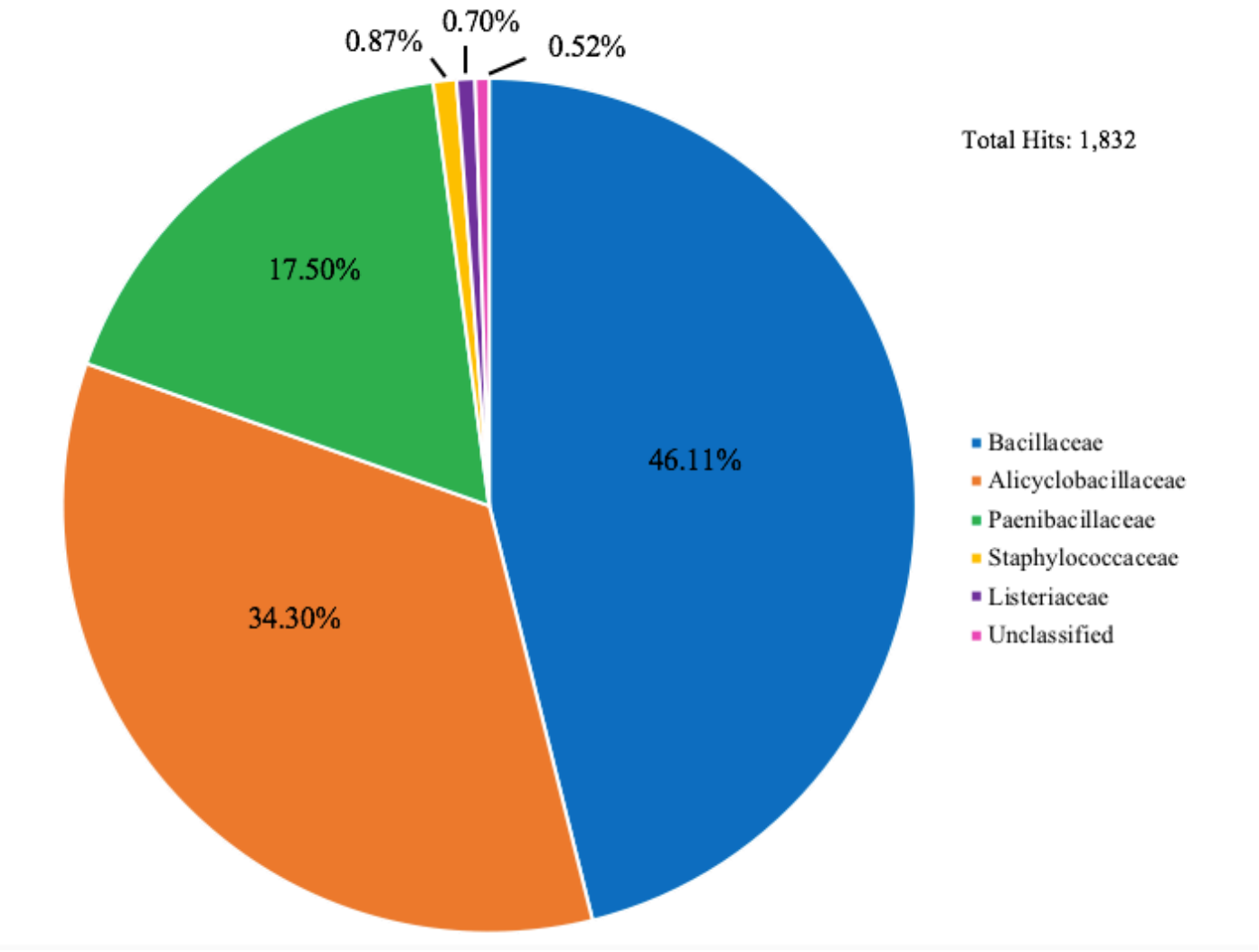

Figure 3.4: **Classification of sequences from the Metagenome 1 sample into families within the Bacillales order**.

Table 3.2: **Subsystem categories identified by MG-RAST from the Metagenome 1 sample that were assigned to the genus *Alicyclobacillus*.**

Subsystem Category	Number of Hits
Amino acids and derivatives	11
Carbohydrates	17
Cell division and cell cycle	1
Cell wall and capsule	1
Clustering-based subsystems	11
Cofactors, vitamins, prosthetic groups, pigments	3
DNA metabolism	6
Dormancy and sporulation	4
Fatty, acids, lipids, and isoprenoids	3
Miscellaneous	9
Motility and chemotaxis	1
Nucleosides and nucleotides	1
Phages, prophages, transposable elements, plasmids	1
Potassium metabolism	3
Protein metabolism	9
RNA metabolism	6
Regulation and cell signaling	1
Respiration	7
Stress response	1
Virulence, disease and defense	3

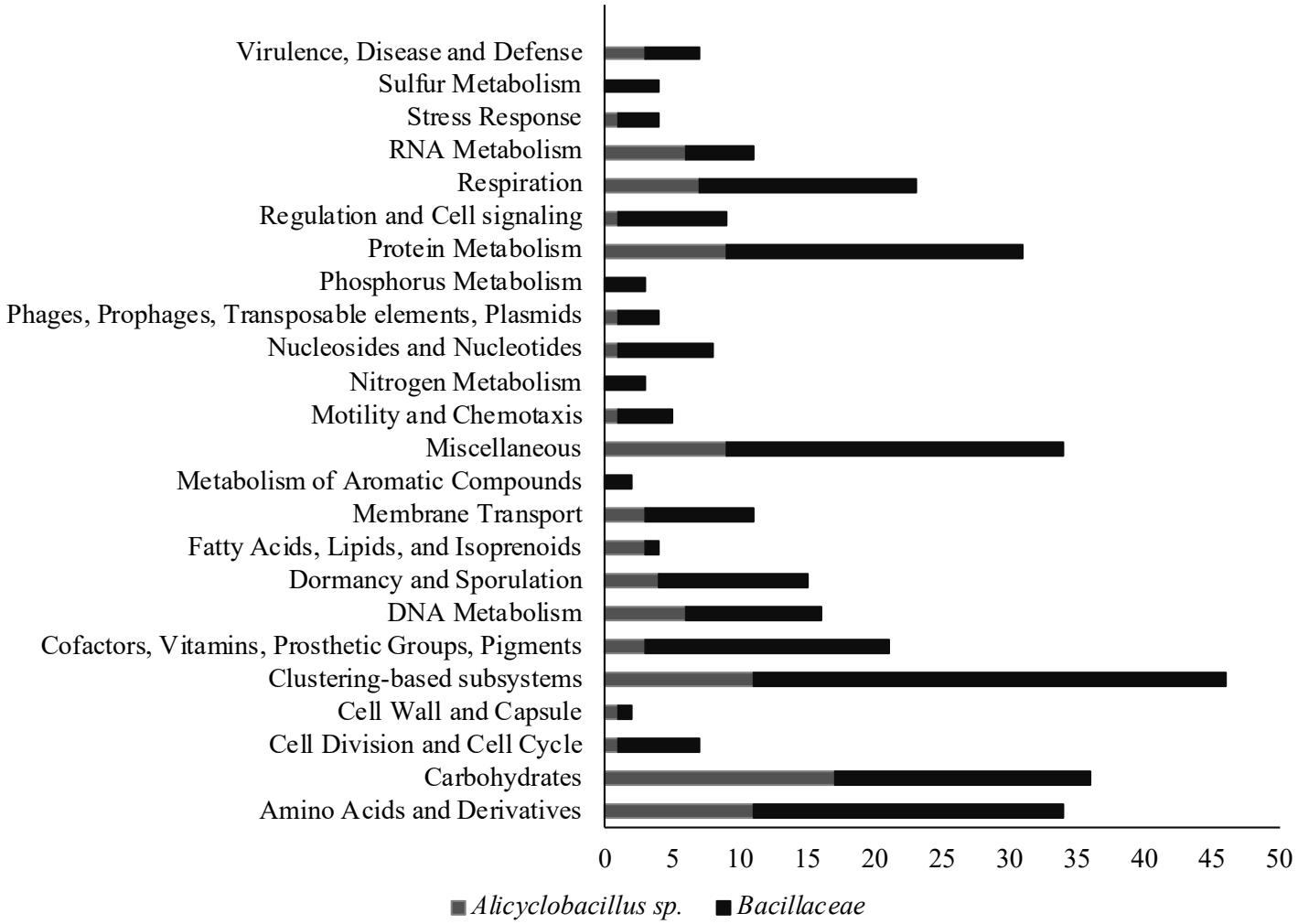

<u>Figure 3.5</u>: Combination of subsystem hits annotated by MG-RAST from the Metagenome 1 sample that were assigned to *Alicyclobacillus* sp. and *Bacillaceae*. Bars are distinguished with different shades. X axis: number of subsystem hits; Y axis: subsystem categories.

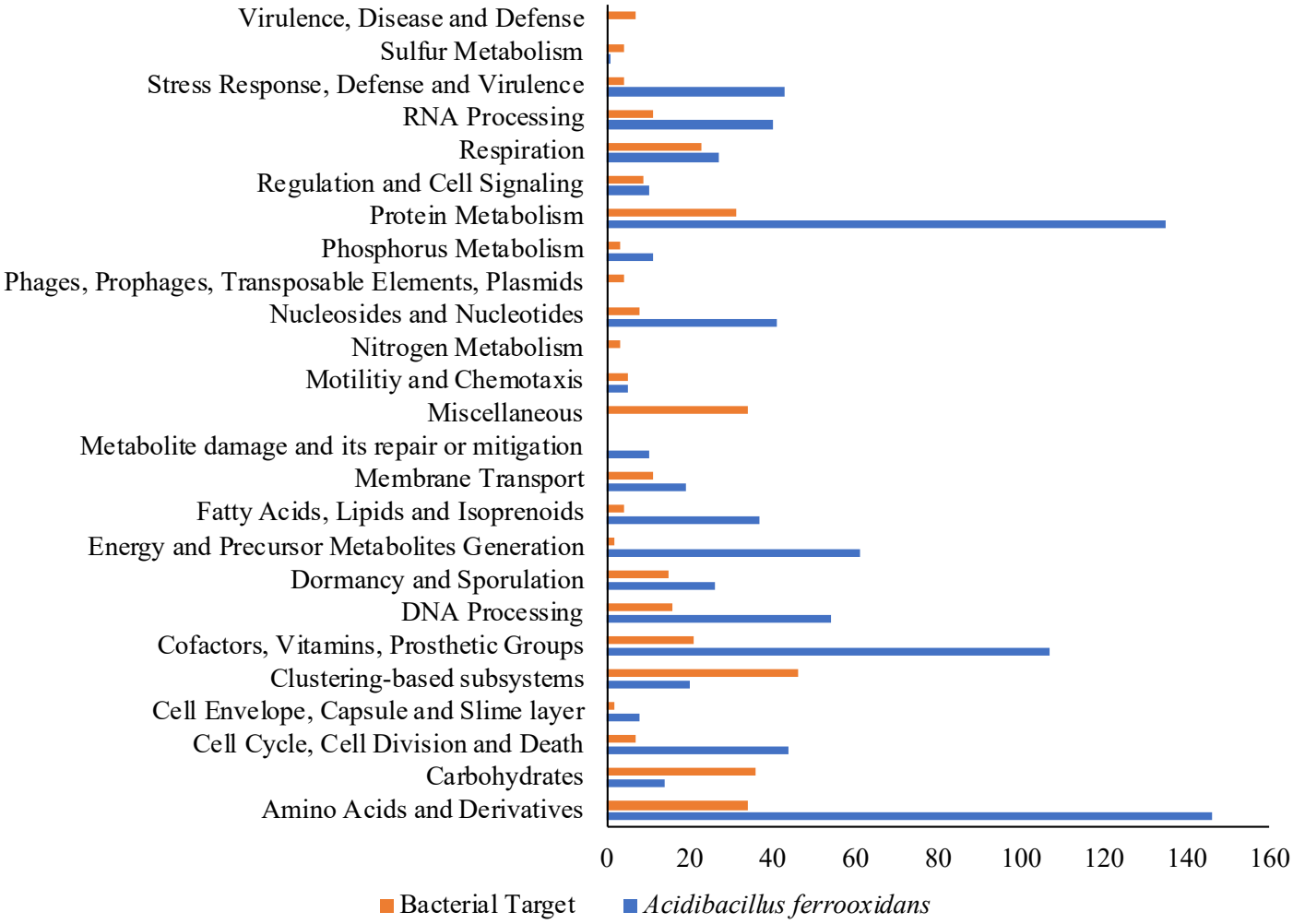

<u>Figure 3.6</u>: Comparison of the number of genes from different subsystem categories between the bacterial target (including hits for *Alicyclobacillus* sp. and *Bacillaceae* family annotated by MG-RAST) and the draft genome of *Ab. ferrooxidans* strain Huett2 (retrieved from PATRIC). Bars are distinguished with different colors. X axis: number of subsystem hits; Y axis: subsystem categories

sequences and 49 RNAs of the 190 contigs which had protein-encoding genes. These genes were assigned to a total of 222 subsystem categories. The N50 value for the scaffolds was 152,821. GC-content of the scaffolds submitted to RAST was reported to be 51.4%.

Nitrogen metabolism and transport

All genes that were found to be involved with dissimilatory or assimilatory pathways for nitrogen are listed in Table 3.3. Seven genes coding for nitrate reductases (EC 1.77.99.4) were identified. No genes were found to code for enzymes that reduce nitrite to ammonium as well as none involved in denitrification that would reduce nitrite to nitric oxide. Many genes found in the data were also found in the draft genomes of *Ab. ferrooxidans* strain SLC66 and *Ab. ferrooxidans* strain Huett2 (Figure 3.7).

Among the nitrate reductases identified, 3 of them were coded by the *napA* gene which is involved in dissimilatory nitrate reduction and were located on various contigs: #2, 4, and 11. Four respiratory nitrate reductase enzymes were coded by *narG* (2), *narX*, and *narY*. These genes are part of two protein complexes that are transcribed by the *narGHI* and *napAB* operons as described by Coelho & Romao (2015). RAST annotated two *narG* genes one after the other on contig #15 which code for the alpha chain of the respiratory nitrate reductase. The remaining gene order was consistent with the organization of this operon that has been established in *Pseudomonas aeruginosa*: beta chain, delta chain, and gamma chain (Blasco et al., 1990). Prokka annotated the beta chain as being the product of the *narY* gene instead (Table 3.3). In addition, it did not identify any genes that code for the delta chain, but it did annotate a hypothetical protein starting at 36,648 bp and ending at 37,238 bp which is exactly where RAST annotated the *narJ* delta chain. The gene *narX* was annotated from 37,279 bp to 38,055 bp and

Table 3.3: **Genes and protein products associated with nitrogen metabolism that Prokka annotated from contigs that were assembled from the Metagenome 1 sample**. Enzyme commission (EC) numbers that are associated to these products are listed if available.

Subsystem	Gene	Protein Product	EC Number	Contig Number
Assimilatory metabolism	*nrgA*	Ammonium transporter	-	1
	gcvT	Aminomethyltransferase	2.1.2.10	2
	rocG	Catabolic NAD-specific glutamate dehydrogenase RocG	1.4.1.2	2
	glnA	Glutamine synthetase	6.3.1.2	2
	gltB	Glutamate synthase [NADPH] large chain	1.4.1.13	2
	asnB	Asparagine synthetase [glutamine-hydrolyzing] 1	6.3.5.4	2
	asnB	Asparagine synthetase [glutamine-hydrolyzing] 1	6.3.5.4	4
	asnO	Asparagine synthetase [glutamine-hydrolyzing] 3	6.3.5.4	4
	glnA	Glutamine synthetase	6.3.1.2	5
Dissimilatory metabolism	*napA*	Nitrate reductase	1.7.99.4	4
	napA	Nitrate reductase	1.7.99.4	11
Energy metabolism	*narG*	Respiratory nitrate reductase 1 alpha chain	1.7.99.4	15
	narG	Respiratory nitrate reductase 1 alpha chain	1.7.99.4	15
	narX	Nitrate reductase-like protein NarX	1.7.99.4	15
	narY	Respiratory nitrate reductase 2 beta chain	1.7.99.4	15
Nitrosative stress	*hmp*	Flavohemoprotein	1.14.12.17	1
	nsrR	HTH-type transcriptional repressor NsrR	-	1
	-	Nitronate monooxygenase	1.13.12.16	2
	ytfE	Iron-sulfur cluster repair protein YtfE	-	7

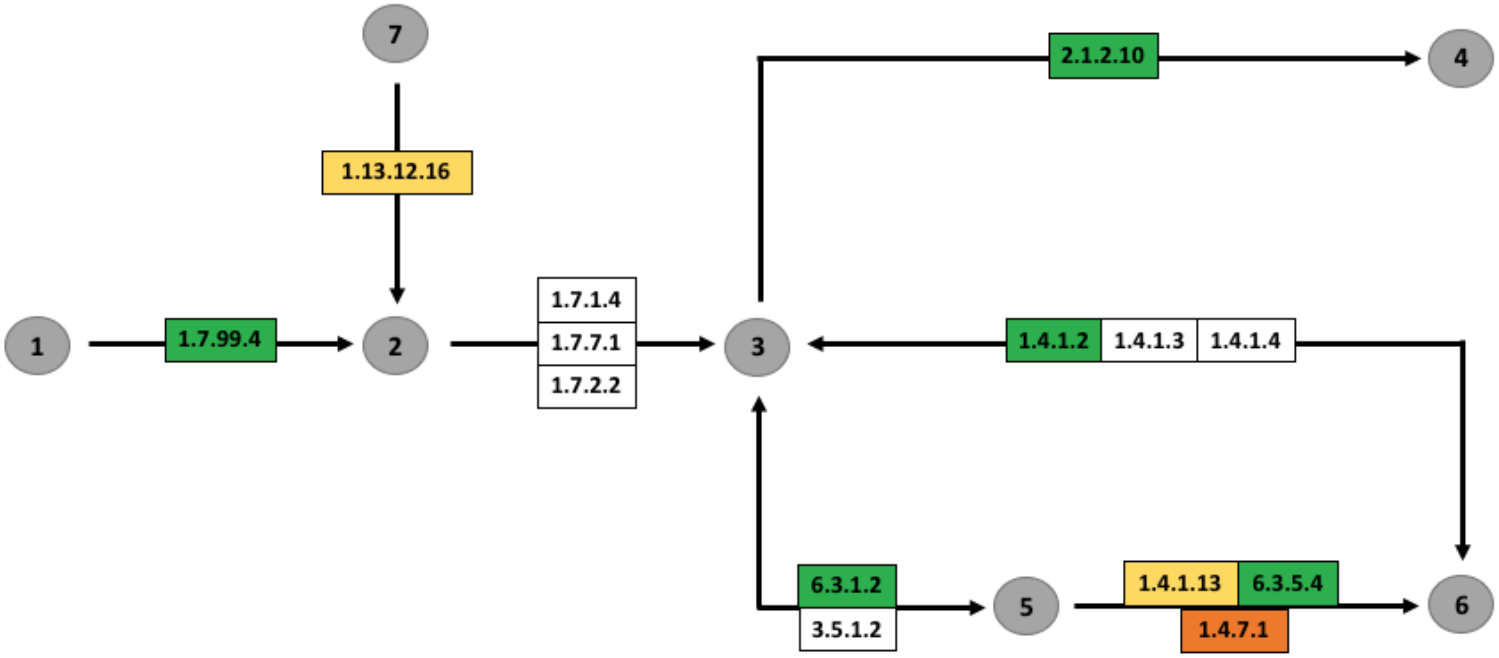

Assigned Number	Reactant/Product
1	Nitrate
2	Nitrite
3	Ammonia
4	Glycine
5	L-Glutamine
6	L-Glutamate
7	Nitroalkane

Figure 3.7: **Respiratory nitrate reduction and catabolic reactions associated with nitrogen metabolism**. Genes are indicated by enzyme commission (EC) numbers for the products that they encode. Green boxes represent the presence of that gene in both the data and draft genomes; Orange represents the gene was only present in the draft genomes; Yellow represents the gene was only found in the data.

this is where RAST annotated that the gamma chain was located (Figure 3.8). In *Ab. ferrooxidans* draft genomes, genes for the alpha, beta, gamma and delta (2) chains were present.

Genes related to nitrosative stress that were identified include the *nsrR* gene on contig #1 which encodes the transcriptional repressor NsrR (Tucker et al., 2008). This gene was present in the draft genomes of *Ab. ferrooxidans*. A gene coding for nitronate monooxygenase (EC 1.13.12.16) was identified on contig #2, and 2 genes were found in the draft genomes coding for a putative oxidoreductase of the nitronate monooxygenase family.

Sulfur metabolism and transport

Most of the genes required for the pathway which reduces sulfate to sulfite, and subsequently to hydrogen sulfide were present in the data and in the draft genomes of *Ab. ferrooxidans* (Figure 3.9). The data did not contain a gene (EC 2.7.1.25) for the reduction of 5'-phosphosulfate (APS) to 3'-phosphoadenylyl-sulfate (PAPS) but the compared draft genomes did. The same gene (EC 1.8.4.8) was found in the data for the next step of reducing PAPS to sulfite, but genes coding for different sulfite reductases were found. They both reduce sulfite to hydrogen sulfide, and the gene from the data encoded a ferredoxin-type sulfite reductase (EC 1.8.7.1) (Table 3.4).

There was no indication from the data or from draft genomes that these organisms possess genes for the dissimilatory oxidation of RISCs. All of the genes that were found in the data were on different contigs except for the genes *sirB*, *sir*, *sat*, and *cysH* which were all found consecutively on contig #3. RAST did not annotate any genes in the sulfur subsystem category.

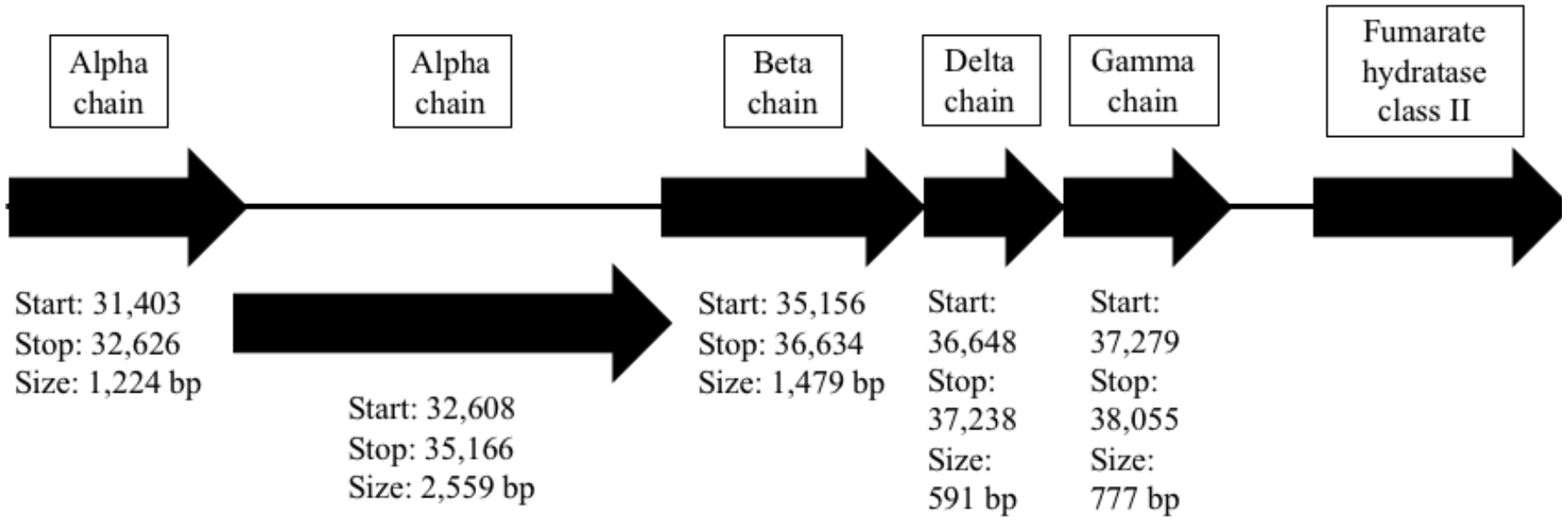

Figure 3.8: **Organization of *nar* genes on contig #15 based on RAST annotation**. Start and stop points as well as gene sizes were used for comparison with Prokka results.

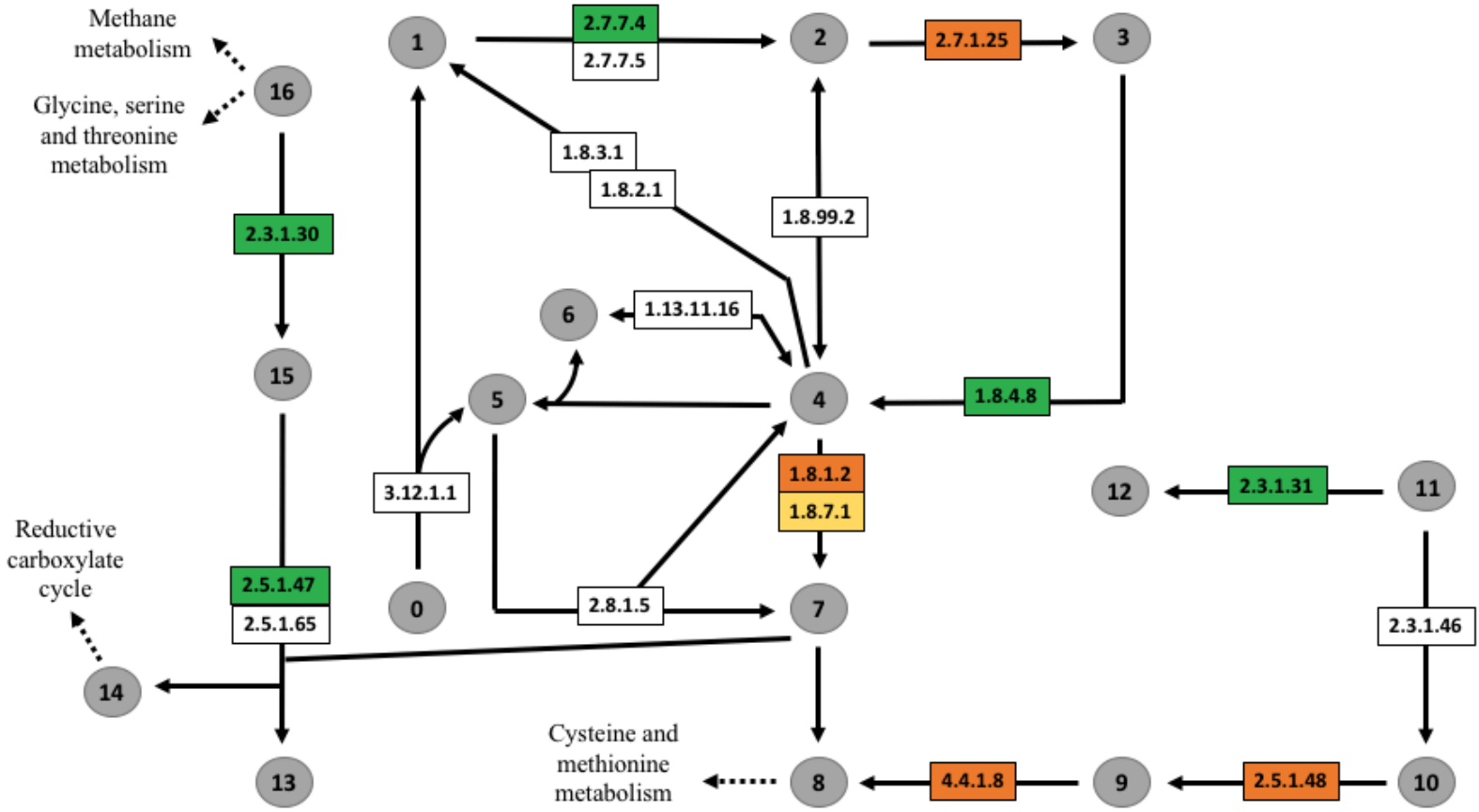

Assigned Number	Reactant/Product
0	Trithionate
1	Sulfate
2	Adenylylsulfate (APS)
3	3'-Phosphoadenylyl-sulfate (PAPS)
4	Sulfite
5	Thiosulfate
6	Sulfur
7	Hydrogen Sulfide

8	L-Homocysteine
9	Cystathionine
10	O-Succinyl-L-homoserine
11	L-Homoserine
12	O-Acetyl-L-homoserine
13	Cysteine
14	Acetate
15	O-Acetyl-L-serine
16	L-Serine

Figure 3.9: **Metabolic pathways for sulfur metabolism**. Genes are indicated by enzyme commission (EC) numbers for the products that they encode. Green boxes represent the presence of that gene in both data and draft genomes; Orange represents the gene was only identified in the draft genomes; Yellow represents the gene was only found in the data.

Table 3.4: **Genes and protein products associated with sulfur metabolism that Prokka annotated from contigs that were assembled from the Metagenome 1 sample**. Enzyme commission (EC) numbers that are associated to these products are listed if available.

Gene	Protein Product	EC Number	Contig
cysG	Siroheme synthase	4.99.1.4	1
metXA	Homoserine O-acetyltransferase	2.3.1.31	2
sirB	Sirohydrochlorin ferrochelatase	4.99.1.4	3
sir	Sulfite reductase [ferredoxin]	1.8.7.1	3
sat	Sulfate adenylyltransferase	2.7.7.4	3
cysH	Phosphoadenosine phosphosulfate reductase	1.8.4.8	3
cysA	Sulfate/thiosulfate import ATP-binding protein CysA	3.6.3.25	6
cysG	Siroheme synthase	4.99.1.4	7
cysK	Cysteine synthase	2.5.1.47	7
metK	S-adenosylmethionine synthase	2.5.1.6	9
cysE	Serine acetyltransferase	2.3.1.30	11
cysK	Cysteine synthase	2.5.1.47	14
cysG	Siroheme synthase	4.99.1.4	15

Iron metabolism and transport

There were no genes identified which were evidently involved in dissimilatory iron reactions in either the data or in the draft genomes of *Acidibacillus* spp. and *Alb. acidocaldarius*. Genes *ctaD* and *ctaC* were found together on contig #10, but these could equally be involved in the oxidative phosphorylation of organic compounds. A *petC* gene was also identified in the data but its predicted product was a cytochrome b6-f complex iron-sulfur subunit instead of a ubiquinol—cytochrome c reductase, which the *petC* gene from Fe^{2+} metabolism codes for. The genes *hmuU* and *hmuV*, that respectively code for a hemin transport system permease protein and a hemin import ATP-binding protein, were found consecutively on contig #1.

Autotrophic carbon metabolism

Almost all of the genes required for the rTCA cycle were detected (Figure 3.10). These genes were also present in the draft genomes of closely-related *Acidibacillus* and *Alicyclobacillus*, except for the gene *frdA* (EC 1.3.5.4) which encodes the fumarate reductase Fe-S subunit. The genes *frdA* and *frdB* were identified consecutively on contig #2 and the gene *sdhC* was directly beside *frdA* (Table 3.5). Key enzymes to regenerate the cycle were missing which included an ATP citrate synthase and a pyruvate synthase. An absence of genes for citrate synthase was also identified in the draft genomes of *Acidibacillus*, but it did have a gene (EC 1.2.7.-) coding for an enzyme to catalyze the reaction from acetyl-CoA to pyruvate. In addition, a gene was present for a pyruvate carboxylase (EC 6.4.1.1) enzyme to bypass the generation of phosphoenolpyruvate in order to directly form oxaloacetate.

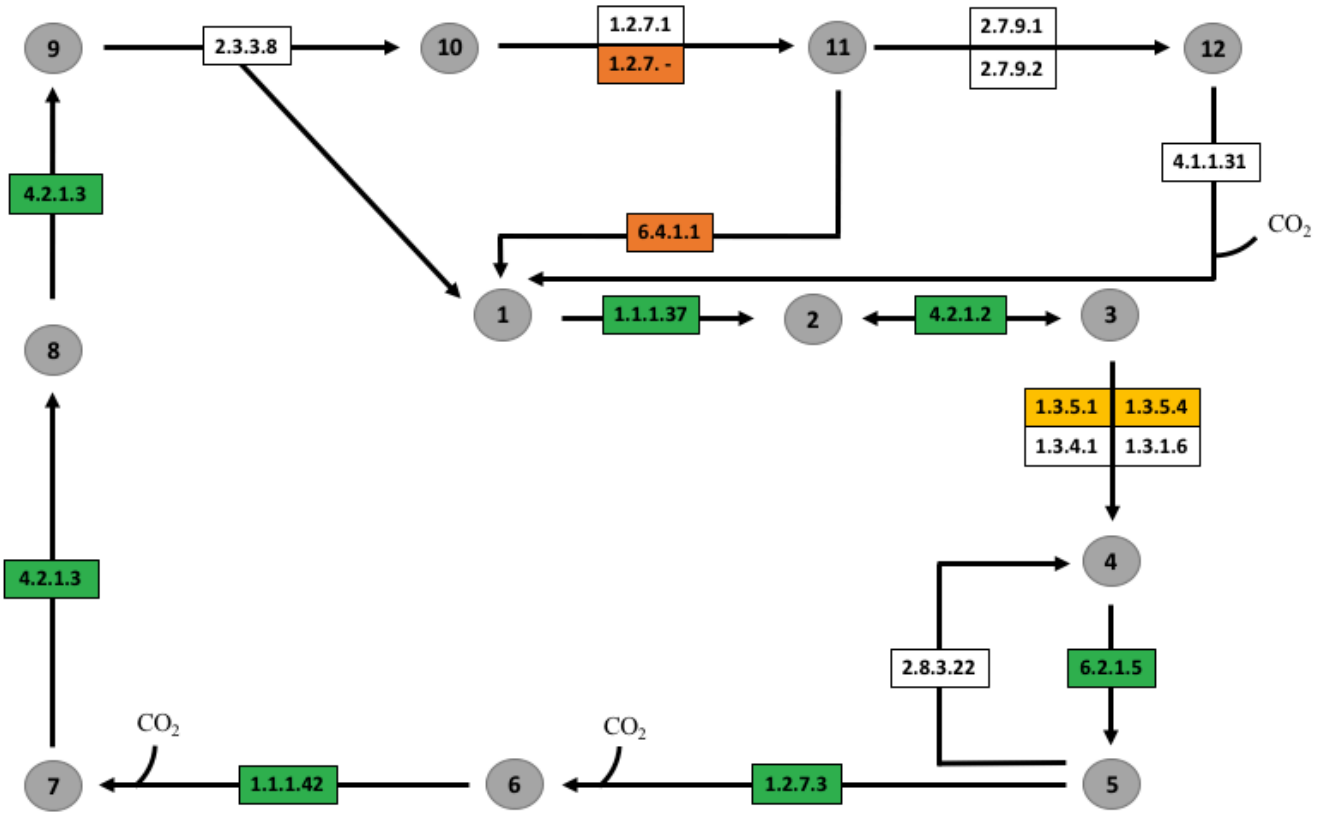

Assigned Number	Reactant/Product
1	Oxaloacetate
2	(S)-Malate
3	Fumarate
4	Succinate
5	Succinyl-CoA
6	2-Oxoglutarate
7	Isocitrate
8	cis-Aconitate
9	Citrate
10	Acetyl-CoA
11	Pyruvate
12	Phosphoenol-pyruvate

Figure 3.10: **CO_2 fixation via the rTCA pathway**. Genes are indicated by enzyme commission (EC) numbers for the products that they encode. Green boxes represent the presence of that gene in both the data and draft genomes; Orange represents the gene was only present in the draft genomes; Yellow represents the gene was only found in the data.

Table 3.5: **Genes and protein products associated with CO_2 fixation pathways that Prokka annotated from contigs that were assembled from the Metagenome 1 sample**. Enzyme commission (EC) numbers that are associated to these products are listed if available.

Pathway	Gene	Protein Product	EC Number	Contig
Reverse citric acid cycle	*icd*	Isocitrate dehydrogenase [NADP]	1.1.1.42	1
	mdh	Malate dehydrogenase	1.1.1.37	2
	frdA	Fumarate reductase flavoprotein subunit	1.3.5.4	2
	frdB	Fumarate reductase iron-sulfur subunit	1.3.5.1	2
	icd	Isocitrate dehydrogenase [NADP]	1.1.1.42	3
	korA	2-Oxoglutarate oxidoreductase subunit KorA	1.2.7.3	5
	sucC	Succinate—CoA ligase [ADP-forming] subunit beta	6.2.1.5	6
	sucD	Succinate—CoA ligase [ADP-forming] subunit alpha	6.2.1.5	6
	citB	Aconitate hydratase A	4.2.1.3	7
	fumC	Fumarate hydratase class II	4.2.1.2	15
Calvin-Benson-Bassham cycle	*pgk*	Phosphoglycerate kinase	2.7.2.3	1
	gap	Glyceraldehyde-3-phosphate dehydrogenase	1.2.1.12	1
	tpiA	Triosephosphate isomerase	5.3.1.1	1
	tkt	Transketolase	2.2.1.1	3
	fba	Fructose-biphosphate aldolase	4.1.2.13	4
	glpX	Fructose-1,6-biphosphatase class II	3.1.3.11	4
Dicarboxylate-hydroxybutyrate	*pccB*	Propionyl-CoA carboxylase beta chain	6.4.1.3	2
	scpA	Methylmalonyl-CoA mutase	5.4.99.2	2
	accA	Acetyl-coenzyme A carboxylase carboxyl transferase subunit	6.4.1.2	3
	accD	Acetyl-coenzyme A carboxylase carboxyl transferase subunit	6.4.1.2	3
	mmgA	Acetyl-CoA acetyltransferase	2.3.1.9	4
	fadN	Putative 3-hydroxyacyl-CoA dehydrogenase	1.1.1.35	5

Two putative genes transcribing for predicted proteins were identified which are involved in the noncyclic carbonic fixation Wood-Ljungdahl (WL) pathway to form acetyl-CoA from CO_2 (Figure 3.11) (de Souza & Rosado, A. S., 2019). *Ab. ferrooxidans* NOWR-5 had a gene coding for an aerobic carbon monoxide (CO) dehydrogenase (EC 1.2.5.3), whereas the draft genomes of *Acidibacillus* contained a gene (EC 1.2.7.4) coding for an anaerobic carbon monoxide dehydrogenase (1.2.7.4). Three genes have been identified in the *Acidibacillus* draft genomes for the methyl branch of the WL pathway including the one coding for the enzyme 5,10-methylenetetrahydrofolate (EC 1.5.1.20). Only the *yitJ* gene was found in the data which codes for an enzyme involved in the methyl branch of the WL pathway.

A substantial number of genes were found in the data as well as in the draft genomes of *Acidibacillus* which are known to be involved in the CBB pathway (Table 3.5). The *gap* gene (EC 1.2.1.12) was found exclusively in the data, whereas both ribose-5-phosphate isomerase coding genes (EC 5.3.1.6) and ribulose-phosphate 3-epimerase coding genes (EC 5.1.3.1) were only identified in the draft genomes. The genes encoding the key enzymes phosphoribulokinase (EC 2.7.1.19), ribulose-biphosphate carboxylase (EC 4.1.1.39), and sedoheptulokinase (EC 2.7.1.14) were missing from the data as well as from the draft genomes of *Acidibacillus* and *Alicyclobacillus* (Figure 3.12). RAST did not annotate any genes in the subsystem category of CO_2 fixation.

Six genes were found in the data and in the *Acidibacillus* draft genomes which are associated to the dicarboxylate-hydroxybutyrate pathway. These included *accA* and *accD* genes (EC 6.4.1.2) that were found consecutively on contig #3 (Table 3.5).

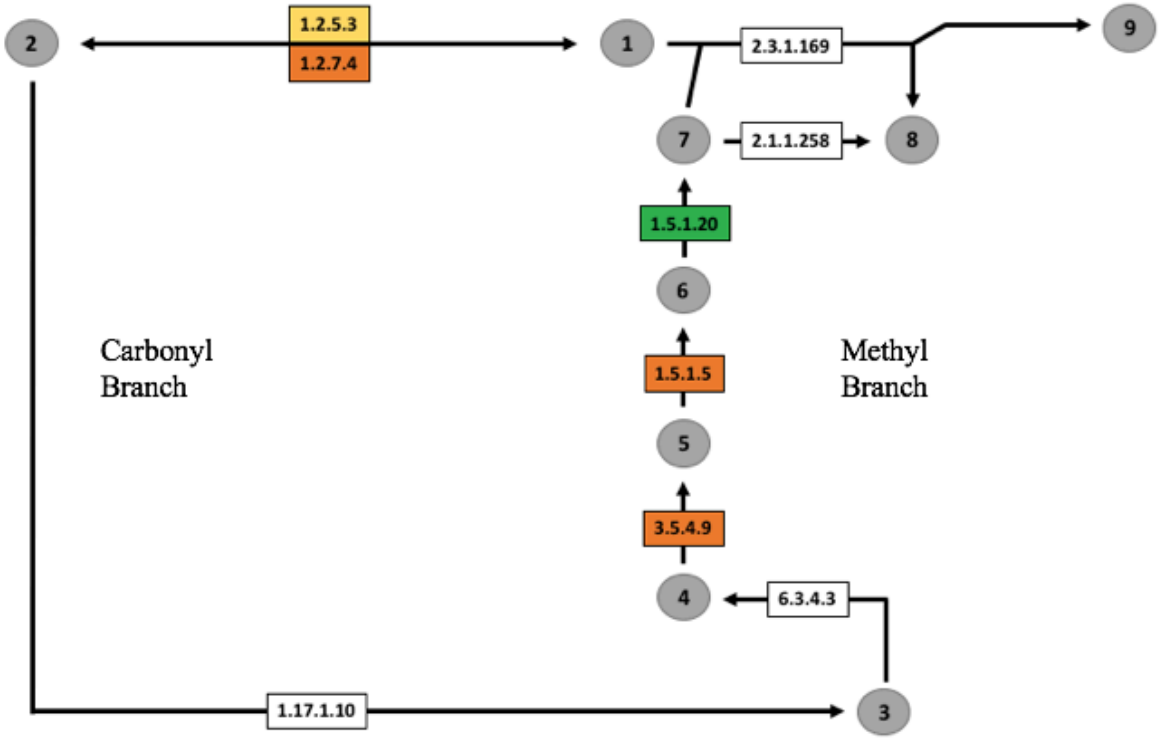

Assigned Number	Reactant/Product
1	Carbon monoxide
2	Carbon dioxide
3	Formate
4	10-Formyl-tetrahydrofolate
5	5,10-Methenyl-tetrahydrofolate
6	5,10-Methylene-tetrahydrofolate
7	5-Methyl-tetrahydrofolate
8	Tetra-hydrofolate
9	Acetyl-CoA

Figure 3.11: **CO_2 fixation via the Wood-Ljungdahl pathway**. Genes are indicated by enzyme commission (EC) numbers for the products that they encode. Green boxes represent the presence of that gene in both the data and draft genomes; Orange represents the gene was only present in the draft genomes; Yellow represents the gene was only found in the data.

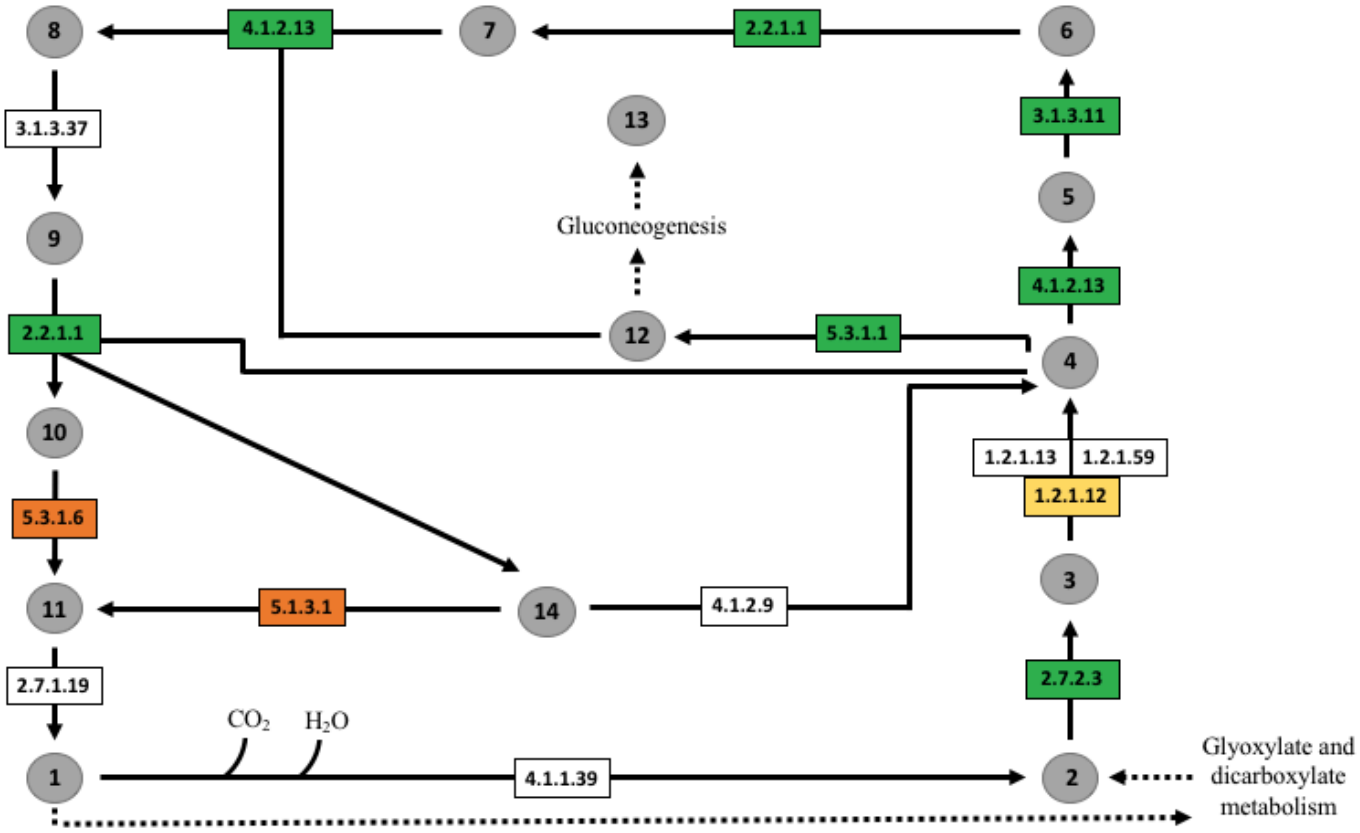

Assigned Number	Reactant/Product
1	Ribulose 1,5-biphosphate
2	3-Phosphoglycerate
3	1,3-Biphosphoglycerate
4	Glyceraldehyde 3-phosphate
5	Fructose 1,6-biphosphate
6	Fructose 6-phosphate
7	Erythrose 4-phosphate
8	Sedoheptulose 1,7-biphosphate
9	Sedoheptulose 7-phosphate
10	Ribose 5-phosphate
11	Ribulose 5-phosphate
12	Dihydroxyacetone phosphate
13	Starch
14	Xylulose 5-phosphate

Figure 3.12: **CO_2 fixation via the Calvin-Benson-Bassham cycle**. Genes are indicated by enzyme commission (EC) numbers for the products that they encode. Green boxes represent the presence of that gene in both the data and draft genomes; Orange represents the gene was only present in the draft genomes; Yellow represents the gene was only found in the data.

Heterotrophic carbon metabolism

All of the genes that were found to be involved in heterotrophic metabolism from glycolysis to the TCA cycle are shown in Table 3.6. Nearly all of the genes required for the metabolic pathways of glycolysis and pyruvate oxidation were present in *Ab. ferrooxidans* NOWR-5 and in the draft genomes.

A substantial number of genes were annotated which can be involved in the PP pathway, however almost none were identified in the data for the oxidative stage of the pathway starting with glucose-6-phosphate to ultimately produce ribose-5-phosphate (Figure 3.13). Only the draft genome of *Alicyclobacillus* had a gene for the transcription of ribose 5-phosphate isomerase (EC 5.3.1.6), and the gene (EC 3.1.1.31) coding for 6-phosphogluconolactonase was not detected in any of the genomes. Many genes were present in the data that take part in the non-oxidative stage of the PP pathway and which accomplish interconversions between glycolytic intermediates.

The only gene missing in the data for the TCA cycle was the one coding for citrate (Si)-synthase (EC 2.3.3.1) that is required for the first step of converting oxaloacetate and acetyl-CoA to citrate (Figure 3.14). The gene *korA* (EC 1.2.7.3) was only found in the data on contig #5.

Both of the genes coding for the key enzymes of the glyoxylate shunt were found in the data as well as in the compared genomes (Figure 3.15). Both *aceB* and *icl1* genes were identified consecutively on contig #3.

Genes identified as part of the oxidative phosphorylation pathway are indicated in Figure 3.16. The enzyme type II NAD(P)H:quinone oxidoreductase (EC 1.6.5.9) was identified

Table 3.6: **Genes and protein products associated with heterotrophic pathways prior to the generation of ATP via the electron transport chain**. Enzyme commission (EC) numbers that are associated to these products are listed if available.

Pathway	Gene	Protein Product	EC No.	Contig
Embden-Meyerhof-Parnas pathway	*glcK*	Glucokinase	2.7.1.2	1
	gap	Glyceraldehyde-3-phosphate dehydrogenase	1.2.1.12	1
	pgk	Phosphoglycerate kinase	2.7.2.3	1
	eno	Enolase	4.2.1.11	1
	pckA	Phosphoenolpyruvate carboxykinase (ATP)	4.1.1.49	1
	-	Putative zinc-binding alcohol dehydrogenase	1.1.1.1	1
	tpiA	Triosephosphate isomerase	5.3.1.1	1
	acsA	Acetyl-coenzyme A synthetase	6.2.1.1	2
	acs	Acetyl-coenzyme A synthetase	6.2.1.1	2
	pfkA	ATP-dependent 6-phosphofructokinase	2.7.1.11	3
	pyk	Pyruvate kinase	2.7.1.40	3
	fba	Fructose-biphosphate aldolase	4.1.2.13	4
	glpX	Fructose-1,6-biphosphatase class II	3.1.3.11	4
	acs	Acetyl-coenzyme A synthetase	6.2.1.1	4
	pgiB	Glucose-6-phosphate isomerase B	5.3.1.9	7
	aceF	Dihydrolipoyllysine-residue acetyltransferase component of pyruvate dehydrogenase complex	2.3.1.12	7
	glcK	Glucokinase	2.7.1.2	18
	pdhA	Pyruvate dehydrogenase E1 component subunit alpha	1.2.4.1	20
	pdhB	Pyruvate dehydrogenase E1 component subunit beta	1.2.4.1	20
	pdhC	Dihydrolipoyllysine-residue acetyltransferase component of pyruvate dehydrogenase complex	2.3.1.12	20
	pdhD	Dihydrolipoyl dehydrogenase	1.8.1.4	20

Pentose phosphate pathway	*prs*	Ribose-phosphate pyrophosphokinase	2.7.6.1	2
	deoB	Phosphopentomutase	5.4.2.7	2
	pgcA	Phosphoglucomutase	5.4.2.2	3
	tkt	Transketolase	2.2.1.1	3
	tal	Transaldolase	2.2.1.2	3
	pfkA	ATP-dependent 6-phosphofructokinase	2.7.1.11	3
	prs	Ribose-phosphate pyrophosphokinase	2.7.6.1	4
	tal	Transaldolase	2.2.1.2	4
	fba	Fructose-biphosphate aldolase	4.1.2.13	4
	glpX	Fructose-1,6-biphosphatase class II	3.1.3.11	4
	pgiB	Glucose-6-phosphate isomerase B	5.3.1.9	7
Citric acid cycle	*icd*	Isocitrate dehydrogenase [NADP]	1.1.1.42	1
	frdB	Fumarate reductase iron-sulfur subunit	1.3.5.1	2
	mdh	Malate dehydrogenase	1.1.1.37	2
	icd	Isocitrate dehydrogenase [NADP]	1.1.1.42	3
	korA	2-Oxoglutarate oxidoreductase subunit KorA	1.2.7.3	5
	citB	Aconitate hydratase A	4.2.1.3	7
	odhA	2-Oxoglutarate dehydrogenase E1 component	1.2.4.2	10
	odhB	Dihydrolipoyllysine-residue succinyltransferase component of 2-oxoglutarate dehydrogenase	2.3.1.61	10
	sucC	Succinate—CoA ligase [ADP-forming] subunit beta	6.2.1.5	12
	sucD	Succinate—CoA ligase [ADP-forming] subunit alpha	6.2.1.5	12
	fumC	Fumarate hydratase class II	4.2.1.2	15
Glyoxylate shunt	*Icl1*	Isocitrate lyase 1	4.1.3.1	6
	aceB	Malate synthase A	2.3.3.9	6

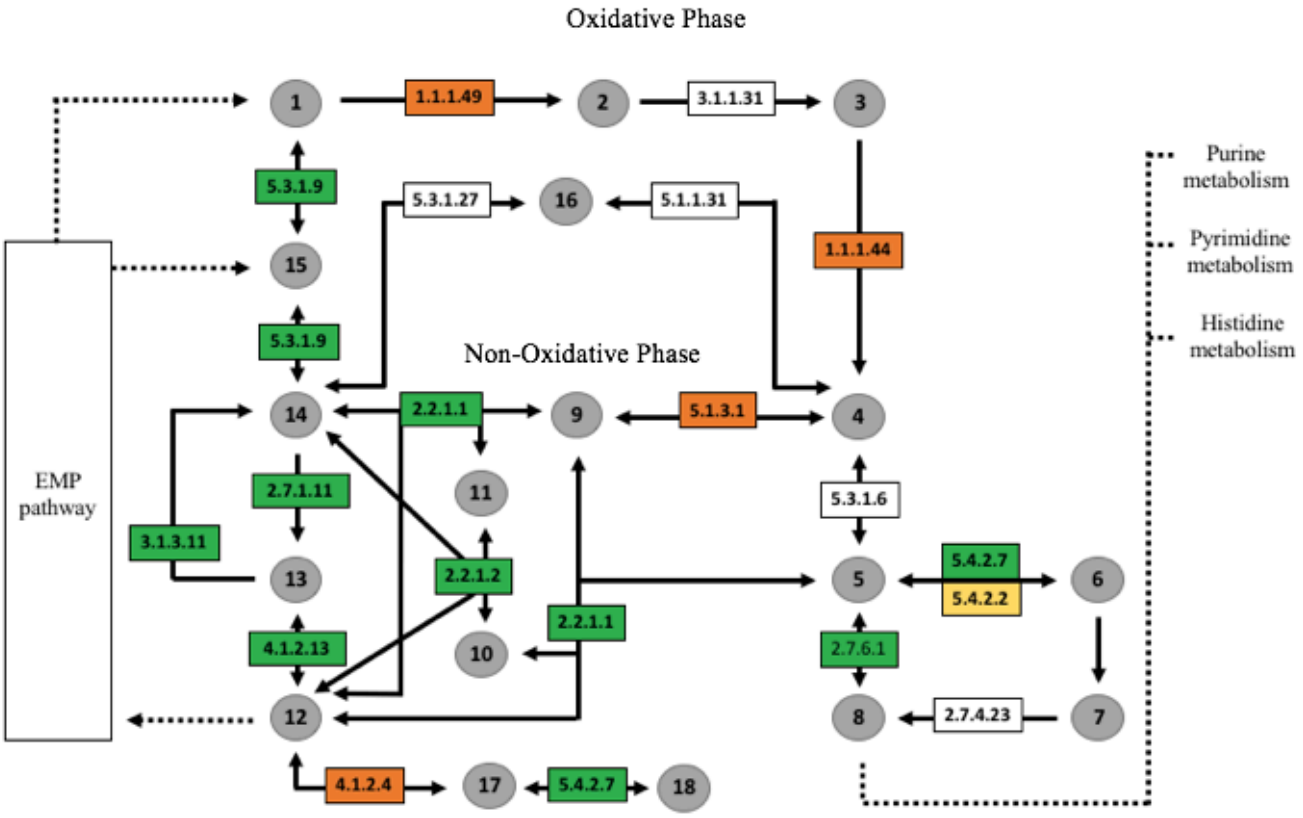

Assigned Number	Reactant/Product
1	Beta-D-glucose 6-phosphate
2	D-glucono-1,5-lactone 6-phosphate
3	6-phospho-D-gluconate
4	D-ribulose 5-phosphate
5	D-ribose 5-phosphate
6	D-ribose 1-phosphate
7	D-ribose 1,5-phosphate
8	Phosphoribosyl pyrophosphate
9	D-xylose 5-phosphate

10	D-sedoheptulose 7-phosphate
11	D-erythrose 4-phosphate
12	D-glyceraldehyde 3-phosphate
13	Beta-D-fructose 1,6-biphosphate
14	Beta-D-fructose 6-phosphate
15	Alpha-D-glucose 6-phosphate
16	D-arabino-hex-3-ulose 6-phosphate
17	2-Deoxy-D-ribose 5-phosphate
18	2-Deoxy-D-ribose 1-phosphate

Figure 3.13: **Pentose phosphate pathway**. Genes are indicated by enzyme commission (EC) numbers for the products that they encode. Green boxes represent the presence of that gene in both the data and draft genomes; Orange represents the gene was only present in the draft genomes; Yellow represents the gene was only found in the data.

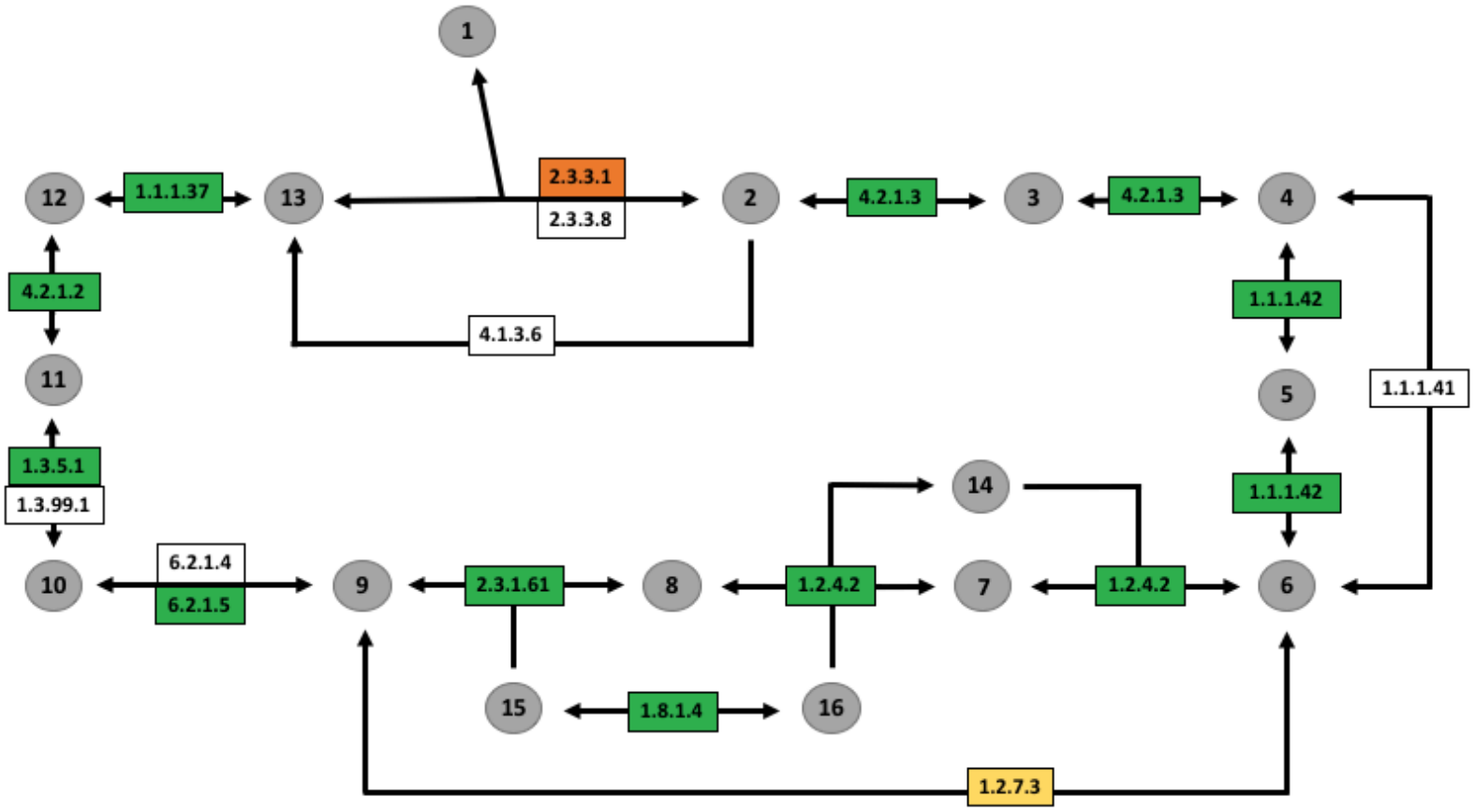

Assigned Number	Reactant/Product
1	Acetyl-CoA
2	Citrate
3	cis-Aconitate
4	Isocitrate
5	Oxalosuccinate
6	2-Oxo-glutarate
7	3-Carboxy-1-hydroxypropyl-thiamine-pyrophosphate
8	S-Succinyl-dihydrolipoamide-E
9	Succinyl-CoA
10	Succinate
11	Fumarate
12	(S)-Malate
13	Oxaloacetate
14	Thiamine pyrophosphate
15	Dihydro-lipoamide-E
16	Lipoamide-E

Figure 3.14: **Citric acid cycle**. Genes are indicated by enzyme commission (EC) numbers for the products that they encode. Green boxes represent the presence of that gene in both the data and draft genomes; Orange represents the gene was only present in the draft genomes; Yellow represents the gene was only found in the data.

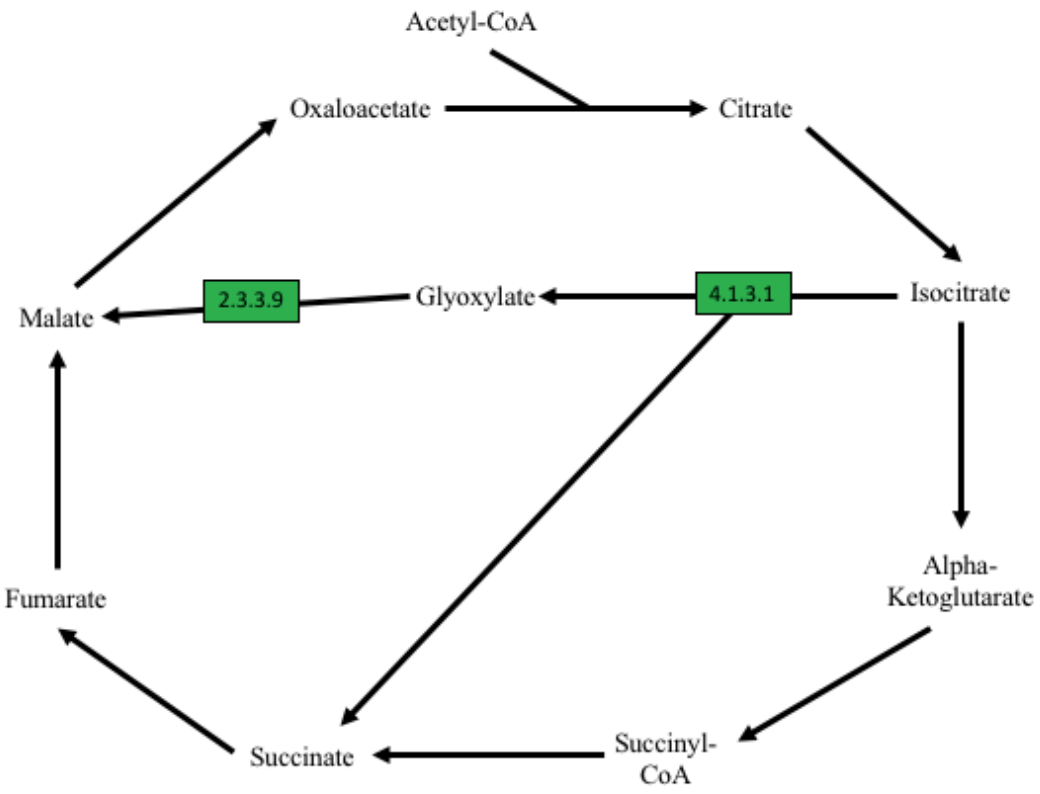

Figure 3.15: **Glyoxylate shunt**. Genes are indicated by enzyme commission (EC) numbers for the products that they encode. Green boxes represent the presence of that gene in both the data and compared draft genomes.

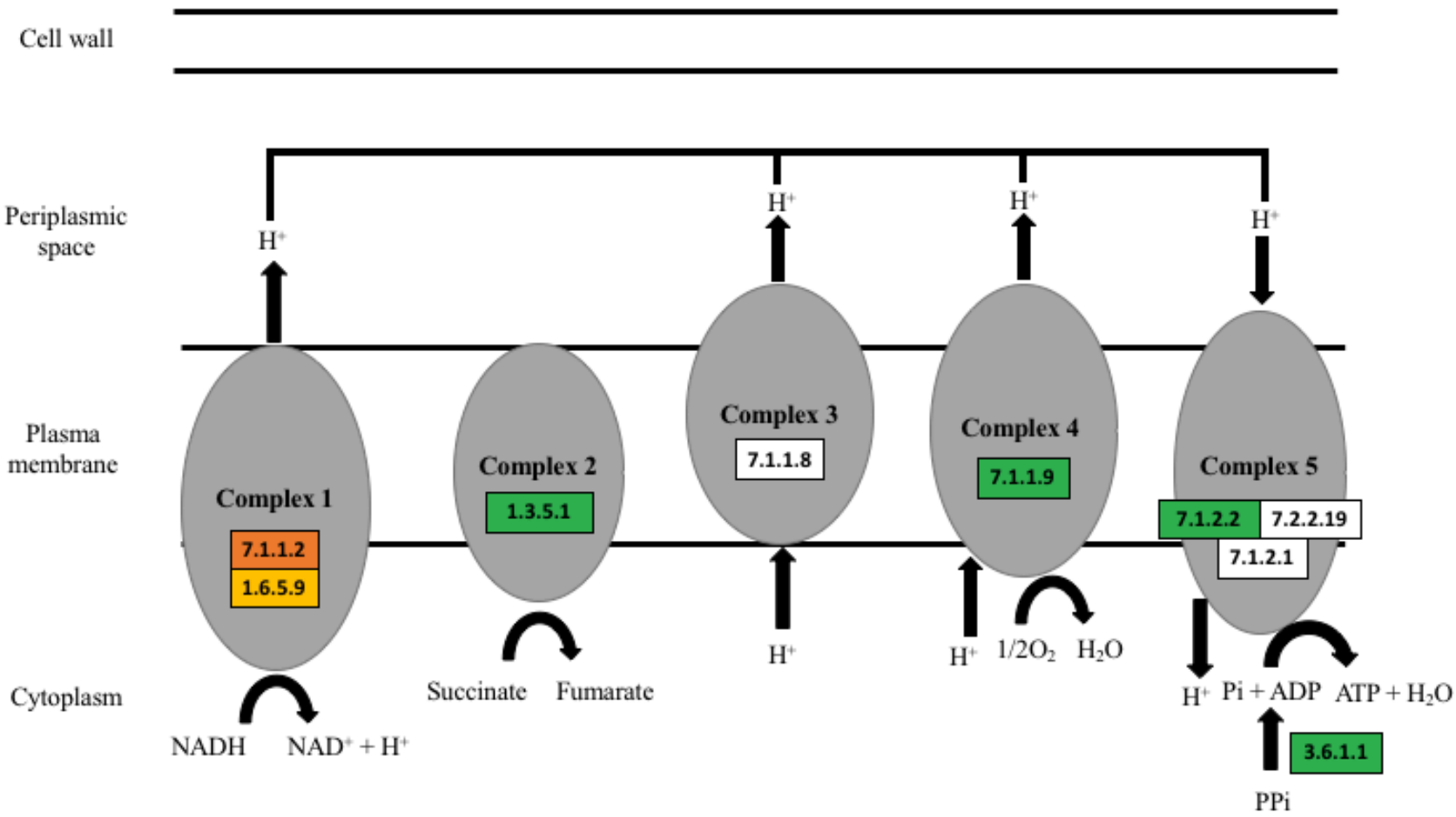

Figure 3.16: **Oxidative phosphorylation via the electron transport chain**. Genes are indicated by enzyme commission (EC) numbers for the products that they encode. Green boxes represent the presence of that gene in both the data and draft genomes; Orange represents the gene was only present in the compared genomes; Yellow represents the gene was only found in the data. Source: KEGG.

in the data whereas complex I of the electron transport chain in the *Acidibacillus* draft genomes was composed of the enzyme NADH ubiquinone reductase (EC 7.1.1.2). Multiple subunits of the enzyme NADH ubiquinone reductase were identified (EC 7.1.1.2), and multiple subunits were encoded by *ndh* and *nuo* genes (Table 3.7). These were identified on various contigs with a large cluster of genes on contig #9 found consecutively: *ndhJ*, *ndhH*, *nuoH*, *nuoI*, *nuoJ*, a gene coding for NADH-quinone oxidoreductase subunit L, *nuoL*, *ndhD1*, and *ndhB*. Subunit chains encoded by the *nuo* genes in *Ab. ferrooxidans* NOWR-5 corresponded with those of the compared draft genomes.

Three genes were found pertaining to complex II of the electron transport chain in the data, and in all of the reference genomes used for comparison. These genes were all found one after the other on contig #2: *sdhC*, *frdA*, *frdB*. However, the gene which codes for quinol cytochrome c reductase (EC 7.1.1.8) that forms the complex III was not identified in the data or in any of the reference genomes. Genes from complex IV (EC 7.1.1.9) coding for cytochrome c oxidase were found in both the data and in the reference genomes. Four quinol oxidases encoded by *qoxA*, *qoxB*, *qoxC*, and *qoxD* genes (EC 1.10.3.-.) were found consecutively on contig #1 encoding subunits 1-4. On contig #7, genes *qoxB* and *qoxC* were annotated a little upstream from *qoxB*, *qoxC*, and *qoxD*. In the *Acidibacillus* draft genomes, multiple *qox* genes were found to code for the aa3-600 menaquinol subunits I, II, and III as well as cytochrome 0 ubiquinol oxidase subunit III.

A total of 10 genes were found to code for subunits of ATP synthase (EC 7.1.2.2). On contig #4, the genes *atpB*, *atpH*, *atpF*, *atpD*, *atpA*, *atpG*, *atpD*, and *atpC* were found consecutively and transcribed for subunits a, c, b, delta, alpha, gamma, beta, and epsilon chains, respectively. All of the subunits which were identified in the data were found in the

Table 3.7: **Genes and protein products associated with components of the electron transport chain that Prokka annotated from contigs that were assembled from the Metagenome 1 sample**. Enzyme commission (EC) numbers that are associated to these products are listed if available.

Gene	Protein Product	EC Number	Contig
ndhB	NAD(P)H-quinone oxidoreductase subunit 2, chloroplastic	1.6.5.9	1
-	NADH-dehydrogenase-like protein	1.6.99.-	1
qoxA	Quinol oxidase subunit 2	1.10.3.-	1
qoxB	Quinol oxidase subunit 1	1.10.3.-	1
qoxC	Quinol oxidase subunit 3	1.10.3.-	1
qoxD	Quinol oxidase subunit 4	1.10.3.-	1
sdhC	Succinate dehydrogenase cytochrome b558 subunit	-	2
frdA	Fumarate reductase flavoprotein subunit	1.3.5.4	2
frdB	Fumarate reductase iron-sulfur subunit	1.3.5.1	2
coxM	Alternative cytochrome c oxidase subunit 2	7.1.1.9	2
ctaD	Cytochrome c oxidase subunit 1	7.1.1.9	2
ppa	Inorganic pyrophosphatase	3.6.1.1	2
ndhC	NAD(P)H-quinone oxidoreductase subunit 3	1.6.5.-	4
nqo6	NADH-quinone oxidoreductase subunit 6	1.6.5.9	4
atpB	ATP synthase subunit a	-	4
atpH	ATP synthase subunit c	-	4
atpF	ATP synthase subunit b	-	4
atpD	ATP synthase subunit delta	-	4
atpA	ATP synthase subunit alpha	7.1.2.2	4
atpG	ATP synthase gamma chain	-	4
atpD	ATP synthase subunit beta	-	4

atpC	ATP synthase epsilon chain	-	4
yglD	NADH-dehydrogenase-like protein	1.6.99.-	5
petC	Cytochrome b6-f complex iron-sulfur subunit	1.10.9.1	6
qoxB	Quinol oxidase subunit 1	1.10.3.-	7
qoxC	Quinol oxidase subunit 3	1.10.3.-	7
qoxB	Quinol oxidase subunit 1	1.10.3.-	7
qoxC	Quinol oxidase subunit 3	1.10.3.-	7
qoxD	Quinol oxidase subunit 4	1.10.3.-	7
ndhJ	NAD(P)H-quinone oxidoreductase subunit J, chloroplastic	1.6.5.9	9
ndhH	NAD(P)H-quinone oxidoreductase subunit H	1.6.5.-	9
nuoH	NADH-quinone oxidoreductase subunit H	1.6.5.9	9
nuoI	NADH-quinone oxidoreductase subunit I	1.6.5.9	9
nuoJ	NADH-quinone oxidoreductase subunit J	1.6.5.9	9
-	NADH-quinone oxidoreductase subunit 11	1.6.5.9	9
nuoL	NADH-quinone oxidoreductase subunit L	1.6.5.9	9
ndhD	NAD(P)H-quinone oxidoreductase chain 4-1	1.6.5.-	9
ndhB	NAD(P)H-quinone oxidoreductase subunit 2, chloroplastic	1.6.5.9	9
ctaD	Cytochrome c oxidase subunit 1	7.1.1.9	10
ctaC	Cytochrome c oxidase subunit 2	7.1.1.9	10

Alicyclobacillus genome and subunits alpha, beta, gamma, a, and c were identified in the *Acidibacillus* draft genomes.

Uptake and utilization of sugars

A total of 21 genes pertaining to the uptake and utilization of 10 different sugars, as well as 5 genes encoding catabolite control proteins were annotated by Prokka in the genome of *Ab. ferrooxidans* NOWR-5 (Table 3.8). The *gal* genes that are part of the Leloir pathway to synthesize the sugar nucleotides UDP-glucose (UDP-Glu) and UDP-galactose (UDP-Gal) appeared to form an operon on contig #3. RAST annotated *galT*, *galK*, *galE*, and *yoxA* that were surrounded by a gene encoding an ABC transporter ATP-binding protein and a gene encoding a transcriptional regulator of the DeoR family. Prokka annotated *galTKEM* that was surrounded by a gene encoding a putative ATP-binding protein and *lacR*. The same organization of genes was identified in the compared genomes from strains of *Ab. ferrooxidans*, and it differed from the organization in the genome of *Alicyclobacillus acidocaldarius* subsp. *acidocaldarius* DSM 446 (Figure 3.17).

Micronutrient uptake and homeostasis

All of the genes related to micronutrient uptake, transport and regulation are listed in Table 3.9. For phosphorus, this included 7 genes with functions including hydrolysis reactions, transport, and regulation. On contig #2, the genes *pstS*, *pstC*, and *pstA* were found consecutively. The genes *pstA2*, *pstC1*, *pstS1*, *pstB3*, and *phoP* were found clustered one after the other on contig #3. Genes *phoU*, *phoP*, and *phoR* (EC 2.7.13.3) were annotated on contig #9 where *phoU* was separated from *phoP* by 1 gene, and *phoR* was beside *phoU*. All of these genes

Table 3.8: **Genes and protein products associated with the uptake and utilization of sugars in *Ab. ferrooxidans* NOWR-5**. Protein products highlighted in green were also found in the compared genomes; Those highlighted in yellow indicate that the draft genomes had a gene encoding a similar enzyme; Sugar highlighted in yellow if compared genomes had different genes for this category. Enzyme commission (EC) numbers that are associated to these products are listed if available

Utilization of Sugar	Gene	Protein Product	EC Number	Contig
Glucose/Mannose Uptake	-	Glucose/mannose transporter GlcP	5.3.1.8	1
Fructose	*tpiA*	Triosephosphate isomerase	5.3.1.1	1
	fba	Fructose-biphosphate aldolase	4.1.2.13	2
	pfkA	ATP-dependent 6-phosphofructokinase	2.7.1.11	3
Glucose and Galactose Interconversions	*galM*	Aldose 1-epimerase	5.1.3.3	3
	galE	UDP-glucose 4-epimerase	5.1.3.2	3
	galK	Galactokinase	2.7.1.6	3
	galT	Galactose-1-phosphate uridylyltransferase	2.7.7.12	3
Galactitol	*gatY*	D-tagatose-1,6-biphosphate aldolase subunit GatY	4.1.2.40	10
	lacC	Tagatose-6-phosphate kinase	2.7.1.144	10
Arabinose	*araQ*	L-arabinose transport system permease proteins AraQ	-	1, 6, 10, 13, 18
	araR	Arabinose metabolism transcriptional repressor	-	1
Lactose	*lacF*	Lactose transport system permease	-	1, 6, 13
	lacR	Lactose phosphotransferase system repressor	-	3
Maltose	*malR*	HTH-type transcriptional regulator	-	1
	nplT	Neopullulanase	-	1
	malG	Maltose transport system permease protein	-	1
	apu	Amylopullulanase	-	7
Trehalose	*sugA*	Trehalose transport system permease protein	-	1, 4, 18
	sugB	Transport system permease	-	1,4
	sugC	Trehalose import ATP-binding protein	-	1
Catabolite Regulation	*ccpA*	Catabolite control protein A	-	1(3), 2, 4

A)

***Acidibacillus ferrooxidans* NOWR-5:**

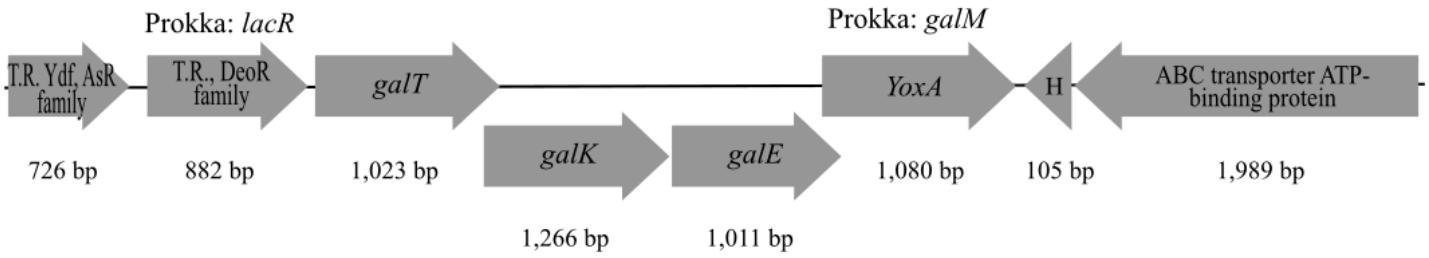

B)

***Acidibacillus ferrooxidans* strain Huett2:**

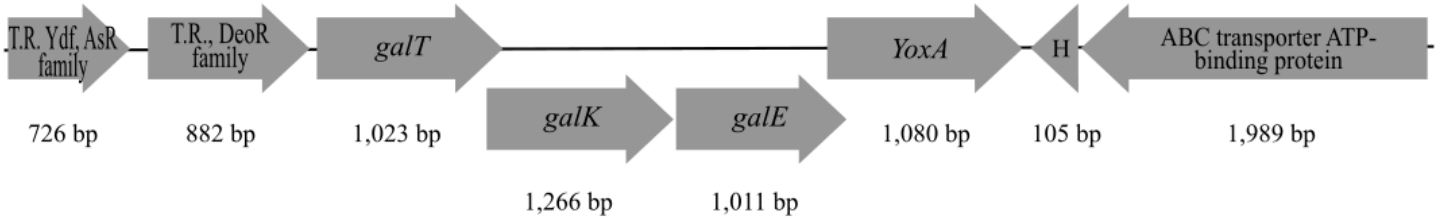

***Acidibacillus ferrooxidans* strain SLC66:**

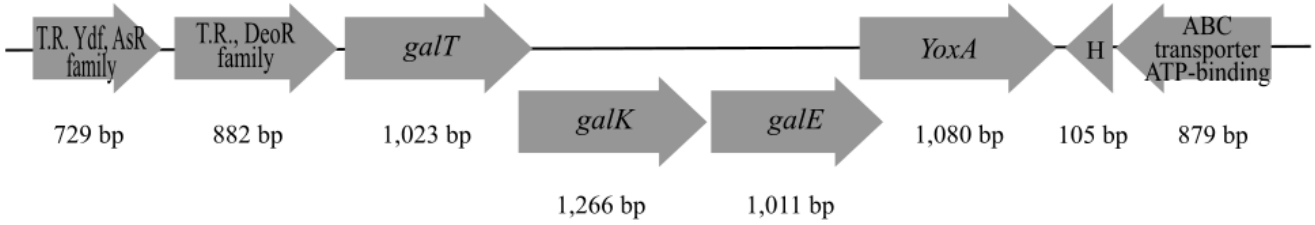

***Alicyclobacillus acidocaldarius* subsp. *acidocaldarius* DSM 446:**

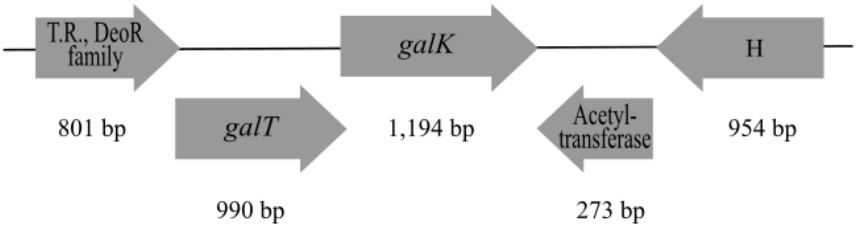

<u>Figure 3.17</u>: Organization of the *gal* operon in A) ***Ab. ferrooxidans* NOWR-5 and** B) **genomes of closely related bacteria available from PATRIC**. Differences between RAST and Prokka annotation indicated above block arrows, and gene length below. "T.R".: transcriptional regulator; "H": hypothetical protein. Protein products indicated if gene name was unavailable.

Table 3.9: **Genes and protein products associated with micronutrient uptake and utilization that Prokka annotated from contigs that were assembled from the Metagenome 1 sample**. Enzyme commission (EC) numbers that are associated to these products are listed if available.

Micronutrient	Gene	Protein Product	EC Number	Contig
Phosphorus	*ppa*	Inorganic pyrophosphatase	3.6.1.1	2
	pstS	Phosphate-binding protein PstS	-	2
	pstC	Phosphate transport system permease protein PstC	-	2
	pstA	Phosphate transport system permease protein PstA	-	2
	pstA2	Phosphate transport system permease protein PstA 2	-	3
	pstC1	Phosphate transport system permease protein PstC 1	-	3
	pstS1	Phosphate-binding protein PstS 1	-	3
	pstB3	Phosphate import ATP-binding protein PstB 3	3.6.3.27	3
	phoP	Alkaline phosphatase synthesis transcriptional regulatory protein PhoP	-	3
	ppx	Exopolyphosphatase	3.6.1.11	5
	phoP	Alkaline phosphatase synthesis transcriptional regulatory protein PhoP	-	8
	phoU	Phosphate-specific transport system accessory protein PhoU	-	9
	phoP	Alkaline phosphatase synthesis transcriptional regulatory protein PhoP	-	9
	phoR	Alkaline phosphatase synthesis sensor protein PhoR	2.7.13.3	9
	ugpC	Sn-glycerol-3-phosphate import ATP-binding protein UgpC	3.6.3.20	13
	ugpA	Sn-glycerol-3-phosphate transport system permease protein	-	13
Potassium	*kdpD*	Sensor protein KdpD	2.7.13.3	1

	kdpE	KDP operon transcriptional regulatory protein KdpE	-	1
	kdpA	Potassium-transporting ATPase potassium-binding subunit	-	1
	kdpB	Potassium-transporting ATPase ATP-binding subunit	3.6.3.12	1
	kdpC	Potassium-transporting ATPase KdpC subunit	-	1
	kdpB	Potassium-transporting ATPase ATP-binding subunit	3.6.3.12	5
	kdpA	Potassium-transporting ATPase potassium-binding subunit	-	6
	kdpB	Potassium-transporting ATPase ATP-binding subunit	3.6.3.12	6
	kdpC	Potassium-transporting ATPase KdpC subunit	-	6
	kdpE	Transcriptional regulatory protein KdpE	-	8
Calcium	-	Ca(2+)/H(+) antiporter	-	5

No annotations were identified pertaining to the transport of magnesium. Genes coding for a magnesium and cobalt transport protein CorA as well as a gene for a magnesium and cobalt efflux protein CorC were found in the *Acidibacillus* genomes.

Metal homeostasis and resistance

A dozen genes related to the resistance of various metals were identified in the data (Table 3.10). The *arsB* gene was found directly beside *arsC* on contig #2, and genes *copA* and *copZ* were found consecutively on contig #30. This contig only contained one other gene that was annotated as coding for a hypothetical protein. Proteins from this category found in *Acidibacillus* genomes included a repressor CsoR of the *copAZ* operon, a copper-translocating P-type ATPase, a mercuric iron reductase, a HoxN/HupN/NixA family nickel/cobalt transporter, and ABC transporter permease proteins (nickel/peptides/opines).

Maintenance of intracellular pH

In the data, 13 genes were annotated which have been documented to maintain intracellular pH in acidic conditions (Table 3.11). Only the *Ab. ferrooxidans* strain Huett2 genome contained a gene encoding a lactate 2-monooxygenase which was annotated on contig #1. A total of 3 *acs* genes were identified in *Ab. ferrrooxidans* NOWR-5 and this was consistent with the compared draft genomes. The data contained 2 *speA* genes, on contig #4 and 5, and *Acidibacillus* draft genomes had the same amount. Other genes which were found in both the data and compared genomes were *clpP* and *clpX* that appeared to form an operon on contig #2. The two genes which were only found in the *Ab. ferrooxidans* NOWR-5 genome were *hup* and

Table 3.10: **Genes and protein products associated with metal homeostasis and resistance that Prokka annotated from contigs that were assembled from the Metagenome 1 sample**. Enzyme commission (EC) numbers that are associated to these products are listed if available.

Gene	Protein Product	EC Number	Contig
czcD	Cadmium, cobalt and zinc/H(+)-K(+) antiporter	-	1
merA	Mercuric reductase	1.16.1.1	1
mntH	Divalent metal cation transporter MntH	-	1
nikB	Nickel transport system permease protein NikB	-	1
arsB	Arsenical pump membrane protein	-	2
arsC	Arsenate reductase	1.20.4.4	2
mntH	Divalent metal cation transporter MntH	-	3
czcR	Transcriptional activator protein CzcR	-	3
arsR	Arsenical resistance operon repressor	-	4
mntP	Putative manganese efflux pump MntP	-	4
mntH	Divalent metal cation transporter MntH	-	7
copA	Copper resistance protein A	-	8
copA	Putative copper-importing P-type ATPase A	3.6.3.54	10
mntP	Putative manganese efflux pump MntP	-	10
nixA	High-affinity nickel-transport protein NixA	-	15
copA	Putative copper-importing P-type ATPase A	3.6.3.54	30
copZ	Copper chaperone CopZ	-	30

Table 3.11: **Genes and protein products associated with maintaining intracellular pH that Prokka annotated from contigs that were assembled from the Metagenome 1 sample**.

Enzyme commission (EC) numbers that are associated to these products are listed if available.

Category	Gene	Protein Product	EC Number	Contig
Maintenance of intracellular pH	-	Lactate 2-monooxygenase	1.13.12.4	1
	napA	Na(+)/H(+) antiporter	-	2
	acsA	Acetyl-coenzyme A synthetase	6.2.1.1	2
	acs	Acetyl-coenzyme A synthetase	6.2.1.1	2
	clpP	ATP-dependent Clp protease proteolytic subunit	3.4.21.92	2
	clpX	ATP-dependent Clp protease ATP-binding subunit ClpX	-	2
	lexA	LexA repressor	3.4.21.88	2
	-	Sodium-lithium/proton antiporter	-	3
	speA	Arginine decarboxylase	4.1.1.19	4
	acs	Acetyl-coenzyme A synthetase	6.2.1.1	4
	speA	Arginine decarboxylase	4.1.1.19	5
	clpP	ATP-dependent Clp protease proteolytic subunit	3.4.21.92	8
	hup	DNA-binding protein HU	-	14
Oxidative stress response	*prxU*	Selenocysteine-containing peroxiredoxin PrxU	1.11.1.15	1
	perR	Peroxide-responsive repressor PerR	-	1
	katA	Vegetative catalase	1.11.16	1
	oxyR	Hydrogen peroxide-inducible genes activator	-	1
	mutM	Formamidopyrimidine-DNA glycosylase	3.2.2.23	3
	mutY	Adenine DNA glycosylase	3.2.2.-	3
	nfo	Putative endonuclease 4	3.1.21.2	5
	bcp	Putative peroxiredoxin bcp	1.11.1.15	5
	-	Manganese catalase	1.11.1.6	6
	ahpE	Alkyl hydroperoxide reductase E	1.11.1.15	7
	fumC	Fumarate hydratase class II	4.2.1.2	15
Cold-shock response	*cspC*	Cold shock protein CspC	-	15

another gene coding for a sodium-lithium/proton antiporter. RAST annotated a total of 28 DNA repair genes in the data (Table 3.12). The draft genome of *Ab. ferrooxidans* strain Huett2 contained 37, and the complete *Alicyclobacillus* genome had 55.

Stress responses

A dozen genes for which the products are involved in oxidative stress response were identified in the data (Table 3.11). Mechanisms included regulating metal uptake and oxidative stress, detoxifying the cell from peroxide, as well as repairing DNA when damaged. All of the genes, except for the regulatory *oxyR* and *perR* for peroxiredoxin products, were also identified in the *Acidibacillus* genomes.

Three cold shock proteins of the CSP family were found in *Alicyclobacillus* genomes, and *cspC* was annotated on contig #15. The *Acidibacillus* draft genomes had multiple genes coding for heat shock proteins that were not annotated in the data. These encoded the heat shock protein 60 kDa family chaperone GroEL, the heat-inducible transcription repressor HrcA, and the heat shock protein 10 kDa family chaperone GroES

Resistance to antibiotics

A total of 17 genes which contribute to the resistance of antibiotics were identified in *Ab. ferrooxidans* NOWR-5 (Table 3.13). The *yheH* and *yheI* genes were found one after the other on contig #2. Most of these genes were absent in the compared genomes. The *Acidibacillus* draft genomes contained genes for protein products including a permease multidrug efflux protein, undecaprenyl-diphosphatase BcrC, and undecaprenyl-diphosphatase. The *Alicyclobacillus* genome contained genes for a heterodimeric efflux ABC transporter,

Table 3.12: **Genes and protein products associated with DNA repair that RAST annotated from contigs that were assembled from the Metagenome 1 sample**. Most were annotated by Prokka as well. Enzyme commission (EC) numbers that are associated to these products are listed if available.

Gene	Protein Product	EC Number	Contig
uvrB	UvrABC system protein B	-	1
uvrA	UvrABC system protein A	-	1
adaA	Bifunctional transcriptional activator/DNA repair enzyme	2.1.1.-	1
uvrC	UvrABC system protein C	-	2
-	DinG family ATP-dependent helicase YoaA	-	2
gph	Phosphoglycolate phosphatase	3.1.3.18	2
xseA	Endodeoxyribonuclease 7 large subunit	3.1.11.6	2
xseB	Endodeoxyribonuclease 7 small subunit	3.1.11.6	2
lexA	LexA repressor	3.4.21.88	2
recN	DNA repair protein RecN	-	2
tag	DNA-3-methyladenine glycosylase 1	3.2.2.20	2
pcrA	ATP-dependent DNA helicase PcrA	3.6.4.12	2
mutY	Adenine DNA glycosylase	3.2.2.-	3
mutM	Formamidopyrimidine-DNA glycosylase	3.2.2.23	3
polA	DNA polymerase I	2.7.7.7	3
dnaE	DNA polymerase III subunit alpha	2.7.7.7	3
mug	G/U mismatch-specific DNA glycosylase	3.2.2.28	4
ssbA	Single-stranded DNA-binding protein A	-	4
gph	Phosphoglycolate phosphatase	3.1.3.18	5
nfo	Putative endonuclease 4	3.1.21.2	5
adaB	Methylated-DNA—protein-cysteine methyltransferase, inducible	2.1.1.63	7
alkA	DNA-3-methyladenine glycosylase	3.2.2.21	7
haeIIIM	Modification methylase HaeIII	2.1.1.37	8
hhaIM	Modification methylase HaeI	2.1.1.37	8
recD2	ATP-dependent RecD-like DNA helicase	3.6.4.12	9
gph	Phosphoglycolate phosphatase	3.1.3.8	10
exoA	Exodeoxyribonuclease	3.1.11.2	10
radA	DNA repair protein RadA	3.6.4.-	11
polC	DNA polymerase III PolC-type	2.7.7.7	12

Table 3.13: **Genes and protein products associated with antibiotic resistance that Prokka annotated from contigs that were assembled from the Metagenome 1 sample**. Enzyme commission (EC) numbers that are associated to these products are listed if available.

Gene	Protein Product	EC Number	Contig
mdtD	Putative multidrug resistance protein MdtD	-	1
-	Putative multidrug-efflux transporter	-	1
tetA	Tetracycline resistance	-	1
mdtC	Multidrug resistance protein MdtC	-	1
yheH	Putative multidrug resistance ABC transporter ATP-binding/permease protein YheH	3.6.3.-	2
yheI	Putative multidrug resistance ABC transporter ATP-binding/permease protein YheI	3.6.3.-	2
bmr3	Multidrug resistance protein 3	-	2
bmr3	Multidrug resistance protein 3	-	2
uppP	Undecaprenyl-diphosphatase	3.6.1.27	2
uppP	Undecaprenyl-diphosphatase	3.6.1.27	5
bcrC	Undecaprenyl-diphosphatase BcrC	3.6.1.27	6
mdtA	Multidrug resistance protein MdtA	-	9
bmr3	Multidrug resistance protein 3	-	10
fsr	Fosmidomycin resistance protein	-	10
stp	Multidrug resistance protein Stp	-	11
sttH	Streptothricin hydrolase	3.5.2.19	13
sttH	Streptothricin hydrolase	3.5.2.19	13

multidrug resistance BmrC and BmrD of the BmrCD subunit, and 4 undecaprenyl-diphosphatases.

Sporulation

A total of 39 genes were identified on various contigs for different stages of sporulation. The *Ab. ferrooxidans* strain Huett2 draft genome contained a total of 21, and the complete genome of *Alicyclobacillus* had 98. All of the genes found in the data are listed in Table 3.14, and those highlighted in green were also found in *Acidibacillus*. Some important sporulation genes were identified in the most similar genomes but were absent from the data, such as the Cot protein coding genes, *spoIIR* and *spoVR*.

Biofilm formation

There were no genes annotated by RAST pertaining to the formation of biofilms. The Prokka data had only a couple genes which appeared to be relevant including a *veg* gene encoding a Veg protein on contig #4, as well as the *gal* genes involved in the Leloir pathway to synthesize exopolysaccharide precursors. The *veg* gene was also found in the genomes of *Acidibacillus*.

Motility and chemotaxis

A total of 20 genes were identified pertaining to flagellar structure and to chemotaxis. In addition, a *pilT* gene was detected, putatively encoding a retraction ATPase that typically depolymerizes the fiber of an extended type IV pilus, suggesting the potential for twitching motility in this bacterium. The *swrD* gene was also detected; it is believed to increase

Table 3.14: **Genes and protein products associated with sporulation that Prokka annotated from contigs that were assembled from the Metagenome 1 sample**. Genes highlighted in green were also present in *Ab. ferrooxidans* draft genomes. Enzyme commission (EC) numbers that are associated to these products are listed if available.

Gene	Protein Product	EC Number	Contig
gerAA	Spore germination protein A1	-	1
yndE	Spore germination protein YndE	-	1
gerBC	Spore germination protein B3	-	1
ydcC	Sporulation protein YdcC	-	1
whiA	Sporulation transcription regulator WhiA	-	1
kinE	Sporulation kinase E	2.7.13.3	1
gerE	Spore germination protein GerE	-	2
sleB	Spore cortex-lytic enzyme	-	2
spoIVFB	Stage IV sporulation protein FB	-	2
spoIIIAE	Stage III sporulation protein AE	-	2
spoIIIAH	Stage III sporulation protein AH	-	2
spo0A	Stage 0 sporulation protein A	-	2
spoIVA	Stage IV sporulation protein A	3.6.1.3	2
spmB	Spore maturation protein B	-	2
spmA	Spore maturation protein A	-	2
ytfJ	Putative spore protein YtfJ	-	2
ylbJ	Sporulation integral membrane protein YlbJ	-	2
rsfA	Prespore-specific transcriptional regulator RsfA	-	3
gerXA	Spore germination protein XA	-	3
soj	Sporulation initiation inhibitor protein Soj	3.6.-.-	4
spo0J	Stage 0 sporulation protein J	-	4
sigK	RNA polymerase sigma-K factor	-	4
sigK	RNA polymerase sigma-28 factor	-	4
yabG	Sporulation-specific protease YabG	3.4.-.-	4

spoVT	Stage V sporulation protein T	-	4
spo0F	Sporulation initiation phosphotransferase F	2.7.-.-	4
yheD	Endospore coat-associated protein YheD	-	5
tlp	Small, acid-soluble spore protein Tlp	-	5
yndE	Spore germination protein YndE	-	6
gerBC	Spore germination protein B3	-	6
gerBA	Spore germination protein B1	-	6
paiB	Protease synthase and sporulation protein PAI 2	-	7
spoIIQ	Stage II sporulation protein Q	-	9
spoIIID	Stage III sporulation protein D	-	9
tlp	Small, acid-soluble spore protein Tlp	-	10
yaah	Spore germination protein YaaH	-	10
lipC	Spore germination lipase LipC	3.-.-.-	11
spoIIE	Stage II sporulation protein E	3.1.3.16	14
yabP	Spore protein YabP	-	14

the power of flagellar motors and is thus implicated in flagella-mediated swarming motility, suggesting the potential for this type of motility in this bacterium (Table 3.15). Most of the genes were found clustered on contig #12, and some were identified directly following each other such as *fliG*, *fliF*, *fliE*, *flgC* and *flgB* as well as *cheD*, *cheC* and *cheW*. The gene *ylxH* was located near *cheW*. Most of the genes were also found in the compared draft genomes.

3.4.2 Metagenome 2: fungal target

A total of 7,968 contigs and 7,891 scaffolds were assembled by SPAdes. The largest (#1) was 217,161 bp with a coverage value of 4.42X. Scaffolds up to and including #30 were over 160,000 bp with coverage values remaining consistent around 4X. Scaffolds following #4,385 were very small (< 200 bp) with slightly higher coverage values that remained under 10X. The uploaded and post QC sequence count from MG-RAST had a total length of 38,434,819 bp and a mean sequence length of 4,871±14,203 bp. MG-RAST predicted 31,014 protein features and 236 rRNA features, as well as identified 13,067 protein features and 29 rRNA features. The reported mean GC-content percentage was 42±8%.

MG-RAST classified that 98.37% of the 27,698 taxonomic hits from the sample belonged to the domain Eukaryota and 1.61% to Bacteria. Analysis of eukaryotic hits indicated that 99.26% of them belonged to the Ascomycota phylum and 0.38% to Basidiomycota. The identification of hits at the class level within the Ascomycota phylum is presented in Figure 3.18. All of the hits from the Eurotiales order (23,930) were identified as belonging to the *Trichocomaceae* family, and Figure 3.19 shows the identification of hits at the genus level. Hits from the Sordariomycetes class were classified into 4 orders (Figure 3.20).

Table 3.15: **Genes and protein products associated with motility and chemotaxis that Prokka annotated from contigs that were assembled from the Metagenome 1 sample**. Genes highlighted in yellow were also present in *Ab. ferrooxidans* draft genomes. Enzyme commission (EC) numbers that are associated to these products are listed if available.

Category	Gene	Protein Product	EC Number	Contig
Flagellar assembly	*flgG*	Flagellar basal-body rod protein FlgG	-	9
	hag	Flagellin	-	9
	flgK	Flagellar hook-associated protein 1	-	9
	ylxH	Flagellum site-determining protein YlxH	-	12
	flhA	Flagellar biosynthesis protein FlhA	-	12
	flhB	Flagellar biosynthetic protein FlhB	-	12
	fliP	Flagellar biosynthetic protein FliP	-	12
	fliM	Flagellar motor switch protein FliM	-	12
	flgG	Flagellar basal-body rod protein FlgG	-	12
	fliG	Flagellar motor switch protein FliG	-	12
	fliF	Flagellar M-ring protein	-	12
	fliE	Flagellar hook-basal body complex protein FliE	-	12
	flgC	Flagellar basal-body rod protein FlgC	-	12
	flgB	Flagellar basal body rod protein FlgB	-	12
Chemotaxis	*pomA*	Chemotaxis protein PomA	-	1
	cheB	Chemotaxis response regulator protein-glutamate	3.1.1.61	2
	cheR	Chemotaxis protein methyltransferase	-	2
	cheD	Chemoreceptor glutamine deamidase CheD	-	12
	cheC	Che-Y phosphatase CheC	-	12
	cheW	Chemotaxis protein CheW	-	12
	cheY	Chemotaxis protein CheY	-	12
	cheB	Chemotaxis response regulator protein-glutamate	3.1.1.61	13
Motility	*pilT*	Twitching motility protein	-	2
	swrD	Swarming motility protein SwrD	-	12

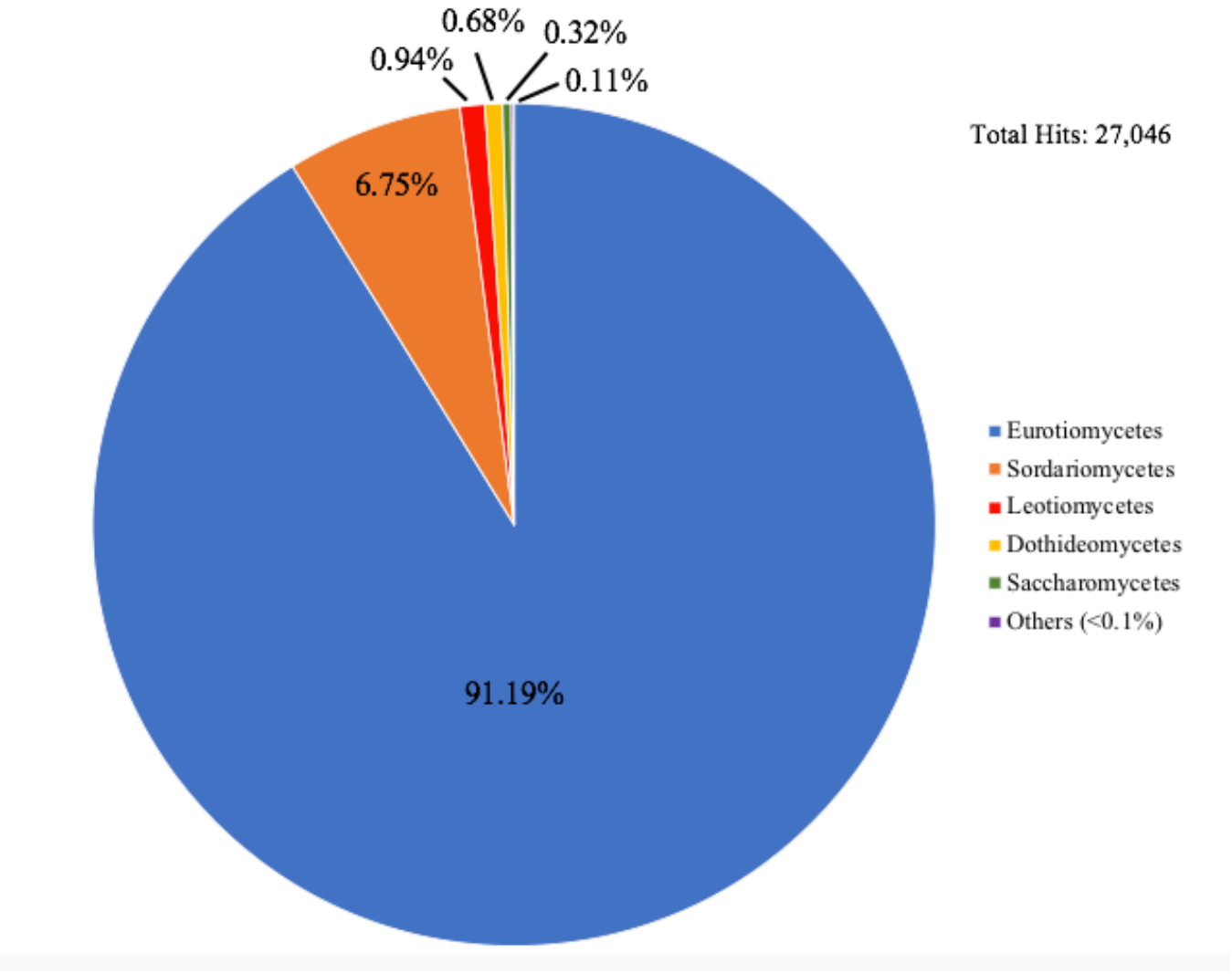

<u>Figure 3.18</u>: Identification of classes within the Ascomycota phylum in the Metagenome 2 sample as annotated by MG-RAST.

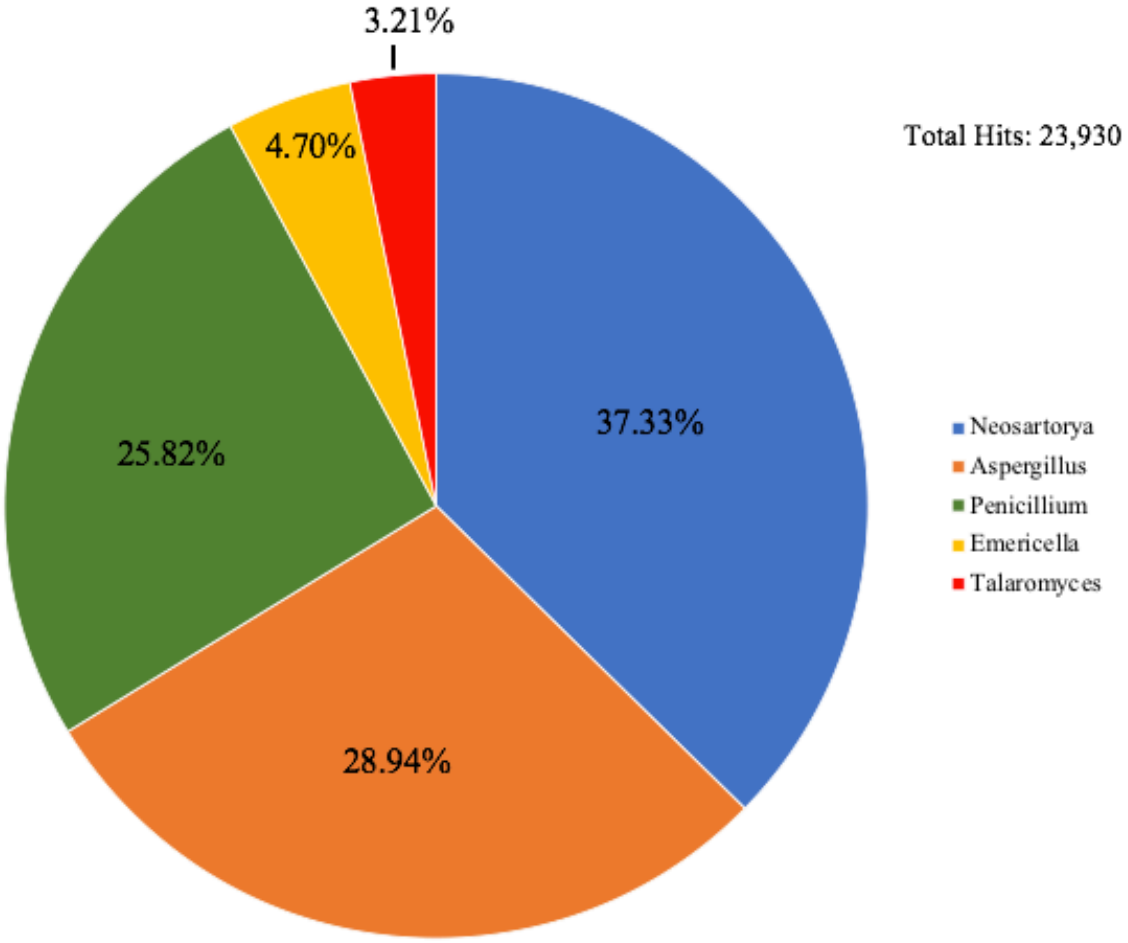

Figure 3.19: **Identification of genera within the *Trichocomaceae* family in the Metagenome 2 sample as annotated by MG-RAST**.

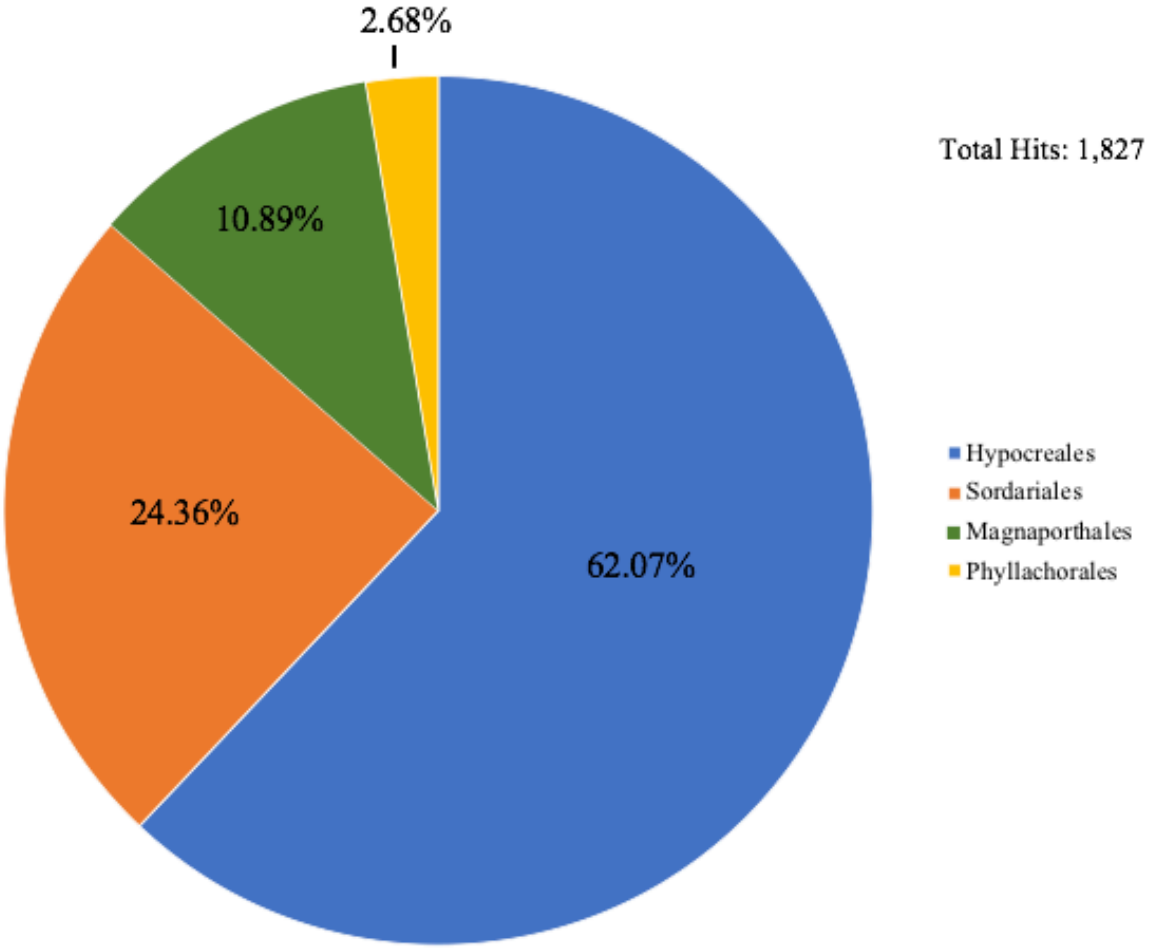

Figure 3.20: **Identification of orders within the Sordariomycetes class in the Metagenome 2 sample as annotated by MG-RAST**.

Identification of the 1.61% of bacterial hits at the phylum level suggested the presence of some notable phyla including Proteobacteria, Actinobacteria, and Firmicutes (Figure 3.21). Within the Firmicutes phylum, 66% of hits were assigned to Bacilli. Hits from the Bacilli class were identified as 81.82% Bacillales, and results showed hits within this order were consistent with the families identified in the Metagenome 1 sample (Figure 3.22). Bacterial classes assigned by MG-RAST to the Proteobacteria phylum are presented in Figure 3.23. Hits from the Actinobacteria phylum were assigned to various families within the order Actinomycetales (Figure 3.24).

Preliminary genetic description of *Penicillium* sp.

MG-RAST annotated 152 hits which belonged to the domain Eukaryota using the subsystems database. Of these 152 subsystem hits, 149 were classified as belonging to the phylum Ascomycota. Only 9 hits were assigned to the Eurotiomycetes class and to the genus *Penicillium*. All of these were associated with respiration. The majority of hits (133/149) from the Ascomycota phylum were classified as belonging to the Sordariomycetes class. Specifically, 78 for the order Hypocreales, 33 for Sordariales, and 22 for Magnaporthales. Subsystem categories in which hits were annotated as belonging to the Ascomycota phylum are listed in Table 3.16.

Hits from the Sordariomycetes class included genes for the uptake and utilization of various sugars such as trehalose (Trehalase: EC 3.2.1.28), L-fructose (L-fuconate dehydratase: EC 4.2.1.68), mannose (Beta-mannosidase: EC 3.2.1.25), xylose (Alpha-xylosidase: EC 3.2.1.-), L-rhamnose (Alpha-L-rhamnosidase: EC 3.2.1.40), D-galacturonate and D-glucuronate (2-deoxy-D-gluconate 3-dehydrogenase: EC 1.1.1.125), fructooligosaccharides and raffinose (Alpha-

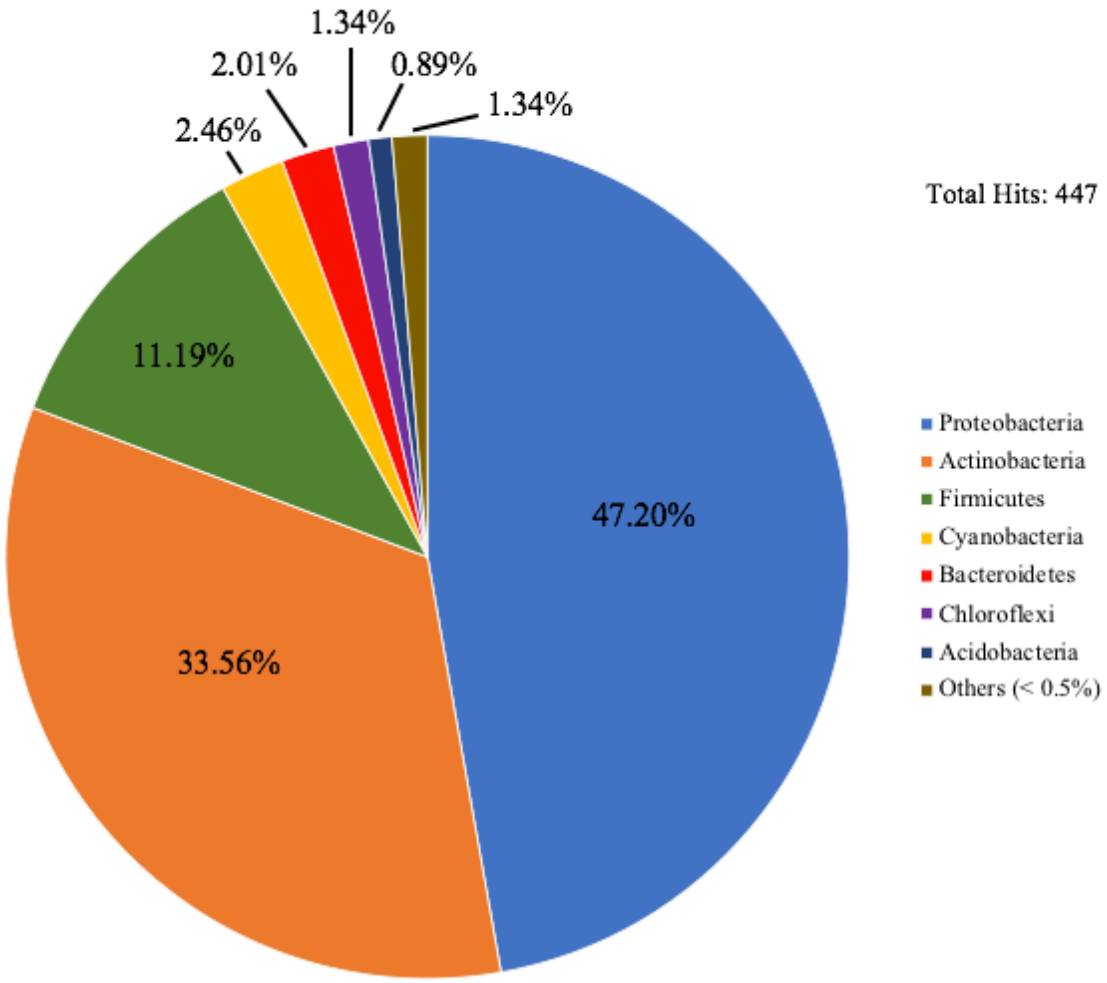

Figure 3.21: **Identification of bacterial phyla in the Metagenome 2 sample as annotated by MG-RAST**.

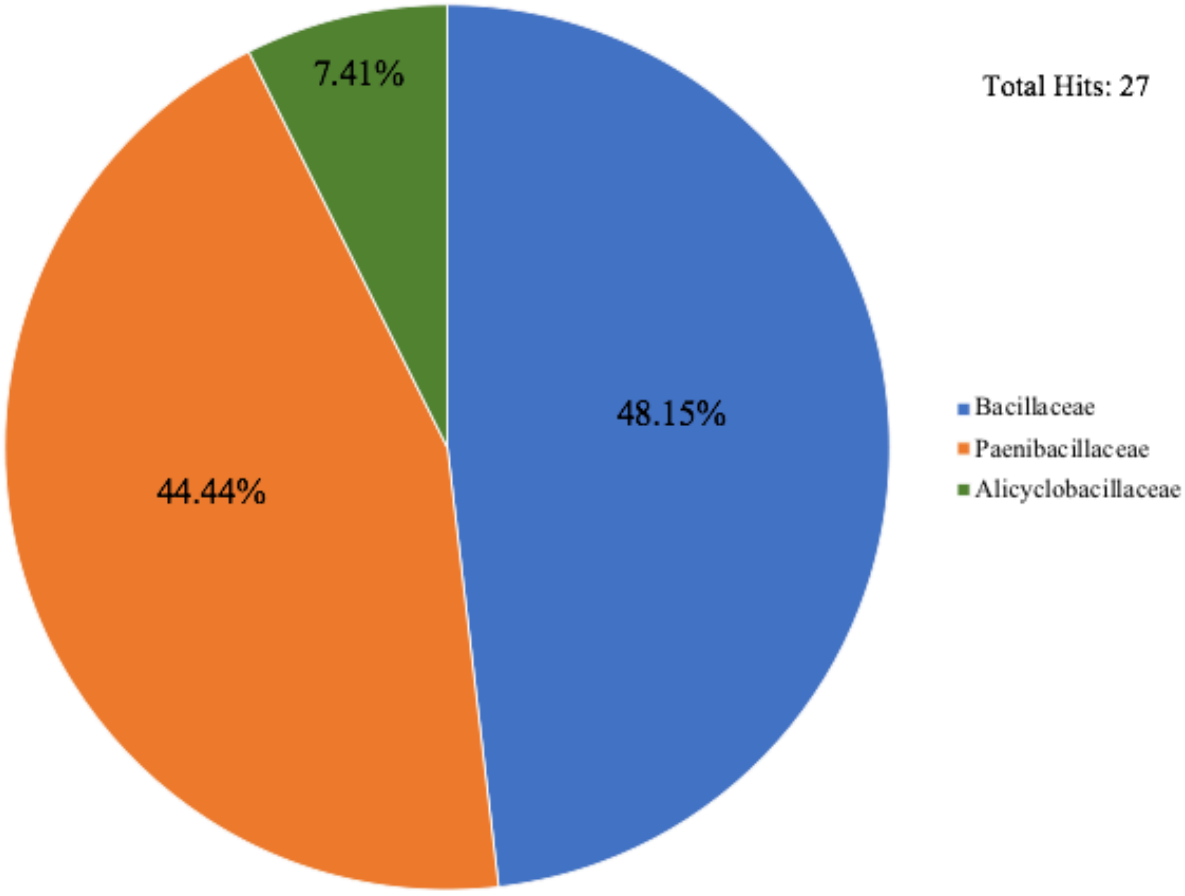

Figure 3.22: **Identification of bacterial families within the Bacillales order in the Metagenome 2 sample as annotated by MG-RAST**.

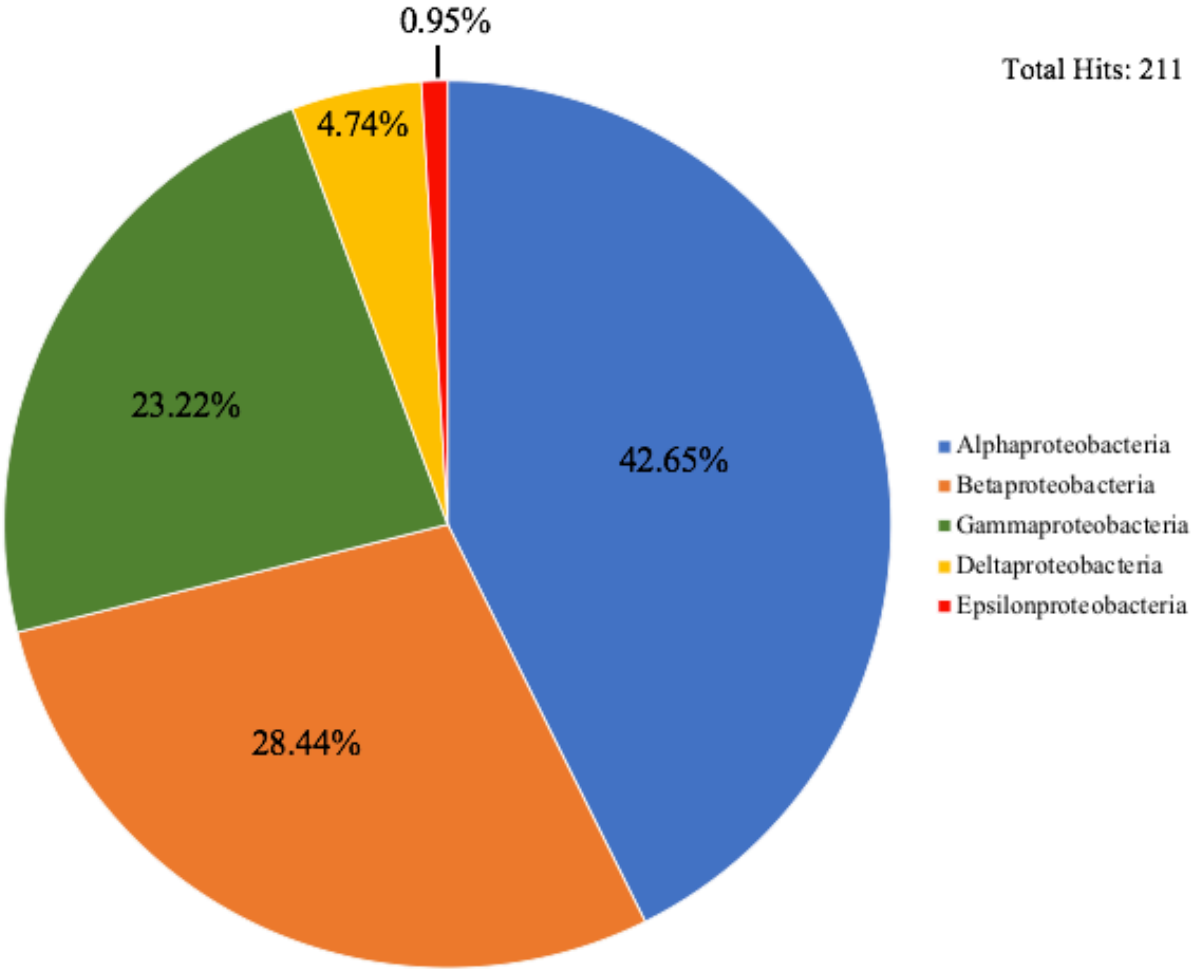

Figure 3.23: **Identification of bacterial classes within the Proteobacteria phylum in the Metagenome 2 sample as annotated by MG-RAST**.

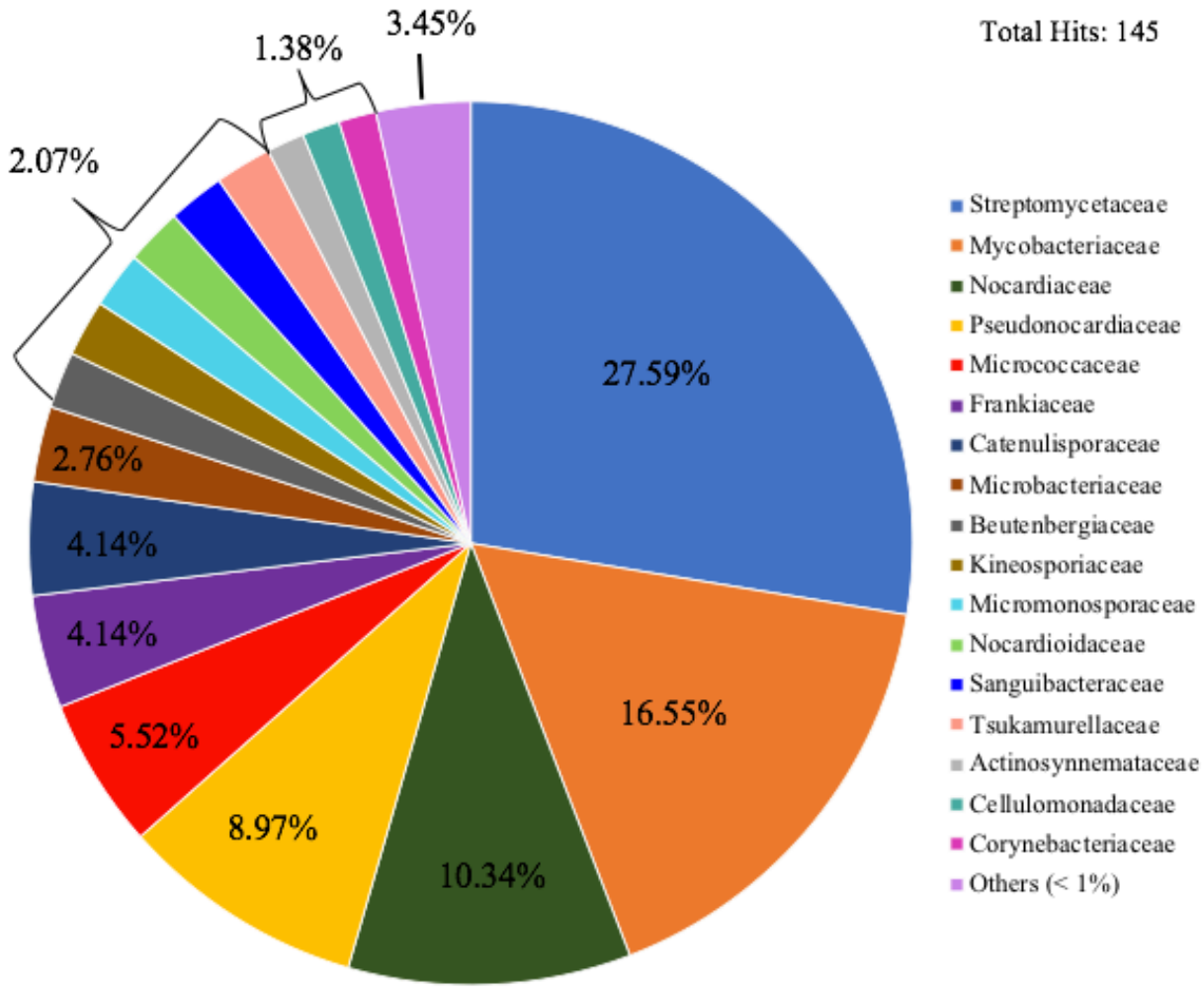

Figure 3.24: **Identification of bacterial families within the Actinomycetales order in the Metagenome 2 sample as annotated by MG-RAST**.

Table 3.16: **Number of subsystem hits for each category that MG-RAST assigned to the phylum Ascomycota**.

Level 1	Level 2	Number of Hits
Amino Acids and Derivatives	Alanine, serine, glycine	5
	Aromatic amino acids and derivatives	4
	Branched-chain amino acids	3
	Histidine metabolism	2
	Lysine, threonine, methionine, and cysteine	5
	Proline and 4-hydroxyproline	2
Carbohydrates	CO_2 fixation	2
	Central carbohydrate metabolism	7
	Di- and oligosaccharides	2
	Fermentation	1
	Monosaccharides	10
	One-carbon metabolism	1
	Sugar alcohols	1
Clustering-based subsystems	Choline bitartrate degradation, putative	1
	Clustering-based subsystems	1
Cofactors, vitamins, prosthetic groups, pigments	Biotin	1
	Coenzyme M	1
	Folate and pterines	2
	NAD and NADP	1
	Tetrapyrroles	1
Fatty acids, lipids, and isoprenoids	Isoprenoids	2
	Phospholipids	5
Membrane Transport	Sugar Phosphotransferase System, PTS	1
Metabolism of aromatic compounds	Metabolism of central aromatic intermediates	1

	Peripheral pathways for catabolism of aromatic compounds	7
Miscellaneous	Plant-Prokaryotic DOE project	15
Nucleosides and nucleotides	Detoxification	2
	Purines	5
Phages, prophages, transposable elements, plasmids	Phages, prophages	1
Protein metabolism	Protein biosynthesis	10
	Protein degradation	4
RNA metabolism	Transcription	2
Respiration	NULL	14
Stress response	Heat shock	1
	Oxidative stress	5
Sulfur metabolism	Inorganic sulfur assimilation	1
Virulence, disease and defense	Resistance to antibiotics and toxic compounds	4

mannosidase: EC 3.2.1.24), as well as mannitol (Multi polyol-specific dehydrogenase: EC 1.1.1.-).

The only gene found in the nitrogen metabolism subsystem encoded a carbonic anhydrase (EC 4.2.1.1) for cyanate hydrolysis.

Predicted proteins associated with fatty acids, lipids and isoprenoids included an acyl-CoA dependent ceramide synthase (EC 2.3.1.4) for sphingolipid biosynthesis, and 4 aldehyde dehydrogenases (EC 1.2.1.3) for glycerolipid and glycerophospholipid metabolism in bacteria. BLAST results for this gene indicated that it was fungal, and the longest sequence matched best to *P. chrysogenum* Wisconsin 54-1255 with 99% query cover and 76.68% identity (Table 3.17). Genes associated with the cell wall and capsule were predicted to encode the proteins N-acylglucosamine-1-phosphate uridyltransferase (EC 2.7.7.23) and anhydro-N-acetylmuramic acid kinase (EC 2.7.1.-) for peptidoglycan biosynthesis and recycling of peptidoglycan amino sugars, respectively. BLAST results supported that both of these belonged to a fungal organism and the gene sequence classified as being involved in peptidoglycan biosynthesis was most similar to a sequence from the genome of *P. chrysogenum* Wisconsin 54-1255 with a query cover of 61% and 71.60% identity (Table 3.18).

Four genes predicted to be involved in maintaining copper homeostasis were identified. The predicted proteins for these genes were multicopper oxidases. BLAST results supported that these sequences correspond to fungal multicopper oxidase-encoding genes (Table 3.19). Sequences in Appx. C.

Table 3.17: **BLAST results for the two largest sequences annotated by MG-RAST as belonging to the phylum Ascomycota and encoding aldehyde dehydrogenase enzymes**. NCBI Accession numbers for most similar sequences are provided.

Gene Size (bp)	Most Similar Sequences in NCBI Database	Query Cover	Percent Identity	Accession Number
1632	*Penicillium chrysogenum* Wisconsin 54-1255 complete genome	99%	76.68%	AM920437.1
	Penicillium arizonense hypothetical protein, partial mRNA	87%	82.14%	XM_022634243.1
	Penicillium expansum aldehyde dehydrogenase, N-terminal, partial mRNA	90%	80.71%	XM_016743136.1
774	*Fonsecaea erecta* aldehyde dehydrogenase, partial mRNA	53%	68.97%	XM_018835952.1
	Westerdykella ornata aldehyde dehydrogenase-like protein, mRNA	50%	69.49%	XM_033800462.1
	Penicillium digitatum Pd1 betaine-aldehyde dehydrogenase, putative mRNA	66%	68.62%	XM_014682515.1
	Penicillium chrysogenum Wisconsin 54-1255 hypothetical protein, mRNA	57%	68.01%	XM_002565590.1

Table 3.18: **BLAST results for sequences annotated by MG-RAST as belonging to the Ascomycota phylum and encoding protein products involved with peptidoglycan**. Enzyme commission (EC) numbers that are associated to these products are listed. NCBI Accession numbers for most similar sequences are provided.

EC Number	Gene Size (bp)	Most Similar Sequences in NCBI Database	Query Cover	Percent Identity	Accession Number
2.7.7.23	1,704	*Penicillium chrysogenum* Wisconsin 54-1255 complete genome	61%	71.60%	AM920437.1
		Penicillium arizonense hypothetical protein, partial mRNA	57%	77.67%	XM_022634223.1
		Penicillium expansum TRAM1-like protein, partial mRNA	55%	74.88%	XM_016743149.1
2.7.1.-	1,143	*Rasamsonia emersonii* CBS 393.64 hypothetical protein mRNA	89%	68.93%	XM_013468124.1
		Exophiala xenobiotica hypothetical protein mRNA	91%	68.50%	XM_013454962.1
		Phialophora attae Anhydro-N-acetylmuramic acid kinase, partial mRNA	81%	73.84%	XM_018146880.1

Table 3.19: **BLAST results for sequences annotated by MG-RAST as belonging to the Ascomycota phylum and encoding multicopper oxidase enzymes**. NCBI Accession numbers for most similar sequences are provided.

Gene Number	Length (bp)	Most Similar Sequences in NCBI Database	Query Cover	Percent Identity	Accession Number
1	1,482	*Aspergillus pseudotamarii* Cupredoxin	39%	68.86%	XM_032062142.1
		Aspergillus mulundensis uncharacterized protein	41%	68.83%	XM_026752204.1
		Rasamsonia emersonii CBS 393.63 Multicopper oxidase, type 3	32%	68.45%	XM_013475134.1
2	1,701	*Penicillium arizonense* hypothetical protein	63%	72.77%	XM_022632490.1
		Penicillium expansum Multicopper oxidase, type 3	50%	72.93%	XM_016744839.1
		Aspergillus candidatus Cupredoxin	46%	71.43%	XM_024815107.1
3	1,761	*Talaromyces rugulosus* strain W13939 chromosome III	95%	73.73%	CP055900.1
		Rasamsonia emersonii CBS 393.64 Multicopper oxidase, type 3	89%	70.36%	XM_013475134.1
		Penicillium expansum Multicopper oxidase, type 3	92%	77.00%	XM_016744839.1
4	423	*Byssochlamys spectabilis* conidial pigment biosynthesis oxidase Arb2/brown2	44%	73.30%	XM_028628779.1
		Aspergillus flavus NRRL3357 multicopper oxidase, putative	48%	72.12%	XM_002382778.1
		Aspergillus oryzae RIB40 unnamed protein product	48%	71.84%	XM_023236768.1

3.5 Discussion

3.5.1 Metagenome 1: bacterial target

The coverage for many of the assembled contigs was relatively low with values around 14X for some of the largest ones. For reference-based assemblies, coverage values of at least 50X have been shown to be most accurate (Pightling et al., 2014). As for *de novo* bacterial genome assemblies, high coverage (100X to ~200X) short sequencing reads typically generate the best results (Al-okaily, 2016). The data was, however, sufficient for preliminary characterization and for a comparative analysis between closely related organisms. Sequence length following assembly was 2,518,408 bp which is smaller than the sequence length of *Ab. ferrooxidans* strain Huett2 (2,990,490 bp) consisting of 50 contigs. The sequence length of the genome from strain SLC66 was 3,202,186 bp which is very close to the length from the complete genome of *Alb. acidocaldarius* subsp. *acidocaldarius* DSM 446. This information suggests that a large portion of the genome was not sequenced, especially if the data contains contigs that consist of fungal DNA. Total GC-content for the assembled contigs was 51.4% according to RAST which is somewhat consistent with GC-contents of *Ab. ferrooxidans* SLC66 (~52.00%) and *Ab. ferrooxidans* Huett2 (52.24%). The GC-content for *Alb. acidocaldarius* was substantially higher at 61.9%.

Of the 40 taxonomic labels that Kraken2 assigned, 30 of those were bacterial IDs, and only contig #3 was assigned to the target organism, *Alb. acidocaldarius* subsp. *acidocaldarius* DSM 446. Nearly all of the other labels were Bacilli, therefore the various IDs may have been caused by general gene sequences matching to relatively similar organisms that have a larger number of publicly available genomes and gene sequences. This method of identification did not appear to be very accurate and failed to identify 150 contigs. In addition,

Kraken2 uses a database that is designed for the identification of bacteria and archaea. Considering that this database also contains sequences from human DNA, 8 contigs consisting of eukaryotic DNA were erroneously classified as *Homo sapiens*. BLAST results to verify this assignment confirmed that these contigs consisted of fungal DNA. Closest matches were *Penicillium* and *Aspergillus* species, such as a strain of *P. chrysogenum*, which indicated that these contigs also likely belong to the target fungal organism that was previously identified as belonging to the *Penicillium* genus by sequencing the ITS region (Chapter 2).

A total of 4 rRNA genes were identified in the Prokka data, which initially suggested the presence of multiple bacterial organisms. Results from searching these genes against the NCBI database indicated that the full 16S rRNA gene (1,500 bp) of *Ab. ferrooxidans* NOWR-5 was located on contig #27. Top hits still included both *Acidibacillus* SLC66 and *Alicyclobacillus*, therefore we could not distinguish which one was most phylogenetically similar to the target bacterium at this point. Contigs #22 and #17 were identified as fungal DNA. The sequence from contig #17 was most similar to a mitochondrial sequence from *Penicillium* ShG4C. This is the acid-tolerant organism that Glukhova et al. (2018) proposed may be a new species that possesses mechanisms of resistance to copper and arsenic.

Based on the data we provided SeaView to construct a phylogenetic tree, we were able to determine with a high level of confidence that the target bacterium was part of the *Ab. ferrooxidans* cluster, and that it was distinct from the clusters of *Alb. acidocaldarius* and *Ab. sulfuroxidans*. Similar strains of *Ab. ferrooxidans* include BOR5, Huett2, and SLC66. These results were based on the assumption that these organisms are closely-related and that recombination was not a factor.

Taxonomic results from MG-RAST also confirmed that most of the sample contained bacterial DNA and a small amount of fungal sequences. Most of the hits were assigned to the Firmicutes phylum in which the target organism belongs, and orders were consistent with the labels from Kraken2 that included *Bacillaceae*, *Alicyclobacillus*, and *Paenibacillus*. Fungal hits were mainly assigned to the genera *Penicillium* and *Aspergillus*, but a few were detected for *Neosartorya* and *Talaromyces*. These results seemed to support that contigs belonged to various organisms, but preliminary binning results obtained from MetaBAT 2 suggested that the sample was almost entirely composed of 2 groups of contigs. Only the presence of *Ab. ferrooxidans* was identified with near certainty, and multiple results supported the presence of *Penicillium*. Therefore, it is likely that the 2 groups of contigs belong to these target organisms.

MG-RAST only annotated 102 subsystem hits as belonging to the target organism, *Alicyclobacillus*. Considering that the genes detected were rather general, it is likely that some of the genes from *Ab. ferrooxidans* NOWR-5 were classified in a broader category, such as those found in the *Bacillaceae* family. The number of hits for each subsystem category in *Bacillaceae* were compared to the number of hits for each category in the draft genome *Ab. ferrooxidans* Huett2. Most categories were underrepresented, which suggests that a number of genes from these subsystems may have been missed in this study. The categories of respiration, regulation and cell signaling, as well as motility and chemotaxis were almost identical. This might indicate that most of the genes that have been annotated in the *Ab. ferrooxidans* draft genome within these categories were annotated in the genomic data we recovered. Subsystems that were overrepresented included virulence, disease and defense, sulfur metabolism, and carbohydrates. These genes could belong to other organisms, but it is also a possibility that they

have not been annotated in the draft genome of *Ab. ferrooxidans* Huett2 yet or that they are unique to *Ab. ferrooxidans* NOWR-5.

Nitrogen metabolism and transport

Multiple genes encoding nitrate reductases were annotated. The NarGHI complex generates proton motive force by using a redox loop to couple quinol oxidation with proton translocation (Coelho & Romao, 2015). There were discrepancies between the RAST and Prokka annotations, but the organization of genes on contig #15 appeared to be consistent with the organization of genes that have been established for the *narGHJI* operon. This is supported by the fact that all of the subunits were found in the draft genomes of *Ab. ferrooxidans*, and that *narY* and *narX* were not on separate operons as has been documented in other studies (Blasco et al., 1990; Egan & Stewart, 1990; Moreno-Vivian et al., 1999). This information indicates the presence of a full operon on contig #15 for respiratory nitrate reduction, and this suggests that *Ab. ferrooxidans* NOWR-5 may be able to use nitrate as an alternative electron acceptor under anaerobic conditions. The coupling of Fe^{2+} oxidation with dissimilatory nitrate reduction in anaerobic conditions is referred to as nitrate-dependent Fe^{2+} oxidation, and it has been documented in various species of bacteria from diverse environments (Kanaparthi et al., 2013; Oshiki et al., 2013). Nitrate reduction has been found to be species specific in *Alicyclobacillus* spp. (Ciuffreda et al., 2015). The only information pertaining to nitrogen metabolism which has been established for *Ab. ferrooxidans* is that it does not have the ability to fix N_2 (Holanda et al., 2016).

Because of its position in the cell, the Nap complex uses a proton-translocation enzyme such as NADH dehydrogenase I to indirectly take part in the electron transport chain

(Moreno-Vivian et al., 1999; Stewart et al., 2002). Nitrate reduction via the Nar complex is more thermodynamically favorable, but the NapAB complex is active by high concentrations of quinone (Sparacino-Watkins et al., 2014). Differences in the organization of genes for this operon in different organisms is described by Sparacino-Watkins et al. (2014). Only *napA* was detected in the data, although all 3 genes were surrounded by putative genes encoding hypothetical proteins which could potentially correspond to other genes from this operon. This complex has been suggested to help bacteria scavenge nitrate when the resource is extremely limited (Chen & Wang, 2015).

Nitric oxide poses a serious threat to microorganisms since it is highly reactive which causes damage to proteins, and it can diffuse through the cell wall (Tucker et al., 2008). Bacteria have therefore evolved proteins that can sense its presence, and which can activate genes coding for detoxification enzymes (Tucker et al., 2008). A nitronate monooxygenase enzyme for the detoxification of nitroalkanes was present in the data, and genes coding for putative oxidoreductases in the nitronate monooxygenase family were identified in the draft genomes of *Ab. ferrooxidans* (Gadda & Francis, 2009). This ability is valuable considering organisms, such as fungi including *Penicillium atrovenetum*, produce the toxic compound 3-nitropropionate (Quintero et al., 2020).

Sulfur metabolism and transport

No genes were found to suggest that *Ab. ferrooxidans* NOWR-5 can oxidize RISCs, and this is consistent with the documented metabolic abilities of *Ab. ferrooxidans*. The gene required for converting APS to PAPS was missing from the data, but it is possible that this gene was not sequenced or annotated considering most of the genes to reduce sulfate to hydrogen

sulfide were present. The *sir* gene identified in the data encoded a ferrodoxin-type sulfite reductase (EC 1.8.7.1), but the draft genomes of *Ab. ferrooxidans* had genes encoding for a sulfite reductase [NADPH] hemoprotein beta-component (EC 1.8.1.2). Sulfite reductase [ferredoxin] has been documented in phototrophic organisms as part of the operon *cysIHDN* (Neumann et al., 2000). The *cysA* gene that was identified is involved in the import of sulfate and thiosulfate prior to assimilatory reduction (Goldman & Roth, 1993).

Iron metabolism and transport

We found no genetic evidence that the target bacterium is able to perform dissimilatory Fe^{2+} oxidation to acquire energy. The only genes present were for hemin transport and acquisition. Despite these results, chemical analyses have demonstrated that *Ab. ferrooxidans* can oxidize Fe^{2+} in laboratory conditions, and a gene related to the one encoding the blue copper rusticyanin protein in *At. ferrooxidans* has been identified with low sequence identity (36%) from its genome (Holanda et al., 2016). Culturing *Ab. ferrooxidans* NOWR-5 in liquid and on solid media also supported its ability to oxidize Fe^{2+} (Chapter 2). The absence of such genes which were expected to be present in the data could have been a result of the challenges associated with annotating iron-related genes.

Hundreds of genes have been identified pertaining to iron metabolism and transport, but only a very small number of them are involved in energy generation via Fe^{2+} oxidation or Fe^{3+} reduction (Garber et al., 2020). These are difficult to identify considering that many common gene annotation pipelines such as RAST, GhostKOALA, MAP, and InterProScan are not able to annotate them (Garber et al., 2020). In addition, many operons that have been established to be involved in iron metabolism also contain many genes which have roles in other

metabolisms, and although these particular genes are important for acquiring and transporting iron, this complicates the annotation process (Garber et al., 2020). For these reasons, Garder et al. (2020) have created a publicly available database containing enzymes for iron acquisition, storage, and energy generation, as well as the FeGenie tool to identify these genes in genomes or metagenomic samples.

In addition, the organization of the Fe^{2+} oxidation pathway in Gram-positive microorganisms, including *Ab. ferrooxidans*, remain poorly understood compared to the well-described pathway in the Gram-negative *Acidithiobacillus* genus (Garber et al., 2020; White et al., 2016). Gram-positive bacteria do not possess an outer membrane, and so Fe^{2+} can diffuse through the cell wall rather than requiring that electrons be shuttled from the cell surface to the cytoplasmic membrane (White et al., 2016). *Sulfobacillus sibiricus* has been documented to perform both Fe^{2+} oxidation and the reduction of O_2 on the inner membrane, but this mechanism is still being investigated (White et al., 2016). The enzyme which is directly oxidizing Fe^{2+} has not been identified, but speculations include that either the oxidation reaction occurs directly by the terminal oxidase or that a cytochrome *b* electron shuttle is responsible for transferring electrons between extracellular Fe^{2+} and terminal oxidase enzymes (White et al., 2016). These findings might be the reason for which there were no genes that were identified in *Ab. ferrooxidans* NOWR-5 that were evidently involved in the respiratory oxidation of Fe^{2+}, and they suggest that annotated genes involved in the electron transport chain could correspond to the Fe^{2+} oxidation pathway in this genus.

Autotrophic carbon metabolism

The CO_2-fixing enzyme 2-oxoglutarate:ferredoxin from the rTCA cycle was present in *Ab. ferrooxidans* NOWR-5 and in the compared genomes (Hugler et al., 2005). The draft genomes also contained a gene for another key enzyme, pyruvate:ferredoxin oxidoreductase, and had a gene encoding a pyruvate carboxylase to bypass the generation of phosphoenolypyruvate in order to form oxaloacetate. The only gene that was missing from any of the genomes to form a complete pathway encoded the key enzyme ATP citrate lyase. It is possible that the gene utilized for this step has not been identified since modifications in the pathway have been found in different species (Berg, 2011). For instance, the two enzymes citryl-CoA synthetase and citryl-CoA lyase, were discovered in *Leptospirillum* spp. and were phylogenetically related to ATP-citrate lyase (Berg, 2011).

In the data, only one gene was identified from the methyl branch to support that the WL pathway is functioning to fix CO_2, and in all cases, the first enzyme from this branch to convert CO_2 to formate was missing as well as enzymes required to complete the pathway by generating acetyl-CoA. Some bacteria, including aerobes and anaerobes, have been documented to perform the WL pathway in reverse to obtain CO_2 and electrons from the degradation of acetyl-CoA (Adam et al., 2018; Techtmann et al., 2012). The aerobic CO dehydrogenase (EC 1.2.5.3) found in the data was assigned to the *coxM* gene. This gene has been identified as part of the *cox*SML complex that oxidizes CO to CO_2 in aerobic organisms (Techtmann et al., 2012). According to KEGG, the CO_2 serves as assimilable carbon for the CBB cycle and electrons are transferred to electron acceptors such as oxygen or nitrate (Techtmann et al., 2012). The putative CO dehydrogenases identified in the draft genomes (EC 1.2.7.4) differed by being the anaerobic enzyme. It is possible that these enzymes are involved in the fixation of CO_2, but Johnson &

Hallberg (2009) identified these enzymes in *Ferroplasma* and concluded that they were more likely involved in obtaining energy from formate for organotrophic metabolism.

Multiple genes were present in the data as well as in the draft genomes which are associated with the CBB cycle. However, this pathway does not appear to be active in these organisms considering that all of these genes are also involved in glycolysis or the PP pathway. In addition, genes for all of the key enzymes were absent from the data and from all compared genomes (Berg, 2011).

Similarly, a few genes were present in the data and draft genomes which can be involved in the dicarboxylate-hydroxybutyrate cycle, but the pathway was barely closed, and these genes are also involved with other pathways such as valine, leucine and isoleucine degradation as well as glyoxylate and dicarboxylate metabolism. For these reasons, this pathway is most likely not functional in these organisms.

The ability to obtain carbon autotrophically would be very beneficial for organisms living in AMD or in bioreactors. The presence of key enzymes for the rTCA cycle in *Ab. ferrooxidans* indicate that this pathway could potentially be active. Most acidophiles have been documented to fix CO_2 via the CBB cycle, but anaerobic or microaerobic organisms often use the rTCA pathway (Bender et al., 2011; Berg, 2011; Johnson & Hallberg, 2009). The complete genome of *Alb. acidocaldarius* subsp. *acidocaldarius* DSM 446 did not contain genes to support that this particular strain exhibits facultative autotrophy. A gene with low sequence identity to *ccbL* for the CBB cycle was identified in 2 strains of *Ab. ferrooxidans* (strain SLC66: 34%; strain ITV01: 36%), but extensive laboratory testing has confirmed that multiple strains require an organic carbon source for growth (Holanda et al., 2016).

Heterotrophic carbon metabolism

Essentially all of the genes were present in both *Ab. ferrooxidans* NOWR-5 and in the compared genomes to suggest that these organisms use the EMP pathway to oxidize glucose and pyruvate prior to the TCA cycle. No evidence was found to support that they have the metabolic ability to use the Entner-Doudoroff (ED) pathway.

Genes coding for enzymes involved in the oxidative stage of the PP pathway were absent from the data. These are the reactions that generate the NAD(P)H which serves as a reducing agent for many biosynthetic reactions (Spaans et al., 2015). Considering that this is one of the main functions of this pathway, and that most of these genes were present in the compared genomes, it is likely that they were either not sequenced or annotated in the data. Most genes required for the non-oxidative stage of the PP pathway were present in the data as well as in the compared genomes (Soderberg, 2005' Wolfe, 2015). These results suggest with confidence that the PP pathway might be active in these organisms if the genes discussed in this section are expressed.

The identification of genes encoding the 2 key enzymes for the glyoxylate shunt, isocitrate lyase and malate synthase, strongly supports that this pathway is functional. These genes were located on contig #6 and appeared to form an operon that was consistent with the *ace*BA that has been described in *Bacillus licheniformis* (Kabisch et al., 2013). Functionality of the glyoxylate shunt would be beneficial for heterotrophic organisms living in AMD or bioreactors that have limited resources of organic carbon. It would allow them to conserve carbon by skipping the steps in the TCA cycle that generate CO_2, as well as to perform gluconeogenesis with acetate and fatty acids when necessary (Ahn et al., 2016).

For complex I of the electron transport chain, *Ab. ferrooxidans* NOWR-5 had the enzyme NADH:quinone reductase whereas the enzyme NADH:ubiquinone reductase was identified in the compared genomes. Some of the *ndh* genes encoded chloroplastic NAD(P)H: quinone oxidoreductases that have been described in chloroplasts as part of photosynthetic electron transport (Crombie et al., 2018). The annotation of chloroplastic genes was likely incorrect, especially since they were found clustered with non-chloroplastic complex I genes. Instead, the *ndh* and *nuo* genes were assigned the EC number 1.6.5.9 which corresponds to type 2 NADH:quinone reductase enzymes that do not contribute to proton translocation, but which have been documented to maintain balance between NADH/NAD^+ (Melo et al., 2004). Quatrini et al. (2009) documented the upregulation of *nuoI* and *nuoK* in *At. ferrooxidans* when it was grown in Fe^{2+}-containing media, and the predicted locations of these genes in the NADH complex suggested their involvement in facilitating the uphill electron flow from quinone to complex I. Genes encoding for type 1 proton-translocating NADH-dehydrogenase-like proteins included *yglD*, as well as another gene for which a name was not assigned (EC 1.6.99.- now covered by EC 7.1.1.2).

The genomes of the closest related organisms had genes coding for the succinate dehydrogenase flavoprotein and Fe-S subunits (EC 1.3.5.1). In aerobic respiration, this enzyme accepts electrons from $FADH_2$ via the oxidation of succinate (Hartman et al., 2014). In the data, one gene coding for the Fe-S subunit (EC 1.3.5.1) was identified but the predicted protein product was a fumarate reductase. Directly beside this gene, labeled *frdA*, was *frdB* encoding for the enzyme fumarate reductase flavoprotein subunit (EC 1.3.5.4). The *frdABCD* operon has been described in *E. coli* and these genes code for the anaerobic electron acceptor fumarate reductase (Latour & Weiner, 1988). These results could indicate that the organism possesses genes to

transcribe both of these aerobic and anaerobic electron transport enzymes, and that some genes were not sequenced or annotated for the expression of all the necessary subunits. Alternatively, *sdhA* and *sdhB* may have been falsely annotated as *frdA* and *frdB* considering that they are very similar enzymes. This would mean that both catalytic subunits for aerobic respiration would be present along with an anchoring polypeptide, *sdhC*, that was identified beside *frdA* (Cecchini et al., 2002).

In all cases, there appeared to be no genes associated with complex III, specifically to form the bc1 complex. This is the most commonly documented structure of complex III, including in the Fe^{2+} oxidation pathway of *At. ferrooxidans*, but the majority of bacteria can complete the electron transport chain without this complex by using alternative pathways (Raquel et al., 2009; Trumpower, 1990). The gene coding for a cytochrome b6-f complex Fe-S subunit on contig #6 in the data has also been described in cyanobacteria and chloroplasts as being structurally and functionally similar to the bc1 complex (Thony-Meyer, 1997).

Genes in the data and in the compared genomes for complex IV encoded mitochondrial aa3-type cytochrome c oxidase enzymes which have been identified in many bacteria (Thony-Meyer, 1997). The *ctaD* gene on contig #2 was directly beside *coxM* coding for an alternative cytochrome c oxidase. The genome of *Bradyrhizobium japonicum* has been described to contain this gene in addition to genes encoding aa3-type cytochrome c oxidase enzymes, but no evidence for the presence of this gene was obtained in the draft genomes of *Ab. ferrooxidans* (Bott et al., 1992). The EC number for *cta* genes and *coxM* was EC 7.1.1.9, and this was consistent with the EC number assigned to the *coxABC* genes in *At. ferrooxidans* that encode

an aa3-type cytochrome c oxidase which is the terminal electron acceptor from the extracellular oxidation of Fe^{2+} in aerobic conditions (Appia-Ayme et al., 1998; Cavazza et al., 1996).

Quinol oxidase encoding genes (*qox*) are structurally related to the family of mitochondrial-type aa3 terminal oxidases, and these were found in the data as well as in *Ab. ferrooxidans* (Santana et al., 1992). The full *qoxABCD* operon described by Villani et al. (1995) in *B. subtilis* appeared to have been annotated on contig #1. Considering that subunit 4 encoded by *qoxD* has been documented to be essential for the proton pumping activity of this enzyme, the *qoxD* gene annotated from *Ab. ferrooxidans* NOWR-5 likely corresponds to the missing gene in the draft genomes (Villani et al., 1995). The presence of these genes suggest that the organisms may be able to directly transport electrons from quinols to O_2, which would be another method to bypass the bc1 complex (Thony-Meyer, 1997).

The *atp* operon in most bacteria consists of *atpIBEFHAGDC* (Liu et al., 2012). The first gene, *atpI*, is not structural and only minor reductions in respiration rates have been observed when it is absent (Liu et al., 2012). All of the remaining structural genes were present on contig #4 and appeared to form an operon *atpBHFDAGDC*. Although the gene organization appears different than the one previously mentioned, protein products were consistent with the order in the established operon (Liu et al., 2012). Quatrini et al. (2009) documented that the genes *atpB* and *atpE* were upregulated in *At. ferrooxidans* when it was grown in media containing Fe^{2+} in order to synthesize larger quantities of ATP by translocating additional protons through the cytoplasmic membrane.

Uptake and utilization of sugars

Holanda et al. (2016) confirmed in biochemical tests that *Ab. ferrooxidans* requires an organic carbon source for growth, and that the complex organic carbon provided by yeast extract was most effectively utilized. They observed that glucose was far less effective, and that the growth rate of most strains in glucose-containing media was limited by Fe^{2+} availability (Holanda et al., 2016). They interpreted these results as support for the theory that *Ab. ferrooxidans* uses Fe^{2+} as the only or main energy source, and that glucose serves only for carbon assimilation (Holanda et al., 2016). They emphasized that the genomes of these organisms should be further annotated in order to understand the restricted utilization of glucose that has been observed in these organisms.

Our findings support that *Ab. ferrooxidans* NOWR-5 may be able to import and assimilate various sugars including glucose. Although sugar metabolism has been found to vary greatly between species of *Alicyclobacillus*, the ability to grow on a wide range of sugars has been documented in some strains. For instance, Lee et al. (2018) found that *Alb. acidocaldarius* strain ATCC 27009 could gain cellular carbon and energy from 5- and 6-carbon sugars including L-arabinose, ribose, D-galactose, D-fructose, D-mannose, lactose, maltose and trehalose. These are among others including more complex polysaccharides, but all of those mentioned are consistent with genes identified in this study (Lee et al., 2018). It would be beneficial for these organisms to assimilate multiple sugars considering that the availability of organic carbon sources in AMD is limited, therefore optimal carbon sources are almost certainly not found in abundant concentrations (if present at all).

The presence of *ccpA* genes encoding the carbon catabolite protein A in *Ab. ferrooxidans* NOWR-5 and in the compared genomes also supports this ability. These are part of

a conserved mechanism in bacteria that allows them to utilize preferred carbon sources when multiple sugars are available (Habib et al., 2017).

This study found no genetic evidence to explain the restrictions in glucose utilization observed by Holanda et al. (2016), however it could potentially be explained by the link between carbon and nitrogen metabolisms as described by Bren et al. (2016). Costa et al. (2002) found that *Pantoea agglomerans* grew well assimilating carbon from soluble starch when yeast extract was provided as a nitrogen source, but the organism grew poorly when yeast extract was replaced with inorganic nitrogen. Similarly, Bren et al. (2016) observed that glucose became one of the worst carbon sources for *E. coli* when a single amino acid was provided as a nitrogen source and that it would consume the glucose prior to other carbon sources, but growth rates were faster once glucose had been fully depleted. This information could explain the results obtained by Holanda et al. (2016) where *Ab. ferrooxidans* grew poorly in iron-rich medium that contained glucose as the sole carbon source and nitrogen from inorganic basal salts. They found that glucose was slowly being consumed but that growth rates were dependent on Fe^{2+}, and so the organism could have been depleting the growth-limiting glucose while relying on its ability to obtain energy from chemolithotrophic metabolism. Analyses of the effects on growth rates when glucose is present in combination with optimal nitrogen sources should be performed to assess this theory. If correct, *Ab. ferrooxidans* NOWR-5 would greatly benefit from the presence of *Penicillium* considering that the latter would consume the glucose at accelerated rates.

Micronutrient uptake and homeostasis

All bacterial phyla have a set of genes that make up the *pho* operons for acquiring and metabolizing molecules that contain phosphorus (Santos-Beneit, 2015). Results indicated

that *Ab. ferrooxidans* uses the ABC-type transport system encoded by the *pst* operon and regulated by the *pho* operon, consisting of *phoR* and *phoP* such as in *B. subtilis*, to transport phosphorus-containing molecules (Santos-Beneit, 2015). All of the *Ab. ferrooxidans* genomes contained *phoU* which has been documented to be absent in *B. subtilis* (Santos-Beneit, 2015). In the genomic data, a similar cluster of genes which could correspond to the second set of *pst* genes in the compared genomes was identified on contig #3. However, it differed by consisting of *pstA2*, *pstC1*, *pstS1*, *pstB3*, and *phoP*. These particular genes have been described in organisms such as *M. tuberculosis* and the cyanobacterium *Nostoc punctiforme* (Hudek et al., 2016; Tischler et al., 2016).

Bacteria have evolved many transport systems to regulate intracellular potassium levels, such as the well-characterized Kdp transport system that is induced by low concentrations of K^+ and which is repressed when concentrations of the cation are high (Asha & Gowrishankar, 1993). Genes forming the full operon which encodes the transporter were identified on contig #1 including *kdpD*, *kdpE*, *kdpA*, *kdpB*, as well as *kdpC*, and genes encoding K^+-transport ATPase products *kdpA*, *kdpB*, as well as *kdpC* were identified on contig #6 (Gowrishankar, 1993). These results were consistent with the *Ab. ferrooxidans* draft genomes that had 2 genes for each KdpA, KdpB, KdpC, and KdpD, as well as only 1 gene for the regulatory KdpE. It can be speculated with confidence that these organisms use this high affinity K^+ transport system.

Considering the importance of regulating micronutrients and that multiple transporters are typically found in organisms, such as 2 or more independent K^+ transport systems, this study certainly missed many genes in this category (Epstein, 2002). This was further supported by the presence of genes in the compared genomes which encoded a P-type Ca^{2+}-transport ATPase, a magnesium and cobalt transport protein CorA, as well as a magnesium

and cobalt efflux protein CorC. However, multiple genes are most likely missing from the draft genomes as well considering the small number of genes associated with vital nutrient homeostasis.

Metal homeostasis and resistance

Genes were found on multiple contigs pertaining to resistance to cadmium, cobalt, zinc, mercury, manganese, copper, and arsenical compounds.

The most commonly used arsenic resistance system in bacteria involves the *ars* operons that are present in most neutrophiles, and which have been documented in acidophiles such as *At. ferrooxidans* (Fekih et al., 2018). The operon typically consists of *arsRBC* to reduce As(V) to As(III) (*arsC*) before exporting it from the cell through a potential driven pump (*arsB*), and these are controlled by the repressor *arsR* (Dopson et al., 2003). An operon consisting of *arsB* and *ars*C was identified on contig #2, and *arsR* was located separately on contig #4. The draft genomes had multiple *arsR* genes, which could explain the finding of *arsR* on contig #4. In addition, a hypothetical protein was annotated directly beside *arsB* which could correspond to the unannotated operon regulator.

Bacteria have evolved different pathways for the maintenance of copper homeostasis which includes the expression of the *cop* operon (Nawapan et al., 2009). The ability of *At. ferrooxidans* to survive in high copper concentrations is due to the presence of at least 10 genes which include *copA1*, *copA2*, *copB*, and *cusCBA* (Barahona et al., 2020). The data contained 3 *copA* genes on different contigs where 2 of them encoded P-type ATPases for copper import, and the other encoded a copper resistance protein. The CopZ chaperone was also located on contig #30. The compared draft genomes also had multiple genes for copper-translocating P-

type ATPases, and a gene encoding a repressor CsoR of the *copZA* operon. This corresponds to the repressor that was not annotated in the data and confirms that the operon in this organism consists of *copZ* and *copA*. This operon was present on contig #30.

Considering that *Ab. ferrooxidans* has demonstrated levels of metal tolerance which are similar to other acidophilic Fe^{2+}-oxidizers in laboratory experiments, it can be assumed that multiple resistance genes have not yet been annotated in this organism. This is suggested because *At. ferrooxidans* has been documented to have at least 10 genes for resistance against copper, and this is nearly the total of genes recovered from *Ab. ferrooxidans* NOWR-5 for all metals (Barahona et al., 2020). In addition, the reduction of Hg^{2+} to Hg^{0} via a mercuric reductase enzyme (*merA*) is the most common pathway of resistance to mercury (Moller et al., 2014). The gene *merA* was identified in the data as well as in the draft genomes, but it is typically part of an operon with transport genes such as *merB* and the *merR* regulator (Moller et al., 2014). In addition, genes from the *czc* system that provide resistance against cobalt, zinc, and cadmium are likely present in the genomes of Ab. ferrooxidans strains because only the *czcD* gene has been identified which regulates the *czc* operon (Anton et al., 1999). The gene *czcR* encoding the transcriptional activator protein CzcR was identified in the data and has been documented to induce the expression of the CzcCBA efflux pump (Dieppois et al., 2012).

Maintenance of intracellular pH

Results indicated that *Ab. ferrooxidans* NOWR-5 uses cation transporters and organic acid degradation to maintain neutral intracellular pH, and that many genes are involved in repairing DNA if biomolecules get damaged from acidity (Baker-Austin & Dopson, 2007). Although no proton antiporters were identified in the genomes of *Ab. ferrooxidans* and *Alb.*

acidocaldarius, the data contained an Na^+/H^+ antiporter as well as a Na-Li/H^+ antiporter. Zhang et al. (2017) reported that the Sulfobacillus strains which they observed appeared to export unnecessary protons via Na^+/H^+ antiporters. However, the NapA-type transporter such as the one found in the data, was characterized in *Thermus thermophilus* by high Li^+/H^+ antiport activity in low pH conditions (Furrer et al., 2007). These active antiporters could enable the efflux of substrates if they become present in toxic concentrations such as Na^+ for the maintenance of osmolarity, as well as regulate the influx of H^+ if alkalinity rises (Krulwich et al., 2009).

In addition, various acidophiles including *Sulfobacillus* spp. use the Kdp-type K^+ transport system to generate a reversed membrane potential for pH homeostasis, and these genes were identified in *Ab. ferrooxidans* NOWR-5 (Zhang et al., 2017). In *At. thioxidans*, K^+ has been observed to be the most efficient cation for the maintenance of a reverse membrane potential (Baker-Austin & Dopson, 2007).

Two *spe*A genes were identified in the data as well as in the draft genomes of *Ab. ferrooxidans*. These catalyze the decarboxylation of arginine which consumes protons that can subsequently be excreted from the cell (Baker-Austin & Dopson, 2007). Zychlinsky & Matin (1983) found that buffer molecules provided by amino acid side chains were the main mechanism of maintaining intracellular pH in acidophilic heterotrophs.

Genes for the degradation of organic acids were also identified. The molecules, such as lactic acid, are cytotoxic for acidophiles in acidic conditions where they can diffuse into the cell and inhibit oxidative phosphorylation by dissociating protons (Baker-Austin & Dopson, 2007). Three genes encoding acetyl-coenzyme A synthetase were found in *Ab. ferrooxidans* NOWR-5 which was consistent with the *Ab. ferrooxidans* draft genomes, and a gene encoding lactate 2-monnoxygenase was identified in the data and exclusively in *Ab. ferrooxidans* strain

Huett 2. These enzymes have been reported from the genomes of multiple extreme acidophiles and they allow them to convert lactate to pyruvate which can also serve as an energy source (Slonczewski et al., 2009).

The genomes of several acidophiles have been documented to contain many genes for DNA and protein repair which has been attributed to the necessity to repair damaged biomolecules quickly when primary defense mechanisms fail to completely protect the cell (Baker-Austin & Dopson, 2007). The data contained 29 genes associated to DNA repair, but some appeared to have been missed considering that the *Ab. ferrooxidans* strain Huett2 draft genome contained 37 genes and the complete genome of *Alb. acidocaldarius* had a total of 55. The data contained 3 genes coding for *clpP* and 1 for *clpX* which was consistent with the compared genomes. Clp proteases have various roles such as degrading misfolded proteins and removing dysfunctional ones, but the ClpXP complex in *E. coli* and *B. subtilis* has been documented as being directly involved in protection against acidity (Guazzaroni et al., 2013). The *lex*A gene which typically regulates SOS response genes also seems to be present in these organisms (Guazzaroni et al., 2013). LexA-like proteins have been found in AMD acidophiles and have been associated with the regulation of genes involved in acid resistance (Guazzaroni et al., 2013). A *hup* gene coding for an HU protein was identified only in the data, but its role in acid stress response has been identified in other AMD acidophiles (Guazzaroni et al., 2013).

Despite the fact that genes appeared to be present for maintaining neutral intracellular pH using various mechanisms, Holanda et al. (2016) have observed that pH values < 2 in bioreactors may be a growth constraint for *Ab. ferrooxidans*, and that it might therefore be most applicable in passive leaching applications where the pH remains at a value of ~2.

Stress responses

Bacteria regulate multi-gene systems, known as stimulons, when faced with various stress-inducing conditions, and under oxidative stress, they express 1 or 2 known stimulons involved in regulation, reactive oxygen species (ROS) detoxification, and DNA repair (Farr & Kogoma, 1991). One of these is the peroxide stimulon that is positively regulated by proteins of the OxyR regulon (Farr & Kogoma, 1991). Many Gram-positive organisms, like *B. subtilis*, have 3 Fur-like repressor proteins for Fe^{3+} uptake, such as the one encoded by *perR* that has a central role in regulating the peroxide stress response (Fuangthong et al., 2002; Zhang et al., 2012). Both of these genes were present in the data, but all compared genomes did not appear to have them.

Thiol-specific peroxiredoxins are encoded by *prxU* and *bcp* genes, and these enzymes reduce hydrogen peroxide and hydroperoxides to alcohol and water (Reeves et al., 2011; Sohling et al., 2001). The peroxiredoxin Bcp protein in *E. coli* has been proposed to potentially serve as a last resort enzyme for defense in highly oxidizing conditions (Reeves et al., 2011). These genes were exclusively identified in the data, as well as the vegetative catalase encoded by *katA*. Almost all aerobic and facultative aerobes have catalases that serve to break down hydrogen peroxide to water and oxygen (Amo et al., 2002).

A nonheme catalase, manganese catalase, was also identified in *Ab. ferrooxidans* NOWR-5 that uses manganese ions in its active site rather than ferric heme (Amo et al., 2002). The spontaneous dismutation of oxygen species can cause the reduction of necessary transition metals and of metal complexes with 4Fe-4S that are involved in multiple enzymatic reactions (Farr & Kogoma, 1991). When dealing with oxidative stress, bacteria will transcribe genes that possess substrate binding sites rather than 4Fe-4S metal-binding sites (Ueda et al., 1991). For

instance, the conversion of fumarate to L-malate in the TCA cycle can be catalyzed by the product of *fumC* which has a substrate binding site rather than *fumA* (Ueda et al., 1991). This backup enzyme was also only found in the data.

The only protein products that appeared in both in *Ab. ferrooxidans* NOWR-5 and in the draft genomes were alkyl hydroperoxide reductase subunits that are associated with protection from organic hydroperoxides (Fleischmann et al., 2002). They did appear to slightly differ as the data contained an alkyl hydroperoxide reductase E encoded by *ahpE*, and the draft genomes had a gene coding for an alkyl hydroperoxide reductase subunit C-like protein. The latter has been associated to the gene *ahpC* which is regulated by *oxyR* that was only identified in the data (Wang et al., 2013).

The repair of damaged DNA increases the survival of bacteria experiencing oxidative stress (Farr & Kogoma, 1991). ROS can cause the spontaneous oxidation of guanine bases forming the product 8-hydroxydeoxyguanosine (8-Oxo-dGTP) which can bind to thymidine rather than cytosine, and subsequently result in mutagenesis (Ock et al., 2012; Tajiri et al., 1995). All of the *Ab. ferrooxidans* genomes assessed in this study had *mutM* and *mutY* genes that are involved in repairing DNA after 8-oxoguanine has been incorporated (Taijiri et al., 1995). ROS can also oxidize the sulfur atoms on the residues of methionine, generating methionine sulfoxide (Singh et al., 2018). The gene *msrC* encodes a free-methionine-R-sulfoxide reductase enzyme that can reduce protein-bound methionine sulfoxide back to methionine, restoring normal protein function (Denkel et al., 2011).

The heat-shock response is universal in prokaryotes but the regulation of genes that express heat-shock proteins differs between species (Roncarati & Scarlato, 2017). Proteases are one group of heat-shock proteins expressed in bacteria that are upregulated in stressful

conditions (Roncarati & Scarlato, 2017). In addition to providing defense from acidity, the proteases encoded by *clpP* and *clpX* are chaperones that are involved in removing polypeptides that have been damaged from high temperatures (Roncarti & Scarlato, 2017). The draft genomes contained more heat-shock genes than were found in the data such as for the chaperones GroEL and DnaK that are important for the formation of proteins even when the cell is not stressed (Roncarti & Scarlato, 2017). Considering the importance of these genes even in normal conditions and their presence in the draft genomes, they were most likely not sequenced or annotated in the data.

The *cspC* gene identified in *Ab. ferrooxidans* NOWR-5 encodes 1 of the 9 cold shock proteins from the Csp family in *E. coli* (Phadtare et al., 2006). During cold shock, it is one of the Csp proteins which bind to RNA and single-stranded DNA to melt and/or destabilize the secondary structures of nucleic acids (Phadtare et al., 2006). The draft genomes contained 3 genes encoding cold shock proteins of the CSP family which could correspond to *cspC* and others such as *cspA* and *cspE* that were not annotated in the data (Phadtare et al., 2006).

Resistance to antibiotics

The majority of genes found in *Ab. ferrooxidans* NOWR-5 and the draft genomes encoded for efflux pumps to extrude the drugs following their entry into the cell, which is a process that ensures significant levels of drug resistance for the organism (Putman et al., 2000). Genes from *Ab. ferrooxidans* NOWR-5 encoded for transporters that have affinities for specific compounds as well as other transporters that can provide defense against various structurally unrelated compounds (Putman et al., 2000). The latter are referred to as multidrug transporters and these were the products of many genes in the data (Putman et al., 2000).

Multiple *bmr3* genes were present, and these have been reported in the genome of *B. subtilis* providing high levels of resistance against tosufloxacin and puromycin as well as lower yet still significant levels of resistance for norfloxacin, acriflavine, ethidium bromide and tetraphenylphosphonium (Murata & Ohki, 1997). The genes *mdtD*, *mdtC* and *mdtA* identified in *Ab. ferrooxidans* NOWR-5 have been characterized as encoding for the MdtABC tripartite complex and the MdtD efflux protein for resistance to novobiocin and deoxycholate (Baranova & Nikaido, 2002; Nagakubo et al., 2002). The *stp* gene encoding another multidrug resistance protein for resistance to spectinomycin and tetracycline was only identified in *Ab. ferrooxidans* NOWR-5 (Ramon-Garcia et al., 2007). Giddings et al. (2020) reported that the most abundant RNA transcript in the transcriptome of an acid rock drainage microbial community encoded the multidrug resistance protein Stp. The genes *bcrABC* which encode an ABC transporter for the efflux of bacitracin have been identified in *Bacillus licheniformis* (Charlebois et al., 2012).

Findings from this study indicated that these organisms also possess genes to inactivate certain antibiotic compounds. Two *uppP* genes encoding undecaprenyl-diphosphatases were identified in the data, and this was consistent with the presence of 2 genes encoding this enzyme in *Ab. ferroxidans* draft genomes as well as 4 of them in *Alb. acidocaldarius*. Bacitracin is a polypeptide antibiotic that is produced by *B. licheniformis* as well as strains of *B. subtilis*, and it inhibits bacterial growth by disrupting cell wall synthesis (Charlebois et al., 2012). This compound binds to undecaprenyl diphosphate (UPP); This prevents its dephosphorylation and subsequent recycling into undecaprenol monosphosphate (UP), which is an essential lipid carrier for the synthesis of extracellular polysaccharides (Charlebois et al., 2012; Kawakami & Fujisaki, 2017). One of the major mechanisms for bacitracin resistance is the possession of undecaprenyl-

diphosphatase enzymes since they catalyze the dephosphorylation of UPP (Charlebois et al., 2012; Ghachi et al., 2005).

The link between antibiotic resistance and heavy metal resistance has been documented since the 1970s (Chen et al., 2019). This relationship is due to mechanisms of co-resistance where bacteria acquire multiple resistance genes simultaneously, and cross-resistance where an organism becomes resistant to multiple substances that have similar effects on the cell by the acquisition of genes for one of these substances (Arsene-Ploetze et al., 2018; Baindara, 2019; Sanders, 2001). It is now known that AMD sites which are contaminated with several heavy metals contain organisms that have a large number of antibiotic resistance genes (Arsene-Ploetze et al., 2018).

Sporulation

Sporulation is a very complex process in bacteria, and *B. subtilis* has been documented to have an abundance of genes to accomplish stages 0-VII, with approximately 80 individual proteins making up the spore coat (Higgins & Dworkin, 2012). One of the main contributors providing resistance to endospores is this coat (Ghosh et al., 2008). Considering that the complete genome of *Alb. acidocaldarius* contained 98 genes encoding proteins involved in sporulation, it can be assumed that quite a few genes have not yet been sequenced or annotated from the draft genomes of *Ab. ferrooxidans* which both only had just over 20 genes classified in this category. Many of these genes were identified in the data, which contained a total of 39 sporulation-related genes. It is possible that some of these additional genes in the data have not yet been annotated in the compared strains of *Ab. ferrooxidans*. All of the genes identified in *Ab. ferrooxidans* NOWR-5 that were absent in the compared genomes were found in strains of *B.*

subtilis (Kodama et al., 1999; Londono-Vallejo et al., 1997). Some necessary genes including *spoIIR* and *spoVR* were only identified in the draft genomes and they were likely missed in this study.

Holanda et al. (2016) have documented that *Ab. ferrooxidans* SLC66^T produces oval endospores that are located terminally in the cell. Endospores were observed by light microscopy from *Ab. ferrooxidans* NOWR-5, but they were mostly found in solution considering the cultures were old and had likely gone dormant. This analysis was performed at a late stage in the experiment based on the findings of a large number of genes involved in sporulation (Chapter 2). Considering that *Ab. ferrooxidans* has been described as generally preferring mesophilic temperatures and pH values of ~2, conditions throughout the bioleaching process in reactors may become unsupportive for growth. When this occurs, the organisms could survive by means of sporulation. Although they would no longer significantly contribute to leaching rates at this point, *Ab. ferrooxidans* could potentially serve in mixed cultures as a dominant member during the early stages of the leaching process that contributes to generating optimal conditions for more extremophilic Fe^{2+}-oxidizers that would take over in later stages.

Biofilm formation

The protein Veg identified in *Ab. ferrooxidans* NOWR-5 and the draft genomes has been characterized to regulate genes for biofilm formation and potentially spore formation in *B. subtilis* (Lei et al., 2013).

In addition, UDP-Gal is a major sugar nucleotide used for the synthesis of exopolysaccharides, and it has been documented as being essential for the formation of biofilms in many microorganisms, such as *B. subtilis* (Barreto et al., 2005; Habib et al., 2017). Genes

involved in producing UDP-Gal include *galE* and *galK* via the Leloir pathway (Habib et al., 2017). In *Ab. ferrooxidans* NOWR-5 and the compared genomes of *Ab. ferrooxidans* strains, genes appeared to form the operon *galTKEM*. The RAST annotation data and publicly available genomes indicated that *galE* was followed by *YoxA* encoding an aldose 1-epimerase enzyme, but results from Prokka suggested that the gene at this position corresponded to *galM*. The organization of genes was very consistent between *Ab. ferrooxidans* NOWR-5 and the genomes of *Ab. ferrooxidans* strain SLC66 as well as Huett2. It was different from the organization in *Alicyclobacillus acidocaldarius* subsp. *acidocaldarius* DSM446 and from the organization of the *gal* operons that have been described in other organisms such as *At. ferrooxidans* (*luxA*-like, *galE*, *galK*, *pgm*, *galM*) and *E. coli* (*galE*, *galT*, *galK*) (Barreto et al., 2005; Chai et al., 2012; Tabachnikov & Shoham, 2012). These results suggest that the organization of genes forming the *gal* operon in *Ab. ferrooxidans* as presented in Figure 3.17 is unique to this organism, and these genes could potentially be involved in producing exopolysaccharide precursors for biofilm matrix formation.

Schieferbein et al. (2017) observed that *Ab. ferrooxidans* Huett2 was able to form microcolonies as precursors for multilayer biofilms on pyrite and chalcopyrite. The formation of an evenly distributed biofilm was observed by *Ab. ferrooxidans*, which differed from the unevenly distributed surface colonization by *At. ferrooxidans* (Schieferbein et al., 2017). Based on these findings, *Ab. ferrooxidans* NOWR-5 may have the ability to colonize mineral surfaces via biofilm formation, and many genes associated with this mechanism have probably not yet been annotated in these organisms.

Motility and chemotaxis

A total of 20 genes associated with flagellar assembly, regulation, as well as function were identified in the data, and the majority of them were also present in the draft genomes of *Ab. ferrooxidans*. Most of them were found on contig #12 with some genes being adjacent to each other, such as *flhA* and *flhB* that form the FlhAB complex (Liu & Ochman, 2007). This complex exports flagellin which is one of the main structural protein components of flagella (Hajam et al., 2017). In addition, the genes *fliG*, *fliF*, *fliE*, *flgC*, and *flgB* were found together. Flagellar genes are often arranged as neighbors but their arrangement is substantially different between species, and throughout evolution, gene complexes became larger with the addition of new genes as well as the fusion of gene units (Liu & Ochman, 2007).

All of the core proteins involved in chemotaxis sensory pathways were present in *Ab. ferrooxidans* NOWR-5 besides the one encoded by *cheA* which may have been missed in this study (Garcia-Fontana et al., 2013). Both *cheB* and *cheW* were not identified in the draft genomes, therefore we may have annotated them for the first time.

B. subtilis can use its rotating flagellum to swim in liquids and for swarming on solid surfaces (Hall et al., 2017). The SwrD protein has been documented to be necessary for increasing flagellar power that is required for swarming motility (Hall et al., 2017). Its presence in the data suggests that *Ab. ferrooxidans* NOWR-5 may be able to use this mechanism for movement over surfaces such as on minerals. In addition, both the data and draft genomes contained a *pilT* gene that is required for twitching motility (Han et al., 2008). This could indicate that these organisms are able to move over moist surfaces by extending and retracting their type IV pili (Mattick, 2002).

Interestingly, *Alb. acidocaldarius* strain 104-IA was reported to possess genes for all of the necessary proteins to assemble a flagellum, but unlike closely related species, it did not express a motile phenotype (Mavromatis et al., 2010). This was explained by the absence of the chaperones *flgN*, *fliJ*, and *fliT* as well as *flhC* and *flhD* (Mavromatis et al., 2010). Although none of these genes were identified in the data or in the draft genomes, motility from *Ab. ferrooxidans* Huett2 has been documented (Schieferbein et al., 2017). It is possible that these genes have not been annotated in the genomes of these organisms yet.

3.5.2 Metagenome 2: fungal target

A big red flag for fungal scaffold assemblies was that coverage values were very low, being mainly between 4X-5X. Values below 25X can affect assembly, but for reliable results, values of at least 10X-15X should be obtained (Ma & Fedorova, 2010; Zoli et al., 2016). Low coverage values in fungal genome sequencing projects can be caused by the presence of repetitive elements and by bacterial DNA in the samples, which complicates the assembly process (Ma & Fedorova, 2010). We know that the latter was the case in this project. Variations exist in fungal genome sizes, but *Penicillium* genomes such as from *P. chrysogenum*, have been documented to be ~32 Mb with a GC-content of 48.9% (van den Berg et al., 2008). A total of 38,434,819 bp were sequenced from the Metagenome 2 sample and the GC-content also did not differ substantially from the one documented in *P. chrysogenum*. However, the sequences obtained certainly did not all belong to the target organism therefore these values are not representative of *Penicillium* sp. that was examined in this study. In fact, results demonstrated that very little genetic information was obtained for the fungus.

Most of the taxonomic hits from the Metagenome 2 sample were assigned to the domain Eukaryota, and nearly all of those hits were identified as belonging to the Ascomycota phylum. This was expected since DNA was extracted from fungal mycelium. Most of the Ascomycota hits also were classified into the Eurotiomycetes class in which *Penicillium* belongs. A small percentage of hits were assigned to other groups such as the classes Sordariomycetes, Leotiomycetes, and Dothideomycetes, as well as the phylum Basidiomycota. These findings were consistent with AMD communities documented in the literature (Kanti Das et al., 2008; Mariner et al., 2008; Oggerin et al., 2016; Wang et al., 2018). Unexpectedly, most of the hits in the *Trichocomaceae* family were assigned to the genus *Neosartorya*.

Based on these results, fungal biomass from the enrichment culture did not only belong to the genus *Penicillium*. As microbial communities in the environment almost always consist of various fungal genera and species, these findings were not surprising, especially since ensuring the isolation of *Penicillium* sp. was a limited pursuit in this study. The presence of multiple fungal organisms in the enrichment culture further supports the important roles they have in these communities, and based on the genera identified, it can be speculated with confidence that these organisms may be contributing to the transformation and accumulation of heavy metals (Hongxiang et al., 2010; Mariner et al., 2008).

Most of the bacterial taxonomic hits from this sample have also been documented in AMD (Chun-bo et al., 2006; Garcia-Moyano et al., 2015; Mariner et al., 2008; Wang et al., 2018). These results supported that multiple bacteria are present in the fungal mycelium including Fe^{2+}-oxidizers that would produce visible Fe^{3+} precipitation on the fungal colonies. This can be beneficial for bacteria in many ways such as by helping them to disperse when the environment is not aqueous (Worrich et al., 2016).

No reports of cyanobacteria in AMD were found in the literature, not even from the Rio Tinto river which has relatively high diversity compared to other sites (Costas et al., 2007). This was attributed to the requirement of a minimal pH value of 4.8 for the proliferation of these organisms (Costas et al., 2007). Symbiotic associations have been documented between fungi and cyanobacteria, including the formation of fungal-cyanobacterial pellets, but it is more likely that the annotation of these taxonomic hits was incorrect (Jiang et al., 2020; Miranda et al., 2015; Siqueira & Lima, 2012).

Preliminary genetic description of *Penicillium* sp.

Given the low coverage values obtained for Metagenome 2 and the complexity of assembling fungal genomes, the genes were only annotated using MG-RAST. Very few genes were identified for a large fungal genome, therefore it appears that most of the *Penicillium* genome was not sequenced in this study. Despite sending at least 50 ng of DNA (based on our measurements), samples should contain more DNA in the future and bacterial DNA should optimally not be present in the sample prior to sequencing. Unexpectedly, less than a dozen subsystem hits were assigned to the genus *Penicillium*, and most of the genes in the Ascomycota phylum were assigned by MG-RAST to the Sordariomycetes class.

We assessed genes associated with the utilization of sugars to compare organic sources that might be used by these fungi with those used by *Ab. ferrooxidans*. Results suggested that the fungus may be assimilating organic carbon from sources including D-glucose, xylose, L-rhamnose, D-galacturonate and D-glucuronate. The ability of fungi to use different sugars varies between species, but a study done on 57 different species established that they could all use glucose, and that nearly all of them could also use fructose and mannose (Virgil Greene &

Barnett, 1953). Sources that might be used by both organisms were identified as trehalose, D-mannose, and fructose. The carbon source provided in the FeTSB medium that was used to cultivate these microorganisms was tryptone soya broth which contained dextrose (D-glucose) rather than yeast extract (HiMedia Laboratories, 2011). In addition, the solidifying agent, gellan gum, is a polysaccharide formed by repeating tetrasaccharide units consisting of 2 residues of D-glucose, 1 D-glucuronic acid residue, and 1 L-rhamnose residue (Morales & Ruiz, 2016). These are all sugars which the fungus appears to be able to utilize, and according to observations by Holanda et al. (2016), *Ab. ferrooxidans* would utilize the D-glucose poorly and would benefit from its accelerated depletion by the heterotrophic fungus.

One gene coding for a carbonic anhydrase that is involved in cyanate hydrolysis was identified. Cyanide is often present in wastewaters such as from mining (Luque-Almagro et al., 2018). Various microorganisms have been documented to degrade or utilize cyanate as a nitrogen source, and this has been investigated for its potential use in removing cyanate from wastewater (Luque-Almagro et al., 2018). The carbonic anhydrase-coding gene identified in the data may be a beta-class enzyme that is required for cyanate hydrolysis via cyanase enzymes (Elleuche & Poggeler, 2009). Genomes of fungi from the phylum Ascomycota have been reported to contain genes for both beta- and alpha-class carbonic anhydrases (Elleuche & Poggeler, 2009).

In the fatty lipid biosynthesis subsystem category, a gene coding for an enzyme involved in sphingolipid biosynthesis was identified, and these are membrane lipids that are often used as taxonomic markers because they're not universally present in bacteria and fungi (Olsen & Jantzen, 2001). Although query cover (~55-61%) and percent identity values (~71-77%) were relatively low from querying the nucleotide sequence of this enzyme against the

NCBI database, the most similar sequences were from species of *Penicillium* which supported that this gene most likely belonged to the target fungus and might belong to the top hit, *P. chrysogenum* Wisconsin 54-1255. This was consistent with the BLAST results of contig #17 from Metagenome 1 as well as with sequences annotated by MG-RAST as aldehyde dehydrogenase-coding genes and a peptidoglycan synthesis-related gene. Aldehyde dehydrogenase enzymes have been identified in almost all species of fungi, and this gene has been reported to reduce ethanol stress in the fungus *Tricholoma vaccinum* (Asiimwe, 1973; Wei et al., 2009).

Siqueira & Lima (2013) reported that species of *Aspergillus* and *Penicillium* which they recovered from a water system could produce biofilms when grown in the laboratory. This study did not find any genetic evidence of fungal biofilm formation. Microorganisms often require hydrophobic interactions to firmly attach to water-solid interfaces (Siqueira & Lima, 2012). Fungi such as *Penicillium* spp. produce a membrane of hydrophobin proteins that are located externally on the surface of their cells (Siqueira & Lima, 2012). Fungal pellet formation relies on hydrophobic interactions, and hydrophobin encoding genes have been found to strongly influence these adhesion forces (Veiter et al., 2018). Due to these hydrophobic interactions, in combination with electrostatic interactions, bacteria can attach to the surface of fungal cells in fungal-bacterial biofilms (Siqueira & Lima, 2012). However, no genetic evidence of hydrophobin encoding genes were identified in this study.

Laccase-like multicopper oxidases (LMCOs) are part of the multicopper oxidase (MCO) superfamily identified in bacteria, fungi and plants (Berni et al., 2019). The genomes of many filamentous fungi have been documented to contain genes for these enzymes including several LMCO gene families in fungi of the phyla Ascomycota and Basidiomycota (Kellner et

al., 2007; Ramos et al., 2011). A total of 13 MCO genes were identified in the genome of *A. niger* ATCC 1015 that were part of 3 different subfamilies including ascomycete laccases, fungal pigment MCOs, and fungal ferroxidases (Ramos et al., 2011). It is known that LMCOs catalyze the oxidation of many substrates and that this reaction is coupled to the reduction of O_2, but they are versatile enzymes and further research is required to understand their roles in different fungal species (Berni et al., 2019; Copete et al., 2015). Several species of *Penicillium* are able to efficiently break down lignin using LMCOs (Kellner et al., 2007). Most importantly, LMCOs can use divalent metal ion substrates (Kues & Ruhl, 2011). Fet3-type ferroxidases have been identified in the genomes of most species of Basidiomycota, and this enzyme has been demonstrated to oxidize Fe^{2+} to Fe^{3+} prior to transporting the metal inside the cell (Kues & Ruhl, 2011). Expression and activity of laccase enzymes is induced by the availability of nutrients such as nitrogen and carbon, as well as by exposure to heavy metals including cadmium, zinc, copper and manganese (Cho et al., 2009; Kues & Ruhl, 2011). This enhanced activity when heavy metals are present suggests that laccase enzymes may contribute to the adaptation of fungi in heavy metal rich environments (Cho et al., 2009). The adsorption of heavy metals onto the biomass of fungi from the study by Cho et al. (2009) was also documented.

BLAST results supported that the 4 multicopper oxidase enzymes which were annotated by MG-RAST most likely belong to either *Penicillium* sp. or *Aspergillus* sp., and that these may be type 3 MCOs. The top hit for one of the genes was a cupredoxin protein from *Aspergillus* sp., which is consistent with multiple domains of MCO enzymes being homologous to cupredoxins (Sedlak et al., 2018). These enzymes have received interest for biotechnological applications and could potentially be contributing to the oxidation of divalent metals by *Penicillium* sp. in this study (Berni et al., 2009; Cho et al., 2009).

3.6 Conclusion

Genomic descriptions provide insight into the potential of different species and strains for bioleaching technology as well as into conditions that best support their growth and leaching rates. In this study, we analyzed genomic data obtained from a bacterium and a fungus that were cultured together from low-sulfur containing waste rock. These organisms were chosen based on their ability to oxidize Fe^{2+} in co-culture as well as when they appeared to be isolated from each other.

By constructing a phylogenetic tree with the 16S rRNA gene sequence from the target bacterium, we were able to conclude with high levels of confidence that it was most similar to sequences from strains of *Ab. ferrooxidans* including SLC66, Huett2, and BOR5. The ID "*Ab. ferrooxidans* NOWR-5" was therefore assigned to this bacterium for the remainder of the study. It was determined that gene sequences from the fungus were consistently most identical to those from species of *Penicillium*, and multiple gene sequences from the Metagenome 1 and 2 samples were specifically most similar to sequences from *P. chrysogenum* Wisconsin 54-1255.

Genes that were evidently involved in respiratory Fe^{2+} oxidation were not identified in the genome of *Ab. ferrooxidans* NOWR-5 or in any of the compared genomes. These results could be explained by the inability of many commonly used pipelines to annotate genes related to iron metabolism, or the fact that Gram-positive iron-oxidizing bacteria do not require porin-cytochrome systems to transfer electrons to terminal oxidase enzymes, such as the aa3-type cytochrome oxidases identified from the genomes of *Ab. ferrooxidans* (White et al., 2016). Genes were identified which suggested that this bacterium might be able to use alternative terminal electron acceptors in anaerobic conditions. Although facultative anaerobic metabolism

using Fe^{3+} has been documented in *Ab. ferrooxidans*, only genes encoding enzymes for respiratory nitrate reduction were identified in the genome of *Ab. ferrooxidans* NOWR-5, and these were absent from all of the compared genomes. These findings indicate that either the genes have not yet been annotated from the submitted draft genomes, or that they might be unique to this particular strain of *Ab. ferrooxidans*.

Results from this study seemed to support that *Ab. ferrooxidans* NOWR-5 can use various sugars, and no genetic information was acquired to explain the observation by others that *Ab. ferrooxidans* grows poorly when glucose is provided as a carbon source. I proposed, based on observations from other studies, that the utilization of D-glucose may be limited due to the presence of poor nitrogen sources (inorganic) in growth media.

The rTCA cycle for the fixation of CO_2 was found to be almost complete in this study, but no evidence has been reported that *Ab. ferrooxidans* possesses this metabolic ability.

We found that *Ab. ferrooxidans* may be able to maintain intracellular pH using various mechanisms such as proton pumps, buffer molecules, and the degradation of organic acids. This genus has been found to be as resistant to heavy metals as other Fe^{2+}-oxidizing bacteria, and this was supported by the findings in this study which identified genes for the resistance of various metals. A large number of genes were also identified for resistance to various antibiotics. This co-resistance is often observed in AMD and is likely a result of the bacterium having been exposed to several heavy metals at the mine waste site.

Sporulation has been observed by the Gram-positive *Ab. ferrooxidans* which is consistent with our findings. Considering the complex mechanism of endospore formation and the large number of proteins involved, it is likely that many genes have yet been annotated in any of the draft genomes of *Ab. ferrooxidans*. We may have identified some of these genes.

Biofilm formation has also been documented by *Ab. ferrooxidans* SLC66, but only a few genes were annotated which may be involved in this process, including the *gal* genes from the Leloir pathway to form extracellular polysaccharides that many microorganisms utilize as precursors for biofilm matrix formation. These genes appeared to form an operon for which the organization was nearly identical in the genomes of *Ab. ferrooxidans* NOWR-5 as well as the compared genomes of strain Huett2 and SLC66, but which was unique from the organization of other well-described *gal* operons. It is likely that many genes have yet been sequenced and characterized. In addition, a large number of genes coding for proteins involved in the assembly of flagella were identified, as well as a couple genes suggesting potential motility by swarming and twitching of the cells.

The important findings described above were combined to produce a whole-cell model illustrating the potential metabolic abilities of *Ab. ferrooxidans* NOWR-5 (Figure 3.25). Certain pathways and system categories are indicated in boxes whereas others are presented in more detail by showing the individual proteins and enzyme complexes (color-coded). Gene names are provided for individual genes, whereas the name of enzyme complexes or of operons are presented if multiple genes constituting them were identified.

Most of the annotated genes by MG-RAST from the Metagenome 2 sample were assigned to Sordariomycetes, but nearly all of the gene sequences that were queried against the NCBI database were most similar to sequences from *Penicillium* spp. or *Aspergillus* spp., which supported that these genes may belong to the fungal target organism. It was hypothesized that genes pertaining to metal-chelating compounds, such as chitin or chitosan, would have been annotated in the fungal genome. LMCO genes were identified that appeared to belong to *Penicillium* spp. or *Aspergillus* spp. and which have been proposed to be a result of fungi

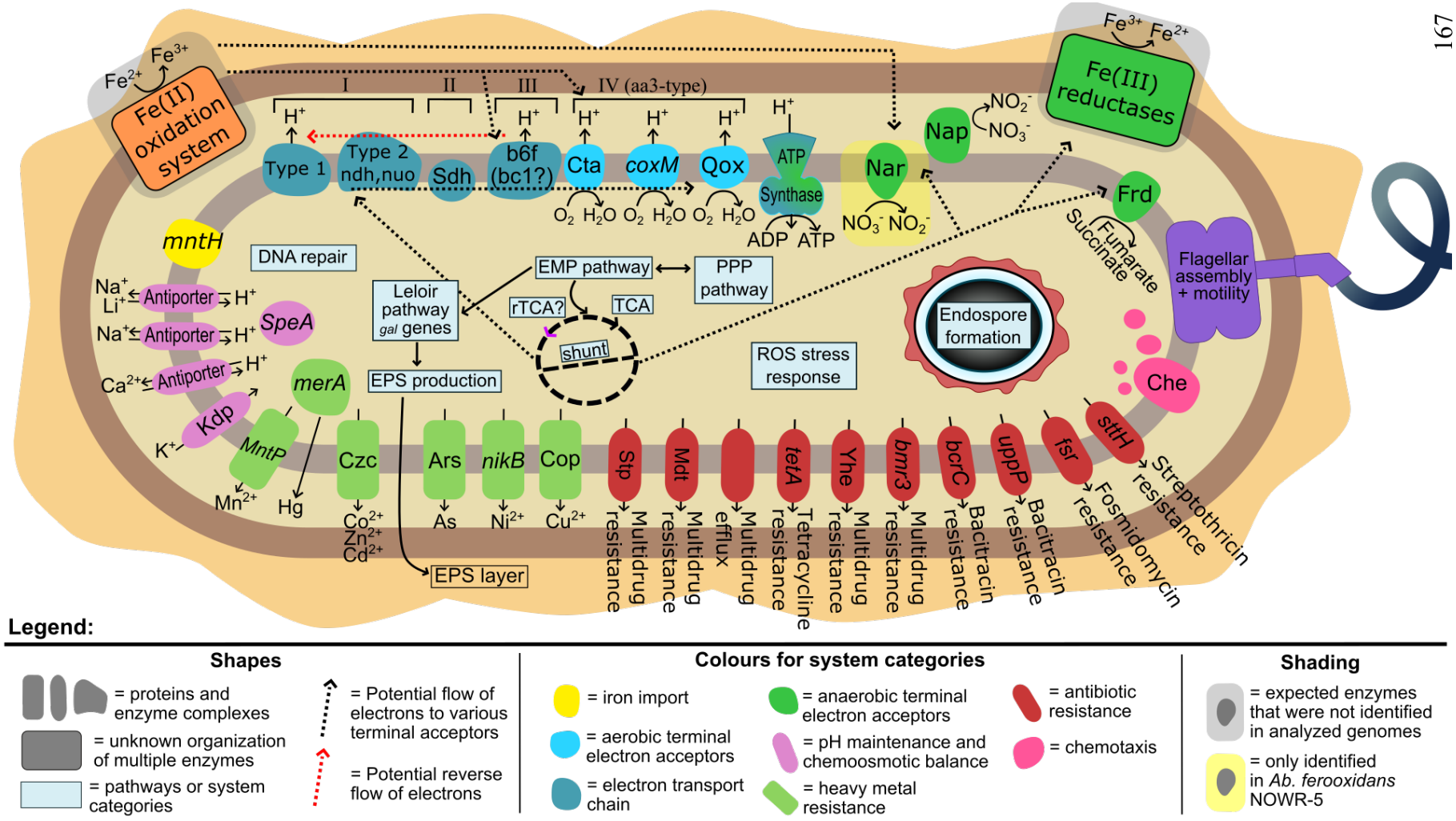

Figure 3.25: **Genome-based whole-cell model indicating the potential metabolic abilities of *Ab. ferrooxidans* NOWR-5.** Constructed by summarizing the important findings from the annotation of genes by Prokka and RAST. Peptidoglycan layer colored brown; Inner membrane colored grey. Question marks indicate uncertainty. Purple arrow represents the reverse direction of the TCA cycle. Type 1 complex I of the electron transport chain corresponds to genes encoding NADH-dehydrogenase-like proteins.

adapting to life in heavy metal-rich environments, and this enzyme might be oxidizing divalent metals such as Cu^{2+} and Fe^{2+}.

We hypothesized that the fungal genome would reveal insights into how the bacterial organism might be benefitting from its presence as observed in Chapter 2. Species of *Penicillium* have been documented to form biofilms that specifically have hydrophobic interactions which can serve as a surface for the adhesion of bacterial cells, but genes encoding hydrophobin proteins and proteins for biofilm formation were not identified. Considering the observation that *Ab. ferrooxidans* grew poorly on D-glucose in the study by Holanda et al. (2016), the fungus could be accelerating the consumption of glucose for this heterotrophic bacterium.

This study provided insight about the relatively uncharacterized genomes of the Fe^{2+}-oxidizing bacterium, *Ab. ferrooxidans*, and the extremophilic fungus, *Penicillium* sp., that were isolated from the BWR enrichment culture (Chapter 2). It identified genes associated with adaptations to acidic- and metal-rich environments, as well as acquired genetic information to support that these microorganisms could potentially be successfully used for bioleaching and/or bioremediation applications.

CHAPTER 4:

INSIGHTS FROM THIS STUDY AND FUTURE DIRECTIONS

4.1 Combined findings from culturing and DNA sequencing

This study aimed to isolate and describe microorganisms from an enrichment culture that was inoculated with low-sulfur waste rock from a mine site in Northern Ontario, and from 2 enrichment cultures which are maintained for the optimization of bioleaching technologies to recover metals from different sulfidic waste materials in bioreactor tanks.

By repeatedly streaking BWR, one type of each bacterial and fungal colonies appeared to have been isolated. Results from Sanger sequencing and whole-genome sequencing identified that sequences from the fungus matched almost perfectly to those from species of *Penicillium*, and 16S rRNA sequences from the bacterium were repeatedly identified as being most similar to sequences from species of *Alicyclobacillus* and strains of *Ab. ferrooxidans*. A phylogenetic analysis confirmed with high levels of confidence that the bacterial organism clustered with Fe^{2+}-oxidizing *Ab. ferrooxidans* strains, such as *Ab. ferrooxidans* strain SLC66, and was distinct from the *Alicyclobacillus* cluster. These identifications were supported by macroscopic colony morphologies as well as microscopic cellular characteristics. They were cultivated on glucose-containing medium which is consistent with their heterotrophic and mixotrophic metabolisms. The growth of *Ab. ferrooxidans* NOWR-5 at ~25-27 °C was also consistent with species of this genus.

Fe^{3+} precipitation persisted even when the fungus appeared to be separated. Despite the fact that the bacterial colony appeared to be isolated, whole-genome sequencing data confirmed that the extracted DNA still contained genetic material from fungal cells.

Penicillium sp. may have been isolated in this study considering that it was repeatedly amplified by Sanger sequencing which would have failed if multiple types of fungi were present, and because sequencing did not detect bacterial DNA from fungal mycelium that accumulated Fe^{3+}. It is however possible that a large amount of fungal DNA suppressed the amplification of bacterial DNA. The extracted sample for Metagenome 2 was fungal mycelium, and taxonomic analyses indicated that it contained genetic material from various groups of fungi and bacteria that have been documented in acidic- and metal-rich environments, including Fe^{2+}-oxidizers and taxonomic hits which likely corresponded to *Ab. ferrooxidans* NOWR-5. It was interesting to note that the target bacterium in the Firmicutes phylum was not a dominant member in the fungal mycelium, but that it was the only colony that was identified with *Penicillium* sp. These findings combined with the difficulty to separate bacterial and fungal growth in cultures support that these organisms may benefit from growing together.

We therefore could not determine with certainty whether the increased rate of Fe^{2+} oxidation was induced by the fungus directly or indirectly by positively influencing *Ab. ferrooxidans* and other chemolithotrophs. However, it appeared as though either Fe^{2+} oxidation was increased by the contribution from both organisms, or that *Ab. ferrooxidans* proliferated more successfully in the presence of *Penicillium* sp. A gene encoding a fungal multicopper oxidase was identified in the genome sequencing data. The presence of this gene in other fungi has been considered to be an adaptation for living in heavy metal-rich environments, and this enzyme could be contributing to the oxidation of divalent metals including Fe^{2+} and Cu^{2+}, as was observed in Chapter 2. Resistance to these particular metals corresponded with the fact that this fungus was obtained from an enrichment culture of low-sulfur waste rock from a nickel-copper-mixed element mine.

We initially hypothesized that *Ab. ferrooxidans* was benefiting from the presence of the fungal organism due to its consumption of organic carbon, which can be inhibitory to chemolithotrophic bacteria. Given the findings of Holanda et al. (2016), the fungus was likely assisting *Ab. ferrooxidans* by depleting growth-limiting glucose at a faster rate than if the bacterium was growing independently in cultures.

Fungal biomass visibly accumulated Fe^{3+} in liquid and on solid media. On plates, the metal was either precipitated on the mycelium or around the colony. The latter was likely caused by the secretion of oxidizing metabolites, but accumulation onto fungal biomass indicated sorption of the Fe^{3+} molecules. In liquid cultures, fungal filaments aggregated either loosely or formed dense pellets. In both cases, the biomass went from white to orange, turbidity of the culture decreased over time, and these cultures appeared to have smaller amounts of settled precipitates than the bacterial culture. Fungal pellets appeared to accumulate less Fe^{3+}.

Most of the bacterial genes identified in this study have been annotated in the draft genomes of *Ab. ferrooxidans* and were consistent with current insights on this organism. For instance, a large number of genes pertaining to sporulation were annotated as well as genes for the assembly of flagella and motility. *Ab. ferrooxidans* is a Gram-positive sporulating organism, and motility has been documented for strain SLC66 (Holanda et al., 2016). We also found genes suggesting resistance to multiple heavy metals and antibiotics. Some of the genes from these categories were not present in the currently available draft genomes and may correspond to genes that have not yet been annotated in these organisms, especially since many of them were present in closely related bacteria such as *Alb. acidocaldarius* subsp. *acidocaldarius* DSM 446. Additionally, the identification of genes which were absent from the draft genomes indicated that the organism may possess metabolic abilities that have yet to be

characterized. These included the use of nitrate as an alternative electron acceptor in the absence of oxygen, which could potentially be coupled to the respiratory oxidation of Fe^{2+}. Finally, genes for Fe^{2+} oxidation were not annotated despite visible precipitation in cultures and on bacterial colonies. Genes identified as part of the electron transport chain could potentially make up the Fe^{2+} oxidation pathway in this Gram-positive bacterium.

We transferred 4 colonies from each bioreactor culture that grew on FeTSB and ISP media. Purity of these cultures and reliable identifications remain to be established. From both ECT and BT, small circular yellow colonies with flat smooth surfaces were obtained which is consistent with colony morphology of *Leptospirillum* spp. and preliminary Sanger sequencing data from ECT grown on modified ISP supported that this bacterium is a chemolithotroph originating from similar extreme environments. Circular orange and red colonies were also obtained from both cultures. Colonies of *Sulfobacillus* spp. have been described as having a "fried egg" shape with an orange center, but preliminary identification supported that the red ECT3 colonies may be cells of a thermophilic bacterium of the *Bacillus* genus.

Substantial fungal growth was also observed from the BT culture. Different colony morphologies were apparent including brown circular colonies and black mold. These did not appear to oxidize or accumulate iron. In addition, grey colonies similar to those from BWR were present and they appeared to be accumulating Fe^{3+} precipitates.

4.2 Environmental implications and industrial applications

We found that *Ab. ferrooxidans* is a Fe^{2+}-oxidizing community member which may be contributing to the leaching of metals from the low-sulfur waste rock at the Northern Ontario mine site. This organism is relatively novel and requires assessment pertaining to

industrial bioleaching potential, but it has been suggested that this bacterium would be most effective for passive treatments. Findings from this study established that fungi also grew from the waste material, and that *Penicillium* sp. might be contributing to mineral weathering, Fe^{2+} oxidation, and Fe^{3+} accumulation. *Ab. ferrooxidans* appeared to grow well with *Penicillium* sp. and its colony was obtained by sub-culturing fungal mycelium. A mixed culture of these organisms might therefore be efficient for biotechnological applications. Bioaccumulation by the fungus would simplify the metal recovery process, and the use of this organism would be cost efficient. This function may be particularly useful for removing metals from contaminated water.

In this study, we began the process of isolating the dominant Fe^{2+}-oxidizers, *Leptospirillum* and *Sulfobacillus*, from the BT and ECT bioreactor enrichment cultures. Obtaining isolated cultures of these bacteria would allow for their assessment in controlled experiments to understand how their leaching rates can be consistently optimized. We found that a fungus capable of accumulating Fe^{3+} also grew from the BT enrichment culture, and that it was capable of growth below pH 2.0. This information supports that the fungus in this culture could potentially serve to increase leaching rates and to facilitate metal recovery in extreme bioreactor tank conditions. However, fungal biomass in leachate collection systems may need to be controlled seeing as how an abundance of growth could clog and disrupt the system, but their complete removal could decrease bacterial leaching efficiencies.

4.3 Future directions

Future work with the BWR enrichment culture should focus on obtaining and confirming the isolation of *Ab. ferrooxidans* and *Penicillium* sp. Fungal colonies can appear to be isolated, but they may have originated from multiple spores and therefore remain to be purified

(Ho & Ko, 1997). Accurate identification of fungi based on phenotypes and genetics requires cultures of single-spore isolates which can be obtained with methods that involve spore suspensions and the transfer of single spores to new media using light microscopy (Choi et al., 1999; Ho & Ko, 1997; Noman et al., 2018). Pure cultures are also required to accurately assess the organism's potential in biotechnological applications by performing controlled experiments (Noman et al., 2018).

Colony morphology of *Penicillium* sp. should be documented on standard media for fungi, such as Czapek media and Potato Dextrose Agar, since its morphology on plates with extreme media in this study was not reliable for identification purposes. However, it is important to remember that the organism could cease to produce enzymes or metabolites when stored in high-nutrient media which could result in the loss of specific functions (Choi et al., 1999).

Obtaining *Ab. ferrooxidans* may be more challenging considering that DNA from fungal spores were still detected from the bacterial colony which grew on a plate without visible fungal growth. Attempts to eliminate the fungus using inhibitory concentrations of copper chloride failed in work done with BWR prior to this study, and we found that antimycotic agents were also unsuccessful, potentially due to their degradation in the extreme media. Separating them by means of filtration probably also would not work because the bacterial cells are likely to be too similar in size to the fungal spores (Madsen et al., 2016; Tianli et al., 2014). Efforts to obtain a pure culture of *Ab. ferrooxidans* should focus on performing dilutions to extinction and streaking onto plates until the fungal organism has been entirely eliminated, or by using light microscopy and optical tweezers to transfer individual bacterial cells to new media (Zhang & Liu, 2008).

The oxidation of Fe^{2+} by *Penicillium* sp. could be assessed with certainty once single-spore isolates are obtained. By controlling cell concentrations of both the bacterium and the fungus, concentrations of precipitated Fe^{3+} could be compared between isolated cultures and mixed cultures. These experiments could be performed using iron assays, but the sorption of Fe^{3+} on fungal biomass would need to be taken into account. Future studies on these organisms should also analyze their potential for solubilizing, precipitating, and accumulating other metals. In order to do so and to optimize their efficiencies, factors such as cell concentrations will need to be strictly regulated. For instance, we unintentionally obtained dense fungal pellets that appeared to accumulate less Fe^{3+}. Using scanning electron microscopy (SEM) and Fourier-transform infrared spectroscopy (FTIR) would provide a clear image of how metals are being accumulated onto the fungal mycelium and of the arrangement of bacterial cells within this network for mixed cultures (Faramarz et al., 2005; Glukhova et al., 2008).

Considering *Penicillium* is a polyphyletic genus, housekeeping genes should be sequenced to assess if this fungus represents a novel species (Glukhova et al., 2018). Efforts to close the assembled genomes of *Penicillium* sp. and *Ab. ferrooxidans* from BWR should continue, especially since their genomes could be unique from others which are available in public databases and that many aspects of the genomes from *Ab. ferrooxidans* remain to be described, such as the Fe^{2+} oxidation pathway. In order to do so, results from short and long read sequencing platforms should be combined.

The annotation of genes pertaining to iron should be performed with the FeGenie tool and the database created by Garder et al. (2020) containing enzymes for iron acquisition, storage, and energy. Genes pertaining to the Fe^{2+} oxidation pathway could also be identified by searching for homologous protein or nucleotide sequences with software such as HMMER

(http://hmmer.org). Considering that *Ab. ferrooxidans* is a Gram-positive Fe^{2+}-oxidizing bacterium, future work should assess the genes identified from the electron transport chain, especially the ones encoding for aa3-type terminal oxidases, to determine whether any of them act as final electron acceptors from the oxidation of Fe^{2+} and/or directly oxidize Fe^{2+} on the inner membrane. The use of transcriptomics to assess if any of the electron transport chain-related genes are upregulated when the bacterium is grown in Fe^{2+}-containing medium could assist in distinguishing those which are involved with this pathway.

Biochemical and phenotypic analyses should be performed to support genomic information, such as our findings of genes from *Ab. ferrooxidans* involved in the utilization of alternate electron acceptors in the absence of oxygen as well as genes for flagellar assembly and motility. Future studies on *Penicillium* from this study should identify which MCO family the enzymes belong to as well as determine whether they're inducing the oxidation of divalent metals to maintain homeostasis. The use of transcriptomics would provide further insights on mechanisms of metal resistance and transformations in these organisms, such as by assessing whether *Penicillium* sp. overproduces organic acids during the TCA cycle, which would indicate that metals are being solubilized by acidolysis and chelation (Deng et al., 2019; Glukhova et al., 2018).

Efforts to obtain pure cultures of bacteria from ECT and BT should continue. If these are not identified as *Leptospirillum* and *Sulfobacillus*, solid selective media could potentially be improved by raising the pH to values between 2.0-2.5. Liu et al. (2007) were able to isolate *L. ferriphilum* on solid media that was adjusted to a final pH of 3.0. Characterization of the important bacterial and fungal organisms from ECT and BT should be characterized as described for the targets in BWR.

This project combined classic culturing techniques and genomic sequencing to isolate and characterize microorganisms of interest from enrichment cultures that were inoculated with different sources of mine waste materials. In order to understand the diversity and complexity of acidophiles from various sites around the world and to optimize biotechnologies for various mine waste materials, multidisciplinary studies such as this one must continue to be conducted.

REFERENCES

Abhilash, Pandey, B. D. (2012). Bioreactor leaching of uranium from a low grade Indian silicate ore. *Biochemical Engineering Journal*, 71: 111-117.

Adam, P. S., Borrel, G. & Gribaldo, S. (2018). Evolutionary history of carbon monoxide dehydrogenase/acetyl-CoA synthase, one of the oldest enzymatic complexes. *Proceedings of the National Academy of Sciences*, 115(6): 1166-1173.

Ahn, S., Jung, J., Jang, I.-A., Madsen, E. L., & Park, W. (2016). Role of Glyoxylate Shunt in Oxidative Stress Response. *J. Biol. Chem.*, 291(22): 11928-11938.

Al-okaily, A. A. (2016). HGA: *de novo* genome assembly method for bacterial genomes using high coverage short sequencing reads. *BMC Genomics*, 17: 193.

Amaral Zettler, L. A., Gomez, F., Zettler, E., Keenan, B. G., Amils, R., & Sogin, M. L. (2002). Microbiology: Eukaryotic diversity in Spain's River of Fire. *Nature*, 417: 137.

Amaral Zettler, L. A., Messerli, M. A., Laatsch, A. D., Smith, P. J. S., & Sogin, M. L. (2003). From Genes to Genomes: Beyond Biodiversity in Spain's Rio Tinto. *Biol. Bull*., 204(2): 205-209.

Amo, T., Atomi, H., & Imanaka, T. (2002). Unique Presence of a Manganese Catalase in a Hyperthermophilic Archaeon, *Pyrobaculum calidifontis* VA1. *J. Bacteriol.*, 184(12): 3305-3312.

Anton, A., Crobe, C., Reibmann, J., Pribyl, T., & Nies, D. H. (1999). CzcD is a Heavy Metal Ion Transporter Involved in Regulation of Heavy Metal Resistance in *Ralstonia* sp. Strain CH34. *J. Bacteriol.*, 181(22): 6876-6881.

Appia-Ayme, C., Bengrine, A., Cavazza, C., Giudici-Orticoni, M. T., Bruschi, M., Chippaux, M., & Bonnefoy, V. (1998). Characterization and expression of the co-transcribed cyc1 and cyc2 genes encoding the cytochrome c4 (c552) and a high-molecular-mass cytochrome c from Thiobacillus ferrooxidans ATCC 33020, *FEMS Microbiol. Lett.*, 167(2): 171-177.

Ardejani, F. D., Marandi, R., Marandi, A., Mirhabibi, A., & Baafi, E. (2005). Effects of pH and biomass concentrations in the removal of selenite from acid mine drainage by Aspergillus niger as biosorbent in Sarcheshmeh porphyry copper mine. *Conference: 9th International Mine Water Association*.

Arguello, J. M., Raimunda, D., & Padilla-Benavides, T. (2013). Mechanisms of copper homeostasis in bacteria. *Front. Cell. Infect. Microbiol.*, 3: 73.

Arsene-Ploetze, F., Chiboub, O., Lievremont, D., Farasin, J., Freel, K. C., Fouteau, S., & Barbe, V. (2018). Adaptation in toxic environments: comparative genomes of loci carrying antibiotic resistance genes derived from acid mine drainage waters. *Environ. Sci. Pollut. Res. Int.*, 25(2): 1470-1483.

Asha, H. & Gowrishankar, J. (1993). Regulation of *kdp* Operon Expression in *Escherichia coli*: Evidence Against Turgor as Signal for Transcriptional Control. *J. Bacteriol.*, 175(14): 4528-4537.

Asiimwe, V. T. (1973). Molecular characterization of a fungal aldehyde dehydrogenase in the *Tricholoma vaccinum*-spruce ectomycorrhiza. *Msc Dissertation*. Pdf.

Auld, R. R. (2014). Re-examining Temporal and Seasonal Microbial Acid Mine Drainage Community Variations. The School of Graduate Studies, Laurentian University, 1-88.

Auld, R. R., Myre, M., Mykytczuk, N. C. S., Leduc, L. G., & Merritt, T. J. S. (2013). Characterization of the microbial acid mine drainage microbial community using culturing and direct sequencing techniques. *Journal of Microbiological Methods*, 93: 108-115.

Auld, R. R., Mykytczuk, N. C. S., Leduc L. G., & Merritt, J. S. (2017). Seasonal variation in an acid mine drainage microbial community. *Can. J. Microbiol.*, 63: 137-152.

Ayling, M., Clark, M. D., & Leggett, R. M. (2020). New approaches for metagenome assembly with short reads. *Briefing in Bioinformatics*, 21(2): 584-594.
Aziz, R. K., Bartels, D., Best, A. A., DeJongh, M, Disz, T., Edwards, R. A., Formsma, K., […] Zagnitko, O. (2008). The RAST Server: Rapid Annotations using Subsystems Technology. *BMC Genomics*, 9: 75.
Baindara, P. (2019). Mechanism of Bacterial Co-resistance. In Mandal, S. & Paul, D. (Eds.), *Bacterial Adaptation to Co-resistance*. Springer, Singapore.
Baker-Austin, C. & Dopson, M. (2007). Life in acid: pH homeostasis in acidophiles. *TRENDS in Microbiology*, 15(4): 165-171.
Baker, B. J. & Banfield, J. F. (2003). Microbial communities in acid mine drainage. *FEMS Microbiol. Ecol.*, 44(2), 139-152.
Baker, B. J., Lutz, M. A., Dawson, S. C., Bond, P. L., & Banfield J. F. (2004). Metabolically Active Eukaryotic Communities in Extremely Acidic Mine Drainage. *Appl. Environ. Microbiol.*, 70(10): 6264-6271.
Baker, B. J., Tyson, G. W., Goosherst, L, & Banfield, J. F. (2009). Insights into the Diversity of Eukaryotes in Acid Mine Drainage Biofilm Communities. *Appl. Environ. Microbiol.,* 75(7): 2192-2199.
Baldrian, P. (2003). Interactions of heavy metals with white-rot fungi. *Enzyme and Microbial Technology*, 32(1): 78-91.
Bankevich, A., Nurk, S., Antipov, D., Gurevich, A. A., Dvorkin, M., Kulikov, A. S., Lesin, V. M., […] Pevzner, P. A. (2012). SPAdes: A New Genome Assembly Algorithm and Its Applications to Single-Cell Sequencing. *Journal of Computational Biology*, 19(5): 455-477.
Barahona, S., Castro-Severyn, J., Dorador, C., Saavedra, C., & Remonsellez, F. (2020). Determinants of Copper Resistance in *Acidithiobacillus Ferrivorans* ACH Isolated from the Chilean Altiplano. *Genes*, 11: 844.
Baranova, N. & Nikaido, H. (2002). The baeSR two-component regulatory system activates transcription of the yegMNOB (mdtABCD) transporter gene cluster in Escherichia coli and increases its resistance to novobiocin and deoxycholate. *J. Bacteriol.*, 184(15): 4168-4176.
Barbas III, C. F., Burton, D. R., Scott, J. K., & Silvermann, G. J. (2007). Quantitation of DNA and RNA. *Cold Spring Harb. Protoc.*.
Barreto, M., Jedlicki, E., & Holmes, D. S. (2005). Identification of a Gene Cluster for the Formation of Extracellular Polysaccharide Precursors in the Chemolithoautotroph *Acidithiobacillus ferrooxidans*, 71(6): 2902-2909.
Bashir, Y., Singh, S. P., & Konwar, B. K. (2014). Metagenomics: An Application Based Perspective. *Chinese Journal of Biology*, (2014): 7 pages.
Baureder, M. & Hederstedt (2011). Production, purification and detergent exchange of isotopically labeled *Bacillus subtilis* cytochrome b_{558} (SdhC). *Protein Expression and Purification*, 80(1): 97-101.
Beale, S. I. (2009). Biosynthesis of Chlorophylls and Hemes. In Harris, E. H., Stern, D. B., & Witman, G. B. (Eds.), *The Chlamydomonas Sourcebook* (Second Edition). Elsevier.
Ben Ali, H. E., Neculita, C. M., Molson J. W., Masqoud, A., & Zagury, G. J. (2019). Performance of passive systems for mine drainage treatment at low temperature and high salinity: A review. *Minerals Engineering*, 134: 325-344.
Bender, G., Pierce, E., Hill, J. A., Darty, J. E., & Ragsdale, S. W. (2011). Metal centers in the anaerobic microbial metabolism of CO and CO_2. *Metallomics*, 3(8): 797-815.
Berg, I. A. (2011). Ecological Aspects of the Distribution of Different Autotrophic CO_2 Fixation Pathways. *Applied and Environmental Microbiology*, 77(6): 1925-1936.
Berni, R., Piasecki, E., Legay, S., Hausman, J.-F., Siddiqui, K. S., Cai, G., & Guerriero, G.

(2019). Identification of the laccase-like multicopper oxidase gene family of sweet cherry (*Prunus avium* L.) and expression analysis in six ancient Tuscan varieties. *Scientific Reports*, 9: 3557.

Bieniek, A. K. (2019). A Metagenomic Analysis of Tailings Microbial Communities from Both Cold and Hot Environments. *A thesis submitted in partial fulfillment of the requirements for the degree of Master of Science (MSc) in Biology, Laurentian Univeristy*.

Blasco, F., Lobbi, C., Ratouchniak, J., Bonnefoy, V., & Chippaux, M. (1990). Nitrate reductases of Escherichia coli: sequence of the second nitrate reductase and comparison with that encoded by the narGHJI operon. *Mol. Gen. Genet.*, 222(1): 104-111.

Bogdanova, T. I., Tsaplina, I. A., Kondrat'eva, T. F., Duda, V. I., Suzina, N. E., Melamud, V. S., Tourova, T. P., & Karavaiko, G. I. (2006). *Sulfobacillus thermotolerans* sp. nov., a thermotolerant, chemolithotrophic bacterium. *Int. J. Sys. Evol. Microbiol.*, 56(5): 1039-1042.

Bogino, P. C., Oliva, M. M., Sorroche, F. G., & Giordano, W. (2013). The Role of Bacterial Biofilms and Surface Components in Plant-Bacterial Associations. *Int. J. Mol. Sci.*, 14(8): 15838-15859.

Bond, P. L., Smriga, S. P., & Banfield, J. F. (2000). Phylogeny of Microorganisms Populating a Thick, Subaerial, Predominantly Lithotrophic Biofilm at an Extreme Acid Mine Drainage Site. *Appl. Environ. Microbiol.*, 66(9): 3842-3849.

Bott, M., Preisig, O., & Hennecke, H. (1992). Genes for a second terminal oxidase in Bradyrhizobium japonicum. *Arch. Microbiol.*, 158(5): 335-343

Bourzama, G., Ennaghra, N., Soumati, B., Benoune, S., & Atriche, N. (2019). Effect of Zinc Metal at High Concentration on Secondary Metabolic Pathways in Penicillium Chrysogenum Strain. *The Journal of Microbiology, Biotechnology and Food Sciences*, 9(2): 307-313.

Bren, A., Park, J. O., Towbin, B. D., Rabinowitz, J. D., & Alon, U. (2016). Glucose becomes one of the worst carbon sources for *E. coli* on poor nitrogen sources due to suboptimal levels of cAMP. *Sci. Rep.*, 6: 24834.

Breuker, A., Blazejak, A., Bosecker, K., & Schippers, A. (2009). Diversity of Iron Oxidizing Bacteria from Various Sulfidic Mine Waste Dumps. *Advanced Materials Research*, 71-73: 47-50.

Brown, J., Pirrung, M., & McCue, L. A. (2017). FQC Dashboard: integrates FastQC results into a web-based, interactive, and extensible FASTQ quality control tool. *Bioinformatics*, 33(19): 3137-3139.

Bullerman, L. B. (2003). Penicillium. In Caballero, B. (Eds.), *Encyclopedia of Food Sciences and Nutrition, 2nd Edition*. Elsevier Science.

Campbell, B. J. & Cary, S. C. (2004). Abundance of Reverse Tricarboxylic Acid Cycle Genes in Free-Living Microorganisms at Deep-Sea Hydrothermal Vents. *Applied and Environmental Microbiology*, 70(10): 6282-6289.

Cavazza, C., Giudici-Orticoni, M. T., Nitschke, W., Appia, C., Bonnefoy, V., & Bruschi, M. (1996). Characterisation of a soluble cytochrome c4 isolated from Thiobacillus ferrooxidans, *Eur. J. Biochem.*, 242(2): 308-314.

Cecchini, G., Schroder, I., Gunsalus, R. P., & Maklashina, E. (2002). Succinate dehydrogenase and fumarate reductase from *Escherichia coli*. *Biochimica et Biphysica Acta (BBA) – Bioenergetics*, 1553(1-2): 140-157.

Chai, Y., Beauregard, P. B., Vlamakis, H., Losick, R., & Kolter, R. (2012). Galactose Metabolism Plays a Crucial Role in Biofilm Formation by *Bacillus subtilis*. *mBio*, 3(4): e00184-12.

Charlebois, A., Jalbert, L.-A., Harel, J., Masson, L., & Archambault, M. (2012). Characterization of Genes Encoding for Acquired Bacitracin Resistance in *Clostridium perfringens*. *PLoS One*, 7(9): e44449.

Chen, J., Li, J., Zhang, H., Shi, W., & Liu, Y. (2019). Bacterial Heavy-Metal and Antibiotic Resistance Genes in a Copper Tailing Dam Area in Northern China. *Front. Microbiol.*, 10: 1916.

Chen, J., Zhou, Z. C., & Gu, J. D. (2014). Occurrence and diversity of nitrite-dependent anaerobic methane oxidation bacteria in the sediments of the South China Sea revealed by ampligication of both 16S rRNA and pmoA genes. *Appl. Microbiol. Technol.*, 98(12): 5685-5696.

Chen, S.-Y. & Lin, J.-G. (2004). Bioleaching of heavy metals from contaminated sediments by indigenous sulfur-oxidizing bacteria in an air-lift bioreactor: effects of sulfur concentration. *Water Research*, 38: 3205-3214.

Chen, X., Schreiber, K., Appel, J., Makowka, A., Fahnrich, B., Roettger, M., Hajirezaei, M. R., […] Gutekunst, K. (2016). The Entner-Doudoroff pathway is an overlooked glycolytic route in cyanobacteria and plants. *PNAS*, 113(19): 5441-5446.

Chen, Y. & Wang, F. (2015). Insights on nitrate respiration by *Shewanella*. *Front. Mar. Sci.*, 1: 80.

Cho, N. S., Wilkolazka, A. J., Staszczak, M., Cho, H. Y., & Ohga, S. (2009). The role of laccase from white rot fungi to stress conditions. *Journal of the Faculty of Agriculture, Kyushu University*, 54(1): 81-83.

Choi, Y. W., Hyde, K. D., & Ho, W. H. (1999). Single spore isolation of fungi. *Fungal Diversity*, 3: 29-38.

Chun-bo, H., Hong-xun, Z., Zhi-hui, B., Qing, H., & Bao-guo, Z. (2006). A novel acidophile community populating waste ore deposits at an acid mine drainage site. *Journal of Environmental Sciences*, 19: 444-450.

Ciuffreda, E., Bevilacqua, A., Sinigaglia, M., & Corbo, M. R. (2015). *Alicyclobacillus* spp.: New Insights on Ecology and Preserving Food Quality through New Approaches. *Micrroorganisms*, 3(4): 625-640.

Coelho, C. & Romao, M. J. (2015). Structural and mechanistic insights on nitrate reductases. *Protein Science*, 24: 1901-1911.

Copete, L. S., Chanaga, X., Barriuso, J., Lopez-Lucendo, M. F., Martinez, M. J., & Camarero, S. (2015). Identification and characterization of laccase-type multicopper oxidases involved in dye-decolorization by the fungus *Leptosphaerulina* sp. *BMC Biotechnology*, 15: 74.

Costa, E., Teixido, N., Usall, J., Atares, E., & Vinas, I. (2002). The effect of nitrogen and carbon sources on growth of the biocontrol agent *Pantoea agglomerans* strain CPA-2. *Letters in Applied Microbiology*, 35: 117-120.

Costas, E., Flores-Moya, A., Perdigones, N., Maneiro, E., Blanco, J. L., Garcia, M. E., & Lopez-Rodas, V. (2007). How eukaryotic algae can adapt to the Spain's Rio Tinto : a neo-Darwinian proposal for rapid adaptation to an extremely hostile ecosystem. *New Physiologist*, 175(2): 334-339

Cotton, C. A. R., Edlich-Muth, C., & Bar-Even, A. (2017). Reinforcing carbon fixation: CO_2 reduction replacing and supporting carboxylation. *Current Opinion in Biotechnology*, 49: 49-56.

Couillard, D. & Mercier, G. (1990). Bacterial leaching of heavy metals from sewadge sludge—Bioreactors comparison. *Environmental Pollution*, 66(3): 237-252.

Crépeau, V., Bonavita, M.-A. C., Lesongeur, F., Randrianalivelo, H., Sarradin, P.-M., Sarrazin, J., & Godfroy, A. (2011). Diversity and function in microbial mats from the Lucky Strike hydrothermal vent field. *FEMS Microbiology Ecology*, 76(3): 524-540.

Crombie, A., T., Larke-Mejia, N. L., Emery, H., Dawson, R., Pratscher, J., Murphy, G. P., McGenity, T. J., & Murrell, J. C. (2018). Poplar phyllosphere harbors disparate isoprene-degrading bacteria. *Proc. Natl. Acad. Sci. USA*, 115(51): 13081-13086.

Dall'Agnol, H., Nancucheo, I., Johnson, D. B., Oliveira, R., Leite, L., Pylro, V. S., Holanda, R., […] Oliveira, G. (2016). Draft Genome Sequence of "*Acidithiobacillus ferrooxidans*" ITV01, a novel Acidophilic Firmicute Isolated from a Chalcopyrite Mine Drainage Site in Brazil. *Genome Announc.*, 4(2): 1748-15

Das, B. K., Roy, A., Koschorreck, M., Mandal, S. M., Wednt-Potthoff, K., & Bhattacharya, J. (2009). Occurrence and role of algae and fungi in acid mine drainage environment with special reference to metals and sulfate immobilization. *Water Research*, 43(4): 883-894.

Deguchi, S. (2011). Versatile Solidified Media for Growth of Extremophiles. In Horikoshi, K. (Eds.), *Extremophiles Handbook*. Springer, Tokyo.

De Lange, J. H. (1989). Significance of autoclaving-induced toxicity from and hydrolysis of carbohydrates in *in vitro* studies of pollen germination and tube growth. *S. Afr. J. Bot.*, 55(1): 1-5.

Deng, X.-H., Chai, L.-Y., Yang, Z.-H., & Wang, Y.-Y. (2014). Influence of heavy metal stress on morphology and physiology of *Penicillium chrysogenum* during bioleaching process. *J. Cent. South. Univ.*, 21: 3254-3262.

Deng, X., Yang, Z., & Chen, R. (2019). Study of Characteristics on metabolism of *Penicillium chrysogenum* F1 during bioleaching of heavy metals from contaminated soil. *Can. J. Microbiol.*, 65: 629-641.

Denkel, L. A., Horst, S. A., Rouf, S. F., Kitowski, V., Bohm, O. M., Rhen, M., Jager, T., & Bange, F.-C. (2011). Methionine Sulfoxide Reductases are Essential for Virulence of *Salmonella tiphymurium*. *PLoS One*, 6(11): e26974

de Souza, Y. P. A. & Rosado, A. S. (2019). Opening the Black Box of Thermophilic Autotrophic Bacterial Diversity. In Das, S. & Dash H. R. (Eds.), *Microbial Diversity in the Genomic Era*. Academic Press.

diCenzo G. C. & Finan, T. M. (2017). The Divided Bacterial Genome: Structure, Function, and Evolution. *Microbiology and Molecular Biology Reviews*, 81(3): e00019-17.

Dieppois, G., Ducret, V., Caille, O., & Perron, K. (2012). The Transcriptional Regulator CzcR Modulates Antibiotic Resistance and Quorum Sensing in *Pseudomonas aeruginosa*. *PLoS One*, 7(5): e38148.

Dong, Y., Kumar, C. G., Chia, N., Kim, P.-J., Miller, P. A., Price, N. D., Cann, I. K. O., […], Fouke, B. W. (2014). Halomonas sulfidaeris-dominated microbial community inhabits a 1.8 km-deep subsurface Cambrian Sandstone reservoir. *Environ. Microbiol.*, 16(6): 1695-1708.

Dopson, M., Baker-Austin, C., Koppineedi, P. R., & Bond, P. L. (2003). Growth in sulfidic mineral environments: metal resistance mechanisms in acidophilic micro-organisms. *Microbiology*, 149: 1959-1970.

Druschel, G. K., Baker, B. J., Gihring, T. M., & Banfield, J. F. (2004). Acid mine drainage biogeochemistry at Iron Mounyain, California. *Geochemical Transactions*: 5-13.

Egan, S. M. & Stewart, V. (1990). Nitrate Regulation of Anaerobic Respiratory Gene Expression in *narX* Deletion Mutants of *Escherichia coli* K-12. *Journal of Bacteriology*, 172(9): 5020-5029.

Elleuche, S. & Poggeler, S. (2009). Evolution of carbonic anhydrases in fungi. *Current Genetics*, 55: 211-222.

Epstein, W. (2002). The roles and regulation of potassium in bacteria. *Progress in Nucleic Acid Research and Molecular Biology*, 75: 293-320.

Fajarningsih, N. D. (2016). Internal Transcribed Spacer (ITS) as Dna Barcoding to Identify Fungal Species: A Review. *Squalen Bulletin of Marine and Fisheries Postharvest and Biotechnology*, 11: 2.

Faramarz, D. A., Reza, M., Amid, M., Reza, M. A., & Ernest, B. (2005). Effects of pH and

biomass concentrations in the removal of selenite from acid mine drainage by Aspergillus niger as biosorbent in Sarcheshmeh porphyry copper mine. *9th Internation Mine Water Congress*.

Farr, S. B. & Kogoma, T. (1991). Oxidative Stress Responses in *Escherichia coli* and *Salmonella typhimurium*. *Microbiological Reviews*, 55(4): 561-585.

Fekih, I. B., Zhang, C., Li, Y. P., Zhao, Y., Alwathnani, H. A., Saquib, Q., Rensing, C., & Cervantes, C. (2018). Distribution of Arsenic Resistance Genes in Prokaryotes. *Frontiers in Microbiology*, 9: 2473.

Flamholz, A., Noor, E., Bar-Even, A., Liebermeister, W., & Milo, R. (2013). Glycolytic strategy as a tradeoff between energy and protein cost. *PNAS*, 110(24): 10039-10044.

Fleischmann, R. D., Alland, D., Eisen, J. A., Carpenter, L., White, O., Peterson, J., Deboy, R., […], Fraser, C. M. (2002). Whole-genome comparison of Mycobacterium tuberculosis clinical and laboratory strains. *J. Bacteriol.*, 184(19): 5479-5490.

Fomina, M., Burford, E. P., & Gadd, G. M. (2006). Fungal dissolution and transformation of minerals: significance for nutrient and metal mobility. In Gadd, G. M. (Eds.), *Fungi in Biogeochemical Cycles*. Cambridge University Press.

Fomina, M., Hillier, S., Charnick, J. M., Melville, K., Alexander, I. J., & Gadd, G. M. (2005). Role of Oxalic Acid Overexcretion in Transformations of Toxic Metal Minerals by *Beauveria caledonica*. *Applied and Environmental Microbiology*, 71(1): 371-381.

Frey-Klett, P., Burlinson, P., Deveau, A., Barret, M., Tarkka, M., & Sarniguet, A. (2011). Bacterial-Fungal Interactions: Hyphens Between Agricultural, Clinical, Environmental, and Food Microbiologists. *Microbiol. Mol. Biol.*, 75(4) : 583-609.

Fuangthong, M., Herbig, A. F., Bsat, N., & Helmann, J. D. (2002). Regulation of the *Bacillus subtilis fur* and *perR* Genes by PerR: Not all Members of the PerR Regulon are Peroxide Inducible. *J. Bacteriol.*, 184(12): 3276-3286.

Fujimura, R., Sato, Y., Nishizawa, T., Oshima, K., Kim S.-W., Hattori, M., Kamjo, T., & Ohta, H. (2012). Complete Genome Sequence of *Leptospirillum ferrooxidans* Strain C2-3, Isolated from a Fresh Volcanic Ash Deposit on the Island of Miyake, Japan. *Journal of Bacteriology*, 194(15): 4122-4123.

Furrer, E. M., Ronchetti, M. F., Verrey, F., & Pos, K. M. (2007). Functional characterization of a NapA Na(+)/H(+) antiporter from Thermus thermophilus. *FEBS Lett.*, 581(3) : 572-578.

Gadd, G. M. (2007). Geomycology: biogeochemical transformations of rocks, minerals, metals and radionuclides by fungi, bioweathering and bioremediation. *Mycol. Res.*, 111(Pt 1): 3-49.

Gadda, G. & Francis, K. (2009). Nitronate monooxygenase, a model for anionic flavin semiquinone intermediates in oxidative catalysis. *Arch. Biochem. Biophys*., 493(1): 53-61.

Galun, M., Keller, P., Malki, D., Feldstein, H., Galun, E., Siegel, S. M., & Siegel, B. Z. (1982). Removal of Uranium(VI) from Solution by Fungal Biomass and Fungal Wall-Related Biopolymers. *Science*, 219(4582): 285-286.

Garber, A. I., Nealson, K. H., Okamoto, A., McAllister, S. M., Chan, C. S., Barco, R. A., & Merino, N. (2020). FeGenie: A Comprehensive Tool for the Identification of Iron Genes and Iron Gene Neighborhoods in Genome and Metagenome Assemblies. *Front. Microbiol.*, 11: 37.

Garcia-Fontana, C., Reyes-Darias, J. A., Munoz-Martinez, F., Alfonso, C., Morel, B., Ramos, J. L., & Krell, T. (2013). High Specificity in CheR Methyltransferase Function. *J. Biol. Chem.*, 288(26): 18987-18999.

Garcia-Moyano, A., Austnes, A. E., Lanzen, A., Gonzelez-Toril, E., Aguilera, A., & Ovreas, L. (2015). Novel and Unexpected Microbial Diversity in Acid Mine Drainage in Svalbard (78 ° N), Revealed by Culture-Independent Approaches. *Microorganisms*, 3(4): 667-694.

Ghachi, M. E., Derbise, A., Bouhss, A., & Mengin-Lecreulx, D. (2005). Identification of

multiple genes encoding membrane proteins with undecaprenyl pyrophosphate phosphatase (UppP) activity in Escherichia coli. *J. Biol. Chem.*, 280(19): 18689-18695.
Gosh, S., Setlow, B., Wahome, P. G., Cowan, A. E., Plomp, M., Malkin, A. J., & Setlow, P. (2008). Characterization of Spores of *Bacillus subtilis* That Lack Most Coat Layers. *J. Bacteriol.*, 190(20): 6741-6748.
Giddings, L.-A., Chlipala, G., Kuntsman, K., Green, S., Morillo, K., Bhave, K., Peterson, H., […], Maienschein-Cline, M. (2020). Characterization of an acid rock drainage microbiome and transcriptome at the Ely Copper Mine Superfund site. *PLoS One*, 15(8): e0237599.
Glukhova, L. B., Frank, Y. A., Danilova, E. V., Avakyan, M. R., Banks, D., Tuovinen, O. H., & Karnachuk, O. V. (2018). Isolation, Characterization, and Metal Response of Novel, Acid-Tolerant Penicillium spp. from Extremely Metal-Rich Waters at a Mining Site in Transbaikal (Siberia, Russia). *Microb Ecol.*, 76(4): 911-924.
Goebel, B. M. & Stackebrandt, E. (1994). Cultural and Phylogenetic Analysis of Mixed Microbial Populations Found in Natural and Commercial Bioleaching Environments, *Applied and Environmental Microbiology*, 60(5): 1614-1621.
Goldman, B. S. & Roth, J. R. (1993). Genetic Structure and Regulation of the *cysG* Gene in *Salmonella typhimurium*. *Journal of Bacteriology*, 175(5): 1457-1466.
Goltsman, D. S. A., Denef, V. J., Singer, S. W., VerBerkmoes, N. C., Lefsrud, M., Mueller, R. S., Dick, G. J., […] Banfield, J. F. (2009). Community Genomic and Proteomic Analyses of Chemoautotrophic Iron-Oxidizing "*Leptospirillum rubarum*" (Group II) and "*Leptospirillum ferrodiazotrophum*" (Group III) Bacteria in Acid Mine Drainage Biofilms. *Applied and Environmental Microbiology*, 75(13): 4599-4615.
Gonzalez-Toril, E., Llobet-Brossa, E., Casamayor, E. O., Amann, R., & Amis, R. (2003). Microbial Ecology of an Extreme Acidic Environment, The Tinto River. *Appl. Environ. Microbiol.*, 69(8): 4853-4865.
Gouy, M., Guindon, S., & Gascuel, O. (2009). SeaView Version 4: A Multiplatform Graphical User Interface for Sequence Alignment and Phylogenetic Tree Building. *Molecular Biology and Evolution*, 27(2): 221-224.
Green, M. R. & Sambrook, J. (2016). Precipitation of DNA with Ethanol. *Cold Spring Harb. Protoc.*, doi: 10.1101/pdb.prot093377.
Gross, S. & Robbins, E. I. (2000). Acidophilic and acid-tolerant fungi and yeasts. *Hydrobiologia*, 433: 91-109.
Guazzaroni, M.-E., Morgante, V., Mirete, S., & Gonzalez-Pastor, J. E. (2013). Novel acid resistance genes from the metagenome of the Tinto River, an extremely acidic environment. *Environmental Microbiology*, 15(4): 1088-1102.
Guibal, E., Roulph, C., & Le Cloirec, P. (1995). Infrared Spectroscopic Study of Uranyl Biosorption by Fungal Biomass and Materials of Biological Orgin. *Environ. Sci. Technol.*, 29(10): 2496-2503.
Guindon, S., Lethiec, F., Duroux, P., & Gascuel, O. (2005). PHYML Online – a web server for fast maximum likelihood-based phylogenetic inference. *Nucleic Acids Research*, 33(2): 557-559.
Habib, C., Yu, Y., Gozzi, K., Ching, C., Shemesh, M., & Chai, Y. (2017). Characterization of the regulation of a plant polysaccharide utilization operon and its role in biofilm formation in *Bacillus subtilis*. *PLoS ONE*, 12(6): e0179761.
Haferburg, G., Reinicke, N., Merten, D., Buchel, G., & Kothe, E. (2007). Microbes adapted to acid mine drainage as source for strains active in retention of aluminum or uranium. *Journal of Geochemical Exploration*, 92(2-3): 196-204.
Hajam, I. A., Dar, P. A., Shahnawaz, I., Jaume, J. C., & Lee, J. H. (2017). Bacterial flagellin – a potent immunomodulatory agent. *Experimental & Molecular Medicine*, 49: e373.

Hall, A. N., Subramanian, S., Oshiro, R. T., Canzoneri, A. K., & Kearns, D. B. (2017). SwrD (YlzI) Promotes Swarming in Bacillus subtilis by Increasing Power to Flagellar Motors. *J. Bacteriol.*, 200(2): e00529-17.

Han, X., Kennan, R. M., Davies, J. K., Reddacliff, L. A., Dhungyel, O. P., Whittington, R. J., Turnbull, L., […], Rood, J. I. (2008). Twitching Motility is Essential for Virulence in *Dichelobacter nodosus*. *J. Bacteriol.*, 190(9): 3323-3335.

Hao, C., Wang, L., Gao, Y., Zhang, L., & Dong, H. (2010). Microbial diversity in acid mine drainage of Xiang Mountain sulfide mine, Anhui Province, China. *Extremophiles*, 14(5): 465-474.

Hartman, T., Weinrick, B., Vilcheze, C., Berney, M., Tufariello, J., Cook, G. M., & Jacobs, Jr., W. R. (2014). Succinate Dehydrogenase is the Regulator of Respiration in *Mycobacterium tuberculosis*, 10(11): e1004510.

Hernandez, G. A. G. (2020). Members of the nitronate monooxygenase gene family from *Metarhizium brunneum* are induced during the process of infection to *Plutella xylostella*. *Applied Microbiology and Biotechnology*, 104: 2987-2997.

Higgins, D. & Dworkin, J. (2012). Recent progress in *Bacillus subtilis* sporulation. *FEMS Microbiol. Rev.*, 36(1): 131-148.

HiMedia Laboratories (2011). Tryptone Soya Broth. *Technical Data*. Retrieved from: http://himedialabs.com/TD/LQ508.pdf

Ho, W.-C. & Ko, W.-H. (1997). A simple method for obtaining single-spore isolates of fungi. *Bot. Bull. Acad. Sin.*, 38: 41-44.

Hohle, T. H. & O'Brian, M. R. (2009). The *mntH* gene encodes the major Mn^{2+} transporter in *Bradyrhizobium japonicum* and is regulated by manganese via the Fur operon. *Mol. Microbiol.*, 72(2): 399-409.

Holanda, R., Hedrich, S., Nancucheo, I., Oliveira, G., Grail, B. M., & Johnson, D. B. (2016). Isolation and characterisation of mineral-oxidizing "*Acidibacillus*" spp. from mine sites and geothermal environments in different global locations. *Research in Microbiology*, 167(7): 613-623.

Hongxiang, O., Yonglai, X., Jianming, P., Chengwu, Y., Xiaohua, Z., & Qian, W. (2010). Biosorption of Pb(II) from aqueous solution by biomass of Neosartorya hiratsukae(M7): Equilibrium and kinetic studies. *The 2nd International Conference on Information Science and Engineering*: 166-170.

Hudek, L., Premachandra, W. A. J., & Brau, L. (2016). Role of Phosphate Transport System Component PstB1 in Phosphate Internalization by *Nostoc punctiforme*. *Appl. Environ. Microbiol.*, 82(21): 6344-6356.

Hugler, M., Wirsen, C. O., Fuchs, G., Taylor, C. D., & Sievert, S. M. (2005). Evidence for Autotrophic CO_2 Fixation via the Reductive Tricarboxylic Acid Cycle by Members of the ε Subdivision of Proteobacteria. *Physiology and Metabolism*, 187(9): 3020-3027.

Hujslova, M., Kubatova, A., Bukovska, P., Chudickova, M., & Kolarik, M. (2017). Extremely Acidic Soils are Dominated by Species-Poor and Highly Specific Fungal Communities. *Microbial Ecology*, 73: 321-337.

Hurst, C. J. (2007). Introduction to Environmental Microbiology. In Hurst, C. J. et al. (Eds.), *Manual of Environmental Microbiolgy; American Society Mic Series.* American Society for Microbiology Press.

Jerez, C. A. (2008). The use of genomics, proteomics and other OMICS technologies for the global understanding of biomining microorganisms. *Hydrometallurgy*, 94: 162-169.

Jiang, L., Li, T., Jenkins, J., Hu, Y., Brueck, C. L., Pei, H., & Betenbaugh, M. J. (2020).

Evidence for a mutualistic relationship between the cyanobacteria *Nostoc* and fungi *Aspergilli* in different environments. *Applied Microbiology and Biotechnology*, 104: 6413-6426.
Johnson, D. B. & Hallberg, K. B. (2009). Carbon, Iron and Sulfur Metabolism in Acidophilic Micro-Organisms. *Advances in Microbial Physiology*, 54: 202-255.
Johnson D. B., Joulian, C., d'Hugues P., & Hallberg, K. B. (2008). *Sulfobacillus benefaciens* sp. nov., an acidophilic facultative anaerobic *Firmicute* isolated from mineral bioleaching operations. *Extremophiles*, 12: 789-798.
Johnson, D. B., Macvicara, J. H. M., & Rolfe, S. (1987). A new solid medium for the isolation and enumeration of Thiobacillus ferrooxidans and acidophilic heterotrophic bacteria. *Journal of Microbiological Methods*, 7(1): 9-18.
Jurtshuk Jr., P. (1996). Bacterial Metabolism. In Baron, S. (Eds.), *Medical Microbiology* (4th Edition). University of Texas Medical Branch at Galveston.
Justice, N. B., Norman, A., Brown, C. T., Singh, A., Thomas, B. C., & Banfield, J. F. (2014). Comparison of environmental and isolate *Sulfobacillus* genomes reveals diverse, carbon, sulfur, nitrogen, and hydrogen metabolism. *BMC Genomics*, 15: 1107.
Kabisch, J., Pratzka, I., Meyer, H., Albrecht, D., Lalk, M., Ehrenreich, A., & Schweder, T. (2013). Metabolic engineering of Bacillus subtilis for growth on overflow metabolites. *Microbial Cell Factories*, 12(1): 72.
Kapoor, A., Viraraghavan, T., & Cullimore, D. R. (1999). Removal of heavy metals using the fungus *Aspergillus niger*. *Bioresource Technology*, 70(1): 95-104.
Kanamarlapudi, S. L. R. K., Chintalpudi V. K., & Muddada, S. (2018). Application of Biosorption for Removal of Heavy Metals from Wastewater. In Derco, J. & Vrana, B. (Eds.), *Biosorption*. IntechOpen.
Kanaparthi, D., Pommerenke, B., Casper, P., & Dumont, M. G. (2013). Chemolithotrophic nitrate-dependent Fe(II)-oxidizing nature of actinobacterial subdivision lineage TM3. *The ISME Journal*, 7: 1582-1594.
Karamanev, D. G., Nikolov, L. N., & Mamatarkova, V. (2002). Rapid simultaneous quantitative determination of ferric and ferrous ions in drainage waters and similar solutions. *Minerals Engineering*, 15: 341-346.
Kawakami, N. & Fujisaki, S. (2017). Undecaprenyl phosphate metabolism in Gram-negative and Gram-positive bacteria. *Bioscience, Biotechnology, and Biochemistry*, 82(6): 940-946.
Keegan, K. P., Glass, E. M., & Meyer, F. (2016). MG-RAST, a Metagenomics Service for Analysis of Microbial Community Structure and Function. In Martin, F. & Uroz, S. (Eds.), *Microbial Environmental Genomics (MEG). Methods in Molecular Biology, vol 1399*. Humana Press, New York, NY.
Kellner, H., Luis, P., & Buscot, F. (2007). Diversity of laccase-like multicopper oxidase genes in *Morchellaceae*: identification of genes potentially involved in extracellular activities related to plant litter decay. *FEMS Microbiology Ecology*, 61(1): 153-163.
Kelly, L. C., Cockell, C. S., Thorsteinsson, T., Marteinsson, V., & Stevenson, J. (2014). Pioneer microbial communities of the Fimmvorduhals Lava Flow, Eyjafjallajokull, Icelan. *Microbiol. Ecol.*, 68: 504-518.
Kodama, T., Takamatsu, H., Asai, K., Kobayashi, K., Ogasawara, N., & Watabe, K. (1999). The *Bacillus subtilis yaaH* Gene is Transcribed by SigE RNA Polymerase during Sporulation, and its Product is Involved in Germination of Spores. *Genetics and Molecular Biology*, 181(15): 4584-4591.
Korabecna, M. (2007). The variability in the Fungal Ribosomal DNA (ITS1, ITS2, and 5.8S rRNA Gene): Its Biological Meaning and Application in Medical Mycology. *Communicating Current Research and Educational Topics and Trends in Applied Microbiology*.

Kracke, F., Vassilev, I., & Kromer, J. O. (2015). Microbial electron transport and energy conservation – the foundation for optimizing bioelectrochemical systems. *Front. Microbiol.*, 6: 575.

Krulwich, T. A., Hicks, D. B., & Ito, M. (2009). Cation/proton antiporter complements of bacteria: why so large and diverse? *Molecular Microbiology*, 74(2): 257-260

Kues, U. & Ruhl, M. (2011). Multiple Multi-Copper Oxidase Gene Families in Basidiomycetes – What for?. *Curr. Genomics*, 12(2): 72-94.

Lane, D. J. (1991). 16S/23S rRNA Sequencing. In Stackerbrant, E. & Goodfellow, M. (Eds.), *Nucleic Acid Techniques in Bacterial Systematic*. John Whiley and Sons, New York.

Larone, D. H. (1995). Medically Important Fungi – A Guide to Identification, 3rd Edition. Elsevier Science.

Latour, D. J. & Weiner, J. H. (1988). Regulation of in vitro expression of the Escherichia coli frd operon: alanine and Fnr represent positive and negative control elements. *Nucleic Acids Res.*, 16(14A): 6339-6352.

Lawton, T. J. & Rosenzweig, A. C. (2011). Chapter Seventeen – Detection and Characterization of a Multicopper Oxidase from *Nitrosomonas europaea*. In Klotz, M. G. & Stein, L. Y. (Eds.), *Methods in Enzymology Volume 496*. Academic Press.

Lei, Y., Oshima, T., Ogasawara, N., & Ishikawa, S. (2013). Functional analysis of the protein Veg, which stimulates biofilm formation in Bacillus subtilis. *J. Bacteriol.*, 195(8): 1697-1705.

Levican, G., Bruscella, P., Guacunano, M., Inostroza, C., Bonnefoy, V., Holmes, D. S., & Jedlicki, E. (2002). Characterization of the *petI* and *res* Operons of *Acidithiobacillus ferrooxidans*. *Journal of Bacteriology*, 184(5): 1498-1501.

Lewinson, O., Lee, A. T., & Rees, D. C. (2009). A P-type ATPase importer that discriminates between essential and toxic transition metals. *PNAS*, 106(12): 4677-4682.

Lior, S., Rosenberg, A., Smith, Y., Segev, E., & Ben-Yehuda, S. (2014). The Molecular Timeline of a Reviving Bacterial Spore. *Mol. Cell.*, 57(4): 695-707.

Liu, J., Hicks, D. B., & Krulwich, T. A. (2012). Roles of AtpI Two YidC-type Proteins from Alkaliphilic *Bacillus pseudofirmus* OF4 in ATP Synthase Assembly and Nonfermentative Growth. *J. Bacteriol.*, 195(2): 220-230.

Liu, J.-S., Xie, X.-H., Xiao, S.-M., Wang, X.-M., Zhao, W.-J., & Tian, Z.-L. (2007). Isolation of *Leptospirillum ferriphilum* by single-layered solid medium. *J. Cent. South Univ. Technol.*, 14(4): 467-473.

Liu, R. & Ochman, H. (2007). Origins of Flagellar Gene Operons and Secondary Flagellar Systems. *J. Bacteriol.*, 189(19): 7098-7104.

Liu, Y., Liao, W., & Chen, S. (2007). Study of pellet formation of filamentous fungi *Rhizopus oryzae* using a multiple logistic regression model. *Biotechnology and Bioengineering*, 99(1): 117-128

Londono-Vallejo, J. A., Frehel, C., & Stragier, P. (1997). SpoIIQ, a forespore-expressed gene required for engulfment in Bacillus subtilis. *Mol. Microbiol.*, 24(1): 29-39.

Lujan, P., Sanogo, S., Puppala, N., & Randall, J. (2016). Factors affecting mycelium pigmentation and pathogenicity of *Sclerotinia sclerotium* on Valencia peanut. *Canadian Journal of Plant Science*, 96(3): 461-473.

Luque-Almagro, V. M., Cabello, P., Saez, L. P., Olaya-Abril, A., Moreno-Vivian, C., & Roldan, M. D. (2018). Exploring anaerobic environments for cyanide and cyano-derivatives microbial degradation. *Appl. Microbiol. Biotechnol.*, 102(3): 1067-1074.

Lyon, J. S., Hilliard, T. J., & Bethell, T. N. (1993). Burden of Gilt: The legacy of environmental damage from abandoned mines, and what America should do about it. *Mineral Policy Center, Washington DC*.

Ma, L.-J. & Fedorova, N. D. (2010). A practical guide to fungal genome projects: strategy, technology, cost and completion. *Mycology*, 1(1): 9-24.
Madsen, A. M., Larsen, S. T., Koponen, I. K., Kling, K. I., Barooni, A., Karottki, D. G., Tendal, K., & Wolkoff, P. (2016). Generation and Characterization of Indoor Fungal Aerosols for Inhalation Studies. *Appl. Environ. Microbiol.*, 82(8): 2479-2493.
Madsen, E. L. (1998). Epistemology of Environmental Microbiology. Environmental Science and Technology, 32(4): 429-439.
Manning, H. L. (1975). New medium for isolating iron-oxidizing and heterotrophic acidophilic bacteria from acid mine drainage. *Applied and Environmental Microbiology*, 30(6): 1010-1016.
Mardanov, A. V., Glukhova, L. B., Gruzdev, E. V., Beletsky, A. V., Karnachuk, O., & Ravin, N. V. (2016). The complete mitochondrial genome of the acid-tolerant fungus *Penicillium* ShG4C. *Genom Data*, 10: 141-143.
Mariner, R., Johnson, D. B., & Hallberg, K. B. (2008). Characterisation of an attenuation system for the remediation of Mn(II) contaminated waters. *Hydrometallurgy*, 94: 100-104.
Martin, M. (2011). Cutadapt removes adapter sequences from high-throughput sequencing reads. *EBMnet.journal*, 17(1): 10-12.
Mattick, J. S. (2002). Type IV pili and twitching motility. *Annu. Rev. Microbiol.*, 56: 289-314.
Mavromatis, K., Sikorski, J., Lapidus, A., Glavina Del Rio, T., Copeland, A., Tice, H., Cheng, J. -F., […] Kyrpides, N. C. (2010). Complete genome sequence of *Alicyclobacillus acidocaldarius* type strain (104-IA^{T}). *Standards in Genomic Sciences*, 2: 9-18.
McCloskey, D., Xu, S., Sandberg, T. E., Brunk, E., Hefner, Y., Szubin, R., Feist, A. M., & Palsson, B. O. (2018). Growth Adaptation of *gnd* and *sdhCB Escherichia coli* Deletion Strains Diverges from a Similar Initial Perturbation of the Transcriptome. *Front. Microbiol.*, 9: 1793.
Melin, L., Magnusson, K., & Rutberg, L. (1987). Identification of the promoter of the Bacillus subtilis sdh operon. *J. Bacteriol.*, 169(7): 3232-3236.
Melo, A. M. P., Bandeiras, T. M., & Teixeira, M. (2004). New Insights into Type II NAD(P)H:Quinone Oxidoreductases. *Microbiol. Mol. Biol. Rev.*, 68(4): 603-616.
Mendez-Garcia, C., Pelaez, A. I., Mesa, V., Sanchez, J., Golyshina, O. V., & Ferrer, M. (2015). Microbial diversity and metabollic networks in acid mine drainage habitats. *Front. Microbiol.*, 6: 475.
Messerschmidt, A. & Huber, R. (1989). The blue oxidases, ascorbate oxidase, laccase and ceruloplasmin. Modelling and structural relationships. *European Journal of Biochemistry*, 187(2): 341-352.
Miranda, A. F., Taha, M., Wrede, D., Morrison, P., Ball, A. S., Stevenson, T., & Mouradov, A. (2015). Lipid production in association of filamentous fungi with genetically modified cyanobacterial cells. *Biotechnology for Biofuels*, 8: 179.
Mohammadian Fazli, M., Soleimani, N., Mehrasbi, M., Darabian, S., Mohammadi, J., & Ramazani, A. (2015). Highly Cadmium tolerant fungi: their tolerance and removal potential. *J. Environ. Health Sci. Engineer.*, 13: 19.
Mohanta, T. K. & Bae, H. (2015). The diversity of fungal genome. *Biol. Proced. Online*, 17: 8.
Moller, A. K., Barkay, T., Hansen, M. A., Norman, A., Hansen, L. H., Sorensen, S. J., Boyd, E. S., & Kroer, N. (2014). Mercuric reductase genes (*merA*) and mercury resistance plasmids in High Arctic snow, freshwater and sea-ice brine. *FEMS Microbiology Ecology*, 87(1): 52-63.
Morales, M. E. & Ruiz, M. A. (2016). 16 – Microencapsulation of probiotic cells: applications in nutraceutic and food industry. In Grumezescu, A. M. (Eds.), *Nutraceuticals: Nanotechnology in the Agri-Food Industry Volume 4.* Academic Press.
Moreno-Vivian, C., Cabello, P., Martinez-Luque, M., Blasco, R., & Castillo, F. (1999).

Prokaryotic Nitrate Reduction: Molecular Properties and Functional Distinction among Bacterial Nitrate Reductases. *J. Bacteriol.*, 181(21): 6573-6584.
Mosier, A. C., Miller, C. S., Frischkorn, K. R., Ohm, R. A., Li, Z., LaButti, K., Lapidus, A., […] Banfield, J. F. (2016). Fungi Contribute Critical but Spatially Various Roles in Nitrogen and Carbon Cycling in Acid Mine Drainage. *Front Microbiol.*, 7:238.
Mousavi, S. M., Yaghmaei, S., Vossoughi, M., Jafari, A., Hoseini, S. A. (2005). Comparison of bioleaching ability of two native mesophilic and thermophilic bacteria on copper recovery from chalcopyrite concentrate in an airlift bioreactor. *Hydrometallurgy*, 80(1-2): 139-144.
Murata, M. & Ohki, R. (1997). Cloning and Characterization of the bmr3, a Third Multidrug Efflux Transporter Gene of *Bacillus subtilis*. *Journal of the Kyorin Medical Society*, 28(2): 155-166.
Mykytczuk, N. (2014). Microbial evaluation of BacTech Environmental microbial leaching mixtures. Industrial report (Unpublished).
Nagakubo, S., Nishino, K., Hirata, T., & Yamaguchi, A. (2002). The Putatibe Response Regulator BaeR Stimulates Multidrug Resistance of *Escherichia coli* via a Novel Multidrug Exporter System, MdtABC. *J. Bacteriol.*, 184(15): 4161-4167.
Nancucheo, I., Oliveria, R., Dall'Agnol, H., Johnson, D. B., Grail, B., Holanda, R., Nunes, G. L., […] Oliveira, G. (2016). Draft Genome Sequence of a Novel Acidophilic Iron-Oxidizing *Firmicutes* Species, "*Acidibacillus ferrooxidans*" ($SLC66^T$). *Genome Announcements*, 4(3): e00383-16.
Natajaran, K. A. (2013). Lecture 3: History and Methods in Biohydrometallurgy. *Course Title: Metals Biotechnology*. Retrieved from: http://content.inflibnet.ac.in/data-server/eacharya-documents/55fbb823e41301c34c843a4b_INFIEP_224/715/ET/224-715-ET-V1-S1__lecture3.pdf
Natajaran, K. A. (2018). History and Methods in Biohydrometallurgy. In Natarajan, K. A. (Eds.), *Biotechnology of Metals*. Elsevier.
Nawapan, S., Charoenlap, N., Charoenwuttitam, A., Saenkham, P., Mongkolsuk, S., & Vattanaviboon, P. (2009). Functional and Expression Analyses of the *cop* Operon, Required for Copper Resistance in *Agrobacterium tumefaciens*. *J. Bacteriol.*, 191(16): 5159-5168.
Neumann, S., Wynen, A., Truper, H. G., & Dahl, C. (2000). Characterization of the cys gene locus from *Allochromatium vinosum* indicates an unusual sulfate assimilation pathway*. *Molecular Biology Reports*, 27: 27-33.
Nogi, Y., Takami, H., Nakasone, K. & Horikoshi, K. (2000). Taxonomical characterization of alkaliphilic *Bacillus* strains used for industrial application: proposal for seven new species. NCBI submission, Unpublished.
Noman, E., Al-Gheethi, A. A., Rahman, N. K., Talip, B., Mohamed, R., N. H., & Kadir, O. A. (2018). Single Spore Isolation as a Simple and Efficient Technique to Obtain Fungal Pure Culture. *IOP Conf. Series: Earth and Environmental Science*, 140: 012055
Norris, P. R., Burton, N. P., & Foulis, N. A. M. (2000). Acidophiles in bioreactor mineral processing. *Extremophiles*, 4: 71-76.
Ock, C.-Y., Kim, E.-H., Choi, D. J., Lee, H. J., Hahm, K.-B., & Chung, M. H. (2012). 8-Hydroxydeoxyguanosine: Not mere biomarker for oxidative stress, but remedy for oxidative stress-implicated gastrointestinal diseases. *World J. Gastroenterol.*, 18(4): 302-308.
Oggerin, M., Tornos, F., Rodriguez, N., del Moral, C., Sachez-Roman, M., & Amils, R. (2013). Specific jarosite biomineralized by Purpureocillium lilacinum, an acidophilic fungi isolated from Rio Tinto. *Environ. Microbiol.*, 15(8): 2228-2237.
Oggerin, M., Tornos, F., Rodriguez, N., Pascual, L., & Amils, R. (2016). Fungal Iron Biomineralization in Rio Tinto. *Minerals*, 6(2) : 37.
Olsen, I. & Jantzen, E. (2001). Sphingolipids in Bacteria and Fungi. *Anaerobe*, 7(2): 103-112.

Oshiki, M., Ishii, S., Yoshida, K., Fujii, N., Ishiguro, M., Satoh, H., & Okabe, S. (2013). Nitrate-Dependent Ferrous Iron Oxidation by Anaerobic Ammonium Oxidation (Anammox) Bacteria. *Appl. Environ. Microbiol.*, 79(13): 4087-4093.

Ouzounis, C. & Sander, C. (1991). A structure-derived sequence pattern for the detection of type I copper binding domains in distantly related proteins. *FEBS Letters*, 279(1): 73-78.

Overmann, J. (2013). Principles of Enrichment, Isolation, Cultivation, and Preservation of Prokaryotes. In Rosenberg, E. et *al.* (Eds.), *The Prokaryotes – Prokaryotic Biology and Symbiotic Associations*. Springer, New York, NY.

Pace, N. R. (1997). A molecular view of microbial diversity and the biosphere. *Science*, 276(5313): 734-740

Panyuskina, A. E., Babenko, V. V., Nikitina, A. S., Selezneva, O. V., Tsaplina, I. A., Letarova, M. A., Kostryukova, E. S., & Letarov, A. V. (2019). *Sulfobacillus thermotolerans*: new insights into the resistance and metabolic capacities of acidophilic chemolithotrophs. *Scientific Reports*, 9: 15069.

Parey, K., Demmer, U., Warkentin, E., Wynen, A., Ermler, U., & Dahl, C. (2013). Structural, Biochemical and Genetic Characterization of Dissimilatory ATP Sulfurylase from *Allochromatium vinosum*. *PLoS ONE*, 8(9): e74707.

Park, M. S., Oh, S., Fong, J. J., Houbraken, J., & Lim, Y. W. (2019). The diversity and ecological roles of *Penicillium* in intertidal zones. *Scientific Reports*, 9: 13540.

Parks, D. H., Imelfort, M., Skennerton, C. T., Hugenholz, P., & Tyson, G. W. (2014). Assessing the quality of microbial genomes recovered from isolates, single cells, and metagenomes. *Genome Research*, 25: 1043-1055.

Phadtare, S., Tadigotla, V., Shin, W.-H., Sengupta, A., & Severinov, K. (2006). Analysis of *Escherichia coli* Global Gene Expression Profiles in Response to Overexpression and Deletion of CspC and CspE. *J. Bacteriol.*, 188(7): 2521-2527.

Pightling, A. W., Petronella, N., & Pagotto, F. (2014). Choice of Reference Sequence and Assembler for Alignment of *Listeria monocytogenes* Short-Read Sequence Data Greatly I nfluences Rates of Error in SNP Analyses. *PLoS ONE*, 9(8): e104579.

Putman, M., van Veen, H. W., & Konings, W. N. (2000). Molecular Properties of Bacterial Multidrug Transporters. *Microbiol. Mol. Biol. Rev.*, 64(4): 672-693.

Quatrini, R., Appia-Ayme, C., Denis, Y., Jedlicki, E., Holmes, D. S., & Bonnefoy, V. (2009). Extending the models for iron and sulfur oxidation in the extreme Acidophile *Acidithiobacillus ferrooxidans*. *BMC Genomics*, 10: 394.

Quatrini, R., Valdes, J., Jedlicki, E., & Holmes, D. S. (2007). The Use of Bioinformatics and Genome Biology to Advance our Understanding of Bioleaching Microorganisms. In Donati, E. R. & Sand, W. (Eds.), *Microbial Processing of Metal Sulfides*. Springer.

Quintero, K. Y. C., Guerrero, I. E. P., Guzman, J. C. T., Martinez, B. G. V., Felix, A. V., & Rainey, F. & Oren, A. (2006). Acidophiles. In Rainey, F. & Oren, A. (Eds.), *Extremophiles* (Volume 35, 1st Edition). Academic Press.

Rambabu, K., Banat, F., Pham Q. M., Ho, S.-H., Ren, N.-Q., & Show, P. L. (2020). Biological remediation of acid mine drainage: Review of past trends and current outlook. *Environmental Science and Ecotechnology*, 2: 100024.

Ramon-Garcia, S., Martin, C., De Rossi, E., & Ainsa, J. A. (2007). Contribution of the Rv2333c efflux pump (the Stp protein) from *Mycobacterium tuberculosis* to intrinsic antibiotic resistance in *Mycobacterium bovis* BCG. *Journal of Antimicrobial Chemotherapy*, 59(3): 544-547.

Ramos, J. A. T., Barends, S., Verhaert, R. M. D., & de Graaff, L. H. (2011). The *Aspergillus niger* multicopper oxidase family: analysis and overexpression of laccase-like encoding genes. *Microbial Cell Factories*, 10: 78.

Ranalli, G., Zanardini, E., & Sorlini, C. (2009). Biodeterioration – Including Cultural Heritage. In Schaechter, M. (Eds.), *Encyclopedia of Microbiology* (Third Edition). Academic Press.
Raquel, Q., Appia-Ayme, C., Denis, Y., Jedlicki, E., Holmes, D. S., & Bonnefoy, V. (2009). Extending the models of iron and sulfur oxidation in the extreme Acidophile *Acidithiobacillus ferrooxidans*. *BMC Genomics*, 10: 394.
Rawlings, D. E. & Johnson, D. B. (2007). The microbiology of biomining: development and optimization of mineral-oxidizing microbial consortia. *Microbiology*, 153: 315-324.
Reeves, S. A., Parsonage, D., Nelson, K. J., & Poole, L. B. (2011). Kinetic and thermodynamic features reveal that Escherichia coli BCP is an unusually versatile peroxiredoxin. *Biochemistry*, 50(41): 8970-8981.
Roncarati, D. & Scarlato, V. (2017). Regulation of heat-shock genes in bacteria: from signal sensing to gene expression output. *FEMS Microbiology Reviews*, 41(4): 549-574.
RoyChowdhury, A., Sarkar, D., & Datta, R. (2015). Remediation of Acid Mine Drainage-Impacted Water. *Current Pollution Reports*, 1: 131-141.
Rygaard, A. M., Thogersen, M. S., Nielsen, K. F., Gram, L., & Bentzon-Tilia, M. (2017). Effects of Gelling Agent and Extracellular Signaling Molecules on the Culturability of Marine Bacteria. *Applied and Environmental Microbiology*, 83(9): e00243-17.
Sanchez-Andrea, I., Rodriguez, N., Amils, R., & Sanz, J. L. (2011). Microbial Diversity in Anaerobic Sediments at Rio Tinto, a Naturally Acidic Environment with High Heavy Metal Content. *Appl. Environ. Microbiol.*, 77(17).
Sanders, C. C. (2001). Mechanisms Responsible for Cross-Resistance and Dichotomous Resistance among the Quinolones. *Clinical Infectious Diseases*, 32(1): S1-S8.
Santana, M., Kunst, F., Hullo, M. F., Rapoport, G., Danchin, A., & Glaser, P. (1992). Molecular cloning, sequencing, and physiological characterization of the qox operon from Bacillus subtilis encoding the aa3-600 quinol oxidase. *J. Biol. Chem.*, 267(15): 10225-10231.
Santelli, C. M., Pfister, D. H., Lazarus, D., Sun, L., Burgos, W. D., Hansel, C. M. (2010). Promotion of Mn(II) Oxidation and Remediation of Coal Mine Drainage in Passive Treatment Systems by Diverse Fungal and Bacterial Communities. *Appl. Environ. Microbiol.*, 76(14): 4871-4875.
Santos-Beneit, F. (2015). The Pho regulon: a huge regulatory network in bacteria. *Front. Microbiol.*, 6: 402.
Saxena, P., Bhattacharyya, A. K., & Mathur, N. (2006). Nickel Tolerance and Accumulation by Filamentous Fungi from Sludge of Metal Finishing Industry. *Geomycrobiology Journal*, 23(5): 333-340.
Schlief, J. & Mutz, M. (2005). Long-term leaf litter decomposition and associated microbial processes in extremely acidic (pH<3) mining waters. *Archiv fuer Hydrobiologie*, 164: 53-68.
Schippers, A. (2007). Microorganisms Involved in Bioleaching and Nucleic Acid-Based Molecular Methods for their Identification and Quantification. In Donati, E. R. & Sand, W. (Eds.), *Microbial Processing of Metal Sulfides*. Springer Netherlands.
Schopf, S., Ullrich, S. R., Heine, T., & Schlomann, M. (2017). Draft Genome of the Heterotrophic Iron-Oxidizing Bacterium "*Acidibacillus ferrooxidans*" Huett2, Isolated from a Mine Ditch in Freiberg, Germany. *Genome Announc.*, 5(19): e00323-17.
Sedlak, E., Zoldak, G., & Wittung-Stafshede, P. (2018). Synergistic Effects of Copper Sites on Apparent Stability of Multicopper Oxidase, Fet3p. *Int. J. Mol. Sci.*, 19(1): 269.
Seemann, T. (2014). Prokka: rapid prokaryotic genome annotation. *Bioinformatics*, 30(14): 2068-2069.
Shrestha, P. M., Nevin, K. P., Shrestha, M., & Lovley, D. R. (2013). When is a microbial culture "pure"? Persistent cryptic contaminant escapes detection even with deep genome sequencing. *mBIO*, 4(2): e00591-12

Shuttleworth, K. L., Unz, R. F., & Wichlacz, P. L. (1985). Glucose catabolism in strains of acidophilic, heterotrophic bacteria. *Appl. Environ. Microbiol.*, 50: 573-579.
Siegel, S. M., Galun, M., & Siegel, B. Z. (1990). Filamentous fungi as metal biosorbents: A review. *Water, Air, and Soil Pollution*, 53: 335-344.
Siegel, S. M. & Speitel, T. W. (1975). Performance of fungi in low temperature and hypersaline environments. *Life Sciences and Space Research*, 14: 351-354
Sigma-Aldrich (2016). Product Information: Ampicillin sodium salt. Retrieved from: https://www.sigmaaldrich.com/content/dam/sigma-aldrich/docs/Sigma/Product_Information_Sheet/a0166pis.pdf
Simonovicova, A., Bartekova, J., Janovova, L., & Luptakova, A. (2010). Behaviour of Fe, Mg, and Ca in Acid Mine Drainage and Experimental Solutions in the Presence of *Aspergillus niger* Species Isolated from Various Environment. *Nova Biotechnologica*, 10: 63-69.
Simonovicova, A., Bartekova, J., Zemberyova, M., Machackova, L., Gaplovska, K., & Luptakova, A. (2013). Bioremediation of Cu, Mn and Zn in acid mine drainage environment through Aspergillus niger wild type strains isolated from different sources. *Fresenius Environmental Bulletin*, 22(10): 2867-2870.
Singh, V. K., Singh, K., & Baurn, K. (2018). The Role of Methionine Sulfoxide in Oxidative Stress Tolerance and Virulence of *Staphylococcus aureus* and Other Bacteria. *Antioxidants (Basel)*, 7(10): 128.
Siqueira, V. & Lima, N. (2012). Surface Hydrophobicity of Culture and Water Biofilm of *Penicillium* spp. *Curr. Microbiol.*, 64: 93-99.
Siqueira, V. M. & Lima, N. (2013). Biofilm Formation by Filamentous Fungi Recovered from a Water System. *Journal of Mycology*, 2013: article ID 152941.
Skousen, J., Zipper, C. E., Rose, A., Ziemkiewicz, P. F., Nairn, R., McDonald, L. M., & Kleinmann, R. L. (2017). Review of Passive Systems for Acid Mine Drainage Treatment. *Mine Water and the Environment*, 36: 133-153.
Slonczewski, J. L., Fujisawa, M., Dopson, M., & Krulwich, T. A. (2009). Cytoplasmic pH Measurement and Homeostasis in Bacteria and Archaea. *Advances in Microbial Physiology*, 55: 79.
Smith, K. S., Plumlee, G., & Hageman, P. L. (2015). Mining for metals in society's waste. *The Conversation*. Web. Retrieved from: https://phys.org/news/2015-10-metals-society.html
Soderberg, T. (2005). Biosynthesis of ribose-5-phosphate and erythrose-4-phosphate in archaea: a phylogenetic analysis of archaeal genomes. *Archaea*, 1(5): 347-352.
Sohling, B., Parther, T., Rucknagel, K. P., Wagner, M. A., & Andreesen, J. R. (2001). A selenocysteine-containing peroxiredoxin from the strictly anaerobic organism Eubacterium. *Biol. Chem.*, 382(6): 979-986.
Spaans, S. K., Weusthuis, R. A., van der Oost, J., & Kengen, S. W. M. (2015). NADPH-generating systems in bacteria and archaea. *Front. Microbiol.*, 6: 742.
Sparacino-Watkins, C., Stolz, J. F., & Basu, P. (2015). Nitrate and periplasmic nitrate reductases. *Chem. Soc. Rev.*, 43(2): 676-706.
Soderberg, T. (2005). Biosynthesis of ribose-5-phosphate and erythrose 4-phosphate in archaea: a phylogenetic analysis of archaeal genomes. *Archaea*., 1(5): 347-352.
St-Germain, G. & Summerbell, R. (1996). Identifying Filamentous Fungi – A Clinical Laboratory Handbook, 1st Edition. Star Publishing Company.
Stewart, E. J. (2012). Growing Unculturable Bacteria. *Journal of Bacteriology*, 194(16): 4151-4160.
Stewart, V., Lu, Y., & Darwin, A. J. (2002). Periplasmic Nitrate Reductase (NapABC Enzyme) Supports Anaerobic Respiration by *Escherichia coli* K-12. *J. Bacteriol.*, 184(5): 1314-1323.
Suzuki, K., Wakao, N., Kimura, T., Sakka, K., & Ohmiya, K. (1998). Expression and Reguation

of the Arsenic Resistance Operon of *Acidiphilium multivorum* AUI 301 Plasmid pKW301 in *Escherichia coli*. *Appl. Environ. Microbiol.*, 64(2): 411-418.
Tabachnikov, O. & Shoham, Y. (2012). Functional characterization of the galactan utilization system of *Geobacillus stearothermophilus*. *FEBS*, 280(3): 950-964.
Tajiri, T., Maki, H., & Sekiguchi, M. (1995). Functional cooperation of MutT, MutM and MutY proteins in preventing mutations caused by spontaneous oxidation of guanine nucleotide in Escherichia coli. *Mutat. Res.*, 336(3): 257-267.
Tarkka, M. T., Sarniguet, A., & Frey-Klett, P. (2009) Inter-kingdom encounters: recent advances in molecular bacterium-fungul interactions. *Curr. Genet.*, 55: 233-243.
Techtmann, S. M., Lebedinsky, A. V., Colman, A. S., Sokolova, T. G., Woyke, T., Goodwin, K., & Robb, F. T. (2012). Evidence for Horizontal Gene Transfer of Anaerobic Carbon Monoxide Dehydrogenases. *Front. Microbiol.*, 3: 132.
Thony-Meyer, L. (1997). Biogenesis of Respiratory Cytochromes in Bacteria. *Microbiology and Molecular Biology Reviews*, 61(3): 337-376.
Tianli, Y., Jiangbo, Z., & Yahong, Y. (2014). Spoilage by *Alicyclobacillus* Bacteria in Juice and Beverage Products: Chemical, Physical, and Combined Control Methods. *Comprehensive Reviews in Food Science and Food Safety*, 13(5): 771-797.
Tianwei, T. & Cheng, P. (2003). Biosorption of metal ions with *Penicillium chrysogenum*. *Appl. Biochem. Biotechnol.*, 104: 119-128.
Tischler, A. D., Leistikow, R. L., Ramakrishnan, P., Voskuil, M. I., & Mckinney, J. D. (2016). *Mycobacterium tuberculosis* Phosphate Uptake System Component PstA2 is Not Required for Gene Regulation or Virulence. *PLoS One*, 11(8): e0161467.
Torres-Cruz, T. J., Hesse, C., Kuske, C. R., & Porras-Alfaro, A. (2018). Presence and distribution of heavy metal tolerant fungi in surface soils of a temperate pine forest. *Applied Soil Ecology*, 131: 66-74.
Trumm, D. (2010). Selection of active and passive treatment systems for AMD—flow charts for New Zealand conditions. *New Zealand Journal of Geology and Geophysics*, 53(2-3): 195-210.
Trumpower, B. L. (1990). Cytochrome bc1 complexes of microorganisms. *Microbiol. Rev.*, 54(2): 101-129.
Tucker, N. P., Hicks, M. G., Clarke, T. A., Crack, J. C., Chandra, G., Le Brun, N. E., Dixon, R., & Hutchings, M. I. (2008). The Transcriptional Repressor Protein NsrR Senses Nitric Oxide Directly via a [2Fe-2S] Cluster. *PLoS ONE*, 3(11): e3623.
Tuovinen, O. H. & Kelly, D. P. (1973). Studies on the growth of *Thiobacillus ferrooxidans* I. Use of membrane filters and ferrous iron agar to determine viable numbers, and comparison with 14+CO2-fixation and iron oxidation as measures of growth. *Arch. Microbiol.*, 88: 285-298.
Turner, S., Pryer, K. M., Miao, V. P., & Palmer, J. D. (1999). Investigating deep phylogenetic relationships among cyanobacteria and plastids by small subunit rRNA sequence analysis. *J. Eukaryot. Microbiol.*, 46(4): 327-338.
Tyson, G. W., Chapman, J., Hugenholtz, P., Allen, E. E., Ram, R. J., Richardson P. M., Solovyev, V. V., […] Banfield, J. F. (2004). Community structure and metabolism through reconstruction of microbial genomes from the environment. *Nature*, 428: 37-43.
Ueda, Y., Yumoto, N., Tokushige, M., Fukui, K., Ohya-Nishiguchi, H. (1991). Purification and characterization of two types of fumarase from Escherichia coli. *J. Biochem.*, 109(5): 728-733.
Valenzuela, L., Chi, A., Beard, S., Orell, A., Guiliani, N., Shabanowitz, J., […] Jerez, C. A. (2006). Genomics, metagenomics and proteomics in biomining microorganisms. *Biotechnol Adv.*, 24(2): 197-211.

Valiquette, N. L. (2018). Genomic Insights into the Psychrotrophic Microbial Leaching of Low Sulfide Waste Rock in Kinetic Testing Systems. *A thesis submitted in partial fulfillment of the requirements for the degree of Master of Science (MSc) in Biology, Laurentian Univeristy*.

Van den Berg, M. A., Albang, R., Albermann, K., Badger, J. H., Daran, J.-M., Driessen, A. J. M., Garcia-Estrada, C., […], Bovenberg, R. A. L. (2008). Genome sequencing and analysis of the filamentous fungus *Penicillium chrysogenum*. *Nature Biotechnology*, 26: 1161-1168.

Van Der Gast, C. J., Whiteley, A. S., & Thompson, I. A. (2004). Temporal dynamics and degradation activity of an bacterial inoculum for treating waste metal-working fluid. *Environmental Microbiology*, 6(3): 254-263.

Vasanthakumar, A., DeAraujo, A., Mazurek, J., Schilling, M., & Mitchell, R. (2015). Pyomelanine production in Penicillium chrysogenum is stimulated by L-tyrosine. *Microbiology (Reading)*, 161(6): 1211-1218.

Veiter, L. & Herwig, C. (2019). The filamentous fungus *Penicillium chrysogenum* analysed via flow cytometry – a fast and statistically sound insight into morphology and viability. *Appl. Microbiol. Biotechnol.*, 103: 6725-6735.

Veiter, L., Rajamanickam, V., & Herwig, C. (2018). The filamentous fungal pellet—relationship between morphology and productivity. *Appl. Microbiol. Biotechnol.*, 102(7): 2997-3006.

Vergil Greene, L. & Barnett, H. L. (1953). The utilization of sugars by fungi. *West Virginia Agricultural and Forestry Experiment Station Bulletins*. 362T.

Villani, G., Tattoli, M., Capitanio, N., Glaser, P., Papa, S., & Danchin, A. (1995). Functional analysis of subunits III and IV of Bacillus subtilis aa3-600 quinol oxidase by in vitro mutagenesis and gene replacement. *Biochim. Biophys. Acta.*, 1232(1-2): 67-74.

Visagie, C. M., Houbraken, J., Frisvad, J. C., Hong, S.-B., Klaassen, C. H. W., Perrone, G., Seifert, K. A., […], Samson, R. A. (2014). Identification and nomenclature of the genus *Penicillium*. *Stud. Mycol.*, 78: 343-371.

Wang, H.-W., Chung, C.-H., Ma, T.-Y., & Wong, H.-C. (2013). Roles of Alkyl Hydroperoxide Reductase Subunit C (AhpC) in Viable but Nonculturable *Vibrio parahaemolyticus*. *Appl. Environ. Microbiol.*, 79(12): 3734-3743.

Wang, H., Zeng, Y., Guo, C., Bao, Y., Lu, G., Reinfelder, J. R., Dang, Z. (2018). Bacterial, archaeal, and fungal community responses to acid mine drainage-laden pollution in a rice paddy soil ecosystem. *Sci Total Environ.*, 616-617:107-116.

Watling, H. R., Perrot, F. A., & Shiers, D. W. (2008). Comparison of selected characteristics of *Sulfobacillus* species and review of their occurrence in acidic and bioleaching environments. *Hydrometallurgy*, 93(1-2): 57-65.

Wei, Y., Lin, M., Oliver, D. J., & Schnable, P. S. (2009). The roles of aldehyde dehydrogenase (ALDHs) in the PDH bypass of Arabidopsis. *BMC Biochemistry*, 10: 7.

White, G. F., Edwards, M. J., Gomez-Perez, L., Richardson, D. J., Butt, J. N., & Clarke, T. A. (2016). Chapter Three – Mechanisms of Bacterial Extracellular Electron Exchange. In Poole, R. K. (Ed.), *Advances in Bacterial Electron Transport Systems and Their Regulation*, 68: 87-138. Academic Press.

Wolfe, A. J. (2015). Glycolysis for the Microbiome Generation. *Microbiol Spectr.*, 3(3): 10.1128/microbiolspec.MBP-0014-2014.

Wood, D. E. & Salzberg, S. L. (2014). Kraken: ultrafast metagenomic sequence classification using exact alignments. *Genome Biology*, 15: R46.

Worrich, A., Konig, S., Miltner, A., Banitz, T., Centler, F., Frank, K., Thullner, M., […], Wick, L. Y. (2016). Mycelium-Like Networks Increase Bacterial Dispersal, Growth, and Biodegradation in a Model Ecosystem at Various Water Potentials. *Appl. Environ. Microbiol.*, 82(10): 2902-2908.

Xue, Y., Zhang, X., Zhou, C., Zhao, Y., Cowan, D. A., Heaphy, S., Grant, W. D., […], Ma, Y. (2006). Caldalkalibacillus thermarum gen. nov., sp. nov., a novel alkalithermophilic bacterium from a hot spring in China. *Int. J. Syst. Evol. Microbiol.*, 56(Pt 6): 1217-1221.
Yadav, H. L. & Jamal, A. (2015). Removal of Heavy Metals from Acid Mine Drainage: A review. *International Journal of New Technologies in Science and Engineering*, 2(3): 77-84.
Zhan, Y., Yang, M., Zhang, S., Zhao, D., Duan, J., Wang, W., & Yan, L. (2019). Iron and sulfur oxidation pathways of *Acidithiobacillus ferrooxidans*. *World Journal of Microbiology and Biotechnology*, 35: 60.
Zhang, H. & Liu, K. K. (2008). Optical tweezers for single cells. *J. R. Soc. Interface*, 5: 671-690.
Zhang, T., Ding, Y., Li, T., Wan, Y., Li, W., Chen, H., & Zhou, R. (2012). A Fur-like protein PerR regulates two oxidative stress response related operons *dpr* and *metQIN* in *Streptococcus suis*. *BMC Microbiology*, 12: 85.
Zhang, X., Liu, X., Liang, Y., Guo, X., Xiao, Y., Ma, L., Miao, B., […], Yin, H. (2017). Adaptive Evolution of Extreme Acidophile *Sulfobacillus thermosulfidooxidans* Potentially Driven by Horizontal Gene Transfer and Gene Loss. *Appl. Environ. Microbiol.*, 83(7): e03098-16.
Zoli, J., Snelders, E., Verweij, P. E., & Melchers, W. J. G. (2016). Next-Generation Sequencing in the Mycology Lab. *Curr. Fungal Infect. Rep.*, 10: 37-42.
Zychlinsky, E. & Matin, A. (1983). Cytoplasmic pH homeostasis in an acidophilic bacterium, *Thiobacillus acidophilus*. *J. Gen. Microbiol.*, 156: 1352-1355.

APPENDICES

Appx. A: Supplemental figures of cultures and colonies

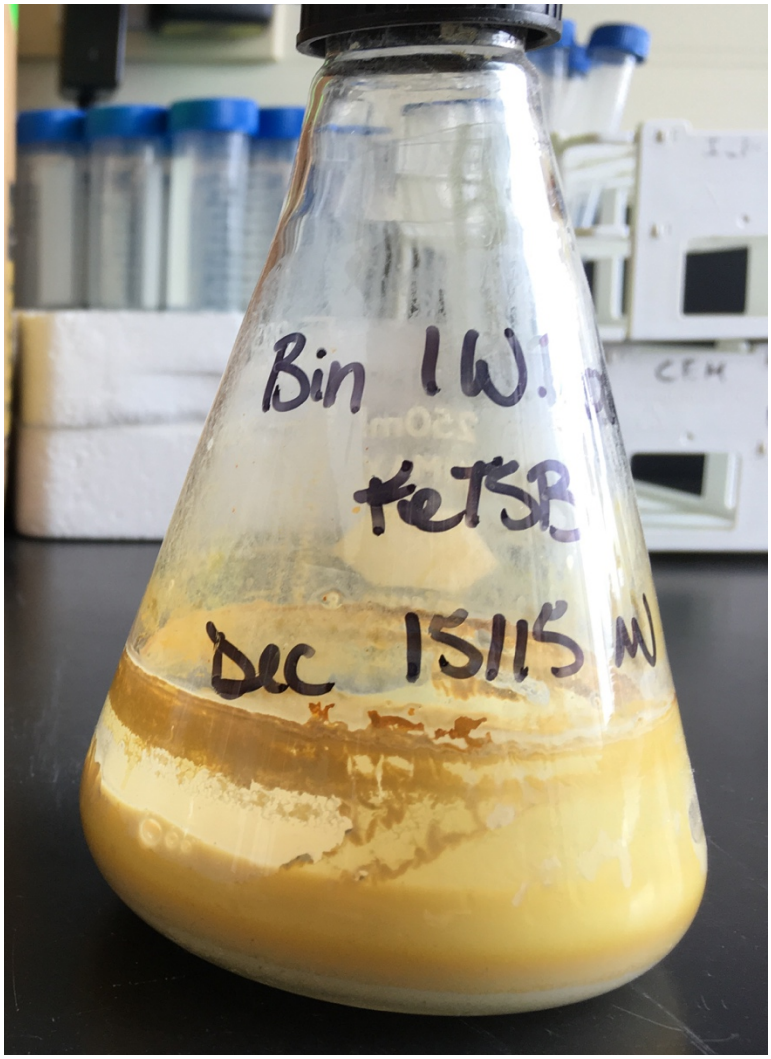

Figure A.A- 1: **Enrichment culture of low-sulfur waste rock from a mine site in Northern Ontario (BWR) used as starting material**.

<u>Figure A.A- 2</u>: **Enrichment cultures maintained for the optimization of bioleaching in bioreactor tanks by BacTech industrial partners**. A) BacTech culture (BT); B) Ecuadorian Tailings culture (ECT).

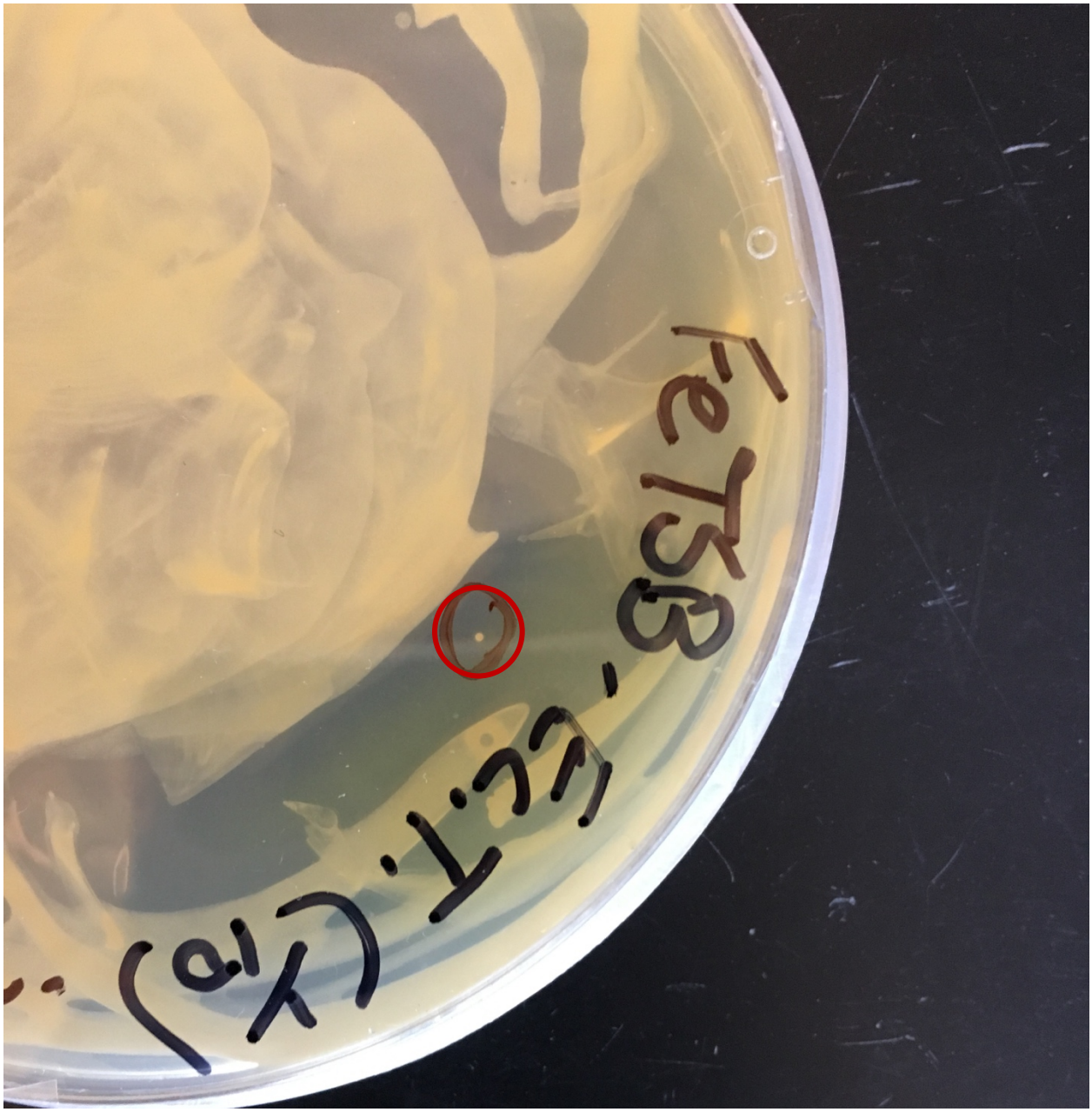

<u>Figure A.A- 3</u>: **Isolated colony from bioreactor enrichment cultures. Circled colony labeled as ECT1**. Isolated from 1/10 dilution of ECT on FeTSB medium by spread-plating.

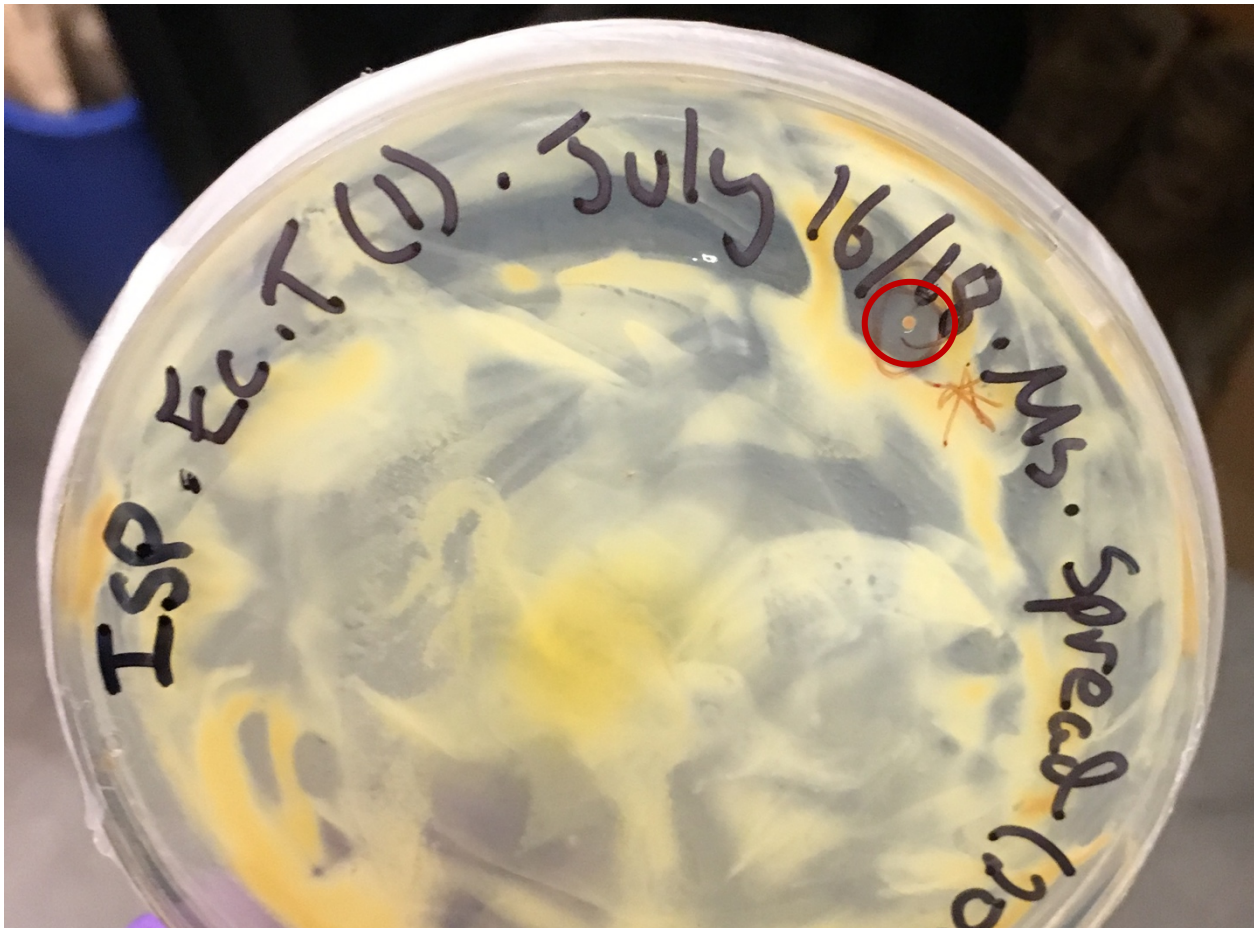

<u>Figure A.A- 4</u>: **Isolated colony from bioreactor enrichment cultures. Circled colony labeled as ECT2**. Isolated from undiluted ECT on ISP medium by spread-plating.

<u>Figure A.A- 5</u>: **Isolated colony from bioreactor enrichment cultures**. Circled colony labeled as ECT3. Isolated from undiluted ECT on FeTSB medium by streaking for isolation.

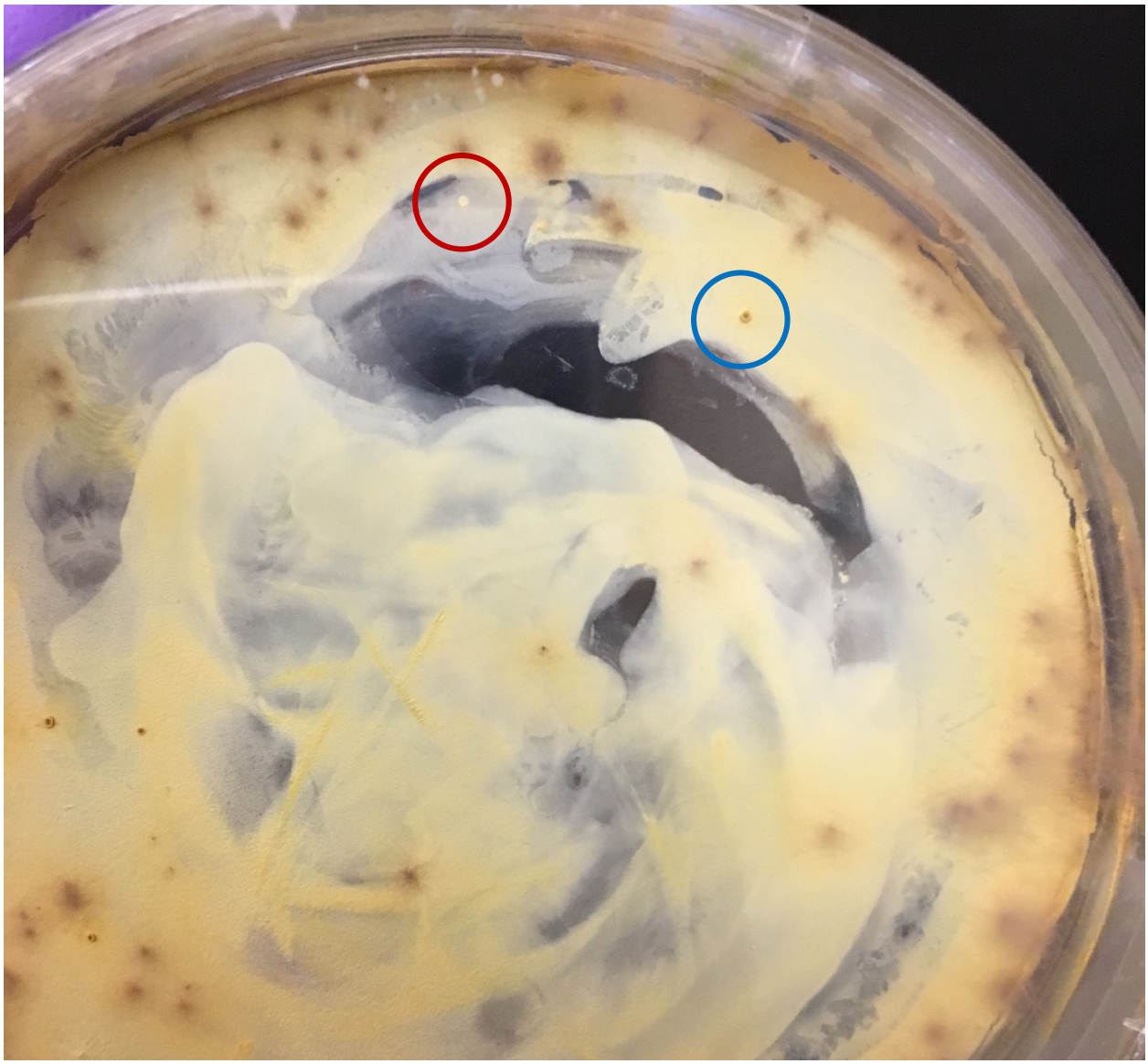

<u>Figure A.A- 6</u>: **Isolated colonies from bioreactor enrichment cultures. Red circled colony labeled as BT1 and blue circled colony labelled as BT2**. Obtained from undiluted BT on FeTSB medium by spread-plating.

<u>Figure A.A- 7</u>: Isolated colony from bioreactor enrichment cultures. Circled colony labeled as BT3. Isolated from undiluted BT on FeTSB medium by streaking for isolation.

Appx. B: Growth inhibiting substances to separate bacteria and fungi

In attempt to separate the bacterial and fungal organisms from BWR, growth inhibiting substances were added to growth media. These included the antifungals Nystatin (NYS) and Amphotericin B (AMB), as well as the antibiotic Ampicillin (AMP). A 5 mg/mL suspension solution of NYS was produced by adding 10 mL of sterile DI water to 50 mg of powder. Based on manufacturer instructions, a 100 mg/mL stock solution of AMP was created by dissolving 1 g of Ampicillin sodium salt into 10 mL of DI water and was sterilized through a 0.2 μm syringe filter. AMB came prepared as a stock solution of 250 μg/mL. The experiment was carried out as shown in Figure A.B.-1. Growth inhibiting substances were added to the samples containing 4 mL of FeTSB and 1 mL of culture at maximum suggested working concentrations. The samples were stagnantly incubated at room temperature until microbial growth was observed.

Microbial growth did not appear to be inhibited and it was suspected that the extreme medium may have caused the chemical breakdown of the antimicrobial agents, especially for AMP, which formed a brown precipitate. Product information states Ampicillin is not very stable at pH values below 7 (Sigma Aldrich, 2016). Furthermore, inoculum sizes were not regulated in this experiment which is a variable that should have been controlled.

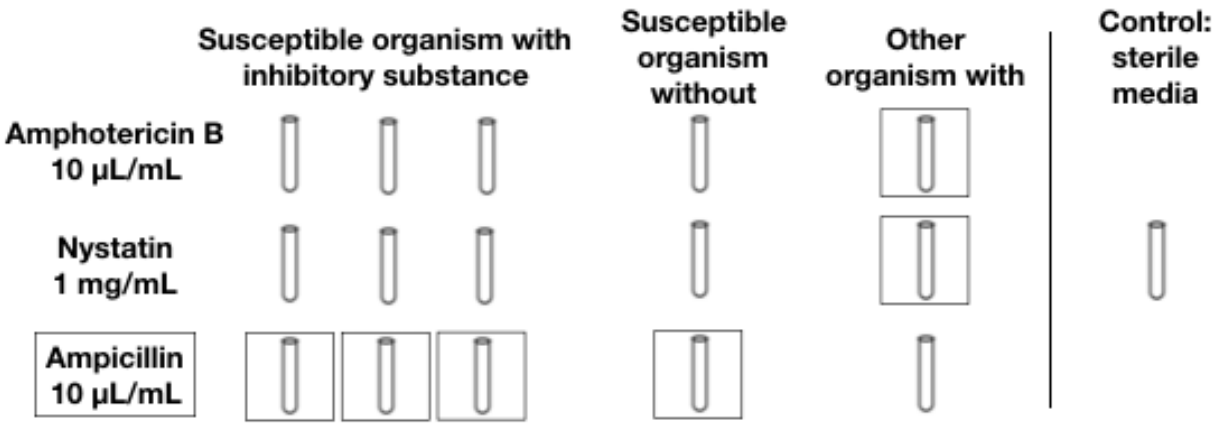

<u>Figure A.B-1</u>: **Experimental design for growth inhibiting substance tests**. For the analysis of each growth inhibiting substance, triplicate test tubes contained the antibiotic/antimycotic along with the target organism. One control sample contained no inhibitory agent, another control contained the drug with the opposite organism, and the final control was sterile. Maximum working concentrations that were added to FeTSB medium are listed below the substance name. Test tubes that are surrounded by squares contained the bacterial organism.

Appx. C: Supplemental data from DNA sequencing

Sequence A.C-1: **16S rRNA gene sequence amplified from *Ab. ferrooxidans* via Sanger sequencing. Forward and reverse reads were aligned, and degenerate bases were not modified**.

TCACCGACTTCGGGTGTTACSCACTCTCRTSGTGTKACGSGCGKKGWSTACMAGGSY
MKSKAATCCTGTWTGCTCMCCRCGSCWTCGCKSMTCMGCGATTACTAGCARTTYCG
GCTYCAKKCAGGCGMSTTCGCMRCYKGYAWTCCTSMACATATSWACGSMTTTCACC
GCTACACGTGGRWTTCSCYYSACCTCTSCGRCYCTCAAGTCTYCCCGTTGTMCAMGS
CCATTGTAGCACGKGTKKAGCCCAKGACMTWWSRSSCMWGAYGCRWWWGACSKC
MTSCSCGCGCTTCCTMCGSYYWGTCATTCCGGCAGTCAWCGMTGWGYCCCCTRCST
ATTACCGCGGCTGCTGKMACRTMGTTAKCMRGGGYTKCGCTCSTTGYGGKACCGTC
TMACCTCGARCATYTCCWCKMMASGTMGCTCGWCGMCAACCATGACACSAMCTGT
YTAGCRWKCCCCGAAGGGACGGATCRTCTCTSATCCCGTCACGCCGRYGTCAWGCY
CTSGTMAGGYTCTTCGCCCRTTGCTTSGAAGWTWMMCYACATGCTSCACTGCYYGT
GMGGRSYCYSGKCMRTKYCTTTSAGTYYCAGTSTKGCGACSGTCACYCTCYCAGGTC
GGCWRYGCWTMGTGSGTTTCCTTCGGYACCGGMSGTGGTACCCTCCGACACCWASC
AGCTMATCGYKTACCGCGTGGMCYAYCAGKKYAKCKAMKCCWGTWWGCKCCYY
WCGCYTYCSCGCCTCATGCGAKCAGGKWTCGTCCAKTCAGGCGCMTTMGCCACYS
GTWTYCAGGCGTTATCCMCATMTSWACGGCAKKTYACCGCTACACGTGKWAYTCA
CCCGTSCRCCKCTCCG

<u>Sequence A.C-2</u>: 16S rRNA gene sequence amplified from *Ab. ferrooxidans* of BWR via Sanger sequencing. Forward and reverse reads were aligned, and bases were called where degenerate base symbols corresponded with bases at this position from the most similar sequences in the NCBI database. These calls are represented by uncapitalized letters.

TCACCGACTTCGGGTGTTACcCACTCTCgTgGTGTgACGgGCGgtGtgTACaAGGcccgg
gAATCCTGTaTGCTCaCCgCGgCaTCGCtgaTCcGCGATTACTAGCAaTTcCGGCTtCAt
gCAGGCGagTTCGCngCctGcAaTCCTgaACATATgaACGgcTTTCACCGCTACACGTGG
gtTTCgCtccACCTCTcCGnCtCTCAAGTCTtCCCGTTGTaCAcGcCCATTGTAGCACGt
GTgtAGCCCAgGACaTaaggggCatGAtGCatttGACgtCaTcCcCGCGCTTCCTcCGgt
ttGTCATTCCGGCAGTCAtCGaTGaGtCCCCTnCnTATTACCGCGGCTGCTGtaACaTcG
TTAtCaaGGGtTgCGCTCgTTGcGGgACCGTCTaACCTCGAaCATcTCCaCgacAcGTaG
CTCGaCGaCAACCATGACACcAcCTGTcTAGCgtgCCCCGAAGGGACGGATCaTCTCTgA
TCCCGTCACGCCGatGTCAaGCcCTgGTaAGGtTCTTCGCCCgTTGCTTcGAAGtTaaaC
cACATGCTcCACTGCttGTGcGGgccCccGtCaaTtcCTTTgAGTttCAGTcTtGCGACc
GTCACtCTCcCAGGTCGGCagtGCtTaGTGgGTTTCCTTCGGcACCGGagGTGGTACCCT
CCGACACCtAgCAGCTcATCGttTACCGCGTGGaCtAcCAGggtAtCtAatCCtGTttGC
tCCccaCGCcTtCgCGCCTCATGCGAtCAGGttTCGTCCAgTCAGGCGCcTTcGCCACtg
GTaTtCAGGCGTTATCCaCATaTctACGGCAttTcACCGCTACACGTGgaAtTCACCCGT
cCgCCgCTCCG

<u>Sequence A.C-3</u>: **Consensus sequence of the ITS region from *Penicillium* sp. (Sample PF) of BWR via Sanger sequencing**.

GAGGTCAACCTGGAAAGATTGAGGGGGGGTCGCCGGCGGGCGCCGGCCGGGCCTAC
AGAGCGGGTGACAAAGCCCCATACGCTCGAGGACCGGACGCGGTGCCGCCGCTGCC
TTTCGGGCCCGCCCCCCGGGAGCCGGGGGGCGGGGGCCCAACACACAAGCCGTGCT
TGAGGGCAGCAATGACGCTCGGACAGGCATGCCCCCCGGAATACCAGGGGGCGCAA
TGTGCGTTCAAAGACTCGATGATTCACTGAATTCTGCAATTCACATTACGTATCGCA
TTTCGCTGCGTTCTTCATCGATGCCGGAACCAAGAGATCCGTTGTTGAAAGTTTTAA
CTGATTTAGCTAAGATGCTCAGACTGCAATCTTCAGACAGCGTTCAATGGTGTCTTC
GGCGGGCGCGGGCCCGGGGGCGGATGCCCCCCGGCGGCCGTGAGGCGGGCCCGCC
GAAGCAACAAGGTACGATAAACACGGGTGGGAGGTTGGACCCAGAGGGCCCTCACT
CGGTAATGATCCTTCCGCA

<u>Sequence A.C-4</u>: **Consensus sequence of the ITS region from *Penicillium* sp. (Sample F1) of BWR via Sanger sequencing**.

GAGGTCAACCTGGAAAGATTGAGGGGGGGTCGCCGGCGGGCGCCGGCCGGGCCTAC
AGAGCGGGTGACAAAGCCCCATACGCTCGAGGACCGGACGCGGTGCCGCCGCTGCC
TTTCGGGCCCGCCCCCCGGGAGCCGGGGGGCGGGGGCCCAACACACAAGCCGTGCT
TGAGGGCAGCAATGACGCTCGGACAGGCATGCCCCCCGGAATACCAGGGGGCGCAA
TGTGCGTTCAAAGACTCGATGATTCACTGAATTCTGCAATTCACATTACGTATCGCA
TTTCGCTGCGTTCTTCATCGATGCCGGAACCAAGAGATCCGTTGTTGAAAGTTTTAA
CTGATTTAGCTAAGATGCTCAGACTGCAATCTTCAGACAGCGTTCAATGGTGTCTTC
GGCGGGCGCGGGCCCGGGGGCGGATGCCCCCCGGCGGCCGTGAGGCGGGCCCGCC
GAAGCAACAAGGTACGATAAACACGGGTGGGAGGTTGGACCCAGAGGGCCCTCACT
CGGTAATGATCCTTCCGCA

<u>Sequence A.C-5</u>: **Consensus sequence of the ITS region from *Penicillium* sp. (Sample F2) of BWR via Sanger sequencing**.

GAGGTCAACCTGGAAAGATTGAGGGGGGGTCGCCGGCGGGCGCCGGCCGGGCCTAC
AGAGCGGGTGACAAAGCCCCATACGCTCGAGGACCGGACGCGGTGCCGCCGCTGCC
TTTCGGGCCCGCCCCCCGGGAGCCGGGGGGCGGGGGCCCAACACACAAGCCGTGCT
TGAGGGCAGCAATGACGCTCGGACAGGCATGCCCCCCGGAATACCAGGGGGCGCAA
TGTGCGTTCAAAGACTCGATGATTCACTGAATTCTGCAATTCACATTACGTATCGCA
TTTCGCTGCGTTCTTCATCGATGCCGGAACCAAGAGATCCGTTGTTGAAAGTTTTAA
CTGATTTAGCTAAGATGCTCAGACTGCAATCTTCAGACAGCGTTCAATGGTGTCTTC
GGCGGGCGCGGGCCCGGGGGCGGATGCCCCCCGGCGGCCGTGAGGCGGGCCCGCC
GAAGCAACAAGGTACGATAAACACGGGTGGGAGGTTGGACCCAGAGGGCCCTCACT
CGGTAATGATCCTTCCGCA

<u>Sequence A.C-6</u>: **Consensus sequence of the ITS region from *Penicillium* sp. (Sample BF) of BWR via Sanger sequencing**.

GAGGTCAACCTGGAAAGATTGAGGGGGGGTCGCCGGCGGGCGCCGGCCGGGCCTAC
AGAGCGGGTGACAAAGCCCCATACGCTCGAGGACCGGACGCGGTGCCGCCGCTGCC
TTTCGGGCCCGCCCCCCGGGAGCCGGGGGGCGGGGGCCCAACACACAAGCCGTGCT
TGAGGGCAGCAATGACGCTCGGACAGGCATGCCCCCCGGAATACCAGGGGGCGCAA
TGTGCGTTCAAAGACTCGATGATTCACTGAATTCTGCAATTCACATTACGTATCGCA
TTTCGCTGCGTTCTTCATCGATGCCGGAACCAAGAGATCCGTTGTTGAAAGTTTTAA
CTGATTTAGCTAAGATGCTCAGACTGCAATCTTCAGACAGCGTTCAATGGTGTCTTC
GGCGGGCGCGGGCCCGGGGGCGGATGCCCCCCGGCGGCCGTGAGGCGGGCCCGCC
GAAGCAACAAGGTACGATAAACACGGGTGGGAGGTTGGACCCAGAGGGCCCTCACT
CGGTAATGATCCTTCCGCA

<u>Sequence A.C-7:</u> Forward and reverse sequences of the 16S rRNA gene amplified from a colony that grew on ISP mod. which was inoculated with the ECT culture.

Forward:

CGGTTTTTGGGGATTATCTCCCCCTCGGGGTTTCGAACCCCTTTNTACCCCCCTTTGT
AACATGTGTGAACCCCNGGANAAAGGGGGNNAGAAAATTTNATTTTNCCCCCCCTT
CCCCCGGTTTTGACCCGGGGTCTCCCTTTANAGTCCCCNCCTAACNGCTGGAAACAA
AGGTAAAGGGTTTNCCNCGTTTTGGGACTTAACCCAACTTNTCNAGANNACGACTGA
CAAGAACCATGNGCCACCNGTTTCNCGTNTCCCCAAAGAAAACCNNCCTTCTCTGG
AGGTANCACGAGGAGGTCAAGCCNGGTNAAGGTTCTCCCNTTNACTT

Reverse:

TTANACAACNGCATGCGGGCGANTNATGCCCCGTAATTTAGATTAACGNTTGCACCC
TCGGAATTACCGGGGGTGTTGTCATGAAGTAAGNNGAAGGTTCTTCCTTTGGTAAAG
TGAACGAGTTCTTGGCATGAAAAAAAAGCTTTTCTTCCCGAAGGNAAGCGTTTTACA
ACCGGAAGGCCTTCTTCAGGCANGCGGCATTGGTGGATNAGGCTTTCGCCCANCGTC
CAATATTNCTCAGNGCTGCCTCCCGTAGGAGTNTGGGCCGTGTATCAGTTCCAGCGG
GGCAGGTCATCTTGTCAGGCCNGGTAGTGATCGTCGCAACGGNGNGCTGTTACCCCG
CCCAATAGGTAATCGGAAACCGGGCGANCACATTNCAANAGGCGGTCAGGTCNCCN
AAGGTCATCTCCGGTNTTAGCNCGGGTTTAGCGGAGGNTATCCACGGTGTTATCNCC
CAGGTAGCGGACAGGTTACCTGATGCAGTACTCACGCTGGATGCAATTCGGTA

<u>Sequence A.C-8:</u> Forward and reverse sequences of the 16S rRNA gene amplified from a colony (ECT3) that grew on FeTSB which was inoculated with the ECT culture.

Forward:

GTTACANACTCTCGGTGGTGTGACGGGCGGGTGGTGATACAAGGCCCGGNAACGTA
TTCACCGCGGCATGCTGATCCGCGATTACTAGCGATTCCGGCTTCATGCAGGCGATT
TGCACCCTGCAATCCAAACTGAGAGCGGCTTTTTGGGATTAGCTCCCCCTCGCGGGT
TCGCAACCCTTTGTACCGCCCATTGTANCACGTGTGTACCCCAGGGCATAGGGGGCA
TGATGATTTGACGTCATCCCCACCTTCCTCCGGTTTGTCACCGGCAGTCCCCTTAGAG
TGCCCAACTNAATGCTGGCAACNAAGGCCAAGGGTTGCGCTCGTTGCGGGACTTAA
CCCAACATCTCACGACACGAGCTGACAACAACCATGCACCACCTGTCACCGGTGTCT
CCAAAGAAAACCCTCCCTCTCTGGAGGTAGCACCGGGATGTCAAGCCCGGGTANGG
TTCTTCGCGTTNCTTAAAAANAAACCACATGCNCCACCGCGTGTGCGGGCCCCCCTC
TNTTCTTTTGANTTTCAGCCTTGCGGCCGTACTCCCGAGGCGGAGTGCTTAATGGTGT
TACCTTCAGCACTGAGGGTGTC

Reverse:

GCCCAGTGATTCAGGACAACGCTCGCCCCNTATGTATTACCGCGGCTGCTAGCAAGT
AGTTAGCCGGGGNTTTCTCGTCAGGTACCGGCAAGGTACCGCCCTTGTTGAACGGTA
GTTGTTCTTCCATGACAACAGAGCTTTACGACCNGAAGGCCTTCNTTTGCACACGCG
GAATCGNTANGTCANGCNTGCGGCCATTGCGGAAGATTCCCTACTGCTGCGTCCTAT
AGGAGTCTGGGCCGTGTCTCAGTCNCANTGGGGCCGGTCACCNTCTCAGGCGGGCT
ATGCATCGTTGCCNCGGTGAGCCGTTACCTCACCAACTAGGTAATGAGCCGCAGGCC
CATCTGTAAGCGGTAGCCGCGCGGCCACCTTTCAACAAACGGTCATGCGAACCGAA
GGTCCTATCACGGTATTAGCCCCGGTTTCCCGGGGTTATTCCCGGTCNTAACATGGC
AGGTAGCNTAGCGTGTTAGCTCAACCCGTCAGCCGCTCGATCCACCTACCCGTCAGC
C

Table A.C- 1: **Taxonomy assigned by Kraken2 to the whole-genome sequencing data of the Metagenome 1 sample containing *Ab. ferrooxidans* from BWR**. Only contig #3 was identified as the closely related species of Alicyclobacillus.

Contig	Length	Coverage	Scientific Name
1	502,177	13.721062	*Bacillus thuringiensis serovar morrisoni*
2	370,406	14.258465	*Bacillus* genus
3	184,596	13.804448	*Alicyclobacillus acidocaldarius* subsp. *acidocaldarius* DSM 446
4	169,885	13.867079	*Bacillus* sp.
5	152,821	13.465125	*Bacillus atrophaeus*
6	145,011	13.111016	*Pseudomonas fluorescens* SBW25
7	121,883	14.539407	*Bacillus* genus
8	107,984	15.205455	*Proteobacteria* phylum
9	106,663	14.292646	*Paenibacillus* genus
10	90,028	14.314871	*Thermoanaerobacteraceae* family
11	83,465	13.360484	*Paenibacillus naphthalenovorans*
12	74,580	14.884287	*Bacillus* sp. FJAT-25496
13	71,077	17.770873	*Paenibacillus brasilensis*
14	58,070	14.362268	*Thermobacillus composti* KWC4
15	45,979	16.51074	*Paenibacillus thiaminolyticus*
18	27,250	15.988776	*Paenibacillus* sp. BIHB4019
20	19,901	13.165658	*Bacillus thermoamylovorans*
21	9,315	22.375839	*Brevibacillus brevis*
22	8,282	153.800853	*Bacillus cereus* m1293
23	7,654	16.20681	*Paenibacillus*
26	5,591	22.645448	*Nostocales cyanobacterium* HT-58-2
27	5,132	47.849258	*Tumebacillus algifaecis*
30	3,288	13.032389	*Paraburkholderia xenovorans* LB400
31	3,231	14.25967	*Bacillales* order
34	2,144	19.549541	*Clostridium perfringens*
36	2,028	15.423885	*Staphylococcus auricularis*
38	1,857	15.232022	*Bacteria* domain
40	1,783	25.499414	*Thermobacillus composti* KWC4
42	1,413	19.622754	*Paenibacillus polymyxa*
50	704	44.606061	*Brevibacillus* sp. SCSIO 07484
51	383	80.098039	*Desulfotomaculum ferrireducens*
57	261	31.608696	*Bacillales* order

<u>Sequence A.C-9</u>: Sequence of ~1,541 bp 16S rRNA gene of *Ab. ferrooxidans* obtained from whole-genome sequencing and annotated by Prokka on contig #27.

AAGGAGGTGATCCAGCCGCACCTTCCGATACGGCTACCTTGTTACGACTTCACCCCA
ATCGCGAATCCCACCTTCGGCGGCTGGCCCCCTTGCGGGTTACCTCACCGACTTCGG
GTGTTACCCACTCTCGTGGTGTGACGGGCGGTGTGTACAAGGCCCGGGAACGTATTC
ACCGCGGCATGCTGATCCGCGATTACTAGCAATTCCGGCTTCATGCAGGCGAGTTGC
AGCCTGCAATCCGAACTATGAACGGCTTTTTGGGTTTCGCTCCACCTCGCGGTCTCG
CTTCCCGTTGTACCGCCCATTGTAGCACGTGTGTAGCCCAGGACATAAGGGGCATGA
TGATTTGACGTCATCCCCGCCTTCCTCCGGTTTGTCACCGGCAGTCATCGATGAGTCC
CCGCCTTTACGCGCTGGTAACATCGATCAAGGGTTGCGCTCGTTGCGGGACTTAACC
CAACATCTCACGACACGAGCTGACGACAACCATGCACCACCTGTCTAGCGTGCCCC
GAAGGGACGGATCATCTCTGATCCCGTCACGCCGATGTCAAGCCCTGGTAAGGTTCT
TCGCGTTGCTTCGAATTAAACCACATGCTCCACTGCTTGTGCGGGCCCCCGTCAATT
CCTTTGAGTTTCAGTCTTGCGACCGTACTCCCCAGGCGGAGTGCTTAGTGGGTTTCCT
TCGGCACCGGAGGTGGTACCCTCCGACACCTAGCACTCATCGTTTACCGCGTGGACT
ACCAGGGTATCTAATCCTGTTTGCTCCCCACGCCTTCGCGCCTCAGCGTCAGGTTTCG
TCCAGTCAGGCGCCTTCGCCACTGGTATTCCTCCACATATCTACGCATTTCACCGCTA
CACGTGGAATTCCCCTGACCTCTCCGACCCTCAAGTCTCCCCGTTTCCAAGGCCATG
TCAGGGTTGAGCCCTGACCTTTCACCCCAGACGCGAAAGACCGCCTGCGCGCGCTTT
ACGCCCAGTCATTCCGGACAACGCTTGCCCCCTACGTATTACCGCGGCTGCTGGCAC
GTAGTTAGCCGGGGCTTCCTCCTTTGGTACCGTCTCACCTCGAGCATTTCCTCTCAAG
GTCGCTCGTCCCAAATGACAGAACTTTACAATCCGAAGACCGTCTTCATTCACGCGG
CGTTGCTCCGTCAGGCTTTCGCCCATTGCGGAAGATTCCCTACTGCTGCCTCCCGTAG
GAGTCTGGGCCGTGTCTCAGTCCCAGTGTGGCCGGTCACCCTCTCAGGTCGGCTACG
CATCGTCGCCTTGGTAGGCCGTTACCCCACCAACCAGCTAATGCGCCGCGGGCCCAT
CGTTCAGCGACGCCAGAAGCGCCTTTCCTTCCCCGCCCATGCGAGCAGGGATCCCAT
TCGGGATTAGCACCCGTTTCCAGGCGTTATCCCCATCTGAACGGCAGGTTACCCACG
TGTTACTCACCCGTCCGCCGCTCCCTTTCCCCGAAGGAAAAGAGCGCTCGACTTGCA
TGTATTAGGCACGCCGCCAGCGTTCGTCCTGAGCCAGGATCAAACTCTCAATA

<u>Sequence A.C-10</u>: Sequence of 932 bp obtained from shotgun whole-genome sequencing that was annotated as rRNA by Prokka on contig #22 and which was most similar to sequences from *Penicillium* spp.

TAATGATCCTTCCGCAGGTTCACCTACGGAAACCTTGTTACGACTTTTACTTCCTCTA
AATGACCGAGTTTGACCAACTTTCCGGCTCTGGGGGGTCGTTGCCAACCCTCCTGAG
CCAGTCCGAAGGCCTCACTGAGCCATTCAATCGGTAGTAGCGACGGGCGGTGTGTA
CAAAGGGCAGGGACGTAATCGGCACGAGCTGATGACTCGTGCCTACTAGGCATTCC
TCGTTGAAGAGCAATAATTGCAATGCTCTATCCCCAGCACGACAGGGTTTAACAAGA
TTACCCAGACCTCTCGGCCAAGGTGATGTACTCGCTGGCCCTGTCAGTGTAGCGCGC
GTGCGGCCCAGAACATCTAAGGGCATCACAGACCTGTTATTGCCGCGCACTTCCATC
GGCTTGAGCCGATAGTCCCCTTAAGAAGCCAGCGGCCCGCAAATGCGGACCGGGCT
ATTTAAGGGCCGAGGTCTCGTTCGTTATCGCAATTAAGCAGACAAATCACTCCACCA
ACTAAGAACGGCCATGCACCACCATCCAAAAGATCAAGAAAGAGCTCTCAATCTGT
CAATCCTTATTTTGTCTGGACCTGGTGAGTTTCCCCGTGTTGAGTCAAATTAAGCCGC
AGGCTCCACGCCTTGTGGTGCCCTTCCGTCAATTTCTTTAAGTTTCAGCCTTGCGACC
ATACTCCCCCCAGAACCCAAAAACTTTGATTTCTCGTAAGGTGCCGAACGGGTCATC
ATAGAATCCCGTCCGATCCCTAGTCGGCATAGTTTATGGTTAAGACTACGACGGTAT
CTGATCGTCTTCGATCCCCTAACTTTCGTTCCCTGATTAATGAAAACATCCTTGGCGA
ATGCTTTCGCAGTAGTTAGTCTTCAGCAAATCCAAGAATTTCACCTCTGACAGCTGA
ATACTGACGCCCCCGACTA

<u>Sequence A.C-11</u>: Sequence of 589 bp obtained from shotgun whole-genome sequencing that was annotated as rRNA by Prokka on contig #22 and which was most similar to fungal sequences including from *Penicillium* sp.

TACGAGCTTTTTAACTGCAACAACTTTAATATACGCTATTGGAGCTGGAATTACCGC
GGCTGCTGGCACCAGACTTGCCCTCCAATTGTTCCTCGTTAAGGGATTTAAATTGTTC
TCATTCCAATTACGAGACCCAAAAGAGCCCCGTATCAGTATTTATTGTCACTACCTC
CCCGTATCGGGATTGGGTAATTTGCGCGCCTGCTGCCTTCCTTGGATGTGGTAGCCG
TTTCTCAGGCTCCCTCTCCGGAATCGAACCCTAATTCCCCGTTACCCGTTGCCACCAT
GGTAGGCCACTATCCTACCATCGAAAGTTGATAGGGCAGAAATTTGAATGAACCAT
CGCCGGCGCAAGGCCATGCGATTCGTTAAGTTATTATGATTCACCAAGGAGCCCCGA
AGGGCGTTGGTTTTTTATCTAATAAATACACCCCTTCCTGAAGTCGGGGTTTTTAGCA
TGTATTAGCTCTAGAATTACCACAGGTATCCATGTAGTAAGGTACTATCAAATAAAC
GATAACTGATTTAATGAGCCATTCGCAGTTTCACAGTATAAAGTGCTTATACTTAGA
CATGCATGGCTTAATC

<u>Sequence A.C-12</u>: Sequence of 1,431 bp obtained from shotgun whole-genome sequencing that was annotated as rRNA by Prokka on contig #17 and which was most similar to a sequence from *Penicillium* sp.

AGAGAGTTTGATGATGGCTCTAACTGAACACTGTCCAAGTACTTGACACATGCTAAT
CGAACGACTAATTAGGTTTAATATAATATTATATTAAACTAAGTAGTAGTGGTGTAC
AGGTGAGTATATGATAAATTGGCTACCTTAAACCAAGGGAAAAATCCCTTATAAAT
AAAGGTAATAAAAATCCGGTTTAAGATGTTAATTTTTATCTCGGTGAGTAGTAGGAA
AGGTAATGACTTTTCTAGCAAGAACCGTAGTCGTGACTGGAAAGTTGATCGACCACA
TTGGGTCTGAAAAAAACCCAATGCTTTTTTGTACAGCAGTGAGGAATATTGGTCAAT
GGCCGAAAGGCTGAACCAGTAACTTGGAAGAATGTAAGTGTATTTGTATAAATACA
GTAGCGATTATATCGCATAAAATTCTAAATAGATTAAAGATAATGACATAATCTATT
TATAAGTCTTGACCAAACTACGTGCCAGCAGTCGCGGTAATACGTAGAAGGCTAGT
GTTAGTTATCTTTATTGGGTTTAAAGGGTATGTAGACGGTAAATTAAACTCTAAAAG
AGTACTTTTTTACTAGAGTTATATATGAGAAGGAAGAATTTCTGGAGTAGAGATAAA
ATTTTTTGATACCAGGAGGACTGTCAACGGCGAAGGCGTCCTTCTATGTAATAACTG
ACGTTGAGAGACGAAGGCTTGGGTAGCAAACAGGATTAGATACCCTAATAGTCCAA
GCAGACAATGATGAATGTCATACATTAGAGAAGATTTAATGTATAAACGAAAGTGT
AAGCATTCCACCTCAAGAGTACTATGGCAACATATAAACTGAAATCATTAGACCGTT
TCTGAAATCAGTAGTGAAGTATGTTATTTAATTCGATGATCCGCGAAAAACCTTACC
ACAGCTTGTATAACTATTTAGTAAATTGTAACAAGCGCTGCATGGCTGTCTTTAGTT
AATGTCGTGAGATTTGGTTAACTCCTTTAATTAACGAAAACCCTCACTTTATTTATTT
ATATAGAGTGGTTCACTACTACATTGGATTAGATAATAGGGATTAAGACAAGTCATT
ATGGCCTAAATGCTGTGGGCTATAGACGTGCCACATACGCCTTTACAAAGGGATGCG
ATATTGTGAAATGGAGCTAATCCTCAAAAAAGGAAATATTATGGATTGTAGTCTGTA
ACTCGACTACATGAAAAAGGAATTACTAGTAATCGTGAATCACCATCGTCACGGTG
AATTTTTTCTCAGTTAGGTACTAACCACTCGTCAGGCGCTGAAAAAAGAAGATGCAG
TAAGTTTGATTTTTTCTATATAAAATTATATATAATTAGGTGTATAAATATGTAGGAA
AGTTTT

<u>Sequence A.C-13</u>: Sequence of gene (1,482 bp) encoding multicopper oxidase obtained from whole-genome sequencing of the Metagenome 2 sample and annotated by MG-RAST as belonging to the Ascomycota phylum.

GACGGGGCAGTTTCCCTTACGCAGTGTCCCATTGCCCCGGGTCAGAGCATGACATAC
CGCTGGCGAGCTACGCAGTACGGAACGACCTGGTACCATTCTCATATGGGACTCCA
GACGTGGGAAGGTGTCTTTGGCGGGATTATCATTAACGGGCCGGCTAGTGCAAACT
ACGACGAGGATAAGGGAACAATCCTATTGACTGACTGGGACCTGAGGACGGTGGAT
GAGCTGTGGGATACGGTGCAAGTGCTGGCCGCCGACGTGGATAATGGGCTTATCAA
TGGGACCAATGTATTTGGGGATGATGGCATGGATCAGGTTGGACGGCGATTTAAGA
TGAAGTTTACGAAAGGGAAATCCTATCGATTAAGGCTGGGAAATGCGGCTTGTGAT
ACGCATTTCAAGTTTAGTATTGATCATCATACTTTGATCGTGATTGCGGTGGATTTGG
TTCCGATTCAACCATATACAACGACTGTTTTGGATATTGCAATTAAAGTAGCACAAT
ACGTCGTTGTTGAAGCACCATCTAACTTCTCCTATCTGACTCTTGGCCTAGGTCAACG
TTACGATGTTATCGTCCACGCCGATCAGTCTGCTCTAAGCAATGCCTTTTGGCTCCGA
GCCATCCCCCAGCTCTCCTGTTCGAAGAGCCTCAACGCCGACAATGTTCGCGGAATT
ATATACTATGACGAGGAAAATATCAATTCTACTATAATCCCCAACTCTACAGCGCAC
AATTTTACCGACAGCTGCCGTGACGAAGACCCCTCAAATCTTATCCCAATGGTTTCC
CAACCCTTCGACCTCACCCCGTCAGAGTTTTTCTACAACGAGACTCTCCCTGTCACA
GTATCCAAGACCAACTCATTCTACCGCTGGCAACTCAATGGCAACTCTTTCTCCATG
AACTGGACACAGCCAACCCTGCGGTCCTTGCACACCTTGGCCCCAAGTCACAGACC
AGACCTACTCCCAAGCTCCAATTCCTGCTTGTCCGCTATCCCCCTACCAGCGAATAG
CATTCCAGTCCCCCAACCAGAAACATGGGTCCTGATAGTAATCGAAAGCACCCTCCC
GATCCCACACCCAATCCACCTACACGGCCACGATTTCATCCTCTTAGCCCAAGGAAC
TGGCCCTTACACTGTCCCAACATCTGCATCTCTACCCTACGCTACTGCTAGCACTATA
CCAAAACGCGATACAGCCCTACTCCCAGCGGGTGGACACCTAGTCCTATCGTTCACA
CTGATAACCCGGGTGTGTGGCTACTACATTGCCATGTTGGATGGCACCNTGGAGCAG
GGGTTTGCGGTGCAGATTATTGAGCAGGGAGAGGAAATTTGTCGGCTGTTAAATGG
CGGTCCTAGTGGTGAGGGTGGGGCGTGGCAGGAGTGGGCGGAGGACCTGGAAGGG
AACTGTCTTGTTTGGGAGGGGTTGAAGGGAGGTTTACAGGGAGTGGAGGATGGGTC
TGGGGTT

<u>Sequence A.C-14</u>: Sequence of gene (1,701 bp) encoding multicopper oxidase obtained from whole-genome sequencing of the Metagenome 2 sample and annotated by MG-RAST as belonging to the Ascomycota phylum.

AAGCCGTTGTATGTTCTTTATTTTTGTATTGAGGACAGCTGCATTCACCATCCCTGGC
CTCGAGGACCGCAAGTCCAAAAAATGCACAGGGAACACAGCCCACACTCGAAACA
AGTGTGTGATTATAACATCGACACTGATTACACGACTGTCGTTCCTGATACAGGCGT
GACTCGTGAGTACTGGTTTTCCATTGACGAAGTCACTGTTGCCCCAGATGGCGTTTC
CTGTCCAGCAATGGCGGTCAATGGGACAATACCTGGACCCACCATCTATGCCGACTG
GGGCGACGAGGTCATTATTCATGTCACAAACCACCTTGATGAATCAAAGAATGGAA
TCAGCATCCACTGGCATGGTATTCGCCAAAATTATACCAATGTAAACGATGGAGTTG
TGTCAATCACCCAGTGTCCCACTGCGCCTGGGCCGAGGGTGACCTATAAATGGCGA
GCTGTTCAATACGGCACATCCTGGTGGCATTCGCACATTGGACTCCAGGCTTGGGAG
GAGATATTTGGGGGAATCATTATCAACGGGCCTGCAAGCTCTAATTACGATGTTGAT
AAAGGTGTCCTATTCCTCAATGACTGGGACCATCAAACTGCAGATGAGCTGTTTACT
TATGCCCAGACCACGGGTCCTCCAACACTCGACACTGGACTGATCAATGGGACCAA
TGTGTACAATTCCACTGGATCACGTTTTACGATAAGAGCCAACAAAGGAGAATCCTA
TCGGTTAAGAGTCATCAATGCGGCAATTGACCCATTGGAAGTTTATACCCTTTCTGTT
ATTGCTATGGACTTGGTGTCAATCAAACATTATACAACGAAGTACATTAACATTGGG
ATGGGAAGTCAAAGCATCTCTAAAATCATAGACTGTACTAACCTGAAATCTGCAGGT
CAGCGATATGACGTGATAGTCACAGCCGACAAGGCTTCTGTAGCTCGAGACTTTTGG
ATTCGCGCAGTACCACAAACGCAATGCTCGGAGAATGACAATGTTGACAATATCAA
GGGGATTCTCCACTACCATACTCAGCTAGGGATACCAGAAACCAATGCGACCCCTTT
GATGATGGCTGCGTTGATGAAAGTCCAAGAATCTCGTCCCGATTGTCTCGAAATCAG
TTTCTGCTGCAAACTGGCAATCTATGAAGATGTGACCGTCAGCAAGAACGCACAGA
ATCTGTTTCGTTGGTACTTAAATAGTACTACTATGCAGGTGGCATGGGAAGATCCCA
CACTGCTCCAACTCTACAATGACGCCACTGATTTCTCGAATTCAAGTGGTGTCATCG
AAGTTCCAAATGCAAATGAATGGGTCTACTTGCTCATTAATACTTCAATTCCCGTCG
CCCATCCGATTCACCTGCATGGCCATGATTTCTTCATTCTAGCTCAGGGAGTCAATCC
TTGGGATGGTACAACTTTGTCTCATCAAATCTTCCCAGAAGGGAACTGTAATTCTGG
AGAGCACGGGGTATTGCTTATTGCGTTTGAAACGGACAATCCAGGCGCGTGGTTGAC
GCATTGTCATATTGGATGGCACACCTCAGAAGGGTTTGCTTTGCAGTTTGTTGAGCG
TTATGACGAGATTAAGAATTTGATTGATTATCCATCTTTGGATCAGAATTGCGCGGC
TTGGACTGCTTATGACTCGACAGTTGGAATAGAGCAAGATGATTCGGGTATT

<u>Sequence A.C-15</u>: Sequence of gene (1,761 bp) encoding multicopper oxidase obtained from whole-genome sequencing of the Metagenome 2 sample and annotated by MG-RAST as belonging to the Ascomycota phylum.

AAGGCCACATCTCTCCTCTTCGGTCTCATTGGTGCAGTACCGCAGCTTCTCTTCGCCA
TCAACACCTCCATCCAAAGCTCAAGCGAGATGTCTGCTCTGGAAACACTGCCAGTGA
AGAAAGACATGGTGCAATACAACATCAGCACGAATTACTACGACGTGGTCCCCAAC
ACAGGTGTGACTCGAGAGTACTATTTCAATATCCAAGAAGTCACAGTTGCACCTGAT
GGCTATTCTCGCTCTGCCATGGCTGTGAACGGCTCCATTCCTGGTCCTACCATCCACG
CCGACTGGGGTGACTACGTTATCGTGCATGTCACGAATAATCTCGCCTCGGCGAAGA
ACGGATCAAGTATTCATTTTCATGGGATCCGTCAGAATTATACCAGCCCCAATGACG
GTGCGCTCGATAACACAATGTCCGACGCACCGGGTAAAACCACGATTTACAAATGG
CGTGCCACGCAGTATGGATCGTCGTGGTACCATTCCCATATTGGACTGCAGGCCTGG
GAGGGTGTCTTTGGTGGCATTGTGATTAACGGGCCGGCCACTGAGAATTATGATGTT
GATAAGGGTAGTTTGTTTTTGAATGACTGGAGCCATCAGACTGTTGATGAGCTTTAT
GATTCTGCTCAAGCGAGTGGTCCGCCAACACTGGACAATGGTCTGATCAATGGTACG
AATGTCTATGGCTATGATAACTCGAGTAGCCAGACGGGATACCGGTTTAATACGTCC
GTCACTGCGGGTACTTCATATCGATTCCGTCTGGTGAATGCTGCGATTGATACGCAC
TTCAAATTTTCCATCGACAACCACACGCTCACCGTGATGACGATGGACTTGGTACCT
ATTGAGCCATTTAATACCACTGTCCTGAGCATCGGCATGGGTATGATCGGAGTGTTC
TCTATAGTCAAGCCGGATATCTGGCTAACGACCATCTCCTATCTAGGCCAACGGTAC
GACATCGTCGTTCACGCGGACCAGTCCACAGGTAACGACACCTATTGGATCCGGGC
CATCCCCCAGGAAGCATGCTCCGACAATGATAGCGTCGACAACATCAAGGGAATCA
TGTACTACGGCAACACACCCTCTACCCCCACCACAACCGAGTACACCTACATCGACA
GCTGCGACGACATGCCCATGTCCGATCTAGTCCCCTACCTCCCTCAGAGCGCCTCAC
TCCCCTACTACAACGCAAGCGAACCTGTCACTCTCGGCGAGAATTCGGAGAACCTTT
TCCGCTGGAAAATGAACGGAACCTCCATGCAGGTCGAATGGGACAATCCCACGCTG
CTACAGATCTGGAACAACGACACCAGCTTCACAAGCTCGAGCGGTGTGGTCGAATT
ACCCCGGGCCAACGAGTGGTCCTACGTTGTCATCGAGACTGCTGACAGTACCACACC
GATCCACCTGCATGGCCACGACTTTTTTGTTCTTGCCCAGGGCTCTGGTACGTACAGC
GGATCGTCGGATATTGCTAGCCTGACGAACCCCCCGCGGCGCGACGTGGCTATGCTA
CCCAGCTCGGGGTATTTGGTTGTGGCGTTCAAGACTGATAACCCAGGGGCGTGGTTG
ATGCATTGTCATATTGGTTGGCACACGGAAGAGGGATTTGCTATTCAGTTCTTGGAA
CGATATGAGGAAGCGCGTAAATTAATTGATTATAGTGCTCTGCACTCTGGGTGCAAG
GCATGGGATGAGTATGTAGAAGAAAGCAGCGTTGAGCAGGAAGACGATGGGATT

<u>Sequence A.C-16</u>: Sequence of gene (423 bp) encoding multicopper oxidase obtained from whole-genome sequencing of the Metagenome 2 sample and annotated by MG-RAST as belonging to the Ascomycota phylum.

CCCTTCAATACGTCAATTCATTTCCACGGCATCGAACAACATGGCACCCCCTGGGCG
GATGGCGTCCCTGGTTTGACCCAAAAGCCTATTCAGCCGGGGCACAGCTGGACATA
CCGCTGGAAAGCTACTCAATATGGAACCTACTGGTACCATGCTCATGCCCGATCCGA
AATGATGGATGGTCTTTATGGCCAATCTGGATCAAGTAAGGTCTTTGGAACCCGTCC
ATATGTTCCTATGCAATCCATGCAGCCGGCTTCTGATGTTCTCGATCCATTCAATTTC
ATTTCCAACAAGAGTGATGACATTGAGGCTATGCGGAAGGCGGAAAAAAATCCTCA
ACTGGTCATGTTGTCGGACTGGGACCACCTAACAGCTGCTGAATACCAGCAGGTGCA
ACAAGATACCCGTGTCGACATCGT